GULF STATES UTILITIES COMPANY
POST OFFICE BOX 2951 • BEAUMONT, TEXAS 77704
AREA CODE 409 838 663

January 23, 1985
RBG- 19,972
File No. G9.5, G9.11, G9.23

Mr. Harold R. Denton, Director
Office of Nuclear Reactor Regulation
U.S. Nuclear Regulatory Commission
Washington, D.C. 20555

Dear Mr. Denton:

River Bend Station - Unit 1
Docket No. 50-458

Enclosed is the Gulf States Utilities Company (GSU) final response to the two letters from A. Schwencer (Nuclear Regulatory Commission - NRC) to W. J. Cahill (GSU) dated June 23 and July 23, 1982 pertaining to containment issues raised by Mr. Humphrey. This submittal supercedes all previous submittals (including the letter from J. E. Booker - GSU to A. Schwencer dated April 29, 1983) by providing complete information on all issues. Attachment 1 provides a cross-reference of containment issues to GSU Action Plans and their status. Attachment 2 contains the GSU detailed responses and although some editorial changes have been made to those action plans previously submitted (i.e. on April 29, 1983) the conclusions reached have not been changed.

In regard to Safety Evaluation Report (SER) Confirmatory Item #14 - Mark-III Related Issues (SER Section 6.2.1.9, pg. 6-18,) the two concerns raised are also addressed in this submittal. Item 1 requested further review of the effects structural encroachments over the suppression pool might have on pool swell and impact loads. Information from the 1/10th scale testing program is included in response to Concern Nos. 1.1 through 1.7 (Action Plan Nos. 1 through 4) and demonstrates that effects of local encroachments is not an issue for River Bend Station (Staff agreement provided by Memorandum from M. B. Fields - NRC to W. R. Butler - NRC dated December 31, 1984.) Item 2 requested further review of the response of the Residual Heat Removal (RHR) System in the Steam Condensing Mode and nearby structures in the suppression pool to loads produced by the steam condensation phenomenon. The response to GSU Action Plan No. 6 discussed the analyses completed which indicate the use of the RHR System in the Steam Condensing Mode is warranted and no restriction on operation is necessary.

Sincerely,

J. E. Booker
Manager-Engineering
Nuclear Fuels & Licensing
River Bend Nuclear Group

JEB/WJR/JWL/je

Enclosures (2)

A001
1/46

ENCLOSURE 1

CONTAINMENT ISSUES CROSS REFERENCE

CONCERN NO.	ADDRESSED IN ACTION PLAN NO.	STATUS
1.1	1	Complete Generic
1.2	1	Complete Generic
1.3	2	Complete P/S Generic
1.4	1	Complete Generic
1.5	3	Complete P/S
1.6	4	Complete P/S Generic
1.7	47	Complete P/S
2.1	5	Complete P/S
2.2	5	Complete P/S
2.3	5	Complete P/S
3.1	6	Complete P/S
3.2	7	Complete Generic
3.3	6	Complete P/S
3.4	8	Complete P/S
3.5	8	Complete P/S N/A
3.6	9	Complete Generic
3.7	6	Complete P/S
4.1	10	Complete P/S
4.2	11	Complete P/S
4.3	12	Complete P/S
4.4	13	Complete P/S
4.5	14	Complete P/S
4.6	15	Complete P/S
4.7	16	Complete Generic
4.8	17	Complete P/S N/A
4.9	18	Complete P/S N/A
4.10	16	Complete Generic
5.1	19	Complete P/S N/A
5.2	50	Complete Generic
5.3	18	Complete P/S N/A
5.4	20	Complete P/S
5.5	21	Complete P/S
5.6	19	Complete P/S N/A
5.7	48	Complete P/S
5.8	22	Complete P/S
6.1	45	Complete P/S
6.2	38	Complete P/S N/A
6.3	23	Complete P/S
6.4	39	Complete P/S
6.5	23	Complete P/S
7.1	13	Complete P/S
7.2	24	Complete P/S
7.3	40	Complete P/S
8.1	25	Complete P/S
8.2	26	Complete P/S
8.3	28	Complete P/S N/A
8.4	27	Complete P/S

CONCERN NO.	ADDRESSED IN ACTION PLAN NO.	STATUS
9.1	11	Complete P/S
9.2	19	Complete P/S
9.3	28	Complete P/S
10.1	29	Complete P/S
10.2	30	Complete P/S
11	31	Complete P/S Generic
12	41	Complete P/S N/A
13	42	Complete P/S N/A
14	32	Complete P/S N/A
15	43	Complete P/S N/A
16	33	Complete P/S
17	46	Complete P/S N/A
18.1	44	Complete P/S
18.2	44	Complete P/S
19.1	34	Complete P/S N/A
19.2	35	Complete Generic
20	36	Complete Generic
21	49	Complete P/S
22	37	Complete Generic

P/S = Plant Specific
N/A = Not Applicable

RIVER BEND STATION - UNIT 1

GULF STATES UTILITIES COMPANY

ACTION PLAN TO ADDRESS

ADDITIONAL CONTAINMENT ISSUES

Action Plan 1

I. Issues Addressed - Generic

1.1 Presence of local encroachments, such as the TIP platform, the drywell personnel airlock, and the equipment and floor drain sumps, may increase the pool swell velocity by as much as 20 percent.

1.2 Local encroachments in the pool may cause the bubble breakthrough height to be higher than expected.

1.4 Piping impact loads may be revised as a result of the higher pool swell velocity.

II. Program for Resolution*

1. Provide details of the one-dimensional analysis which was completed and showed a 20-percent increase in pool velocity.

2. The two-dimensional model will be refined by addition of a bubble-pressure model and used to show that pool swell velocity decreases near local encroachments. The code is a version of SOLA.

3. The inherent conservatisms in the code and modeling assumptions will be listed.

4. The modified code will be benchmarked against existing clean pool PSTF data.

5. A recognized authority on hydrodynamic phenomena will be retained to provide guidance on conduct of the analyses.

6.a. An evaluation will be made with drawings of various plant encroachments and pool geometries to establish that the results of the Grand Gulf Analysis are bounding or representative.

6. The effects of the presence of local encroachments on pool swell will be calculated with the two-dimensional code. These calculations will be based upon the worst-case encroachment geometry identified in Item 6.a. Three-dimensional effects (such as bubble breakthrough in nonencroached pool regions) will be included based upon empirical data.

7. A 1/10 linear Froude scaled Mark III encroachment test will be performed to benchmark the SOLA-VOF code and provide additional information on the pool response with varying encroachment geometries. This additional information will aid in determining any areas and/or loads of liquid or froth impact not previously considered.

III. Status*

Items 1 through 3 are complete and included in MP&L's August 19, 1982, submittal (Reference No. AECM-82/353, Attachment 1.1). Items 4 and 6 are complete and included in MP&L's October 22, 1982, submittal (Reference No. AECM-82/497, Attachment 1.2). Item 5 is complete and included in MP&L's December 3, 1982, submittal (Reference No. AECM-82/574, Attachment 1.3). Results of Items 6A and 7 are included in this submittal.

IV. Final Program Results*

Item 6A

The only significant encroachment in RBS is the TIP platform. This encroachment is similar to the encroachment that has been analyzed for Grand Gulf Nuclear Station (GGNS) as shown in Table 1 below.

Table 1 Comparison of GGNS and RBS Pool Encroachment

	River Bend	Grand Gulf
Radial width	11' 4"	10' 8"
Circumferential extent	15'	22'
Vertical height	7'	9'
Clearance to HCU floor from HWL	21.125'	22'
Pool width	20.5'	20.5'
PDW-Max (psig)	19.1	22.0

Since the encroachment geometry in the two plants is similar, and the driving pressure in the River Bend is less than that of GGNS, it may be concluded that the TIP platform in the River Bend plant produces a local response less severe than that of the GGNS. Based on this response, this issue is considered closed for RBS.

Item 7

In early 1984, a series of 1/10 linear Froude scaled Mark III encroachment tests were performed under the auspices of the Containment Issues Owners Group (CIOG). The CIOG concluded on the basis of this test series that local encroachments in the suppression pool do not produce pool swell (Reference 1) loadings in excess of the unencroached or clean pool design loads. This conclusion was based on the observations that:

1. The encroached pool response is always bounded by the clean pool responses.

2. The encroached pool breakthrough height is always less than the design breakthrough height.

3. The encroached pool liquid profile on the containment wall is smaller radially than the clean pool wall profile.

The NRC and its consultants disagreed with the CIOG conclusions. The NRC believed that "there will be a significant solid water impact at the Hydraulic Control Unit (HCU) floor level for type A encroachment (3 cells x 50%)" (Reference 2). However, the NRC did not believe that the smaller encroachments (i.e., B cells x 50%) would cause an increase in design loads. In the NRC's opinion, "for the 'C' encroachment, the ligament has... become broken up and has also virtually stopped rising by the time it reached the HCU floor level" (Reference 2).

The River Bend Station (RBS) traversing incore probe (TIP) platform, which is the only significant encroachment in the suppression pool, is essentially a C series encroachment. Figure 1 shows the geometry of this encroachment. Since the encroachment is a rectangular block in an annular pool, some ambiguity exists in defining the circumferential extent of the encroachment. If the vent spacing at the drywell wall is used, the circumferential coverage is 2.6 cells; if the midpoint spacing is used, the circumferential coverage is 2.1 cells; while if outer edge spacing is used, the circumferential coverage is 1.9 cells. It is most appropriate to use a radial vector through the edge of the encroachment to determine the appropriate circumferential extent. With this rationale, the geometry of the vents is relative to the encroachment, since this is the path of least resistance. Thus only one bubble would remain in the encroached area, which test results indicate would produce significant pool curvature and loadings less than the design values.

Sketch No. SK-5-4712-2 (Figure 2) shows equipment and structures above the tip drive platform encro·hment for River Bend. The crosshatching denotes the .·ne of influence for froth impact loads caused when the pool rises around a Type C encroachment and begins to break up (Reference 2, Figures 7 and 8). The only structures and equipment potentially affected by rising water are termination cabinets containing cables not required for large break LOCAs (Item 7), a plate (Item 6) which protects cables entering the control rod drive position multiplexer cabinet (the loss of which would not offset safe shutdown), and the structural framing shown within the crosshatched area.

This equipment, located on elevation 114 ft, is designed to withstand froth impact loads as described in FSAR Appendix 6A, Sections 10, 11, and 12.

Other equipment in this vicinity, also shown, is outside the zone of influence and/or is shielded by the tip drive platform itself.

Sketch No. SK-5-4713-2 (Figure 3) shows Section AA. The underside of elevation 114 ft is shown in isometric Sketch No. SK-5-4738-1 (Figure 4).

In summary, there is only one significant encroachment for RBS, and it is representative of the tested encroachment configuration which produced no increase in design pool swell loads. The loading specification which has already been considered for design in this area is the very conservative froth impact load method specified in the Mark III acceptance criteria. This specification was based on the 50-ft/sec design froth velocity with the duration of the loading tuned to the natural period of the structure. Since the ligament has become broken up and has also virtually stopped rising by the time it reaches the HCU floor level, the expected loading in the vicinity of the encroachment will be substantially reduced. Therefore, the encroachment issue should be closed for RBS.

References

1. McNamara, E. J. (et. al., General Electric Co.), Mark III Encroachments Summary Report, November 1984 (Attachment 1.4).

2. Sonin, A. A., Comments on the 1/10 Scale Tests for the Effect of Encroachments on Mark III Pool Swell, September 27, 1984 (Attachment 1.5).

*This revision replaces the GSU submittal dated April 1, 1983.

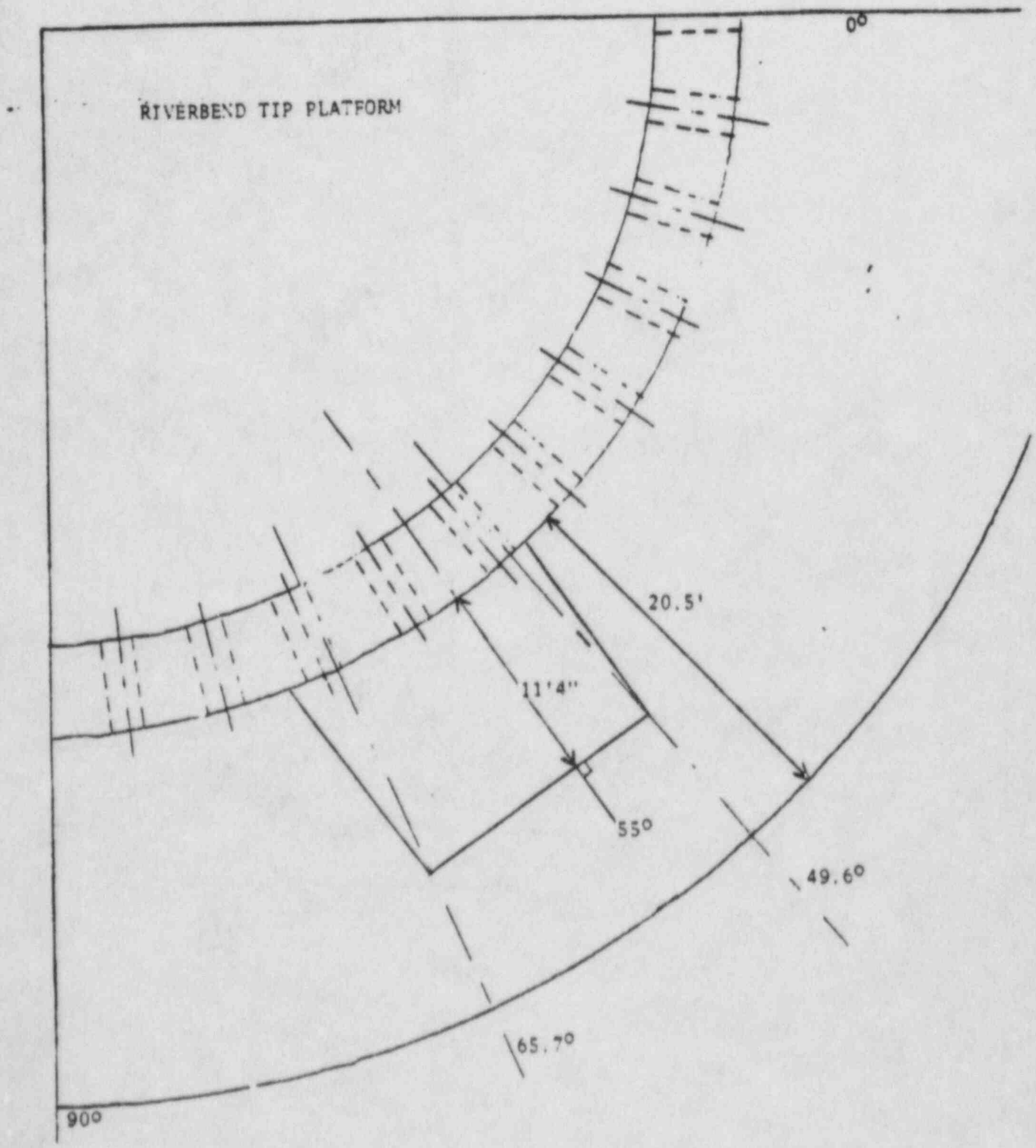

FIGURE - 1
1 - 2c

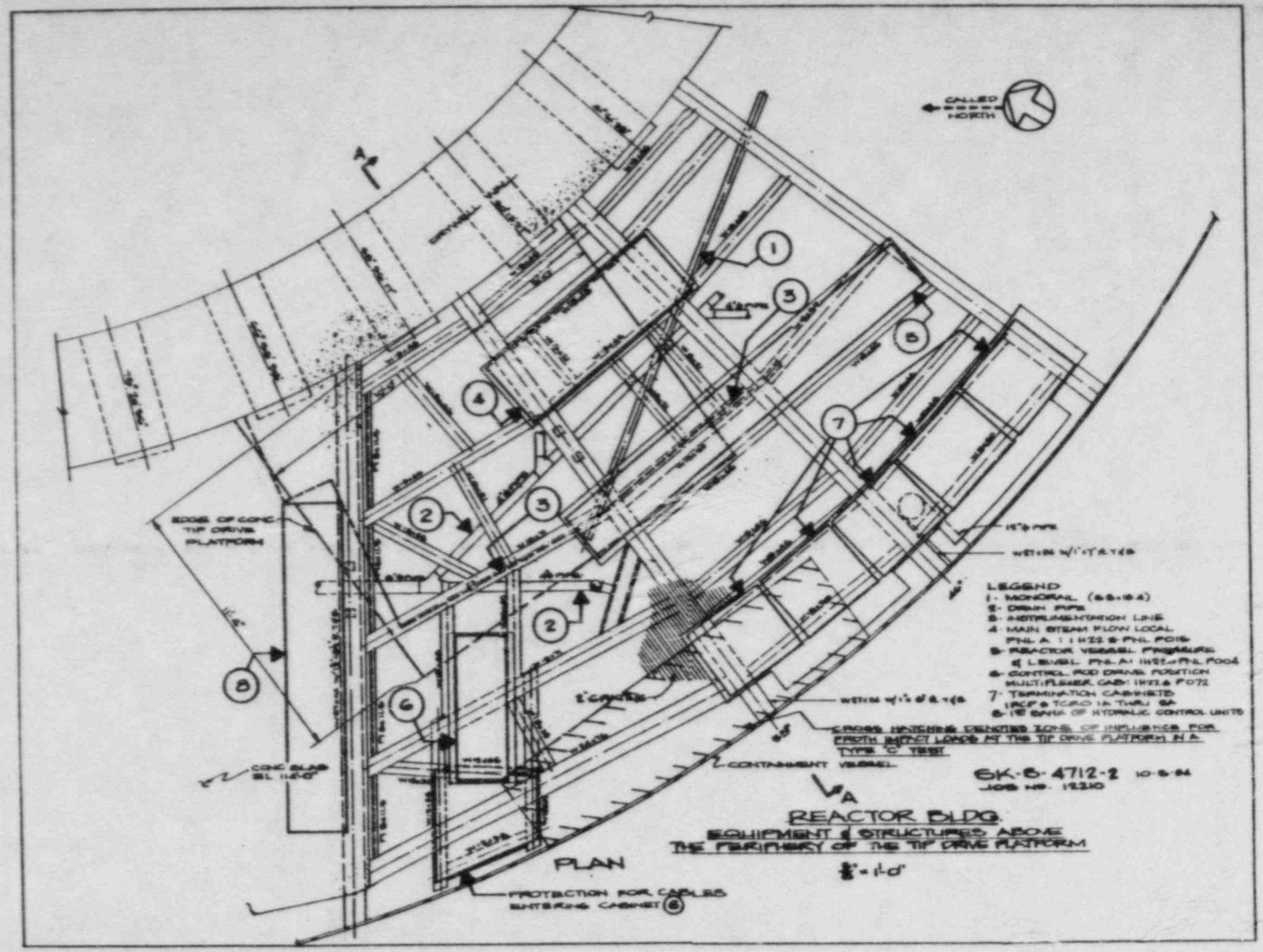
CALLED NORTH
EDGE OF CONC TIP DRIVE PLATFORM
CONC SLAB EL 114'-0"
PROTECTION FOR CABLES ENTERING CABINET
LEGEND
1- MONORAIL (A&B-104)
2- DRAIN PIPE
3- INSTRUMENTATION LINE
4- MAIN STEAM FLOW LOCAL
5- REACTOR VESSEL
7- TERMINATION CABINETS
8- HYDRAULIC CONTROL UNITS
CONTAINMENT VESSEL
6K-5-4712-2
JOB NO. 1230
REACTOR BLDG.
EQUIPMENT & STRUCTURES ABOVE THE PERIPHERY OF THE TIP DRIVE PLATFORM
PLAN

FIGURE - 2
1 - 2d

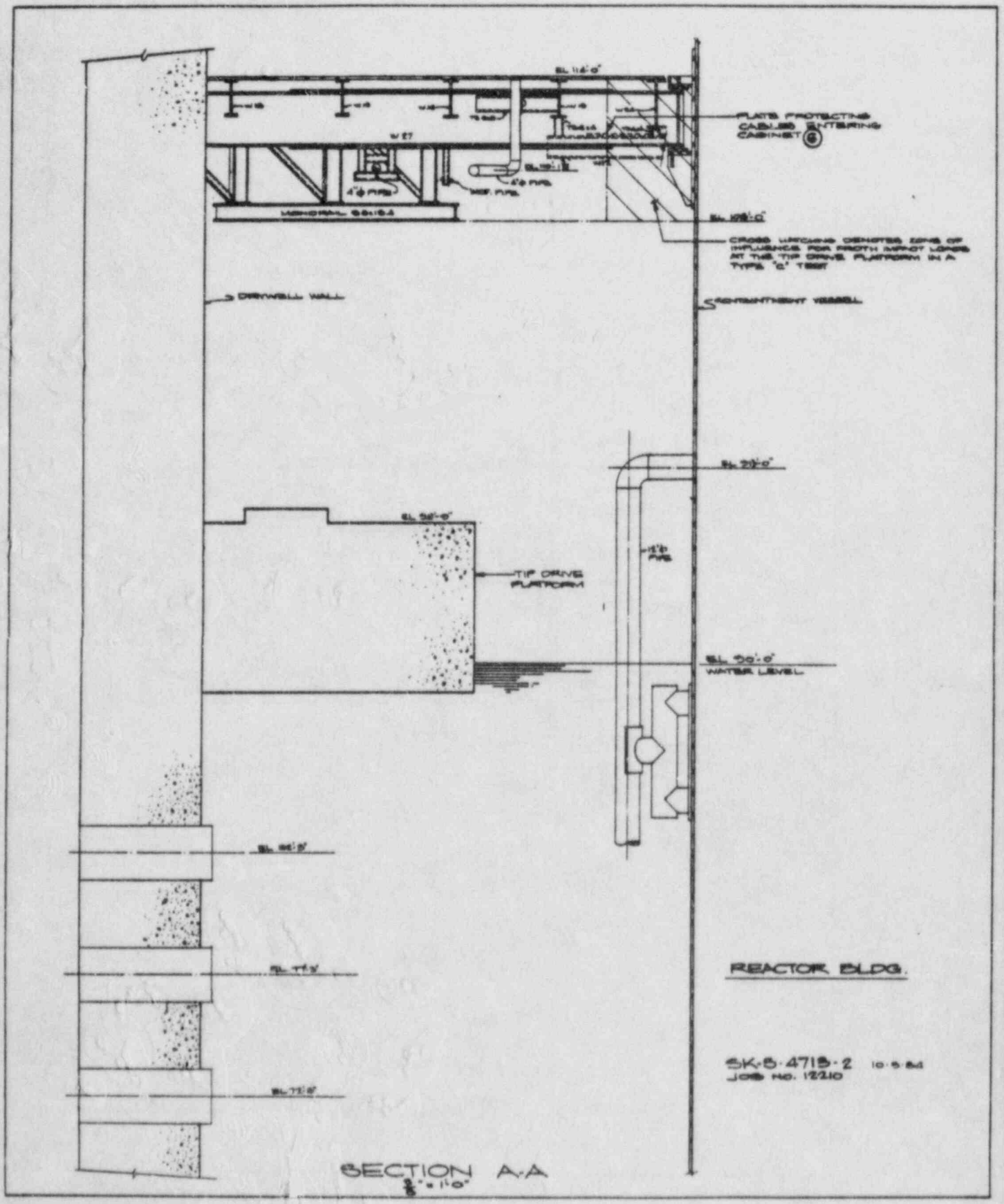
PLATES PROTECTING CABLES ENTERING CABINET
DRYWELL WALL
CONTAINMENT VESSEL
TIP DRIVE PLATFORM
WATER LEVEL
REACTOR BLDG.
SK-5-4715-2
JOB NO. 12210
SECTION A-A

FIGURE - 3

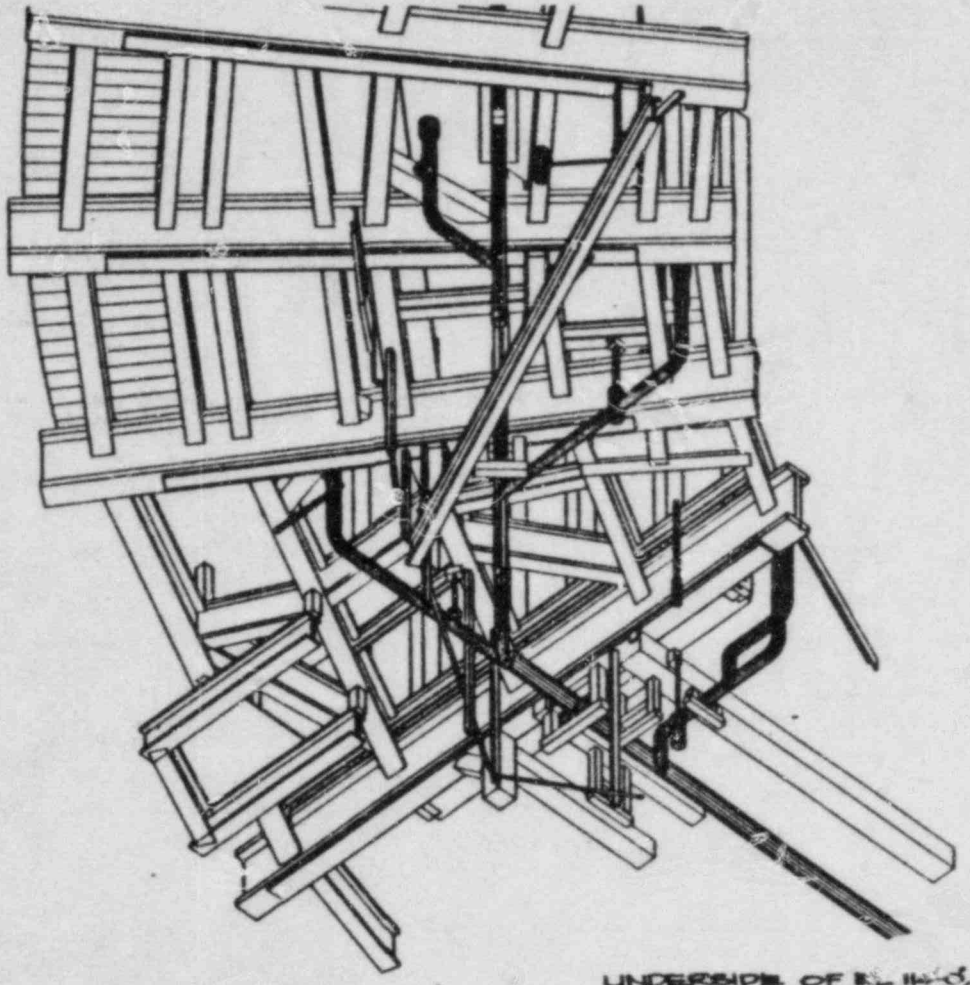

FIGURE - 4
1 - 2f

UNDERSIDE OF EL. 116'-3", CONTAINMENT
ABOVE THE PERIPHERY OF THE
TIP DRIVE PLATFORM

REACTOR BUILDING

SK-S-4758-1
JOB NO. 12210 10-10-84

ATTACHMENT 1.1

The results of Items 1 and 2 and portions of Items 3 and 4 are attached.

Ref: AECM 82/353

The one-dimensional (1-D) scoping analysis discussed in Item 1 of the program for resolution was initially performed by General Electric to determine the effect of pool encroachments on the pool swell transient. The conclusions of this study were: (a) Encroachments typically found in Mark III containments have only a small effect on the pool swell transient; and (b) A more refined 2-D analysis would have to be performed to determine the actual magnitude of the effect.

This analysis was performed using a GE computer code (M3CPT04) which is based on the General Electric Mark III Pressure Suppression Containment Analytical Model (References 1, 2). A pool swell model (Reference 3) has been incorporated into this code. This analysis modeled the pool encroachment as being a blockage in the pool of uniform width (the width of the TIP platform) around a 360° pool sector. Thus, this analysis implied 47% of the GGNS pool to be covered, while only 4% of the pool is actually covered. The effect of the 47% encroachment was found to cause the drywell pressure (pool swell driving force) to increase 10%. The increase which might be expected for GGNS based upon this extremely conservative analysis is 10% x 4%/47% = 1%. Thus, the pool is somewhat overdriven by this particular modeling.

The 1-D assumption sets the encroachment at infinite vertical extent. The modeling also constrains the bubble into the reduced annulus formed by the encroachment edge (extended vertically) and the containment wall, as shown in Figure 1-1. Thus, an assumption must be made with regard to the water which was initially under the encroachment. This analysis assumed half of the water under the top vent stagnates while the other half moves (at time t = 0) to the open portion of the pool; thus, the initial pool submergence was assumed to increase with encroachment size.

The code does not have a bubble breakthrough mechanism. In fact, in the 1-D modeling, the water slug above the top vent does not thin with time. There is no relief of driving force — either radially over the encroachment or circumferentially after breakthrough occurs in surrounding cells. Therefore, a further assumption must be made regarding where breakthrough occurs. Based on test data, the best estimate for where breakthrough occurs is 1.6 times the initial submergence above the initial (t = 0) pool surface. This corresponds to a breakthrough elevation of 12 feet above the initial pool surface for the unencroached pool. For the encroached pool, the breakthrough elevation will again be assumed to be 1.6 times the initial submergence above the initial pool surface, except the initial submergence is larger due to the assumption that half of the water under the encroachment is added to the open portion of the pool. Resulting breakthrough heights for various pool area fractions blocked by encroachments are plotted in Figure 1-2.

Figure 1-3 provides analysis results presented as peak pool swell velocity versus pool area fractions blocked by encroachments. For annular encroachments having the Grand Gulf TIP floor centerline width, 1-D analysis predicts a 23% velocity increase. These results are within the design margin of the load definition. The design velocity (60 ft/sec) is 33% larger than expected (40 ft/sec), and thus the 33% margin bounds the 23% (worst-case) projected velocity increase.

This analysis estimates an upper bound of the effect of encroachments. This represented a first-attempt to assess such effects. However, General Electric (GE) felt that the 1-D analysis results were excessively conservative and potentially misleading. Accordingly, GE stopped the 1-D analysis work, without performing detailed verification of that study, and initiated work on 2-D analyses since 2-D analyses appeared to be necessary to obtain a realistic assessment of encroachment effects on pool swell velocities.

SOLA-VOF, a computer program for solution of 2-dimensional transient flows, developed by Los Alamos Scientific Lab (Reference 4), was modified to include a hydrodynamic model of the bubble and vent system to conform with the work discussed in Item 2 of the program for resolution. SOLA-VOF solves the Navier-Stokes equations for an incompressible fluid on a two-dimensional rectangular mesh, with the capability to track fluid region interfaces and multiple free surfaces. For pool swell problems, additional capability was needed to relate the bubble pressure to the drywell pressure and the flow losses through the vent systems; which necessitated the addition of bubble and vent system modeling.

The vent flow model incorporated into SOLA-VOF is based on the assumptions of a perfect gas with constant specific heat adiabatically flowing through a constant-area duct with friction. Air is assumed as the constant temperature fluid medium. The modeling considers only subcritical flow and the bubble pressure is not allowed to drop below the critical vent exit pressure. Isentropic flow is assumed upstream from the vents.

The user controls several important input parameters to the modeling. These include the ratio of specific heats, the gas constant, the temperature, the vent area, the vent loss coefficient, and a 3-D volume correction factor. The user also inputs the pool and vent system geometry, fluid properties, and drywell and wetwell pressure histories. Currently, the ratio of specific heats and the gas constant for air are used. The temperature used is the average drywell temperature. Vent area is obtained from geometry data. The vent loss coefficient used is the same as that used in final safety analysis report modeling. The 3-D volume correction factor is found by taking the ratio of bubble volume in three dimensions to bubble volume in two dimensions for the same radial cross-section. This is done for several bubble volumes and input in tabular form, with volume ratio as a function of 2-D computed volume.

The added modeling contains routines to compute the vent flow pressure losses due to friction based on the vent flow computed from the bubble expansion rate. The vent loss modeling is based on the Fanno frictional flow model. With knowledge of the stagnation and back pressures, the properties at the vent entrance (state 1) and the Mach numbers at the vent entrance and exit (state 2) can be computed. Then, the properties at state 2 are giver by the Fanno relations:

$$\frac{T_2}{T_1} = \frac{1+\frac{(k-1)}{2}M_1^2}{1+\frac{(k-1)}{2}M_2^2} \tag{1}$$

$$\frac{P_2}{P_1} = \frac{M_1}{M_2}\sqrt{\frac{1+\frac{(k-1)}{2}M_2^2}{1+\frac{(k-1)}{2}M_1^2}} \tag{2}$$

$$C_2 = \sqrt{kRT_2} \tag{3}$$

$$v_2 = M_2 C_2 \tag{4}$$

The two subroutines which solve these equations in the General Electric computer program SHEX were incorporated into SOLA-VOF. The methodology used in the SHEX program is described in detail in references 1 and 2.

Mass conservation for the bubble may be written as follows:

$$-\dot{M}_v + \frac{dM_b}{dt} = 0 \tag{5}$$

where $\dot{M}_v$ is the vent mass flux M_b is the bubble mass. The vent mass flux is computed from the properties at state 2:

$$\dot{M}_v = P_2 v_2 A \tag{6}$$

where A is the vent area. The derivative of bubble mass may be expressed as

$$\frac{dM_b}{dt} = \frac{d}{dt}\left(P_b V_b\right) = P_b \frac{dV_b}{dt} + V_b \frac{dp_b}{dt} \tag{7}$$

Thus, equation (5) becomes

$$-V_2 A + \frac{dVb}{dt} + \frac{V_b}{P_b}\frac{dp_b}{dt} = 0 \tag{8}$$

The modeling incorporated into SOLA-VOF iterates at each timestep to find a back pressure (bubble pressure) for which the exit conditions predicted by the Fanno model satisfy equation (8).

The solution of equation (8) requires knowledge of the bubble volume at each timestep. Since SOLA-VOF is a two-dimensional code, the volumes computed are not representative of a 3-D bubble. To account for this, the volume computed by the SOLA-VOF algorithm is multiplied by the correction factor discussed above. This multiplier must be empirically determined for each geometry.

The bubble and vent system modeling (i.e., computing the airflow into the bubble) only accomodates flow through the top vent. The second vent clears so late into the transient that its flow will not significantly affect the bubble growth and, consequently, will not significantly affect the breakthrough height or velocity. For tracking the interface motions at the bottom two vents, the bubble pressure of the first bubble is applied at the middle vent interface and then still later, at the bottom vent interface after the respective vents clear.

The changes in pool swell velocity and bubble breakthrough height are being predicted by use of a multiplier. The multiplier is calculated using a ratio of computer predictions for encroached pools to unencroached pools. Although numerous conservatisms exist in the computer predictions, the multiplier ratio essentially "cancels out" these conservatisms. Consequently the conservatisms discussed in item 3 of the program for resolution are limited to the conservatisms in the clean pool peak velocity and breakthrough height specification. The conservatisms in these specifications are listed in GESSAR II Appendix 3B, Attachment 0, Response to NRC questions 3 and 9.

Bench marking of the modified version of SOLA-VOF for pool swell calculations is being performed as discussed in Item 4 of the program for resolution by simulating pool swell tests that were run at the GE Pressure Suppression Test Facility (PSTF). These simulations will include ten cases selected from the 1/9, 1/3, and full-scale tests (References 5, 6, 7). Geometry, pressure histories, bubble parameters and initial conditions will be input to the computer program and pool swell response will be calculated. The pool swell results from the modified SOLA-VOF, including velocity and elevation, is being compared to the test data.

At present, a preliminary simulation of a 1/9-Area Scale test has been completed. This case is Test 6002 Run 7, a 5-ft vent submergence, 100% main steamline break simulation. Figure 1-4 shows the pool surface elevation as a function of time as computed by the modified SOLA-VOF and as indicated by the test data. Current predictions are close to the test data, although the calculated displacement is consistently low by about 10%.

The pool surface velocity as a function of height for the 1/9-Area Scale simulation is shown in Figure 1-5. The predicted velocity is consistently higher than that indicted by PSTF data. Also, the transient continued well past the end of the PSTF data, demonstrating the need for a breakthrough criterion.

Final iterations to this model are still in progress to refine its capability to predict both pool displacement and velocity.

References

1. Bilanin, W. J., "The General Electric Mark III Pressure Suppression Containment System Analytical Model", NEDO-20533, June 1974.

2. Bilanin, W. J. et al, "The General Electric Mark III Pressure Suppression Containment System Analytical Model (Supplement 1)", NEDO-20533, September 1975.

3. Ernst, R. J. et al, "Mark II Pressure Suppression Containment Systems: An Analytical Model of the Pool Swell Phenomenon", NEDE-21544P, December 1976.

4. Nichols, et al, "SOLA-VOF: A Solution Algorithm for Transient Fluid Flow with Multiple Free Boundaries", LA-8355, August 1980.

5. Kingston, R. E., "Mark III Confirmatory Test Program 1/9-Area Scale Multivent Pool Swell Tests (Test Series 6002)", NEDE-24648-P, May 1979.

6. Ernst, R. J., et al, "Mark III Confirmatory Test Program One-Third Scale Three Vent Tests (Test Series 5801 Through 5809)", NEDM-13407-P, May 1975.

7. Myers, L. L., et al, "Mark III Confirmatory Test Program Phase I-Large Scale Demonstration Tests - Test Series 5701 Through 5703", NEDM-13377, October 1974.

V. Details of Planned Analyses

The 2-D SOLA-VOF Computer Program modified with the inclusion of a bubble model will be utilized to determine the effect of local encroachments on pool swell as discussed in Item 6 of the program for the resolution. When the implementation and qualification of the modified code version is complete, the GGNS geometry will be simulated. The containment response analytical model will be run for the GGNS pool geometry and GGNS initial conditions to determine the drywell and wetwell pressure time histories. Standard FSAR assumptions will be made for the determination of these time histories with the exception that the pool surface area will be decreased by the total encroachment area in order to maximize this pool swell driving pressure and assure an upper bound on resulting

pressure histories will be input into the modified version of SOLA-VOF and the bounding clean pool peak bubble pressure, peak pool surface velocity and the breakthrough elevation will be determined.

To determine the effect of the encroachments, these drywell and wetwell pressure histories will be input into SOLA-VOF with the bubble model incorporated and the GGNS TIP platform modeled. This case will be run up until the time the reference clean pool case predicted bulk breakthrough. The modified SOLA-VOF will then be restarted with the driving pressure being ramped to the wetwell airspace pressure to determine the peak pool swell height. This approach is justified on the basis that PSTF tests indicate that the adjacent pool swell bubbles coalesce circumferentially. If breakthrough occurs elsewhere in the pool, the higher bubble pressure under the encroachment would be vented circumferentially to the wetwell airspace through the path of least resistance.

There is also the potential for breakthrough to occur over the encroachment. To determine if this will occur, a criterion will be developed which predicts when radial breakthrough (breakthrough over the encroachment) would occur. If this criterion is satisified in the analysis, the modified SOLA-VOF run will be terminated at the moment of breakthrough, and restarted with the bubble pressure being ramped to the wetwell airspace pressure.

The resulting peak velocity and breakthrough elevation from the encroached pool will then be compared with the like quantities in the reference clean pool case to determine the effect of the encroachments.

It is anticipated that the effect of the encroachment will be to lower the pool swell velocity in the vicinity of the encroachment. Preliminary results show the pool surface acceleration to be substantially less in the encroached case than in the clean pool case. Hence, when breakthrough occurs in unencroached pool regions, the driving pressure will be removed. High velocities and breakthrough heights will therefore not occur near encroachments.

VI. Justification For Full Power Operation

The results which have been obtained from preliminary one dimensional analysis indicate a net effect of less than 1% in terms of the composite pool swell phenomena. Extensive margins exist in the existing GGNS analyses such as assuming a pool swell velocity of 60 ft/sec, applying the absolute bubble pressure methodology to definition of submerged structure loads, and the HCU floor is higher above the suppression pool than the GESSAR plant. Preliminary assessments indicate that the pool swell velocity and bubble breakthrough heights may actually decrease near the encroachment. Extensive conservatisms have been employed in defining peak pool swell velocity and maximum bubble breakthrough height. Based upon the aforementioned argument, full power operation of GGNS should be permitted pending completion of analyses which are in progress.

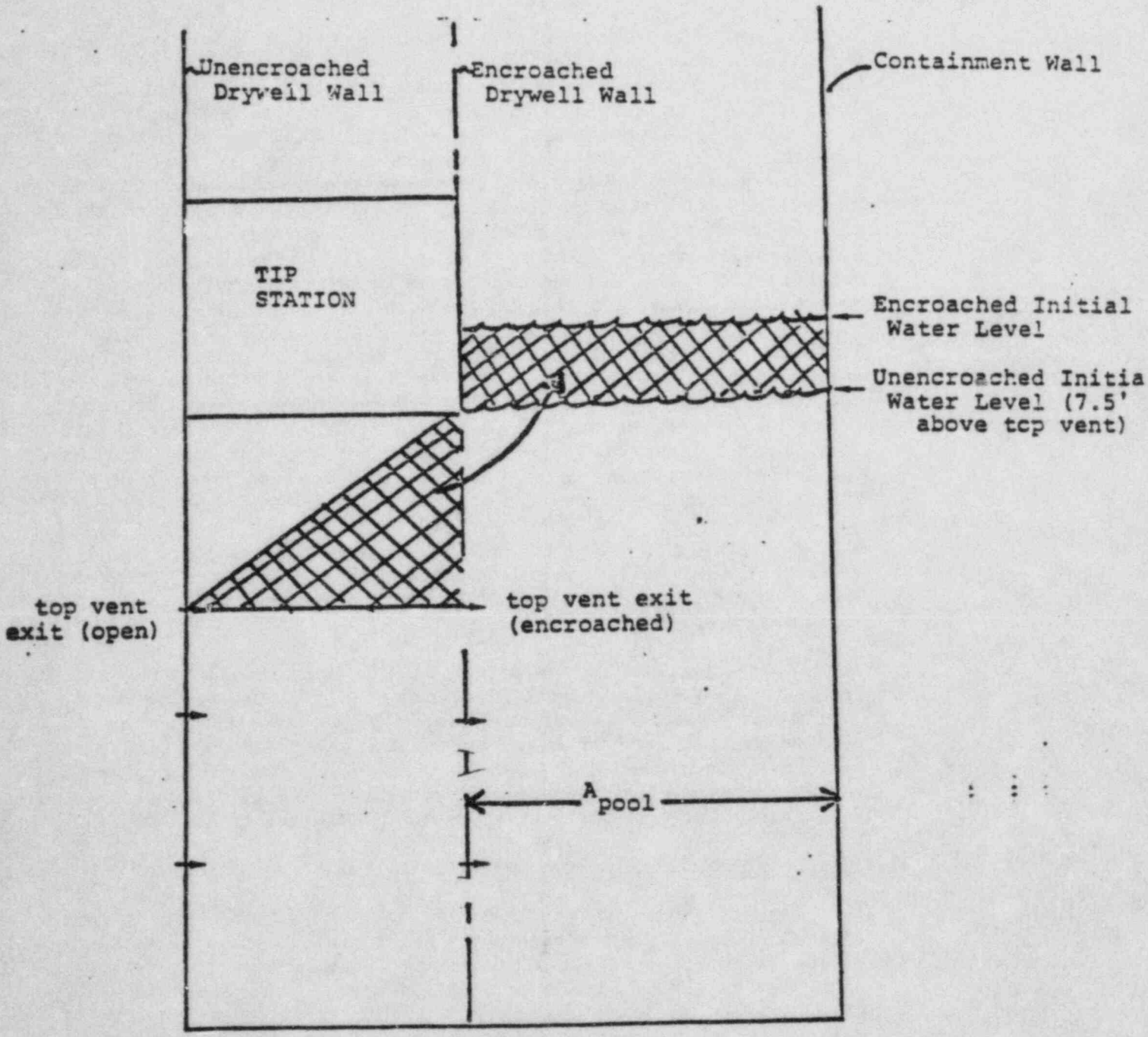

Figure 1-1 1-D Pool Model

Figure 1-2 Effect of Encroachments Breakthrough Height (1-D Assumption)

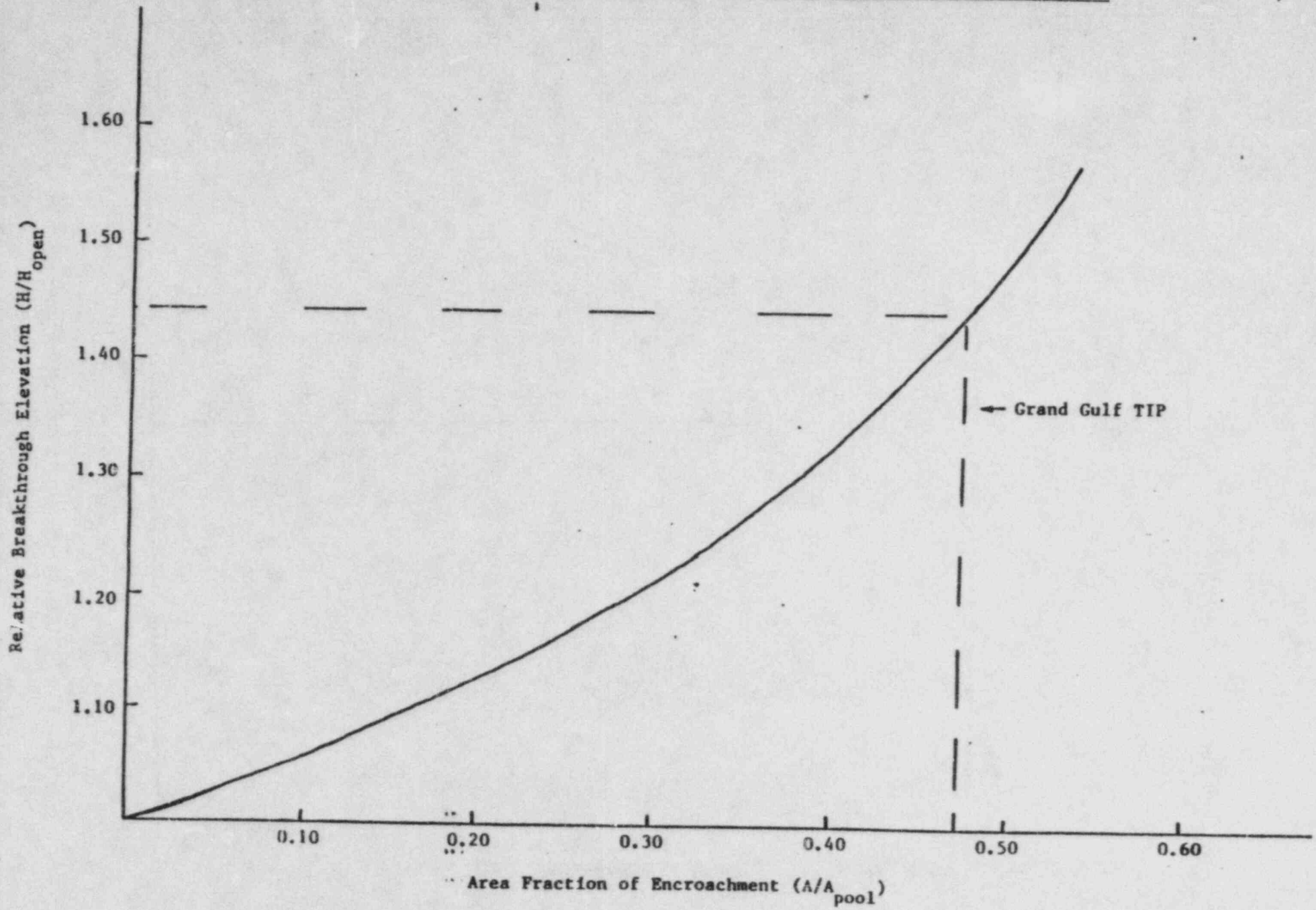

Figure 1-3 Effect of Encroachments on Peak Pool Swell Velocity (1-D Analysis)

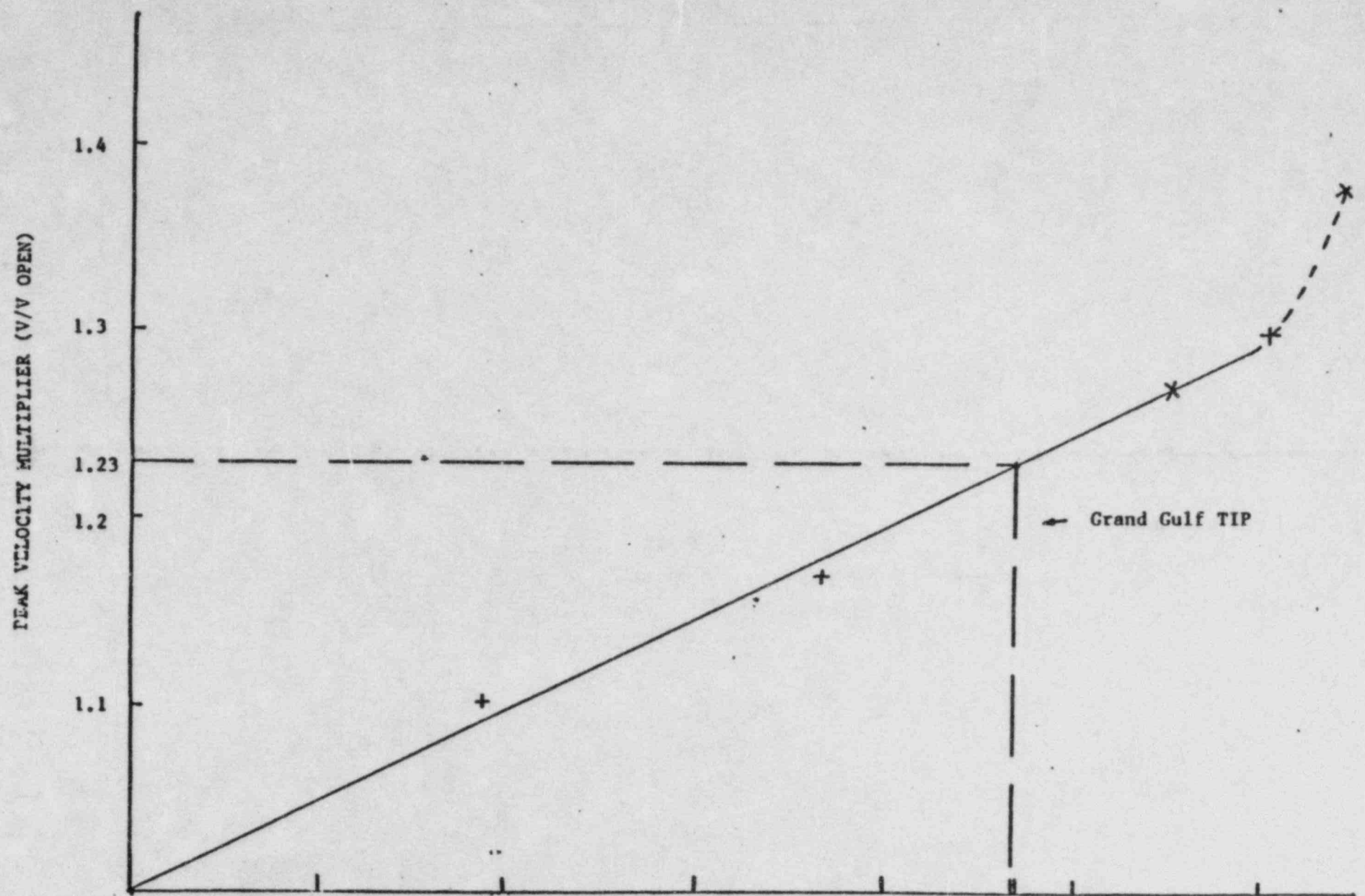

Pages 1-13 and 1-14

These pages represent General Electric Company Proprietary Figures 1-4 and 1-5. These figures have been previously provided to the NRC via MP&L's August 19, 1982 submittal (Reference No. AECM-82/353).

ATTACHMENT 1.2

The results of Items 3, 4, and 6 are attached.

Ref: AECM 82/497

Item 3

The methodology used to predict peak pool swell velocity and maximum swell height is extremly conservative.

The output of the modified SOLAVOl code is used directly to obtain the encroached case peak velocity and maximum swell height. The peak velocity obtained (31 ft/sec) is conservative (i.e., higher than actually will occur) since:

1) Condensation is not accounted for. The effects of condensation are discussed in detail under item six of this action plan; however, condensation is expected to cause approximately a 20% reduction in peak surface velocity.

2) The driving drywell pressure was calculated by the containment analytical model which is known to overpredict drywell pressure by approximately 15% (GESSAR II, Appendix 3B, Attachment O, Response to NRC Question 3).

3) Comparisons between test measurements and code predictions presented under item 4 of this action plan show SOLA tends to overpredict pool swell velocities, including air blowdown cases without condensation.

4) The pressure in the bubble is not allowed by the code to drop below the pressure which would choke the flow exiting from the vent. In both the real and calculated situations, the bubble expansion is such that the pressure decreases below the critical pressure. Thus, both the clean pool and the encroached pool are overdriven by this effect after approximately 1.1 sec.

The other critical output of the CGNS encroached pool SOLAV run is the peak pool swell height. Since local bubble breakthrough does not occur in the vicinity of the encroachment, the peak swell height is a strong function of the peak velocity. Once peak velocity is obtained, the slug slows under the influence of gravity. As previously demonstrated, the peak velocity is conservatively high; therefore, the peak swell height is likewise extremely conservative. When the conservatisms on velocity are considered, it is expected that the slug would not reach the HCU floor.

Item 4

Extensive simulations of pool-swell tests have been conducted using SOLAVOl to verify the accuracy of added modeling. The simulations include tests from the 1/9-, 1/3-, and full-area-scale facilities.

The actual runs used for comparison were 5701-5, 5706-2, -3, 5801-9, -10, -11, 5906-1, -2, and 6002-6, -7. Both air and steam blowdowns from the 1/3- and full-scale facilities were simulated. A representative simulation of the 1/9-, 1/3-, and full-scale test is discussed in detail below.

Input Assumptions

For each facility, the geometry was obtained from pertinent test reports. The most difficult constraint upon two dimensional modeling is simultaneously retaining the ratio of weir annulus surface area to vent flow area and the weir annulus surface area to suppression pool surface area ratio. The effect of failure to simultaneously maintain these ratios is only significant before vent clearing, and typically results in a delay of vent clearing on the order of 0.1 - 0.2 seconds. The use of cylindrical or rectangular geometry was evaluated and rectangular geometry was selected for the subsequent analyses since it provided better agreement with test results. The vent height was shown to have a significant effect on vent clearing; in all simulations, the height was set to the vent diameter, rather than preserving vent flow area. For the 1/9-scale simulations, the vent was shortened to preserve vent volume; however, in the 1/3- and full-scale simulations, the true length of 5 ft was used, as preserving vent volume would result in vent length longer than 5 ft. In all cases, the true suppression pool width was used, and the weir annulus width was scaled to preserve the ratio of pool surface area to weir annulus surface area.

A bubble volume correction factor is used to compensate for the modeling of a three dimensional bubble in two dimensions. The methodology employed in calculating these correction factors is discussed in detail in reference 1. The ratio of true bubble volume to 2-D computed volume was determined for several assumed bubble shapes. The assumed shapes included a hemispherical bubble over the vent exit, a spherical bubble tangent to the vent exit and the sides of the pool sector, and a large bubble nearly filling the pool. These computations were made for the 1/3-scale geometry and extrapolated for use in the 1/9-scale and full-scale tests by normalizing to the ratios of true pool surface area to 2-D pool area.

For each test, drywell and wetwell pressure histories were obtained from the test records. Other inputs obtained from test data included initial pool and weir annulus water levels, water temperature (from which fluid properties are obtained), and the average drywell air temperature, which was used as the stagnation temperature in the vent flow model. Air was used as the fluid in the vent flow model to eliminate uncertainty due to the effects of condensation and to provide direct comparisons with air blowdowns. The flow loss coefficient (fL/D) was obtained from previously-performed best-estimate calculations.

S3

Comparison Results

Figures 1-1 and 1-2 show the pool and bubble surface configurations at several times into the pool swell transient for run 6002-7. This run is a 1/9- scale steam blowdown with 5-ft vent submergence. The test data are shown for comparison. The calculated surface rises somewhat faster than the test data indicates. Figure 1-3 shows average surface elevation as a function of time. The solid line is the average of the SOLAVOI results; the dashed line is a corrected average which accounts for the difference in bubble volume between the true geometry and the 2-D model. Since average surface elevation is a direct function of bubble displacement, the 2-D effect tends, as expected, to cause overprediction of surface elevation. Figure 3 shows that, with the correction, the SOLAVOI prediction is very close to the test data.

Figures 1-4 and 1-5 show the pool and bubble surfaces for run 5801-9. This run is a 1/3-scale steam blowdown with 5-ft vent submergence. The pool surface prediction is very close to the test data, falling slightly below the test data at 1.3 seconds. The predicted bubble surface is generally lower than the test data, due to a vent-clearing delay of about 0.1 seconds. Figure 1-6 shows the pool surface elevation transient, compared with test data at several radial locations. The prediction shows similarity between the predicted and measured surface curvature. The elevations shown are not corrected for the 2-D bubble, and an average surface elevation curve is not presented since the average surface elevation calculations are not applicable to cases with surface curvature. However, correction for the 2-D bubble would lower the elevation predictions by about 1 ft.

Figures 1-7 and 1-8 show the surface predictions for run 5706-2. This run is a full-scale air blowdown with 6-ft vent submergence. The prediction is very close to the test data, but exhibits somewhat less surface curvature. Figure 1-9 shows the surface elevation transient, which again shows good correlation between test results and code predictions, especially in the center of the pool.

Significant Trends

As previously mentioned, vent clearing tends to be delayed by about 0.1 seconds in most cases. The delay does not cause appreciable errors in the remainder of the transient. In fact, the pool elevation transient tends to lead the test data in some cases. This may be a combined effect of the 2-D considerations and steam condensation, which will be discussed in more detail.

Another general trend noted from the comparisons is that velocity tends to be somewhat higher in the simulations, especially for tests which employed steam blowdowns. This trend is largely due to the lack of steam condensation modeling in the code. Steam condensation reduces the mass in the bubble, and consequently the

pressure. This argument is supported by two observations. First, the velocity effect tends to be more pronounced in runs with higher submergence. The higher submergence increases condensation effects both by delaying pool swell until a higher percentage of steam is in the bubble, and by increasing the hydrostatic head. Second, the velocity predictions are much closer to test data in the air blowdowns (1/3- and full-scale), in which large drywell volume reduced the percentage of steam in the blowdown mixture. The trend toward higher velocity error with increasing submergence is not noted in the 1/3-scale air test.

The comparisons between SOLAVOI predictions and measured test results provides assurance that the modeling of phenomena with the SOLAVOI code accurately represents physical processes. In particular, the comparisons completed to date have validated the methodology used to calculate geometric factors which account for discrepancies between two dimensional modeling and three dimensional phenomena. These comparisons have included a wide range of initial conditions including variations in blowdown composition and initial vent submergence. Several inherent conservatisms in the modeling have been demonstrated. The principle result of the aggregate of these conservatisms is that pool swell velocity predictions tend to exceed measured test data.

Item 6

The modified SOLAVOI computer code described in reference 1 and verified above was used to determine the effect of the Grand Gulf TIP platform on the pool swell transient. To determine the encroachment effect, it was first necessary to develop a reference clean pool base case. This was done by first running the containment response analytical model (M3CPT04 - References 2, 3) for the GGNS pool geometry and GGNS initial conditions to determine the drywell and wetwell pressure-time histories. Standard FSAR assumptions were made for the determination of these time histories with the exception that the pool surface area was decreased by the total encroachment area to maximize the pool swell driving pressure and assure an upper bound on resulting encroachment effects. These reference pressure histories were input into the modified SOLAVOI code, and the bubble pressure and pool surface elevation time histories were determined. Figure 1-10 shows the input drywell and wetwell pressure histories and the resultant bubble pressure history for the GGNS clean pool case. Figure 1-11 shows how the bubble and pool surfaces evolve during the transient. The growth patterns are consistent with the design peak velocity of 50 ft/sec.* The predicted breakthrough elevation is 17.4 feet above the initial pool surface. This elevation is much higher than the breakthrough elevation which would be expected for the GGNS vent submergence based on test data. This increase in breakthrough height occurs because the slug thins more slowly than prototypically in the 2-D SOLAVOI results.

* The expected peak velocity is approximately 40 ft/sec because PSTF test data show condensation has a 20% effect on peak velocity (Reference 4).

To determine the effect of the encroachments, the same drywell and wetwell pressure histories were input into the modified SOLAVOI code with the CGNS TIP platform modeled. Since SOLA is a 2-D code, the implicit assumption is that the encroachment covers a 360° arc and the bubble pressure accordingly remains unrealistically high.

This case was used to determine when the bubbles coalesce circumferentially. The assumption is made that the bubble expands circumferentially and radially at the same rate. Using this criterion, adjacent bubbles would be expected to come together approximately 0.17 seconds following vent clearing, or about 1 second into the transient. This neglects the fact that the higher bubble pressure under the encroachment would create additional circumferential expansion, causing the actual coalescence to occur even earlier. The encroached bubble pressure following coalescence was then ramped down to the clean pool bubble pressure in the time it takes for the acoustic wave to make two round trips between the encroached bubble and free bubble (t =0.047 sec). From 1.047 sec into the transient, the clean-case bubble pressure was used to drive the water slug. After breakthrough (t = 1.275 sec), the bubble pressure is ramped to the wetwell airspace pressure in approximately 0.2 sec. The bubble pressure history calculated assuming a 360° encroachment is shown in Figure 1-12. The final bubble pressure history used in the CGNS encroached-case is shown in Figure 1-13.

The pool elevation profiles and pool velocities for the CGNS encroached pool simulation are presented in Figure 1-14. The peak pool surface velocity is 31 ft/sec, only 62% of the clean pool velocity. Taking credit for a 20% condensation effect would indicate a maximum encroached pool velocity of around 25 ft/sec. Breakthrough for this encroached case does not occur, because the slug does not thin with the encroachment present. The maximum rise of the surface is about 23.5 feet, or to just below the bottom of the CGNS grating. Two feet below the grating, (where impact on beams might occur) the peak velocity is only on the order of 10 ft/sec. When condensation effects on the pool swell transient along with the other conservatisms identified under item 3 of this action plan are considered, no impact on these beams should occur.

References

1. Mississippi Power & Light letter number AECM-82/353 from L. F. Dale to Harold R. Denton dated August 19, 1982.

2. Bilanin, W. J., "The General Electric Mark III Pressure Suppression Containment System Analytical Model", NEDO-20533, June 1974.

3. Bilanin, W. J. et al, "The General Electric Mark III Pressure Suppression Containment System Analytical Model (Supplement 1)", NEDO-20533, September, 1975.

4. GESSAR II, Question/Response 3BO.3.2.3, 22A7000, Rev 2.

Pages 1-21 through 1-29

These pages represent General Electric Company Proprietary Figures 1-1 through 1-9. These figures have been previously provided to the NRC via MP&L's October 22, 1982 submittal (Reference No. AECM-82/497).

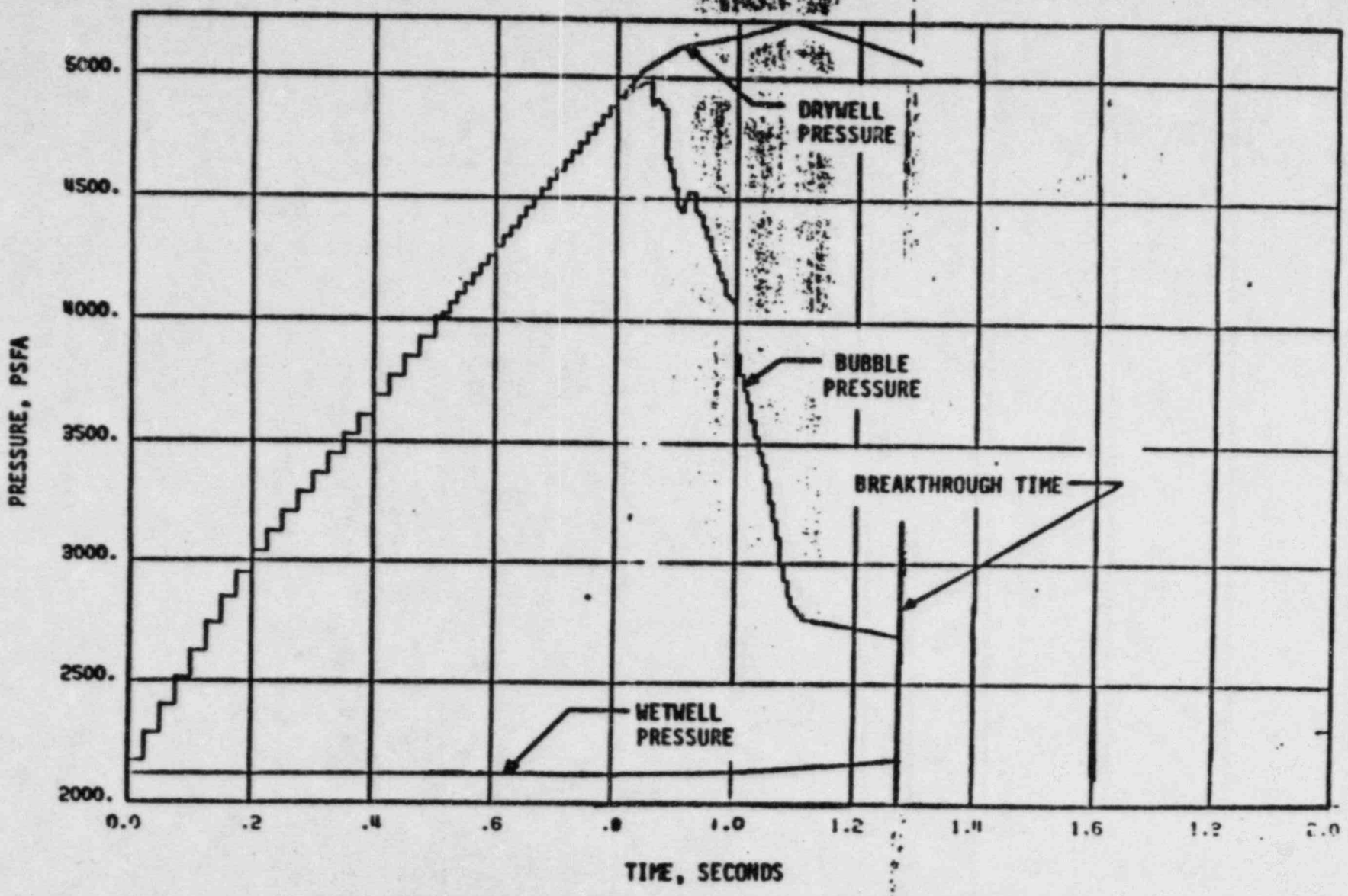

FIGURE 1-10 PRESSURE HISTORIES, GRAND GULF UNENCROACHED CASE

Figure 1-11
GRAND GULF CLEAN POOL SIMULATION

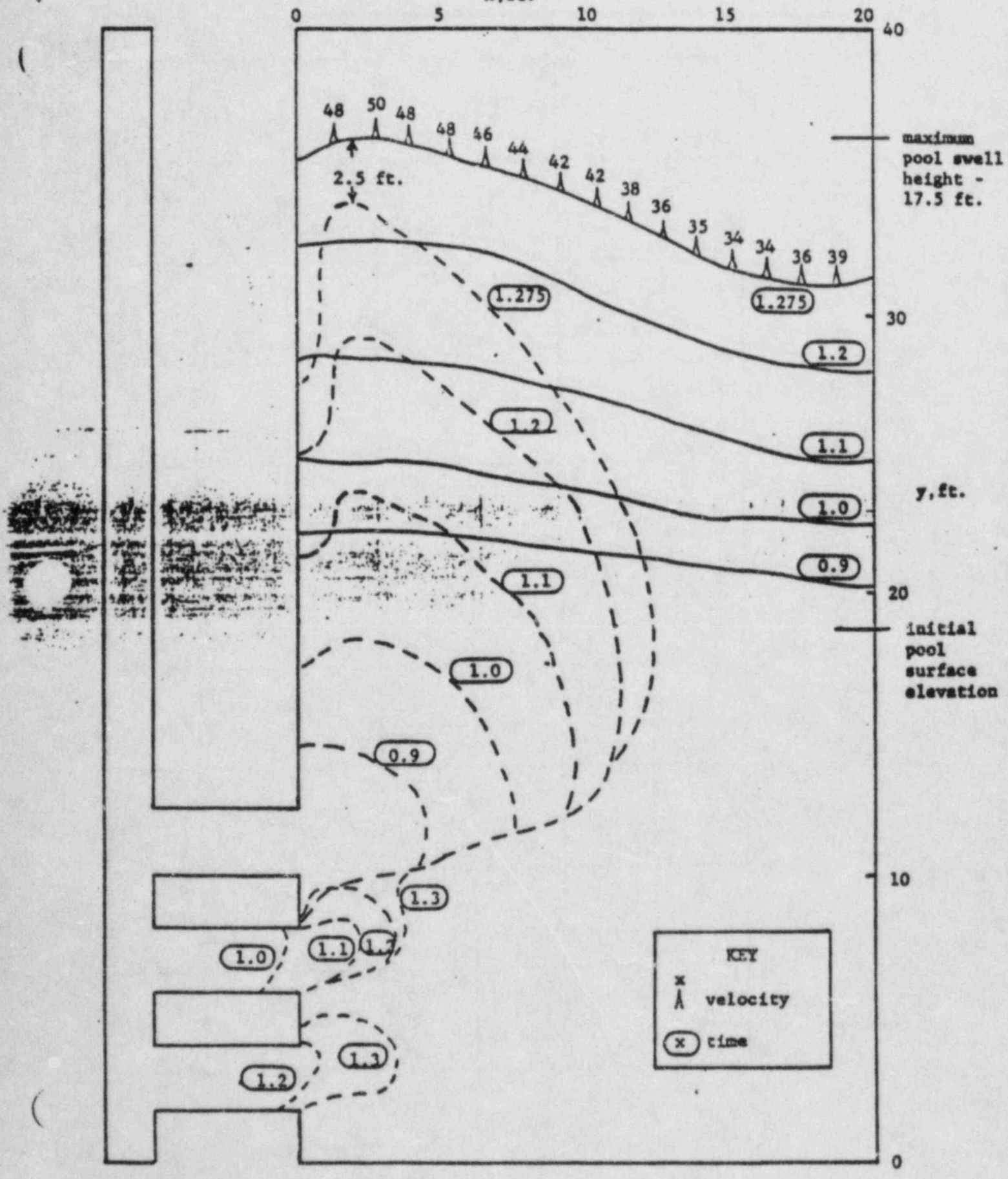

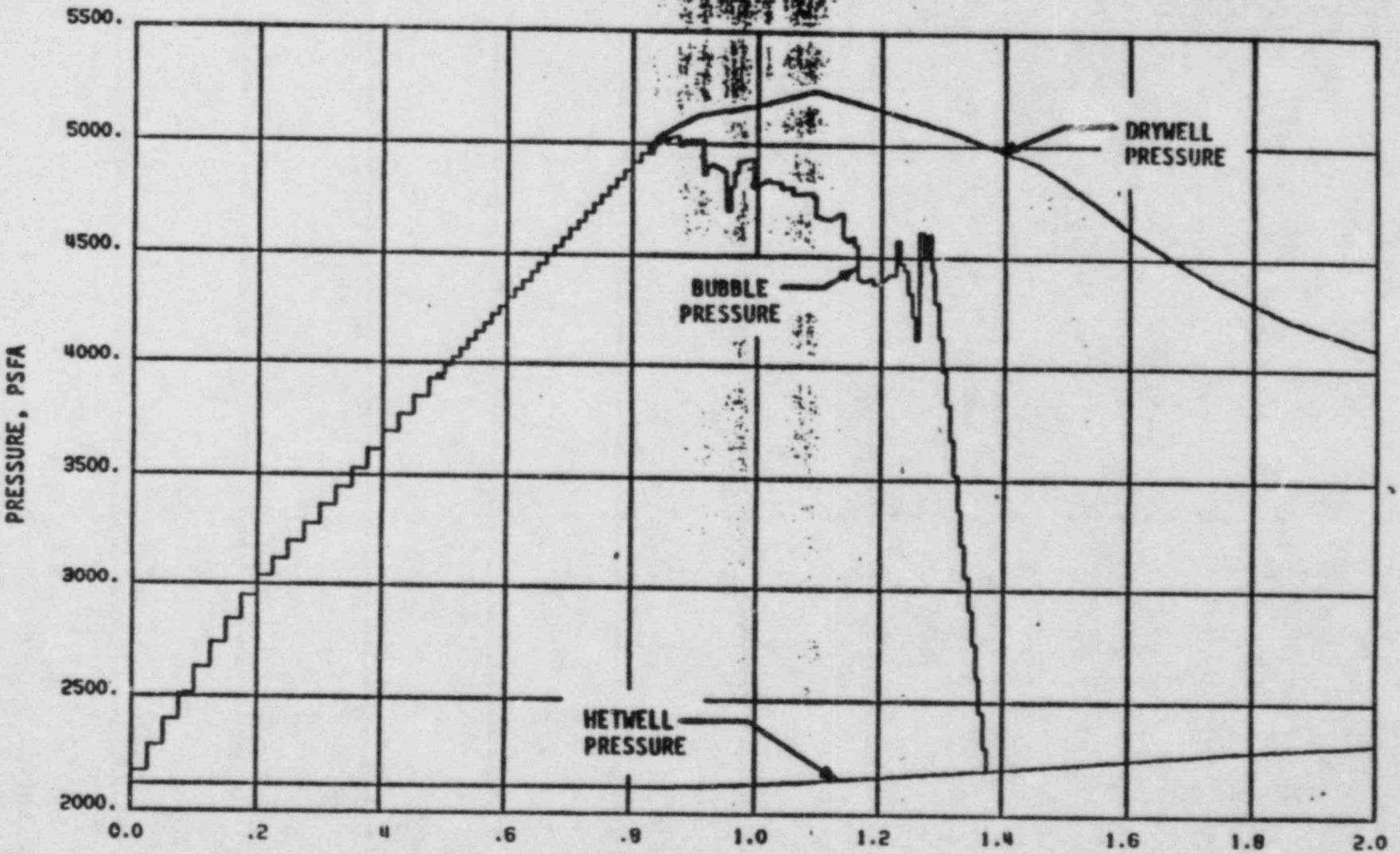

FIGURE 1-12 PRESSURE HISTORIES GRAND GULF 360° ENCROACHED CASE

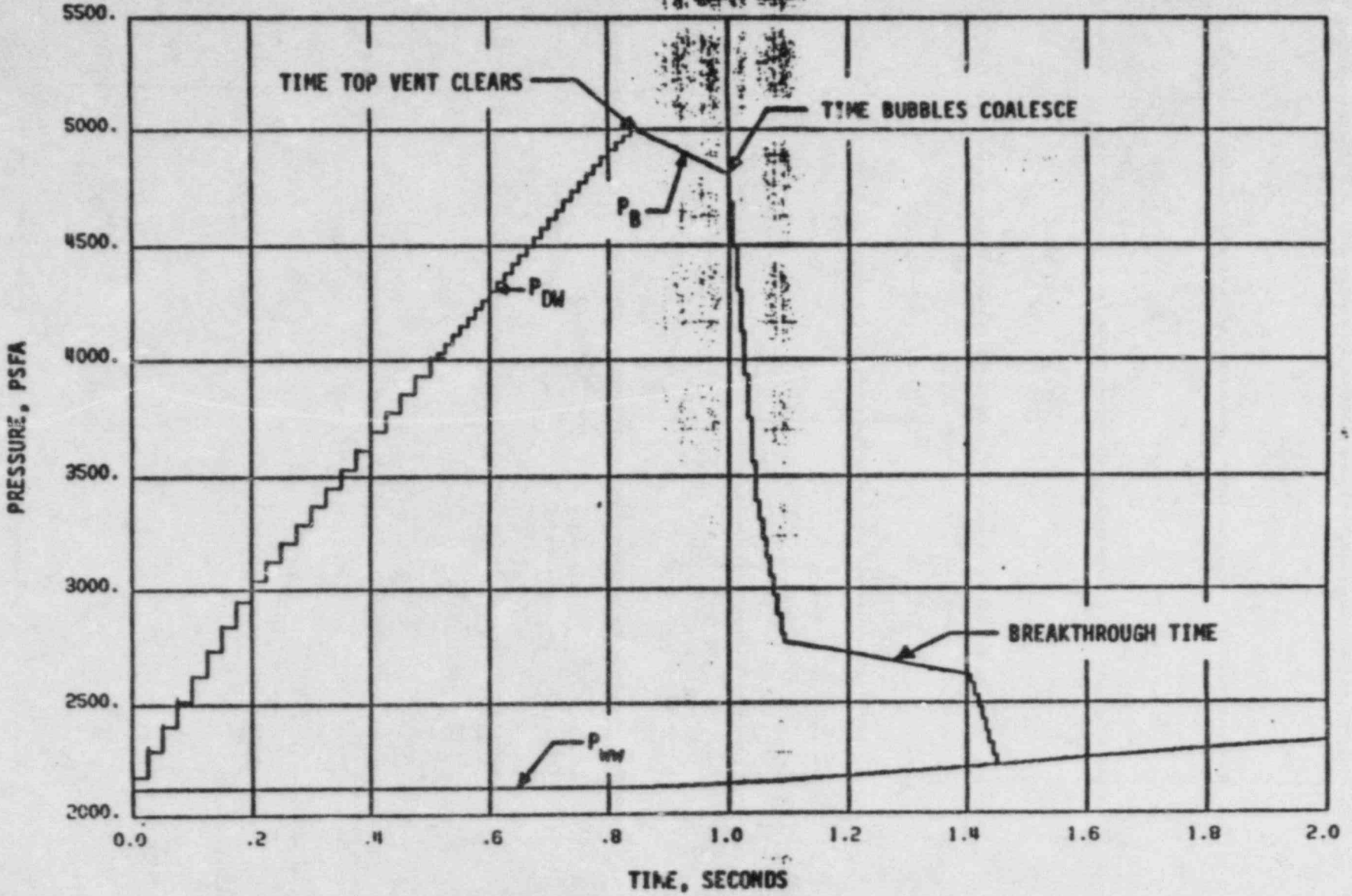

FIGURE 1-13 GRAND GULF ACTUAL ENCROACHED CASE (BUBBLES COALESCE AT 1 SEC.)

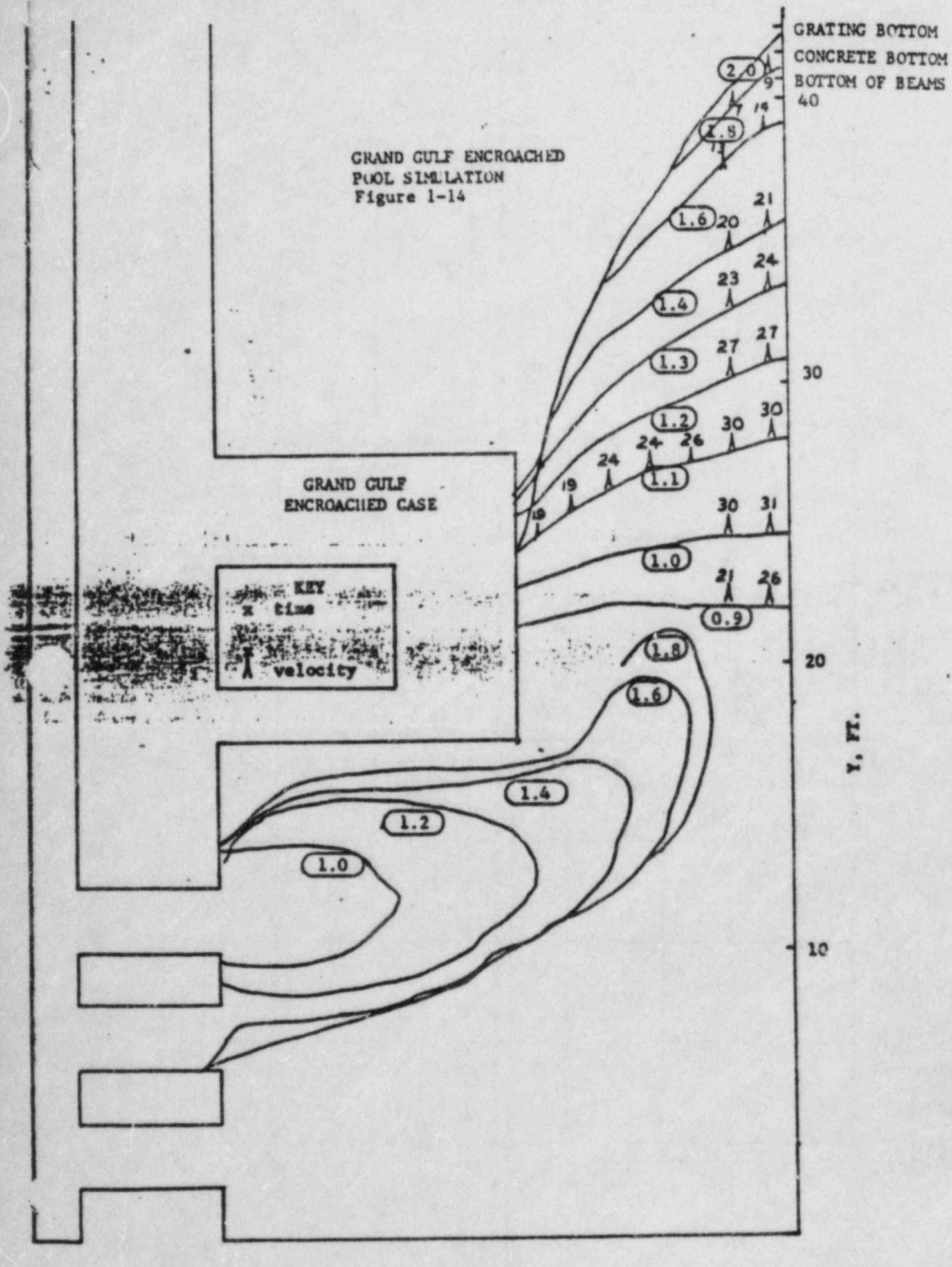
GRATING BOTTOM
CONCRETE BOTTOM
BOTTOM OF BEAMS
40
30
20
10
Y, FT.
GRAND GULF ENCROACHED
POOL SIMULATION
Figure 1-14
GRAND GULF
ENCROACHED CASE
KEY
x time
velocity
2.0
1.8
1.6
1.4
1.3
1.2
1.1
1.0
0.9
9
14
11
21
20
24
23
27
27
30
30
24
26
24
19
19
30
31
21
26

ATTACHMENT 1.3

AECM-82/574

Flow Science, Inc.'s Evaluation
Report on Modified SOLA-VOF CODE

The results of Item 5 are attached.

Flow Science Inc.
Post Office Box 933
1325 Thirty Drive
Los Alamos, New Mexico 87544
Telephone (505) 662-2636

EVALUATION REPORT

on

MODIFIED SOLA-VOF CODE

October 18, 1982

For: Grand Gulf Nuclear Station Humphrey Containment Concerns

Prepared by

Cyril W. Hirt

James M. Sicilian

Subject: Grand Gulf Nuclear Station
Humphrey Containment Concerns

Evaluation Report

on

Modified SOLA-VOF Code

Flow Science, Inc. has reviewed the findings presented in the G.E. Design Review Report: Effects of Local Encroachment on Pool Swell, dated 9/24/82. At the request of Mississippi Power & Light Company, we have prepared the following additional comments concerning our evaluation of the Design Review Report and of the applicability of SOLA-VOF to pool swell phenomena.

1. Basic Capability of SOLA-VOF

The SOLA-VOF code has been used for a wide variety of fluid dynamic applications. Its capability for solving incompressible flow problems with free surfaces has been demonstrated through numerous comparisons with analytic and experimental data. Documentation of these comparisons is given in the following references:

a. B.D. Nichols, C.W. Hirt, and R.S. Hotchkiss, "SOLA-VOF: A Solution Algorithm for Transient Fluid Flow with Multiple Free Boundaries," Los Alamos Scientific Laboratory report LA-8355 (1980) [see pp. 44-58 and pp. 108-117].

b. C.W. Hirt and B.D. Nichols, "A Computational Method for Free Surface Hydrodynamics," ASME Jour. Pressure Vessel Technology, 103, 136 (1981).

c. B.D. Nichols and C.W. Hirt, "Hydroelastic Phenomena in Boiling Water Reactor Suppression Pools," Proc. 5th International Conf. on Structural Mech. in Reactor Tech., Berlin, W. Germany (1980).

d. B.D. Nichols and C.W. Hirt, "Numerical Simulation of BWR Vent Clearing Hydrodynamics," Nuc. Sci. Eng., 73, 196 (1980).

e. C.W. Hirt, B.D. Nichols, and L.R. Stein, Electric Power Research Institute report NP-1856 (1981)
Vol. 1: "Numerical Simulation of BWR Suppression Pool Dynamics,"
Vol. 2: "Multidimensional Analysis for Pressure Suppression Systems,"
Vol. 3: Studies of Bracing Influence on BWR Pool Swell Dynamics."

References c - e contain the most relevant data comparisons for pool swell phenomena.

2. Assumptions in SOLA-VOF

SOLA-VOF provides a numerical solution algorithm to the Navier-Stokes equations (mass and momentum conservation equations). These equations assume incompressible water and only consider viscous stresses associated with a constant coefficient of viscosity (i.e., no turbulence is included). There should be no question of the suitability of the differential equations. The Numerical Solution algorithm is based on a well established finite-difference method that has been used and refined over a period of 17 years (J.E. Welch, F.H. Harlow, J.P. Shannon, and B.J. Daly, "The MAC Method," Los Alamos Scientific Laboratory report LA-3425, 1965).

The principal limitation in SOLA-VOF solutions is that they

cannot describe phenomena whose scales are less than the size of the underlying finite-difference grid. This, of course, is the basic limitation of any numerical solution method. For pool swell phenomena this limitation has an important consequence related to bubble breakthrough times. Breakthrough is known to be enhanced by small scale Taylor instabilities. For water, the dominant unstable wavelength is on the order of a centimeter, which is far smaller than the smallest mesh cell used to model the pool region. By not allowing this small scale penetration to occur, the SOLA-VOF calculations will have delayed bubble breakthrough times. Consequently, bubble pressures, which remain above the wet well pressure until breakthrough, will accelerate the pool surface to a higher velocity in the calculations than in a real case. This, therefore, is a conservatism. Some of this conservatism has been reduced in the G.E. calculations because they include a model for breakthrough which ramps the bubble pressures to the wet well pressure at a time determined from test data. It should also be noted that three-dimensional bubbles will break through sooner than two-dimensional bubbles (see below) so this too is a conservatism in the SOLA-VOF calculations.

3. Effect of 2D versus 3D Bubbles on Pool Swell

The two-dimensional, axisymmetric bubbles modeled in SOLA-VOF are slower to break through pool surfaces than spherical

bubbles with the same pressure history. The reason for this is evident from a simple 2D, cross-sectional picture of the two cases:

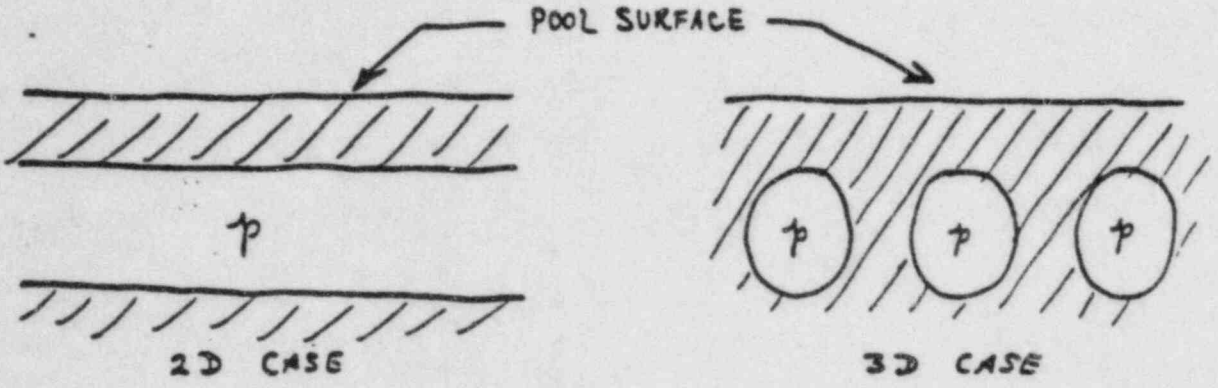

In the 2D Case the top water layer will accelerate upward uniformly (assuming no variations normal to the page) and no breakthrough will occur! In the 3D Case fluid will be accelerated most above the top of each bubble (where the fluid layer is thinest). Fluid will also be pushed left and right above each bubble center, allowing the bubbles to deform and push through the surface as shown schematically here:

Bubble penetration accelerates in time because the amount of water to be accelerated above the bubble is continually reduced.

The net upward fluid momentum will also be less in the 3D

Case than the 2D Case because the horizontal area on which the bubble pressure acts is less in the 3D Case.

From these examples it is clear that increasing the surface curvatures of bubbles will increase their ability to penetrate the pool surface. Therefore, we see that bubbles generated in Mark III suppression pools by multiple inlet vents will more readily penetrate the pool surface than an axisymmetric bubble at the same pressure and located the same distance below the surface.

By the same argument, the distortion of an axisymmetric bubble by a limited encroachment will induce local curvatures that can lead to earlier breakthrough.

The influence of bubble pressure on pool surface velocity can also be understood from the above picture. The vertical velocity acceleration above the center of a bubble is primarily the result of the local pressure gradient and gravity accelerations. The average pressure gradient is the difference in bubble pressure and wet well pressure divided by the thickness of the water layer. Thus, higher bubble pressures (or smaller water layers) produce larger pressure gradients, hence, larger upward accelerations.

4. Influence of Steam Condensation

By the last argument, any steam condensation that would reduce bubble pressures would also reduce the upward

accelerations, resulting in smaller pool swell velocity. Therefore, assuming equal mass flow rates through the vents, flow with some steam versus a pure air flow will result in lower bubble pressures and lower pool swell velocities.

5. Deflection of Pool Surface by Encroachment

In calculations with a 360° encroachment the pool surface is significantly tilted from the horizontal with its outer edge (i.e., at maximum radius) much higher. This feature is a direct consequence of the deflection of the flow by the bottom of the encroachment. Fluid trapped between the bubble and the encroachment is forced to move radially outward as the bubble grows. This radial momentum persists as the fluid rises and causes the pool surface to tilt as observed.

6. General Electric Modifications to SOLA-VOF

A basic assumption used in G.E.'s modification of SOLA-VOF is that bubble pressures are uniform within the bubble. This assumption is acceptable when the fluid interfaces are moving at speeds which are slow compared to the speed of sound in air. Because water/air interface speeds in these problems are at worst a few tens of feet per second, this condition is satisfied by a fair margin.

Not having to compute gas flows within bubbles is a great simplification, for then it is only necessary to follow the time dependence of global bubble properties such as total gas mass and

total volume. G.E.'s implementation of these global properties is based on standard gas dynamic relations connecting different gas states. Their formulation based on pressure drop, stagnation conditions, computed volume changes, and standard ideal gas relations is logically correct. We have not reviewed the actual programming of these relations into the SOLA-VOF code. Also, we have not reviewed the prescribed dry well pressure history nor the flow loss used at the vents.

The G.E. staff has performed extensive comparisons between their modified code, SOLAV01, and test data from 1/9, 1/3, and full-area-scale test facilities. These data comparisons provided an operational procedure for the scaling of code results with data. That is, the code had to be run in rectangular geometry to properly model vent clearing, and bubble volume corrections were based on pool area ratios. There is no way to rigorously justify these procedures, but the data comparisons are quite good and provide confidence in the method for the type of problems considered.

7. Summary

The weakest point in the G.E. study is still the point at which bubbles are assumed to coalesce so that bubble pressures can be ramped from the 360° encroached case to the case with no encroachment. This was the one Open Item reported in the Design Review Report. Bubble growth and coalescence is a strictly

three-dimensional phenomena, which cannot be directly modeled with SOLAV01. It is this feature that has required the introduction of volume correction factors and other model approximations. Under the two-dimensional limitations of the SOLA-VOF code, the G.E. analysis has been well done. Extensive data comparisons have been made with tests having no encroachments that provide an operational procedure for how to run and interpret SOLAV01 calculations. By combining the 360° encroached and unencroached cases into a composite model G.E. has constructed an approximation of pool swell behavior under actual plant conditions. Bubble pressures are computed using the 3D corrected bubble volumes (smaller volumes), but these pressures are applied in the 2D bubbles. Both effects should enhance pool swell velocities (i.e., higher bubble pressures and a more coherent water layer over the bubbles). Thus, these model approximations give conservative estimates for pool swell.

It's somewhat harder to judge whether the bubble pressure ramping procedure is conservative or not. Using the 360° encroached case pressure out to t = 1.0s is conservative because a higher pressure generated under a limited encroachment will tend to be relieved through azimuthal expansion. On the other hand, the selection of 1.0s as the time to start ramping down the pressure and the total ramp time of approximately 0.05s is an engineering judgement for these parameters. The assumption is that bubbles generated at different vents will coalesce at 1.0s

and thereafter have the same pressure. Near the encroachment, however, higher pressures may slow bubble growth and coalescence. Unfortunately, this flow region is strongly three-dimensional and a priori estimates are difficult to make.

To go beyond the present model would necessitate fully three-dimensional calculations. Such calculations would eliminate the need to introduce 3D bubble volume corrections and the need to select a time for ramping bubble pressures between the full and unencroached cases.

ATTACHMENT 1.4

This General Electric Company Proprietary document "Mark-III Encroachments Summary Report", November 1984 has been previously provided to the NRC via the Containment Issues Owners Group submittal dated December 19, 1984 (Reference LAE-OG-133).

Action Plan 2

I. Issues Addressed - Generic/Plant Specific

1.3 Additional submerged structure loads may be applied to submerged structures near local encroachments.

II. Program for Resolution

1. The results obtained from the two-dimensional analyses completed as part of the activities for Action Plan 1 will be used to define changes in fluid velocities in the suppression pool which are created by local encroachments. Supporting arguments to verify that the results from two-dimensional analyses will be bounding with respect to velocity changes in the suppression pool will be provided.

2. The new pool velocity profiles will be used to calculate revised submerged structure loads using the existing or modified submerged load definition models.

3. The newly defined submerged structure loads will be compared to the loads which were used as a design basis for equipment and structures in the River Bend Station suppression pool.

III. Status*

Items 1, 2, and 3 are complete and the results are included in this submittal.

IV. Final Program Results*

Item 1

Additional loadings may be applied to both submerged structures and the pool boundary due to the effect of local encroachments.

Due to similarities in pool encroachments between RBS and GGNS as indicated in Table 1 of Action Plan 1, Item 6a, the results of GGNS analyses are applicable to RBS.

Item 2

The results obtained from the two-dimensional SOLA analysis indicated a maximum pool swell velocity of 31 ft/sec. This is enveloped by the 40 ft/sec drag load velocity specified as the design basis for the Grand Gulf Nuclear Station in the CLR and the RBS FSAR.

The RBS design basis for piping and structures above the pool surface is 60/110 psi impact load, depending on the structure shapes, followed by drag load based on 40 to 50 ft/sec pool swell velocities. The newly defined pool swell velocities are enveloped by the design basis. For piping and structure below the pool surface, the load is bounded by the LOCA vent clearing drag load.

Item 3

The pressure loadings on piping and structures above the pool surface in the vicinity of the TIP platform as a result of encroachment effects are enveloped by the 60/110 psi design impact load for piping/flat structures respectively as identified in GESSAR II. For piping and structures below the pool surface, the pressure loadings produced as a result of the encroachment are bounded by the LOCA vent clearing loads specified as the design basis for the River Bend Nuclear Station in GESSAR II.

Based on this response, this issue is considered closed for RBS.

*This revision replaces the GSU submittal dated April 1, 1983.

Pool Boundary Loads

The present load definition specifies the pool swell boundary load on the drywell wall to be the peak drywell pressure. Even with encroachments, this limit will not be affected.

The pool boundary load definition on the containment wall is 10 psid, based on PSTF full scale test data. An evaluation was performed to address the concern that the encroachment may increase the bubble pressure and cause the bubble to be translated closer to the containment wall, which could result in increased loading.

Pressure on the containment wall is a direct output of the SOLAV01 code. In the full scale PSTF geometry, the containment wall is located 19 ft from the vent exit as opposed to 20.5 ft for RBS. Since the River Bend pool is wider, the 10 psid design load is extremely conservative. The base case for evaluating the potential increase in pool boundary loads on the containment wall was established as the GGNS geometry with a 19-ft pool width. The pressure loading curve on the containment wall was calculated and then normalized so that the peak pressure corresponded to the design pressure of 10 psid. The pressure loading curve was then recalculated for the GGNS encroached case, and again normalized to the design pressure. A comparison of the base case and the design base case is presented in Figure 2-1.

The encroachment causes the wall pressure to increase by approximately 15 percent. This is, of course, only a local loading increase in the vicinity of the encroachment. This increase poses no concern from a design standpoint because the loading is of sufficient duration (0.5 sec) to be considered a static load. The 15 percent increase over the 10 psid design value is easily bounded by the 15 psid containment design pressure. Thus, encroachments do not adversely affect the boundary design loads.

The use of a 2-D code in this analysis is conservative because the encroachment is assumed to cover 360°, maximizing the wall loading. In addition, pressure gradients will exist in the areas between the projections of the vents on the containment shell. This effect will not be seen in any two-dimensional analysis, nor is it accounted for in the containment shell bubble pressure load definition.

Figure 2-1 Effect of GGNS Encroachment on Containment Wall Boundary Load During Pool Swell

Note: A comparison of RBS and GGNS pool encroachments is given in Table 1 of Action Plan 1.

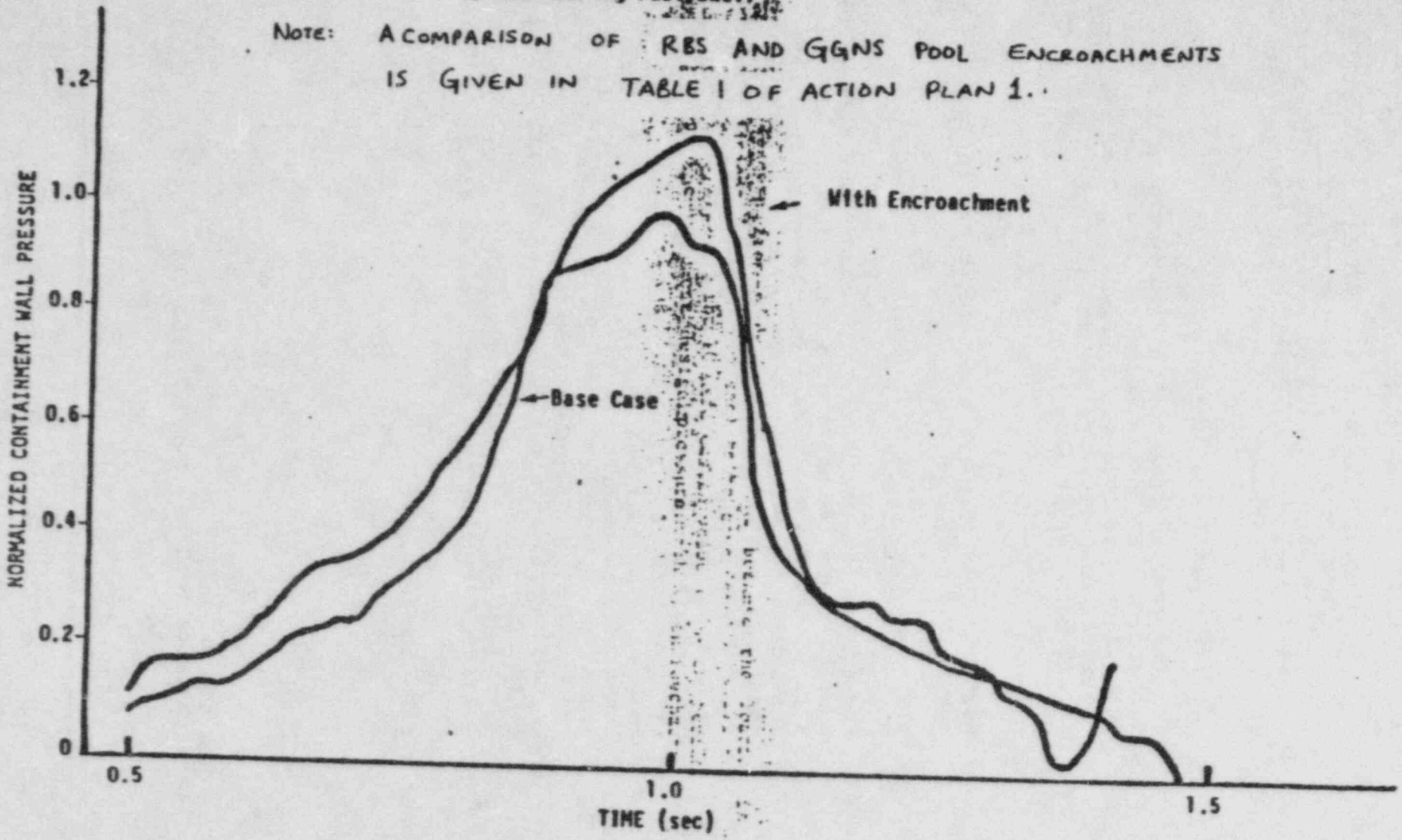

1.5 Impact loads on the HCU floor may be imparted and the HCU modules may fail, which could prevent successful scram if the bubble breakthrough height is raised appreciably by local encroachments.

II. Program for Resolution

If the results from Action Plan 1 show that the bubble breakthrough height is increased to the height of the HCU floor, additional analyses will be performed to determine the structural capabilities of the HCU floor to withstand water sloshing impacts.

III. Status

Resolution is complete and results are included in this submittal.

IV. Final Program Results*

The SOLAV01 analyses and 1/10 scaled Mark III encroachment test results obtained from Action Plan 1 demonstrate that the pool swell for the encroached case will not impact the HCU floor when the effects of steam condensation and a variety of other identified conservatisms are included in the analysis. In addition, the peak pool swell height is extremely dependent on distance from the drywell wall. The maximum elevation of 21.125 ft above the initial pool surface is only reached by an extremely small fraction of the pool. Therefore, no significant loading on the HCU floor will occur as a result of the presence of local encroachments. Therefore, GSU does not believe that an evaluation of any new loads on the HCU floor is warranted.

Based on this response, this issue is considered closed for RBS.

*This revision replaces the GSU submittal dated April 1, 1983.

Action Plan 4 - Generic/Plant Specific

I. Issues Addressed

1.6 Local encroachments or the steam tunnel may cause the pool swell froth to move horizonally and apply lateral loads to the gratings around the HCU floor.

II. Program for Resolution*

1. A bounding analysis for determining the horizontal liquid and air flows created by the presence of the steam tunnel and HCU floor will be performed. The forces imposed on the HCU floor supports and gratings will be calculated from this information.

1.a. An assessment will be made of the potential effects which variations in HCU floor support arrangement and grating location may produce. This assessment will result in the selection of a bounding arrangement for defining lateral loads.

2. Either it will be demonstrated that the affected structures can withstand the lateral loads, or required modifications will be proposed.

III. Status

Items 1, 1a, and 2 are complete and results are included in this submittal.

IV. Final Program Results*

Item 1

A bounding, steady, potential flow analysis was performed to determine the free jet flow field passing through the HCU floor. This analysis assumed all the rising fluid passed through the HCU floor open area (i.e., no separation of liquid droplets following impact on the solid portion of the HCU floor), and the velocities of the liquid and gas phases were equal.

This potential flow model was driven with the same conditions used for calculation of the GGNS plant unique HCU floor differential pressure model. The HCU floor differential pressure model is documented in Reference 1 and assumes that the pool swell froth mix-

ture impacts on the HCU floor, stagnates, and then is reaccelerated due to wetwell pressurization.

The analysis has demonstrated that horizontal loads on the HCU floor are small and vary with location. For beams, the horizontal source is a maximum of .85 psid. For grating, the horizontal force is a maximum of .24 psid. The details of the load definition are given in Attachment 4.1.

The analysis which yields these results is conservative, due to the assumptions of steady flow, equal phase velocities, and stagnation of liquid droplets upon impact with solid portions of the HCU floor. In reality, the flow is highly transient. Most of the rising two-phase mixture is expected to impact the solid floor, stagnate, and fall back to the pool surface. Hence, the flow which actually passes through the HCU floor will have total momentum substantially less that the value determined with this analysis. The calculated loads are thus expected to be bounding.

Item 2

RBS analyses show that the stresses due the horizontal loads are a small fraction of the total stresses. When the 0.24 psid load is applied to the grating, the stresses induced in the grating can be considered negligible.

Based on the above results, this issue is considered closed for RBS with this submittal.

Reference

1. Bilanin, W. J., Mark III Containment Analytical Model, NEDO-20533, Supplement 1, June 1974.

*This revision replaces the GSU submittal dated April 1, 1983.

ATTACHMENT 4.1

1. The River Bend-unique HCU floor horizontal beam load is defined as:

$$\Delta P_{\text{beam, max}} = 0.85 \text{ lbf/sq. in.}$$

This load was applied to the first major radial beam (depth greater than or equal to 24 inches) under each grating section. This load was also applied to minor beams located closer to the concrete sections of floor than the first major beam.

The load on major beams was reduced as follows:

a) The load was reduced, linearly, from $\Delta P_{\text{beam max}}$ to zero between the first major beam and the zero shear plane. The zero shear planes are located at:

$$\phi = 66°$$
$$\phi = 181°$$
$$\phi = 293°$$

(All angles per azimuthal coordinate system on SWEC Drawing No. 12210-ES-53D-7.)

b) For beams not directed radially outward from the reactor centerline, the pressure was reduced by:

$$\Delta P_{\text{beam}} = \Delta P_{\text{beam, Max}} \cos\alpha$$

where α is the angle between that of the subject beam and a radially outward line through the reactor centerline.

In all cases, the direction of loading is from concrete areas toward the zero shear plane.

Since the flow was assumed to stagnate between beams which extend below the HCU floor, there was no horizontal loading under concrete areas.

2. The River Bend-unique HCU floor grating load was defined as:

$$\Delta P_{\text{grating}} = 0.24 \text{ lbf/sq in.}$$

This load was to be applied uniformly to all vertical surfaces of all grating components.

Action Plan 5 - Generic/Plant Specific

I. Issues Addressed

2.1 The annular regions between the safety relief valve lines and the drywell wall penetration sleeves may produce condensation oscillation (CO) frequencies near the drywell and containment wall structural resonance frequencies.

2.2 The potential CO and chugging loads produced through the annular area between the SRVDL and sleeve may apply unaccounted-for loads to the SRVDL. Since the SRVDL is unsupported from the quencher to the inside of the drywell wall, this may result in failure of the line.

2.3 The potential CO and chugging loads produced through the annular area between the SRVDL and sleeve may apply unaccounted-for loads to the penetration sleeve. The loads may also be produced at or near the natural frequency of the sleeve.

II. Program for Resolution

1. The existing condensation data will be reviewed to verify that no significant frequency shifts have occurred. The data will also be reviewed to confirm that the amplitudes were not closely related to acoustic effects.

2. The driving conditions for CO at the SRVDL exit will be calculated. Based on these calculations, existing test data will be used to estimate the frequency and bounding pressure amplitude of CO at the SRVDL annulus exit.

3. A wide difference between the CO frequency and structural resonances will be demonstrated. The margin between the new loads and existing loads will be quantified.

4. A detailed description of all hydrodynamic and thermal loads that are imposed on the SRVDL and SRVDL sleeve during LOCA blowdowns will be provided.

5. Ensure that thermal loads created by steam flow through the annulus have been accounted for in the design.

6. State the external pressure loads that the portion of the SRVDL enclosed by the sleeve can withstand.

7. Calculate the maximum lateral loads which could be applied to the sleeve by phenomena analogous to the Mark I and Mark II downcomer lateral loads.

III. Status*

Items 1 through 7 are complete under a previous submittal; however, some additional information has now been added to Items 5, 6, and 7 in this submittal.

IV. Final Program Results*

Item 1

CO frequency shifts which occurred in the 1/9 area scale PSTF data are discussed in some detail in References 1 and 2. The unique size of the 1/9 scale PSTF vent caused these frequency shifts to occur. Late in the transient, the CO frequency content excited the quarter standing wave (20-24 Hz) in the PSTF pool. This caused the root mean square pressure amplitude to increase by a factor of approximately 2. The amplitude of oscillation is consequently related to acoustic effects only for the 1/9 area scale PSTF tests. Similar acoustic effects were not observed in 1/3 area scale or full scale tests.

The size of the SRVDL sleeve annulus is such that the CO frequency is much higher than the frequency which occurred in the 1/9 scale PSTF vent. The first fundamental frequency of sleeve CO is relatively close to the three-quarter standing wave in the pool. However, when standing waves have been detected in Mark III pool tests, it is only the one-quarter standing waves which have appeared. The conservative analysis performed under Item 2 of this action plan demonstrates that the factor of 2 margin exists within the design basis, which should easily encompass any acoustic effects.

The frequency in the sleeve is expected to decrease with time. Chugging should occur in the main vents effectively eliminating CO in the SRVDL-sleeve annulus before the CO frequency can approach a frequency capable of exciting the pool quarter standing wave.

Item 2

A calculation of the steam mass flux at the SRVDL sleeve discharge during a postulated LOCA shows the CO can be expected to occur in the sleeve. The GESSAR II CO load definition pressure time-history was modified to include higher frequency components attributable to CO in the SRVDL sleeve. A comparison of amplified response spectra (ARS) of the CO pressure time-histories, which included the contribution of the sleeve with chugging and pool swell load definitions, shows that the CO loads produced in the sleeve are easily bounded by other Mark III load definitions.

SRVDL Sleeve Steam Mass Flux

The condensation mode (CO or chugging) is determined, to a large extent, by the steam mass flux. Thus, prediction of the condensation mode for discharges from the SRVDL sleeve annulus requires an estimate of the steam mass flux through the annulus. This estimate has been made by considering the SRVDL sleeves and the top row of main vents as parallel flow paths, each with a different resistance to flow. Since the sleeve annuli have a much smaller total area than the top vents, it is logical to expect that the total flow through the annuli will be small compared to the total vent flow. For parallel flow paths, the ratio of the mass fluxes can be determined from:

$$\frac{G_{sleeve}}{G_{vent}} = \sqrt{\frac{K_{vent}}{K_{sleeve}}}$$

where G is mass flux and K is a pressure loss coefficient,

$$K = P/(\rho v^2/2\, g)$$

Using the dimension of the Grand Gulf SRVDL or River Bend SRVDL sleeves

$\frac{G_{sleeve}}{G_{vent}}$ is approximately equal to 0.8

Since this ratio is relatively close to unity, CO will occur in the sleeve during nearly the same time period of a LOCA as it occurs in the vent. To illustrate this, Figure 5-1 shows the vent and sleeve steam mass flux time-history calculated with M3CPT04 (Reference 3) for a Grand Gulf DBA. Assuming that transition from CO to chugging occurs near 10 lb/sq ft/sec, Figure 5-1 shows that generally the vent and sleeve will experience CO simultaneously.

Defining the Load on the Pool Boundary

The CO occurring in the SRVDL sleeve annuli is expected to add a high-frequency component to the basic vent CO load definition. To evaluate the effect of SRVDL sleeve CO, a modified CO pressure time-history was developed by summing the individual components of the main vent and SRVDL sleeve CO pressure histories. It was assumed that the SRVDL sleeves behave as small horizontal vents, allowing application of the Mark III CO methodology.

No data on condensation in slanted annular geometry currently exists. Therefore, a very conservative load definition has been provided to bound these geometric uncertainties. Reference 4 suggests that the wall pressure amplitude varies as the ratio of vent area to pool surface area. To account for uncertainties in the condensation processes which might occur in the annular SRVDL sleeve opening, the assumption was made that the amplitude varies as the square root of the vent area to pool area ratio. This assumption increases the SRVDL sleeve CO amplitude by a factor of 4 over the result contained in Reference 4. This large factor of conservatism is used to assure that a bounding response is obtained.

For additional conservatism, the maximum local CO amplitude will be considered to act azimuthally on the entire pool boundary. Globally, the SRVDL sleeve CO effect will be smaller since there are only 20 SRVDL sleeves compared to the 45 sets of vents present. Thus, an additional factor of approximately 2 exists over the expected global response. It should be noted that RBS has only 16 SRVDL sleeves and 43 vents per row. Therefore, GG's results envelop RBS.

A CO pressure time-history was calculated as:

$$\Delta P(t) = \Delta P_{vent}(t) + \Delta P_{sleeve}(t)$$

Where $P_{vent}(t)$ is the pool pressure time-history as currently defined in the GESSAR II and using the best correlation of Mark III CO frequency and amplitude test data (Reference 5). The term $\Delta P_{sleeve}(t)$ represents the expected pool pressure time-history resulting from CO only in the sleeve. This term was calculated using the same techniques and data correlations as P_{vent} but amplitude and frequency were modified by the scaling assumptions previously described. The sleeve CO pressure time-history was determined to be:

$$\Delta P_{sleeve}(t) = \frac{AMP(t)}{2}$$

$$\{0.8 \sin (2\pi\tau(t) f_s(t)) + 0.3 \sin (4\pi\tau(t) f_s(t)) + 0.15 \sin (6\pi\tau(t) f_s(t)) + 0.2 \sin (8\pi\tau(t) f_s(t)) \}, \text{ psid}$$

where:

$\Delta P_{Sleeve}(t)$ = pressure amplitude contribution of the SRVDL sleeve on the drywell wall

AMP (t) = peak-to-peak amplitude variation with time, psid

$$= \sqrt{A_{sleeve}/A_{VENT}} \times 5.5 \times PPA_{(G,a,T)}$$

$f_s(t)$ $\frac{D_{h\,VENT}}{D_{h\,sleeve}} \times f(G_s, a, T)$

= relative time within each cycle, seconds

= time from initiation of LOCA blowdown, seconds

PPA = CO amplitude correlation on containment wall, psid

f = CO vent frequency correlation

G = sleeve steam mass flux, lb/sq ft/sec

a = vent air content, percent

T = bulk pool temperature, °F

D = hydraulic diameter

A = area

A portion of the resulting pressure time-history on the drywell wall for Grand Gulf is shown in Figure 5-2

(vent CC only) and Figure 5.3 (simultaneous vent and sleeve CO).

Significance of the SRVDL Sleeve CO Load

The pressure time-histories of Figures 5-2 and 5-3 were digitized and ARS plots were prepared. Peak broadening of 15 percent was used, as in the GESSAR II CO load, to account for uncertainty in the predicted frequencies. The ARS resulting from the time-histories given in Figures 5-2 and 5-3 are shown in Figures 5-4 and 5-5. As evident from these plots, the SRVDL sleeve CO has no impact below 30 Hz. Superimposed on Figure 5-5 is the ARS of the chugging load on the drywell wall (Reference 6). In the frequency range of the sleeve CO pressure, signal, the chugging load is bounding by a substantial margin, even though an unrealistically large pressure due to the sleeve CO was utilized and credit was not taken for attenuation of the SRVDL sleeve CO as distance away from the sleeve increases.

Figure 5-4 does not correspond directly to the design basis accident (DBA) ARS presented by Grand Gulf in support of the LOCA Licensing defense. Due to limitations in the existing code, a smaller number of cycles was used in Figure 5-4 to obtain the DBA CO peak response at the low-frequency range than were used in developing the DBA CO ARS. At the high-frequency range, however, the number of cycles used is adequate to reach the peak response and Figures 5-5 and 5-6 adequately represent the maximum amplitudes produced by the high frequency components of the CO load.

To determine the effect of the SRVDL sleeve CO on the containment wall loading, the drywell composite CO loading was attenuated to the containment wall. The resulting ARS is shown in Figure 5-6. As is evident from this curve, the ARS of the pool swell containment wall load definition bounds the combined effect of the main vent CO and the SRVDL sleeve CO Note that the global pool swell load is compared to the local SRVDL CO load, so the additional factor of conservatism previously discussed (on the order of 2) is present.

In summary, a bounding and extremely conservative analysis shows that the CO produced by the SRVDL sleeve adds high frequency components to the basic main vent CO load definition. This additional contribution is bounded by other loads. Also, since the response is increased in only the high frequency range, the structural impact of this loading is very small.

Item 3

Based on analysis for the loading provided in Figure 5-3, the resulting increases in structural forces and moments are not significant and are enveloped by other LOCA cases.

Item 4

A detailed description of the hydrodynamic and thermal loads on the SRVDL piping and the SRVDL sleeve during LOCA blowdown is given below.

SRVDL Piping

1. Inertia loads caused by building excitation. The loading cases include CO, chugging, and pool swell.

2. Drag loads on SRVDL piping, quencher, and quencher supports. The load cases include LOCA vent clearing, LOCA bubble and pool fallback, CO and chugging.

3. Lateral load due to chugging.

4. LOCA caused by the drywell negative pressure transient. The loading conditions include weir impact and weir drag.

5. The thermal loads on the piping are based on drywell and the suppression pool temperature during accident conditions.

SRVDL Sleeve

1. Inertia loads caused by building excitation. The load cases considered are pool swell, CO, and chugging.

2. Drag loads, including LOCA bubble, pool fallback, CO, and chugging.

3. Thermal loads. The thermal loads imposed on the sleeve from steam flow through the annulus have been accounted for in the design.

Items 5 and 6

External drag loads due to the sleeve CO have been generated for the DBA condition. Evaluation of this new sleeve CO drag loads and the thermal loads created by steamflow has been performed. Results showed that

both the SRVDL and the penetration sleeve have sufficient margin to accommodate the new loads. The maximum external pressure loads which the safety relief valve discharge lines (SRVDL) can withstand in the region enclosed by the drywell penetration sleeve are 300 psi (Upset) and 450 psi (Faulted). These pressures are orders of magnitude higher than maximum calculated drywell pressure.

Item 7

Lateral loads on the SRVDL sleeve have been calculated by scaling the Mark II downcomer lateral load data to the outside diameter of the SRVDL sleeve. No credit is taken for the presence of SRVDL in the bubble, providing a very conservative loading. The maximum lateral load is found to be 22 kips, distributed over 1 to 4 feet from the sleeve exit. The piping and SRVDL sleeves are qualified to this load.

References

1. A.M. Varzaly, et al, Mark III Confirmatory Test Program - Test Series 6003, NEDE-24720P, January 1980

2. GESSAR II, Question/Response 3B.11, 22A7000, Rev. 2, 1981

3. W.J. Bilanin, The General Electric Mark III Pressure Suppression Containment System Analytical Model, General Electric Report No. NEDO-20533, June 1974, and Supplement 1, September 1975

4. General Electric Company, Comparison of Single and Multivent Chugging at Two Scales, NEDE-24781-1-P, January 1980

5. A.M. Varzaly, et al, Mark III Confirmatory Test Program -1/3 scale Condensation and Stratification Phenomena - Test Series 5807, General Electric Report No. NEDE-21596-P, March 1977

6. GESSAR II, Figure 3B.18.2, page 3BO.3.2.18, 22A7000, June 1981

7. Dynamic Lateral Loads on a Main Vent Downcomer - Mark II Containment, NEDE-24106-P, General Electric Company, March 1978

8. S.T. Nomanbhoy, Loads on the Vent Struts Due to Condensation of Steam in a Water Pool, NEDE-23627-P, General Electric Company, June 1977

*This revision replaces the GSU submittal dated April 1, 1983.

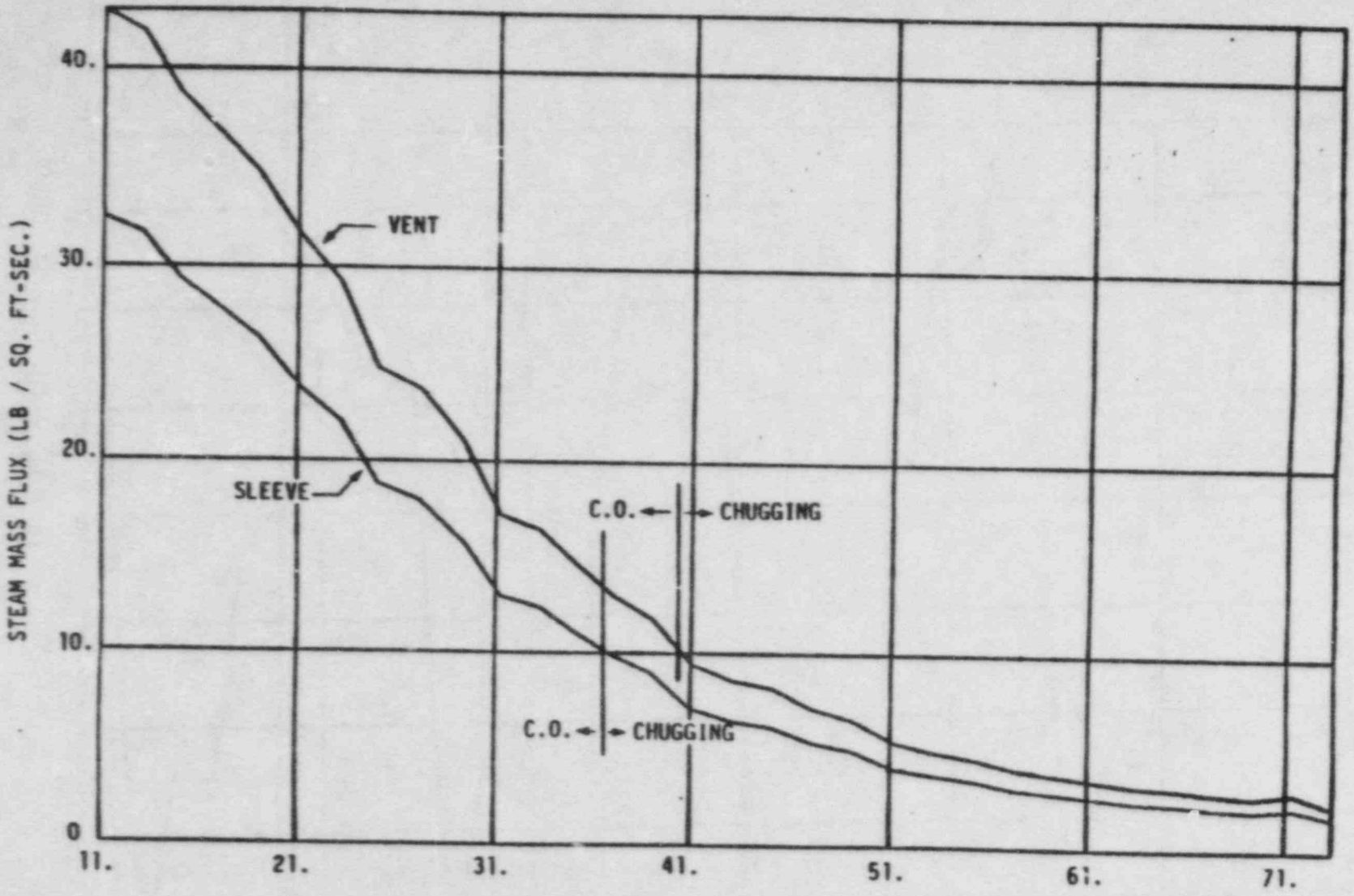

CALCULATED VENT AND SLEEVE STEAM MASS FLUX FOR GRAND GULF 100% BREAK SIZE

FIGURE 5-1

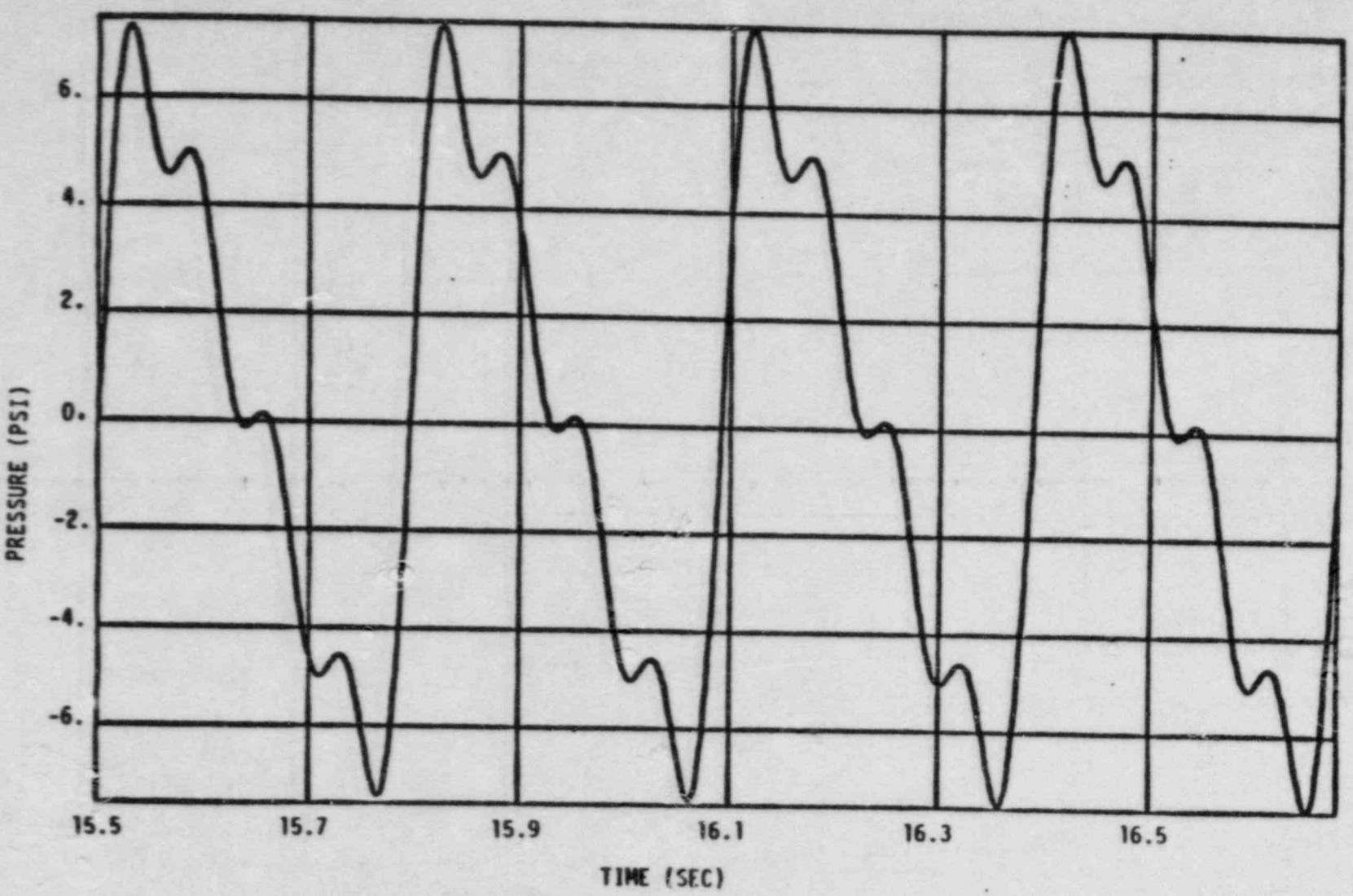

PRESSURE TIME HISTORY WITH C.O. IN THE VENT ONLY

FIGURE 5-2

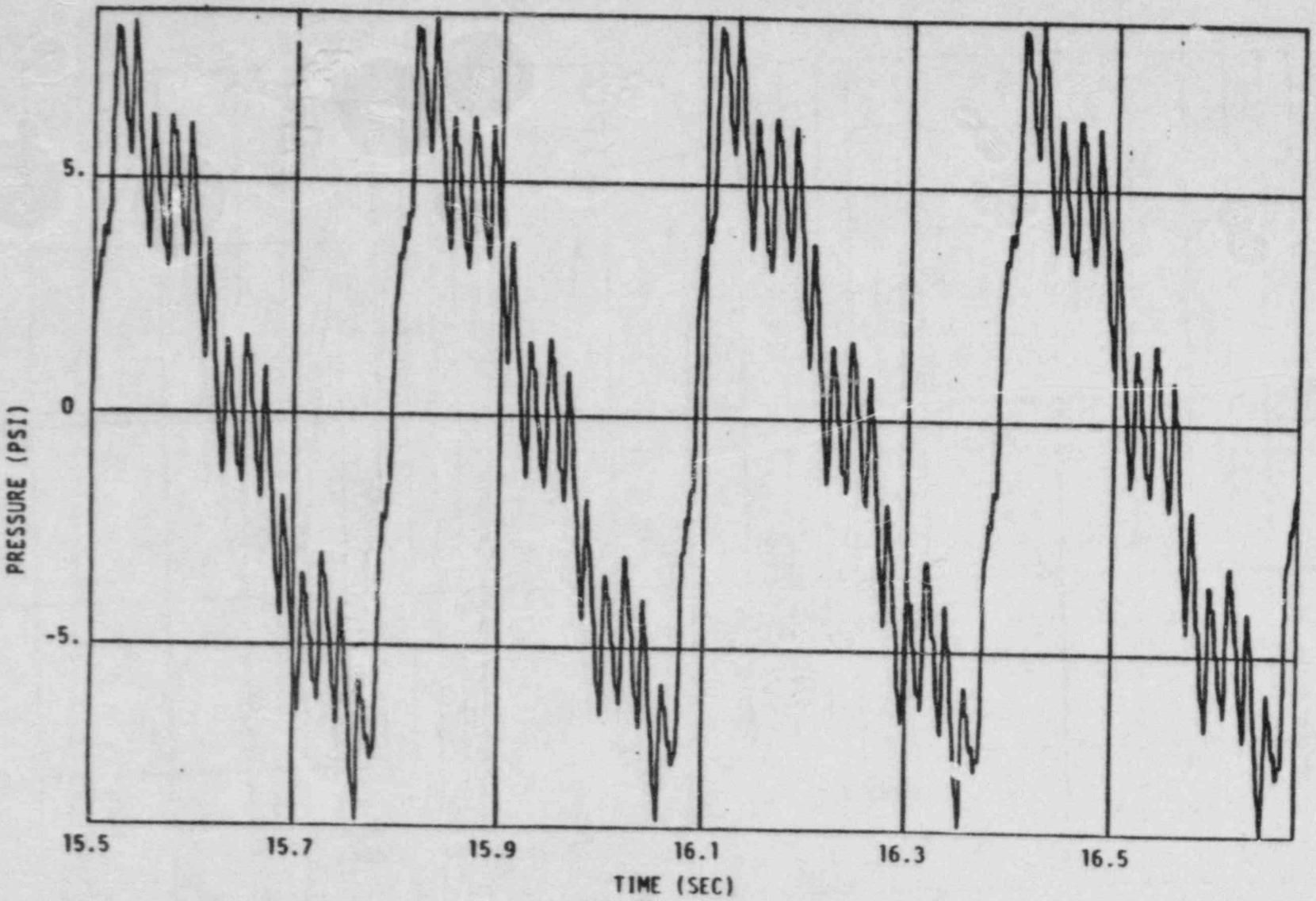

PRESSURE TIME HISTORY ON DRYWELL WALL WITH C.O. IN THE VENT AND THE SRVDL SLEEVE

FIGURE 5-3

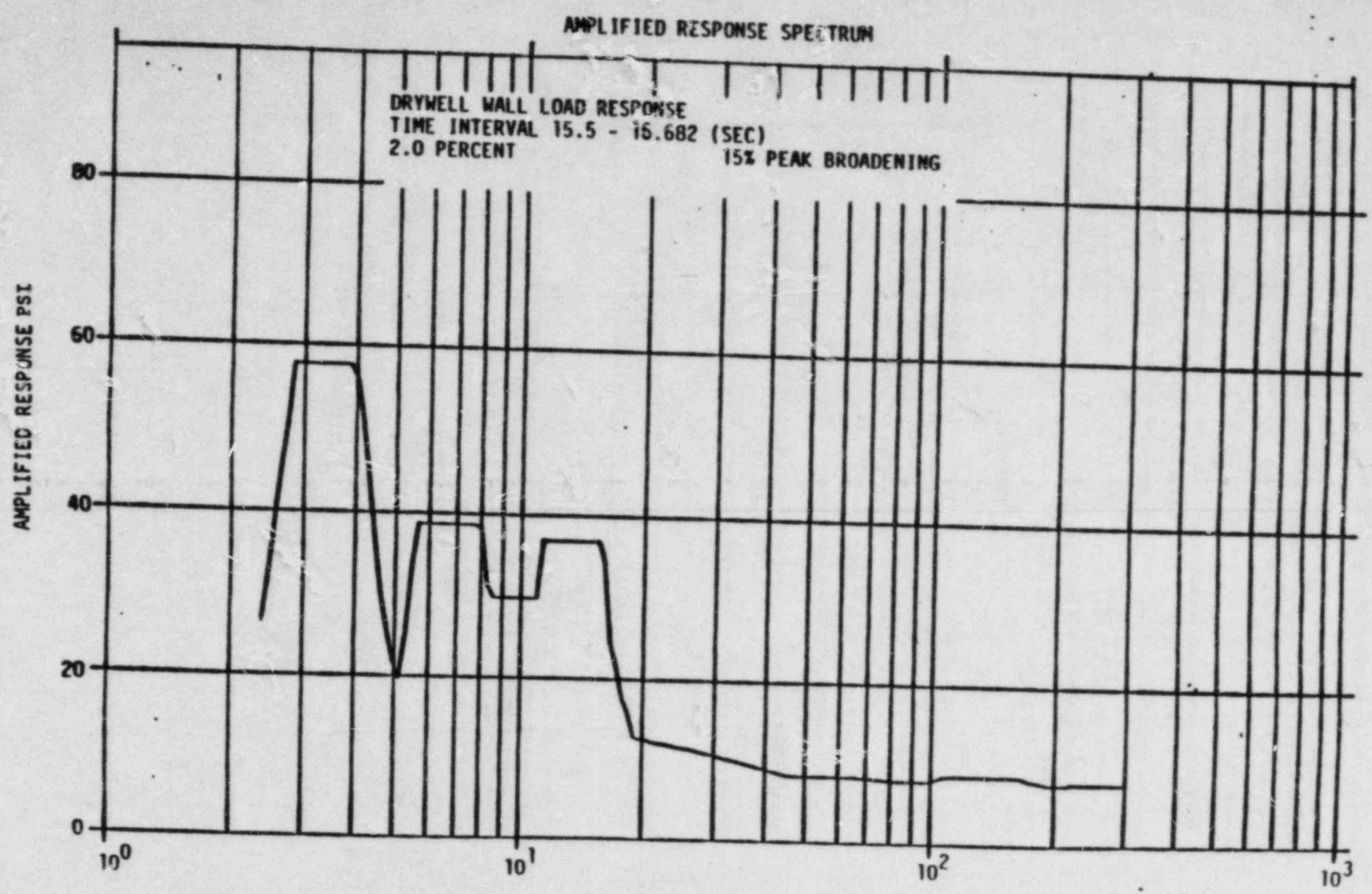

ARS OF PRESSURE TIME HISTORY WITH C.O. IN THE VENT ONLY

FIGURE 5-4

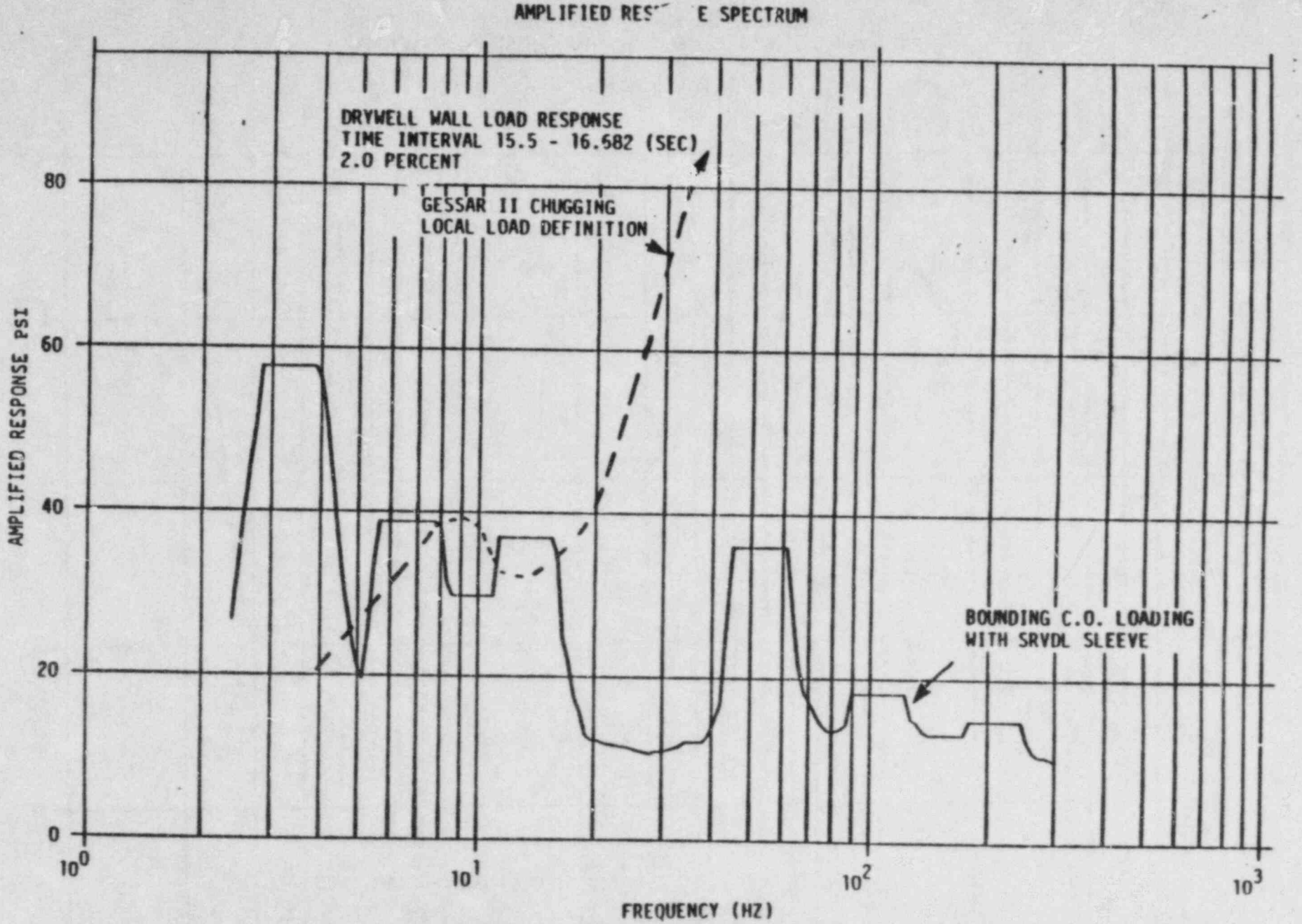

COMPARISON OF GESSAR II LOCAL CHUGGING LOAD DEFINITION AND EXPECTED C.O. LOADING WITH SRVDL SLEEVE ON DRYWELL WALL

FIGURE 5-5

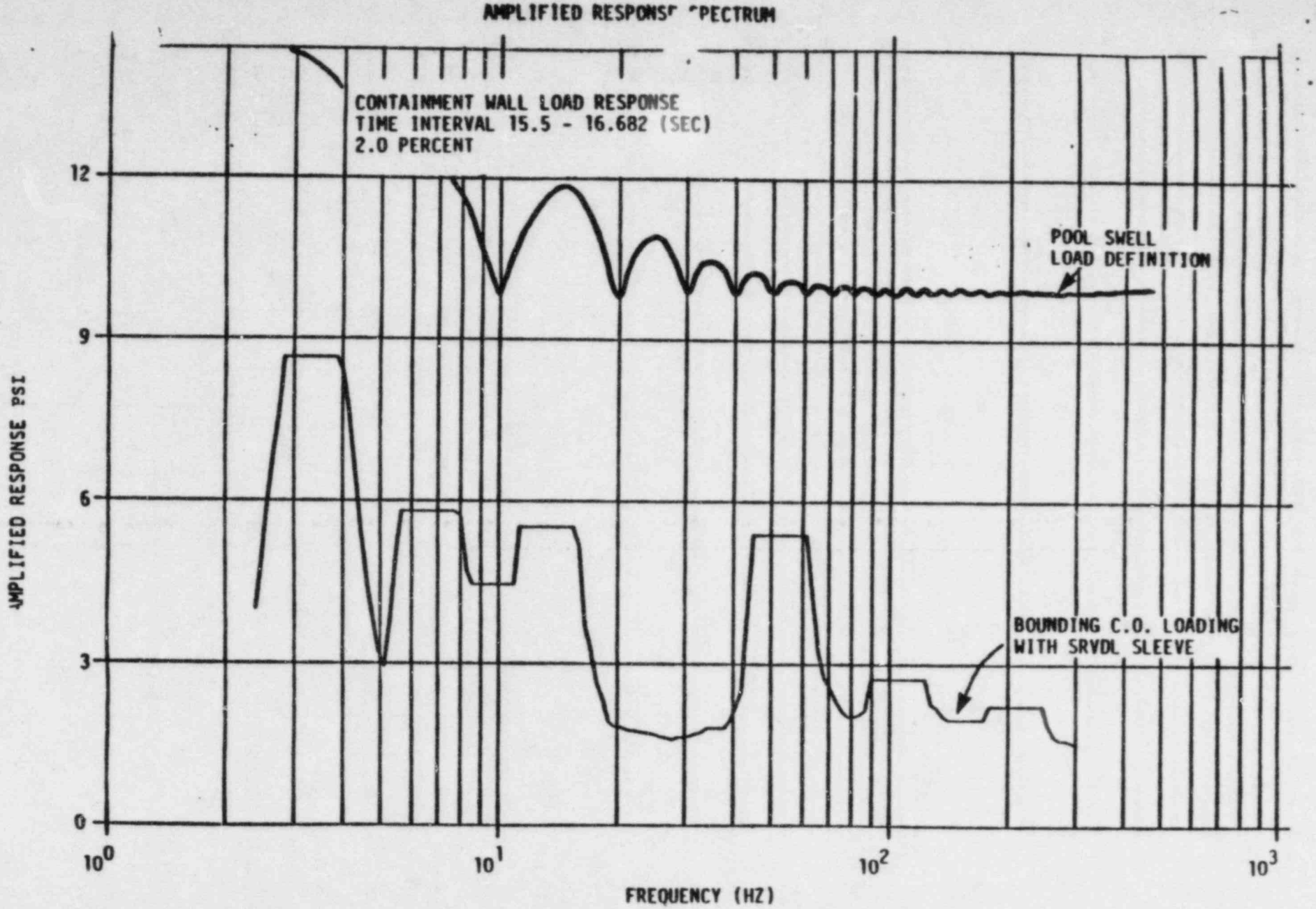

COMPARISON OF POOL SWELL LOAD DEFINITION AND EXPECTED C.O.
LOADING WITH SRVDL SLEEVE ON CONTAINMENT WALL

FIGURE 5-6

Action Plan 6 - Plant Specific

I. Issues Addressed

3.1 The design of the STRIDE plant did not consider vent clearing, CO, and chugging loads which might be produced by the actuation of the residual heat removal (RHR) heat exchanger relief valves.

3.3 Discharge from the RHR relief valves may produce bubble discharge or other submerged structure loads on equipment in the suppression pool.

3.7 The concerns related to the RHR heat exchanger relief valve discharge lines should also be addressed for all other relief lines that exhaust into the pool.

II. Program for Resolution*

1. The vent clearing and chugging loads produced by the actuation of the RHR heat exchanger relief valves will be calculated and compared with the main steam SRV bubble loads.

The following information will be submitted for all relief valves that discharge to the suppression pool.

2. The piping drawings and piping and instrumentation diagrams (P&IDs) showing line and vacuum breaker locations will be provided. This information will include the following:

   - The geometry (diameter, routing, height above the suppression pool, etc) of the pipeline from immediately downstream of the relief valve up to the line exit.
   - The maximum and minimum expected submergence of the discharge line exit below the pool surface.
   - Any lines equipped with load-mitigating devices (e.g., spargers or quenchers).

3. The range of flow rates and character of fluid (i.e., air, water, steam) that is discharged through the line and the plant conditions (e.g., pool temperatures) when discharges occur will be defined.

4. The sizing and performance characteristics (including make, model, size, opening characteristics, and flow characteristics) of any vacuum breakers provided for relief valve discharge lines will be noted.

5. The potential for oscillatory operation of the relief valves in any given discharge line will be discussed.

6. The potential for the failure of any relief valve to reseat following initial or subsequent opening will be evaluated.

7. The location of all components and piping in the vicinity of the discharge line exit and the design bases will be provided.

8. The CO load resulting from the RHR heat exchanger relief valve actuation will be calculated and compared with the SRV bubble and LOCA hydrodynamic loads.

III. Status*

Items 1 through 8 are considered complete with this submittal.

IV. Final Results*

Analysis was performed for the RHR heat exchanger relief valve actuation line. It was found that the vent clearing load produced by the actuation of the RHR heat exchanger relief valves has been calculated without considering the steam venting effect of the noncondensible vent. The peak boundary pressure was found to be 8.93 psid on the wall and 2.4 psid on the basemat; the peak negative pressure on the wall is -3.53 psia. These values are considerably lower than the RBS SRV design load of 16.56 psid and -7.41 psid. Furthermore, the RHR bubble load frequency is about 7.5 Hz, which is enveloped by the SRV bubble load design frequency of 5 to 12 Hz. Thus the vent clearing load due to RHR heat exchanger relief valve discharge is not a concern for the RBS containment.

The majority of the information described in Items 2 through 7 is included in the attached tables and the attached FSAR Figures 5.4-12, 6.3-1, and 6.3-4; piping Drawing Nos. 12210-EP-71A, 71F, 83A, and 13A; and valve Drawing No. 12210-0228.213-058-001G. The minimum and maximum suppression pool levels are 89 feet-6 inches

and 90 feet-0 inches, respectively. None of the relief valve discharge lines have a load-mitigating device.

When the RHR pressure control valves E12*PVF051A and B begin to cycle in an undefined manner, the RHR heat exchanger relief valves experience cyclic behaviour. However, the vent valves which pressurize this relief valve discharge line in the steam-condensing mode depress the water leg out of the piping. Additionally, since the most rapid travel time for the RHR pressure control valve is 10.5 seconds as a result of the valve design, any postulated oscillation would be quite slow.

There is also a possibility that the RHR heat exchanger relief valve may fail open during RHR system operation or that the relief valve may fail to reseat following normal actuation. The water hammer analyses performed for Action Plan 8, Program for Resolution, Item 2 will bound all conditions associated with the postulated failure of any relief valves discharging to the suppression pool.

Drawing No. EP-71A shows components in the vicinity of the RHR heat exchanger relief valve discharges. The loads produced by discharge from these relief valves will bound all postulated loads which could be produced by other relief valves discharging to the suppression pool, including the LPCS relief valves which discharge through these lines. The GE design criteria for the HPCS and LPCS strainers, given in the HPCS and LPCS design specifications, require them to be located at least 8 feet from the discharge of the main steam safety relief valve ram's head. In RBS design, only one component (high-pressure core spray strainer 1CSH*STR1) is less than 8 ft (3 ft 7 in) away from the discharge point. While River Bend does not use a ram's head on the main steam safety relief valves, this criteria is applicable to the RHR relief valves since the ram's head configuration, an open-ended pipe, is similar to the RHR relief valve discharge lines. Since the flow from the RHR heat exchanger relief valves is much less than the main steam safety relief valves, the present design is acceptable. Drawing No. EP-83A shows that the flow from valves of components in the vicinity of the HPCS relief valves is low, and submerged structure loads are negligible. A tee has been installed at the end of each RHR relief valve discharge line. These tees are aligned and oriented such that no structures will be impacted by the vent cleaning jets. The induced drag loads are also bounded by LOCA and SRV loads.

RBS has participated in a generic Mark III containment evaluation program for the RHR-induced condensation oscillation (RHRCO). The RBS RHRCO load was calculated and is found to be bounded by SRV loads. Comparison was made between the RHRCO and the SRV load definition. It is found that the maximum positive pressure due to a single SRV actuation exceeds that due to RHRCO, except in a small region on the containment in the neighborhood of the RHR discharge point and that the actuation of all SRVs produces a peak positive pressure that exceeds the maximum positive pressure generated by RHRCO. Thus, it is concluded that RHRCO load is bounded by the design basis SRV load specification.

*This revision replaces the GSU submittal dated April 1, 1983.

TABLE 6-1

ECCS Relief Valve Discharges into Suppression Pool - Design Conditions

Valve I.D. No.	System	Size (In.)	Relief Flow (lb/hr)	Set Press. (psig)	Discharge Line Number	Function (Component protected)	Relief Mode	R/V Inlet Temp. (°F)	Discharged Fluid	Minimum Submergence (ft)
E12-F055A	RHR	4x6	1.3×10^5	500	1RHS-012-148-2	RHR HX A	Steam Condensing	480	Steam	5 1/2
E12-F055B	RHR	4x6	1.3×10^5	500	1RHS-012-145-2	RHR HX B	Steam Condensing	480	Steam	5 1/2
1RHS*RV3A	RHR	4x6	1.3×10^5	485	1RHS-012-148-2	RHR HX A	Steam Condensing	480	Steam	5 1/2
1RHS*RV3B	RHR	4x6	1.3×10^5	485	1RHS-012-145-2	RHR HX B	Steam Condensing	480	Steam	5 1/2
E12-F025A	RHR	1 1/2x2	4.97×10^4	500	1RHS-012-148-2	RHR Pump A Disch.	Surveillance Test	358	Steam	5 1/2
E12-F025B	RHR	1 1/2x2	4.97×10^4	500	1RHS-012-145-2	RHR Pump B Disch.	Surveillance Test	358	Steam	5 1/2
E12-F025C	RHR	1 1/2x2	4.97×10^4	500	1RHS-012-145-2	RHR Pump C Disch.	Surveillance Test	358	Steam	5 1/2
E12-F005	RHR	3/4x1	6.75×10^3	200	1RHS-012-148-2	RHR Shutdown Suc.	Shutdown Cooling	358	Steam	5 1/2
E12-F036	RHR	6x8	7.38×10^5	75	1RHS-012-148-2	RHR Shutdown Disch.	Steam Condensing	140	Water	5 1/2
E12-F017A	RHR	3/4x1	6.75×10^4	200	1RHS-012-148-2	RHR Pump A Suc.	System Standby	358	Steam	5 1/2
E12-F017B	RHR	3/4x1	6.75×10^4	200	1RHS-012-145-2	RHR Pump B Suc.	System Standby	358	Steam	5 1/2
E12-F101	RHR	3/4x1	7.5×10^4	150	1RHS-012-145-2	RHR Pump C Suc.	System Standby	212	Steam	5 1/2

TABLE 6-1 (CONT)

Valve I.D. No.	System	Size (In.)	Relief Flow (lb/hr)	Set Press. (psig)	Discharge Line Number	Function (Component protected)	Relief Mode	R/V Inlet Temp. (°F)	Discharged Fluid	Minimum Submergence (ft)
E12-F030	RHR	3/4x1	6.75×10^4	200	1RHS-012-145-2	RHR Flushing HDR	Thermal R/V	212	Steam	5 1/2
E21-F018	LPCS	1 1/2x2	5.01×10^4	570	1RHS-012-148-2	LPCS Pump Disch.	Accident Conditioning	185	Water	5 1/2
E21-F031	LPCS	1 1/2x2	5.01×10^3	100	1RHS-012-148-2	LPCS Pump Suc.	System Isolation	185	Water	5 1/2
E22-F014	HPCS	3/4x1	9.02×10^3	100	1CHS-010-18-2	HPCS Pump Suc.	System Standby	185	Water	12 1/2
E22-F035	HPCS	3/4x1	Thermal R/V	1560	1CHS-010-18-2	HPCS Pump Disch.	Accident Conditions	185	Water	12 1/2
E22-F039	HPCS	3/4x1	Thermal R/V	1560	1CHS-010-18-2	Test Line R/V	Thermal R/V	185	Water	12 1/2
(1)RCIC Turbine	RCIC	-	302×10^4	-	(2)1ICS-012-52-2	Turbine Exhaust	-	250	Steam	4 1/2

(1) Not an ECCS relief valve
(2) This line is equipped with a sparger (1440 1/2 in. diameter holes)

TABLE 6-2

Vacuum Breaker Data

Velan 3/4-In. Spring-Loaded Piston Check Valve
(Drawing No. 0228.213-058-001G)

Disc area - 0.3068 sq in.
Flow area - 0.3068 sq in.
Full open flow coefficient - Cv = 3.2
Maximum disc travel - Approximately 1/4 in.

Valve Mark Nos. E12*VF103A, B, E12*VF104A, B
Function - RHR Relief Valve Discharge Line Vacuum Breakers

TABLE 6-3

Components and Piping in the Vicinity of the Discharge Line Exit

	Centerline Coordinates			Minimum Distance
	X	Y	Z	
1RHS-012-148-2				
Discharge point	40'-7 7/8"	82'-2"	40'-7 7/8"	-
1CSL*STR1(J-)	44'-11 9/16"	76'-6 1/2"	36'-4 15/16"	9'-7 1/4"
1RHS*PSR3013	40'-3 3/4"	7[illegible]'-4 3/4"	35'-10 1/3"	9'-9 3/8"
1RHS-020-56-2	38'-10 9/16"	73'-4 3/4"	38'-10 9/16"	10'-1 1/16"
1T23*G024S	30'-10 5/8"	75'-7 2/3"	32'-0 7/16"	11'-7 1/8"
1RHS-012-145-2				
Discharge point	40'-7 7/8"	82'-2"	-40'-7 7/8"	-
1RHS-020-1-2	40'-7 7/8"	73'-4 3/4"	-40'-7 7/8"	9'-9 1/4"
1T23*G024L	35'-2 11/16"	75'-7 2/3"	-27'-2 3/8"	12'-8"
1CSH*STR1(J-)	39'-5 1/2"	78'-7"	-42'-3 3/4"	7'-8 3/4"
1CSH-010-18-2				
Discharge point	49'-1"	77'-0"	-30'-3 1/4"	-
1ICS-012-52-2	47'-3 1/3"	71'-3 1/2" on up to 82'-5 1/2"	-29'-6 1/2"	1'-11 1/3"
1RHS-020-1-2	47'-8"	73'-4 3/[illegible]"	-29'-4 3/4"	3'-2 3/4"

TABLE 6-3

	Centerline Coordinates			
	X	Y	Z	Minimum Distance
1RHS*PSR3036	48'- 11 2/3"	73'- 4 3/4"	-26'- 5 1/2"	3'- 5 1/2"
1ICS*PSR3001	47'- 3 1/3"	75'- 3 3/4"	-29'- 6 1/2"	2'- 7 1/3"

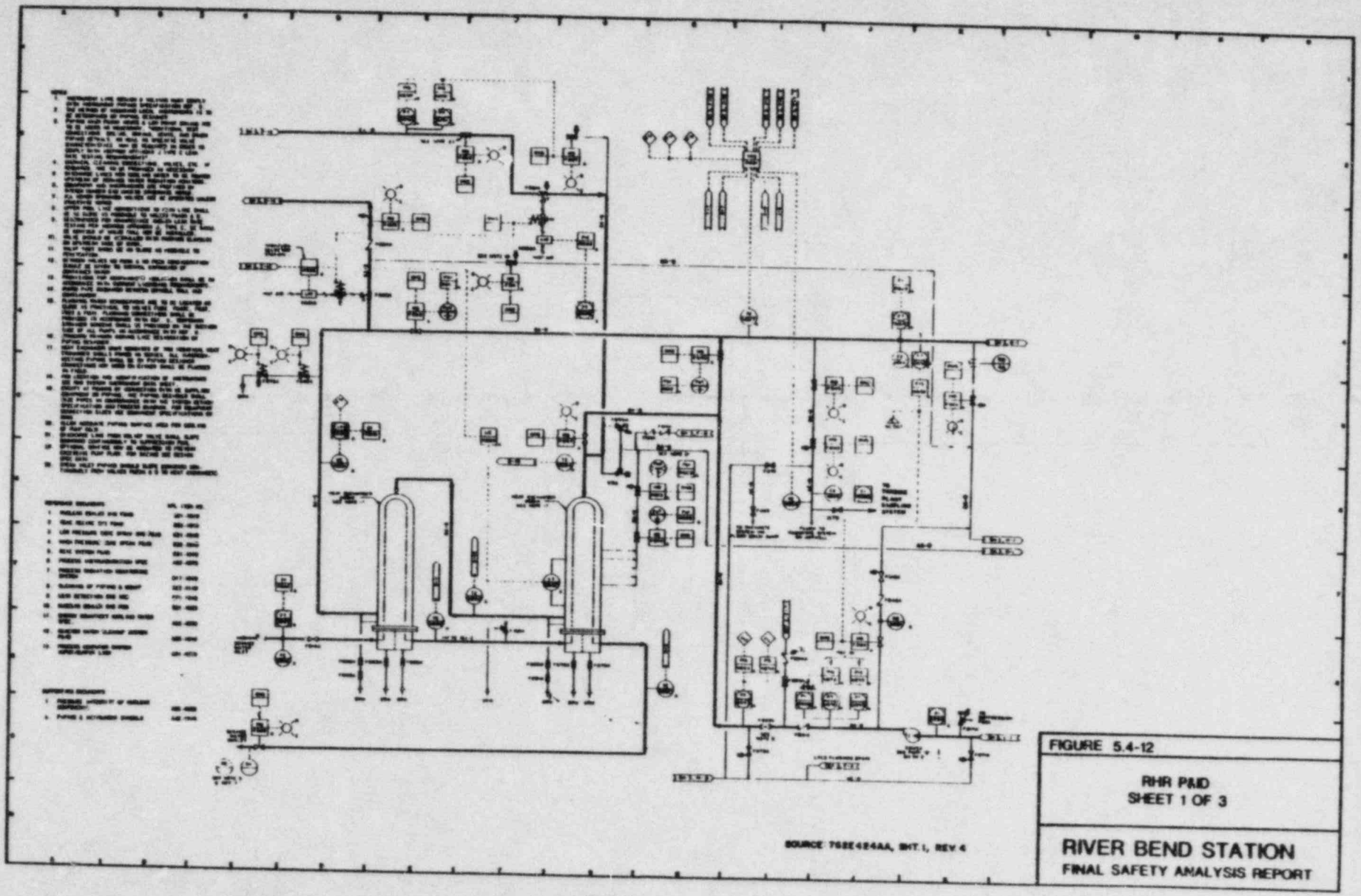

SOURCE 7E2E424AA, SHT. 1, REV. 4

FIGURE 5.4-12

RHR P&ID
SHEET 1 OF 3

RIVER BEND STATION
FINAL SAFETY ANALYSIS REPORT

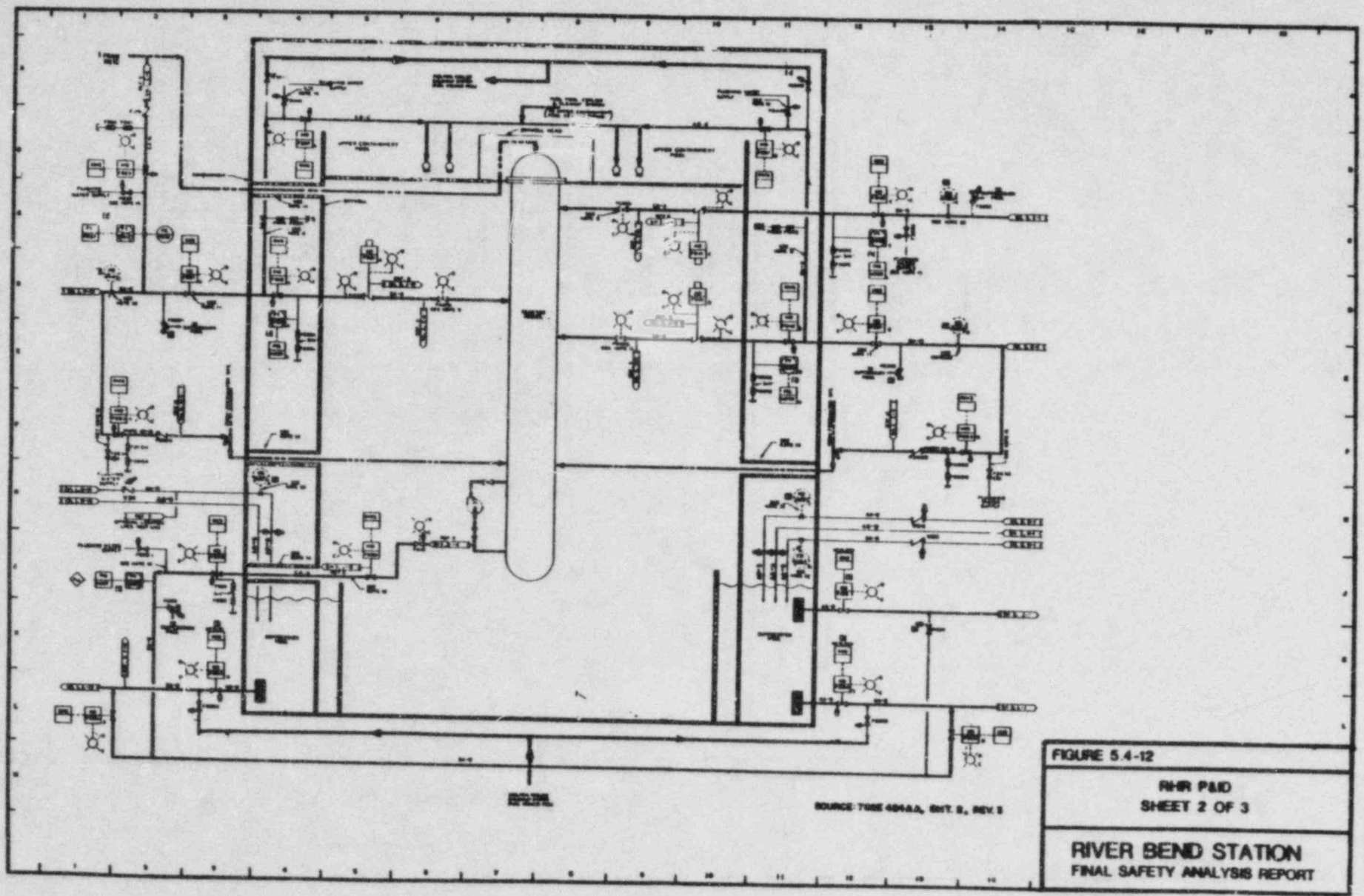

FIGURE 5.4-12

RHR P&ID
SHEET 2 OF 3

RIVER BEND STATION
FINAL SAFETY ANALYSIS REPORT

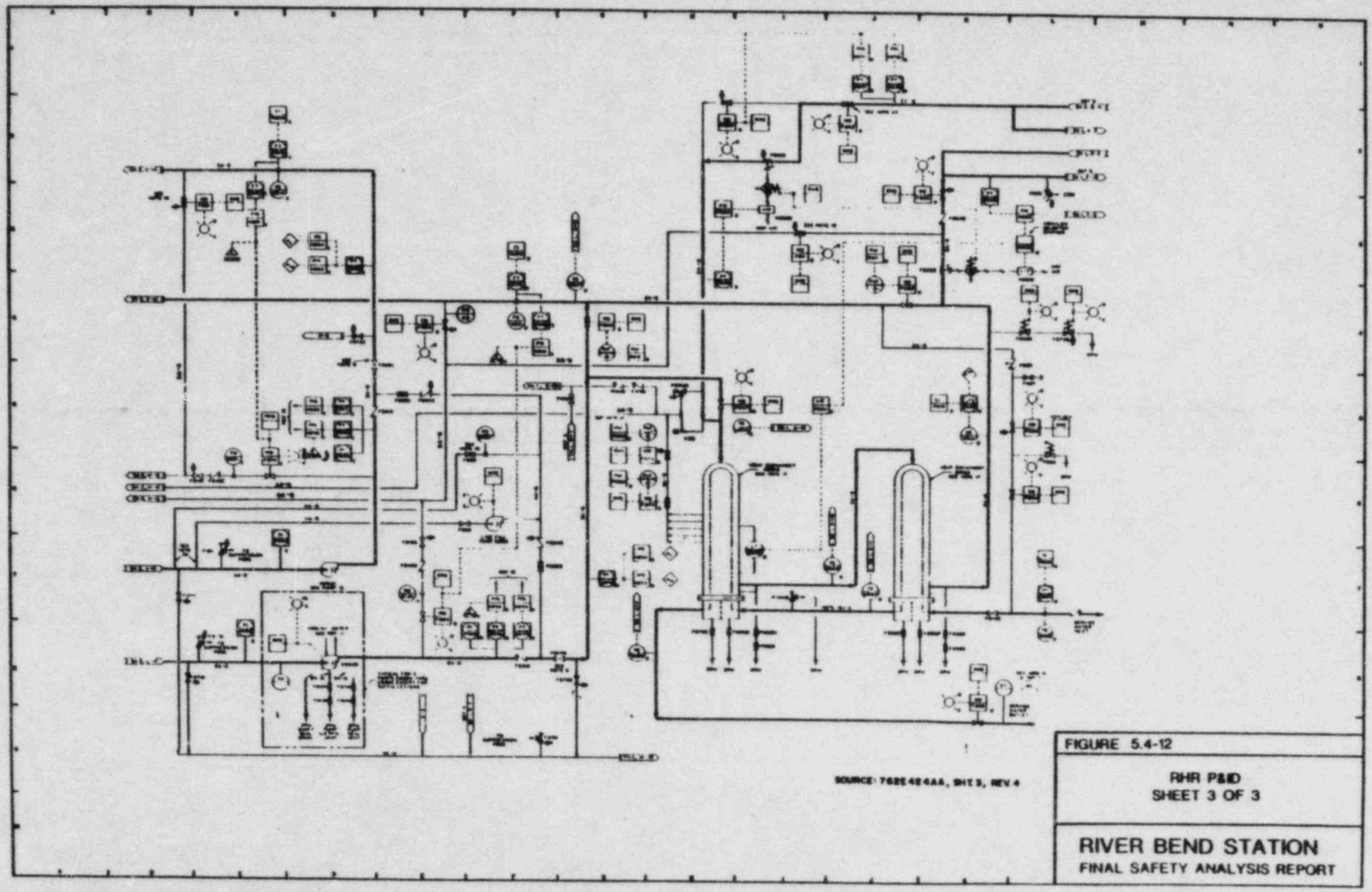

SOURCE: 7GEE424AA, SHT 3, REV 4

FIGURE 5.4-12

RHR P&ID
SHEET 3 OF 3

RIVER BEND STATION
FINAL SAFETY ANALYSIS REPORT

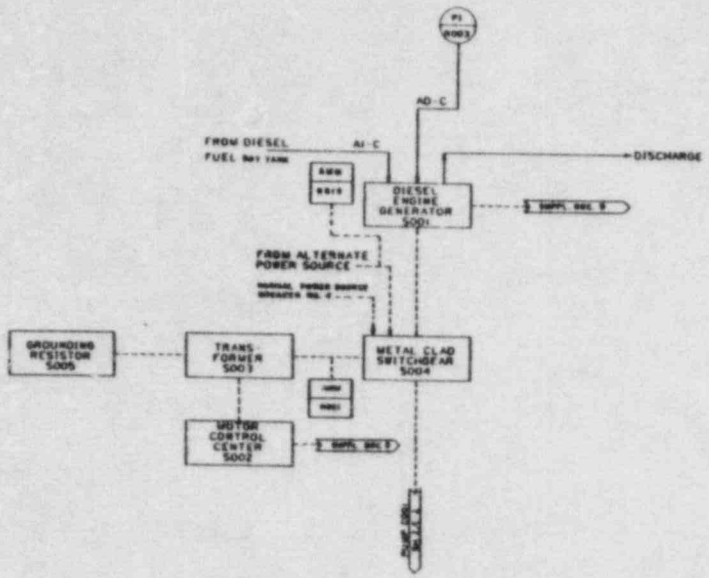

NOTES:

1. EQUIPMENT AND INSTRUMENTS ARE PREFIXED BY SYSTEM NUMBER (E22 UNLESS OTHERWISE SPECIFIED)
2. PIPING HIGH POINT VENTS AND LOW POINT DRAINS ARE TO BE ADDED AS NECESSARY. ADDITIONAL TEST CONNECTIONS, ORIFICES, DRAINS, VENTS, AND STUB-S PIPING DETAIL S, AS WELL AS SPECIFIC VALVE CHARACTERISTICS, MAY BE REQUIRED TO COMPLY WITH SECTION XI APPENDIX J TYPE C LEAK RATE TESTING REQUIREMENTS.
3. CHEMICAL CLEANING CONNECTIONS (FITTED, ETC.) AS NECESSARY, ARE TO BE PROVIDED AS NECESSARY.
4. INSTRUMENT LINE ORIFICES AND FLOW LOOPS SHALL BE IN ACCORDANCE WITH THE REQUIREMENTS SPECIFIED IN NOTE 5.
5.
6. VALVE E22F... SHALL BE INSTALLED WITH THE PACKING GLAND ON THE UPSTREAM SIDE OF THE VALVE DISC.
7. VALVE E22F... SHALL BE LOCATED AS CLOSE AS PRACTICAL TO VALVE E22F...
8. FOR ADDITIONAL CONTROL, PANEL ALARM, SYSTEM ALARMS AND DETAILED MANUAL SEQUENCING, SEE APPLICABLE LOGIC DIAGRAMS AND ELECTRICAL SAR LOAD DIAGRAM FIG. 8.3-1.
9. PROTECTION FOR ISOLATION SHALL BE IN ACCORDANCE WITH CURRENT LOCKOUT REQUIREMENTS AND SECTION 6.8.4.
10. THIS LINE MAY BE CLOSED "B" IF IT IS 3/4 INCH OR LESS IN DIAMETER. IF LARGER THAN 3/4 INCH THE LINE SHALL BE CLOSED "A".
11. THE PIPE BARRIER SHALL PROVIDE ADEQUATE PIPE SUPPORT AND ANCHOR THE SPARGERS TO INSURE NOZZLE OF ZONE TO ASSURE SUFFICIENT CONNECTION WITH END OF CONT SPRING
12. VALVE E22F... SHALL BE LOCATED AT AN ELEVATION LOWER THAN THE SUPPRESSION POOL MINIMUM WATER LEVEL AND CONDENSATE SYSTEM MINIMUM WATER LEVEL.
13. FLUSHING WATER CONNECTIONS ARE LOCATED AS CLOSE AS PRACTICAL TO E22F... AND E22F...
14.
15.
16. FLUSHING CONNECTIONS SHALL BE PROVIDED IN ACCORDANCE WITH NOTE 5. TEMPORARY STRAINER SCREENS SHALL BE PROVIDED ON THE SUCTION SIDE OF ALL PUMPS IN ACCORDANCE WITH NOTE 5.
17. VALVE E22F... IS RECOMMENDED FOR MAINTENANCE AND/OR LEAK RATE TESTING PER SECTION APPENDIX J, TYPE C. E22F... SHALL BE DELETED IF VALVE WILL NOT BE INSTALLED.
18. CHECK VALVE E22F... SHALL BE LOCATED AS CLOSE AS PRACTICAL TO THE HIGH PRESSURE CORE SPRAY NOZZLE NOZZLE.
19. VALVES E22F... AND E22F... SHALL BE LOCATED AS CLOSE AS PRACTICAL TO THE CONTAINMENT PENETRATION OF THE SUCTION LINE TO THE SUPPRESSION POOL.
20. COOLING WATER FOR E22F... MOTOR WINDINGS AND SEALS, IF REQUIRED, IS SPECIFIED IN NOTE 4.
21. OPTIONAL ORIFICE MAY BE REQUIRED TO PREVENT EXCESSIVE PUMP FLOW. FOR SIZING SEE HPCS SYSTEM PROCESS DIAGRAM NOTES 16 AND 17.
22. ALL MOTOR OPERATED VALVES ARE AC OPERATED UNLESS OTHERWISE NOTED.
23. FOR NOT

SUPPLEMENTAL DRAWINGS	MECHANICAL
1. MAIN SYSTEM P&ID	E22-M002
2. PROCESS COMPUTER SYSTEM INPUT/OUTPUT LIST	C51-M030
3. LEAK DETECTION SYSTEM P&ID	
4. EMERGENCY EQUIP COOLING WATER	M52-M230
5. PROCESS INSTRUMENTATION	M57-M070
6. CLEANING OF PIPING & EQUIPMENT	M57-M140
7. PRESSURE INTEGRITY OF INSTEAD COMPONENTS	M57-M030
8. PIPING & INSTRUMENT SYMBOLS	M42-010
9. APCS ONE LINE DIAGRAM	E22-M000
10. NUCLEAR BOILER SYSTEM P&ID	M51-M002

LEGEND
AMM AMMETER

SOURCE 105050E5AA, SH. 1 OF 2, REV. 0

FIGURE 6.3-1
HIGH PRESSURE CORE SPRAY SYSTEM P&ID SHEET 1 OF 2

RIVER BEND STATION
FINAL SAFETY ANALYSIS REPORT

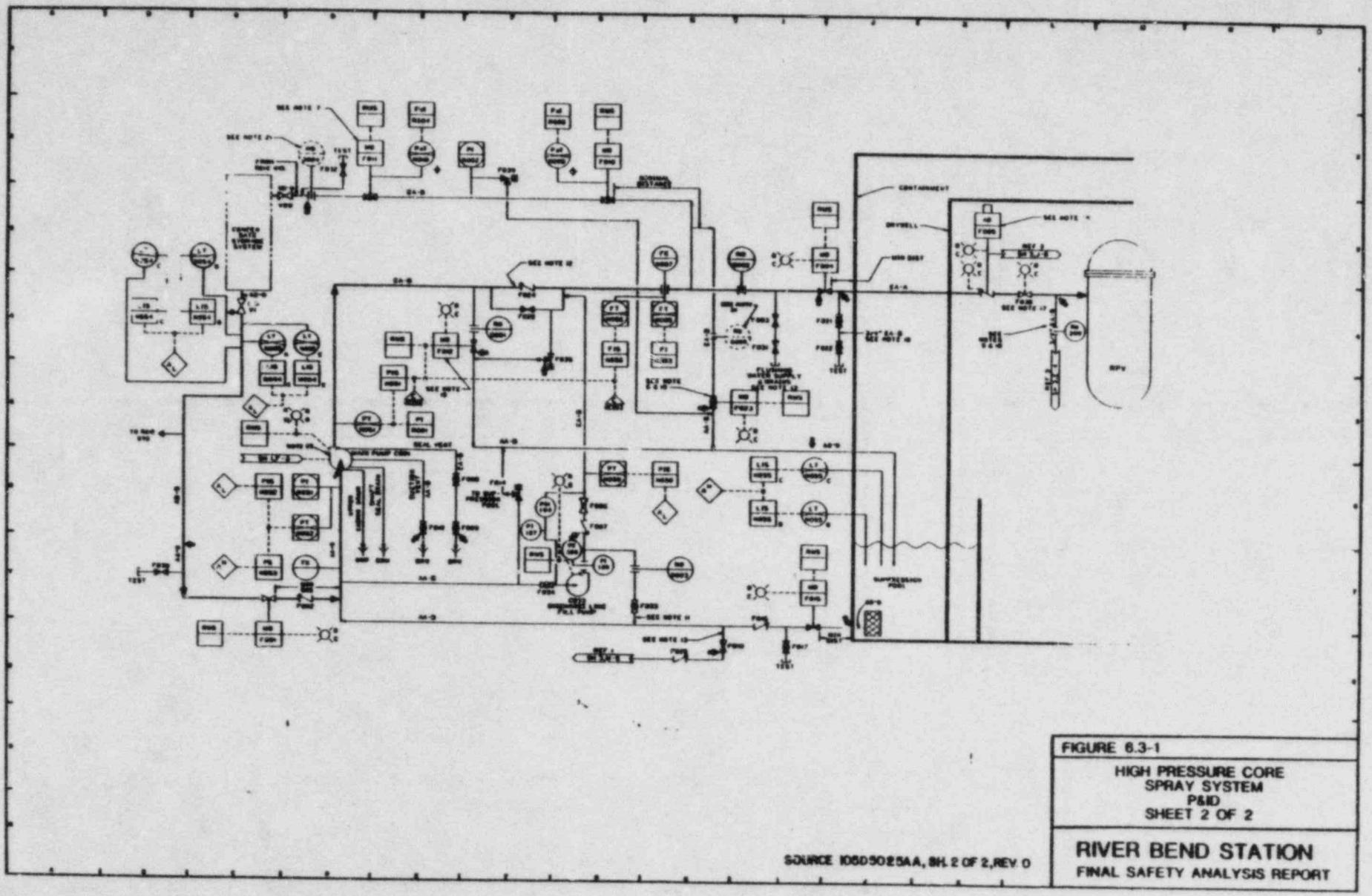

SOURCE 10SD502SAA, SH. 2 OF 2, REV 0

FIGURE 6.3-1

HIGH PRESSURE CORE SPRAY SYSTEM P&ID SHEET 2 OF 2

RIVER BEND STATION
FINAL SAFETY ANALYSIS REPORT

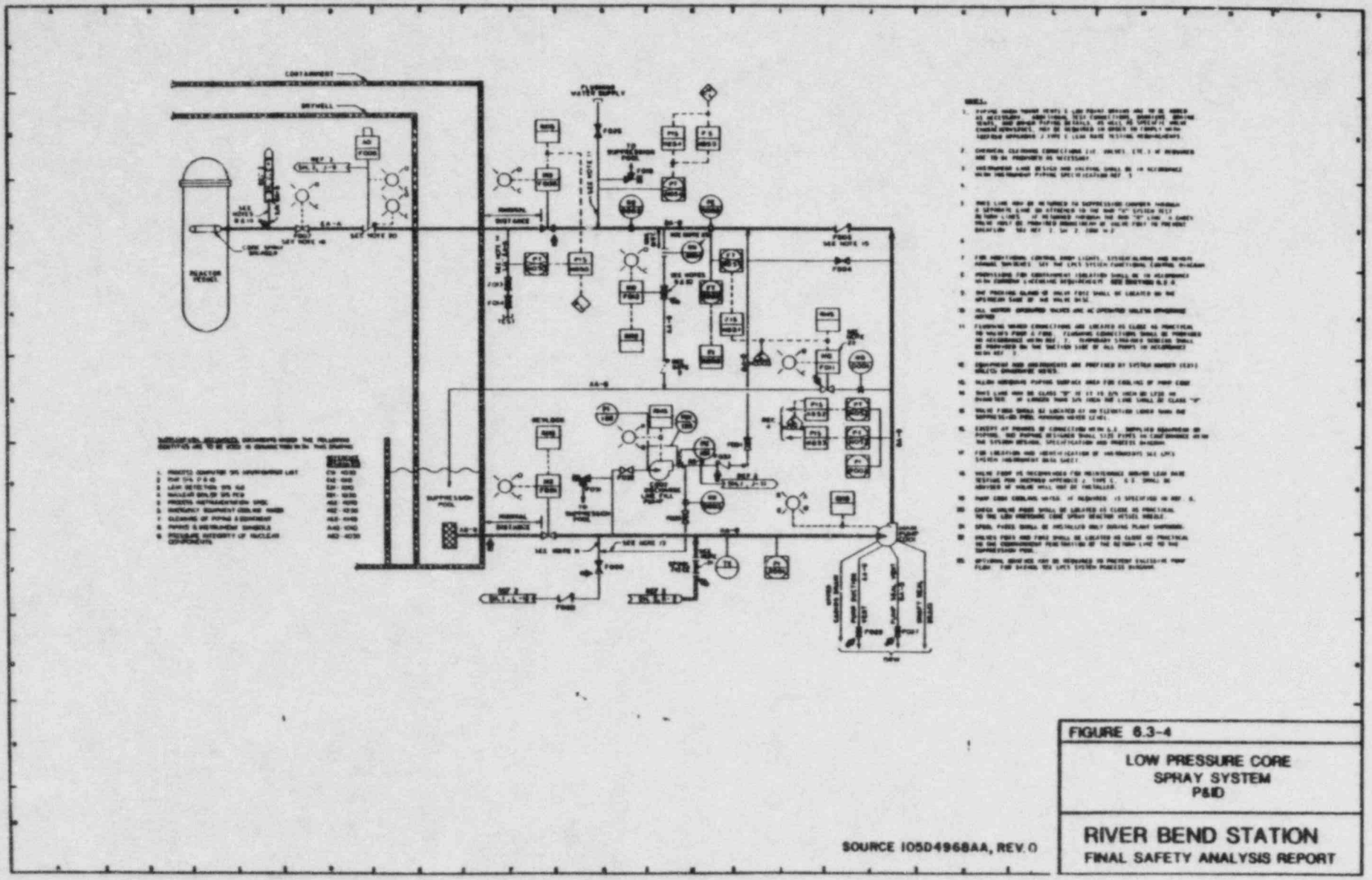

SOURCE I05D4968AA, REV.0

FIGURE 6.3-4

LOW PRESSURE CORE SPRAY SYSTEM P&ID

RIVER BEND STATION
FINAL SAFETY ANALYSIS REPORT

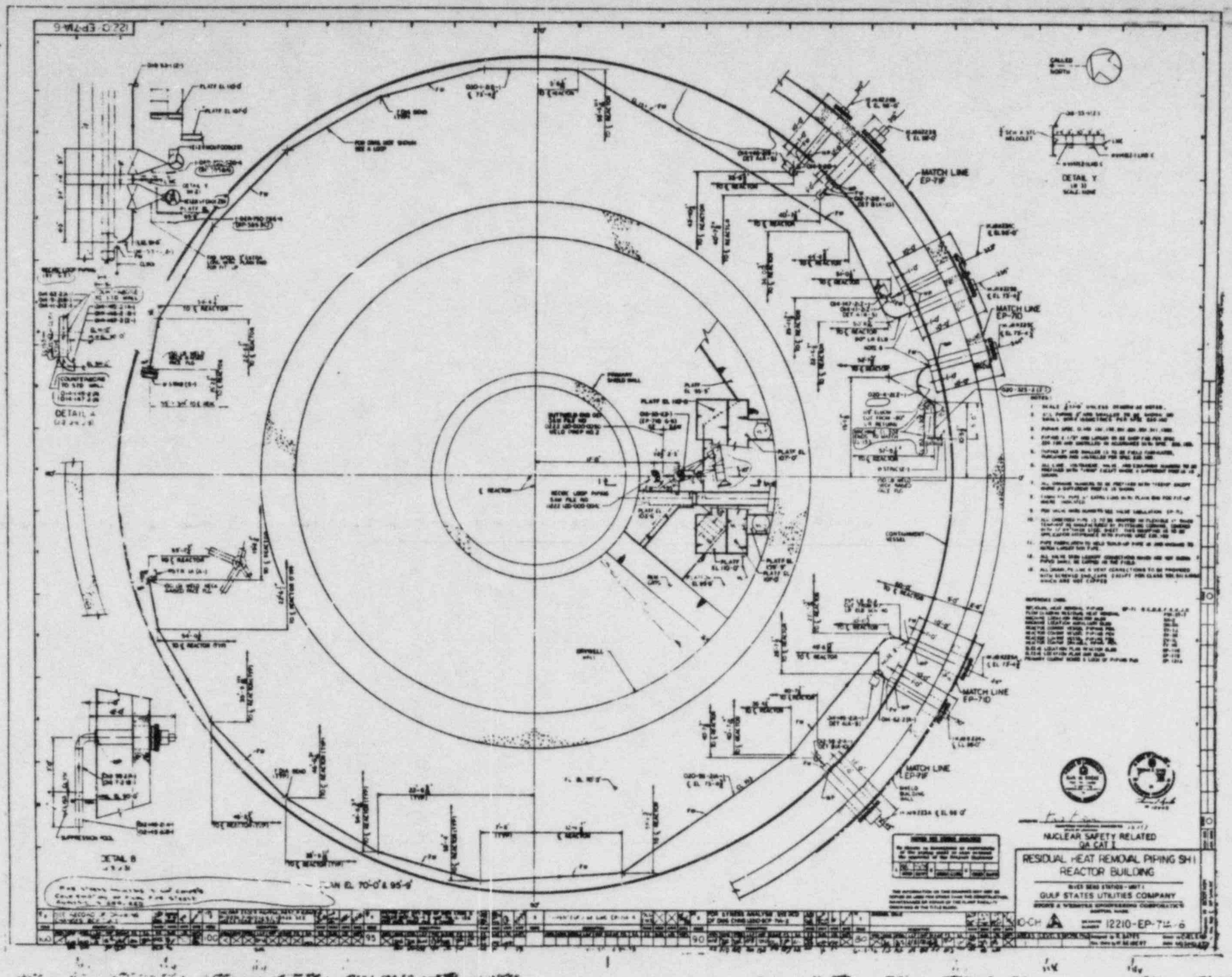
MATCH LINE EP-7F
MATCH LINE EP-7G
MATCH LINE EP-7D
MATCH LINE EP-7F
DETAIL A
DETAIL B
DETAIL Y
CONTAINMENT VESSEL
NUCLEAR SAFETY RELATED
QA CAT I
RESIDUAL HEAT REMOVAL PIPING SHI
REACTOR BUILDING
GULF STATES UTILITIES COMPANY
12210-EP-7

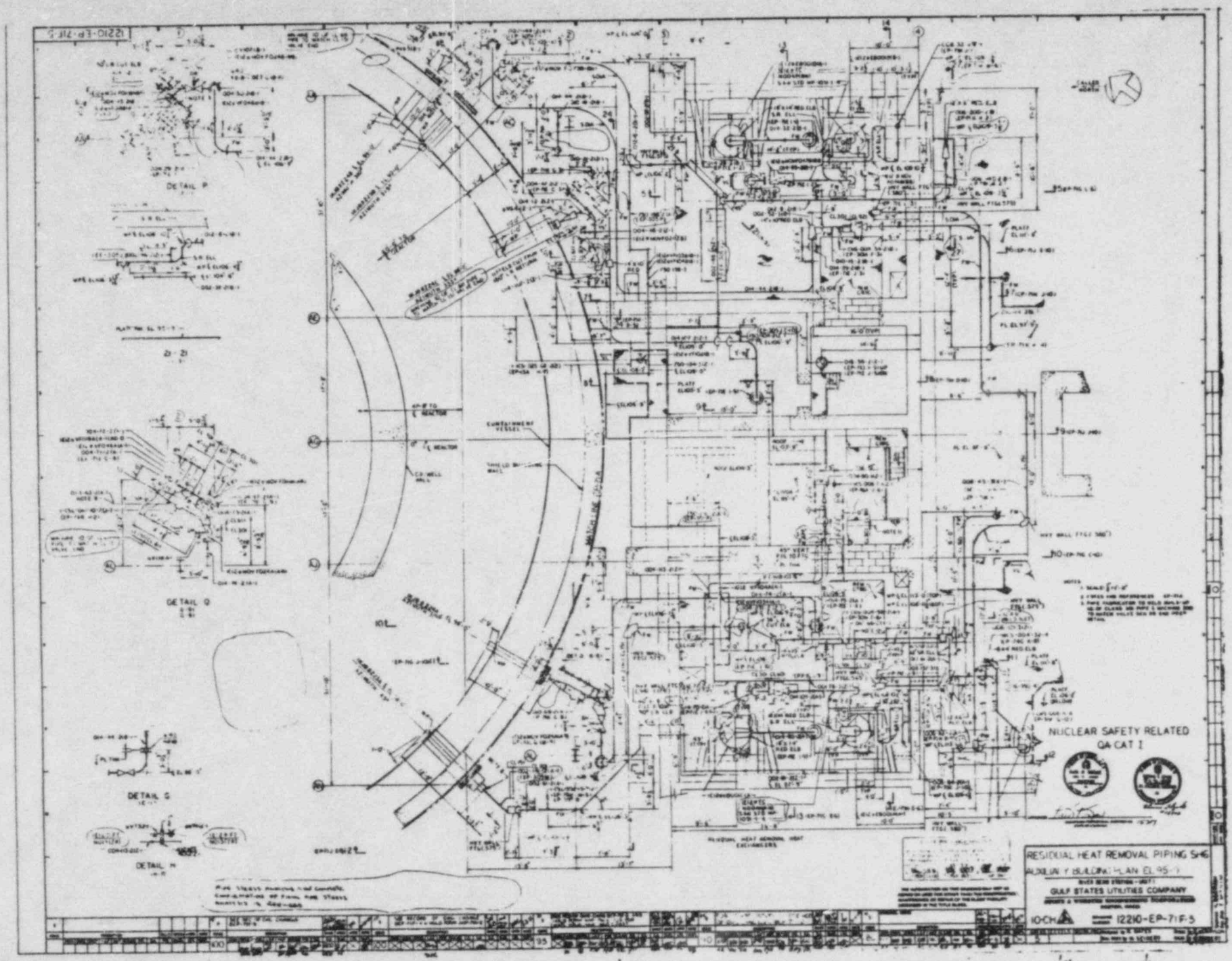
DETAIL P
DETAIL Q
DETAIL S
DETAIL N
NUCLEAR SAFETY RELATED
QA CAT I
RESIDUAL HEAT REMOVAL PIPING SHG
AUXILIARY BUILDING PLAN EL 95'-0"
GULF STATES UTILITIES COMPANY
10-CH-A
12210-EP-71F-5

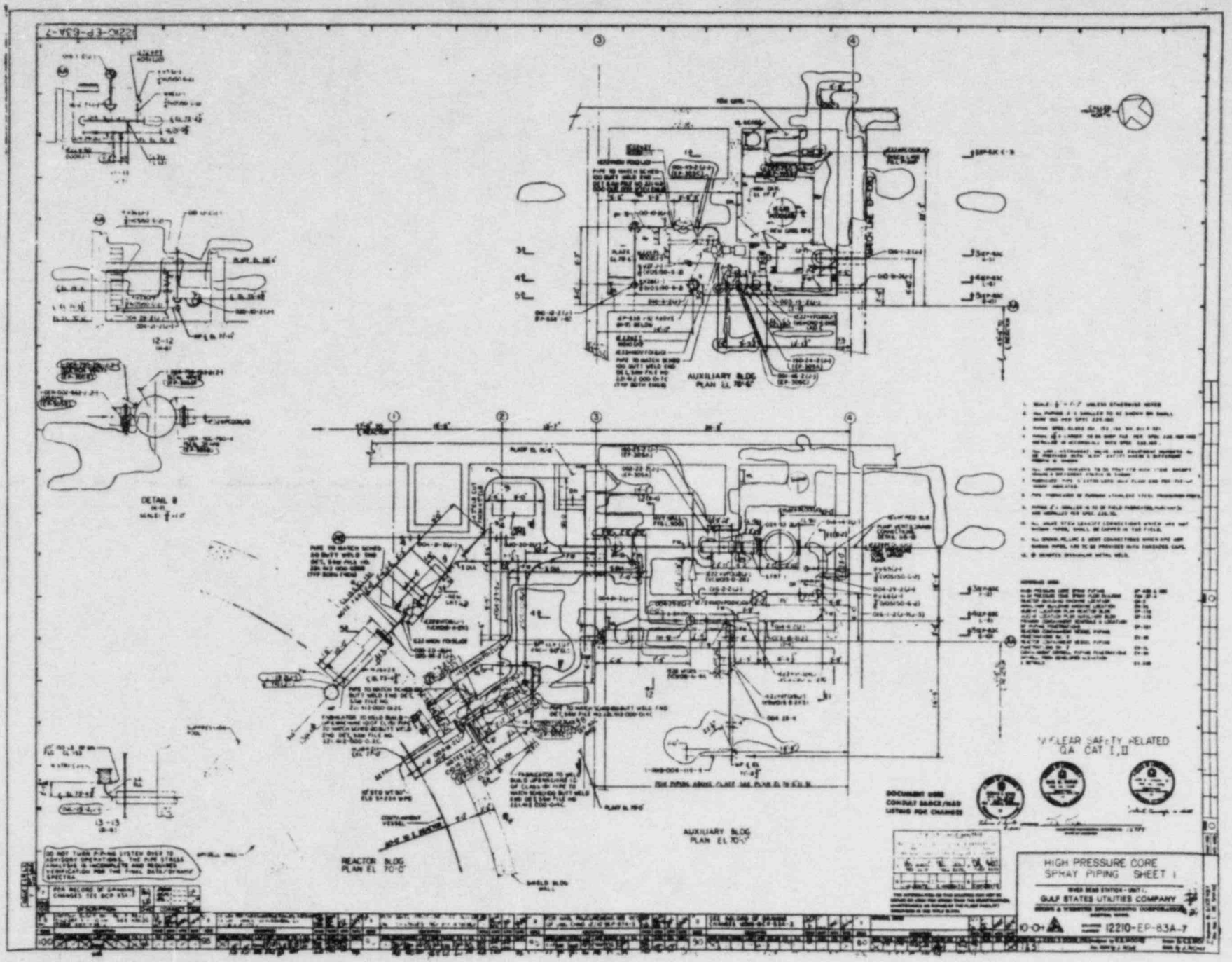
DETAIL B
AUXILIARY BLDG PLAN EL 70'-6"
AUXILIARY BLDG PLAN EL 70'-0"
REACTOR BLDG PLAN EL 70'-0"
NUCLEAR SAFETY RELATED QA CAT I, II
HIGH PRESSURE CORE SPRAY PIPING SHEET 1
GULF STATES UTILITIES COMPANY
12210-EP-83A-7

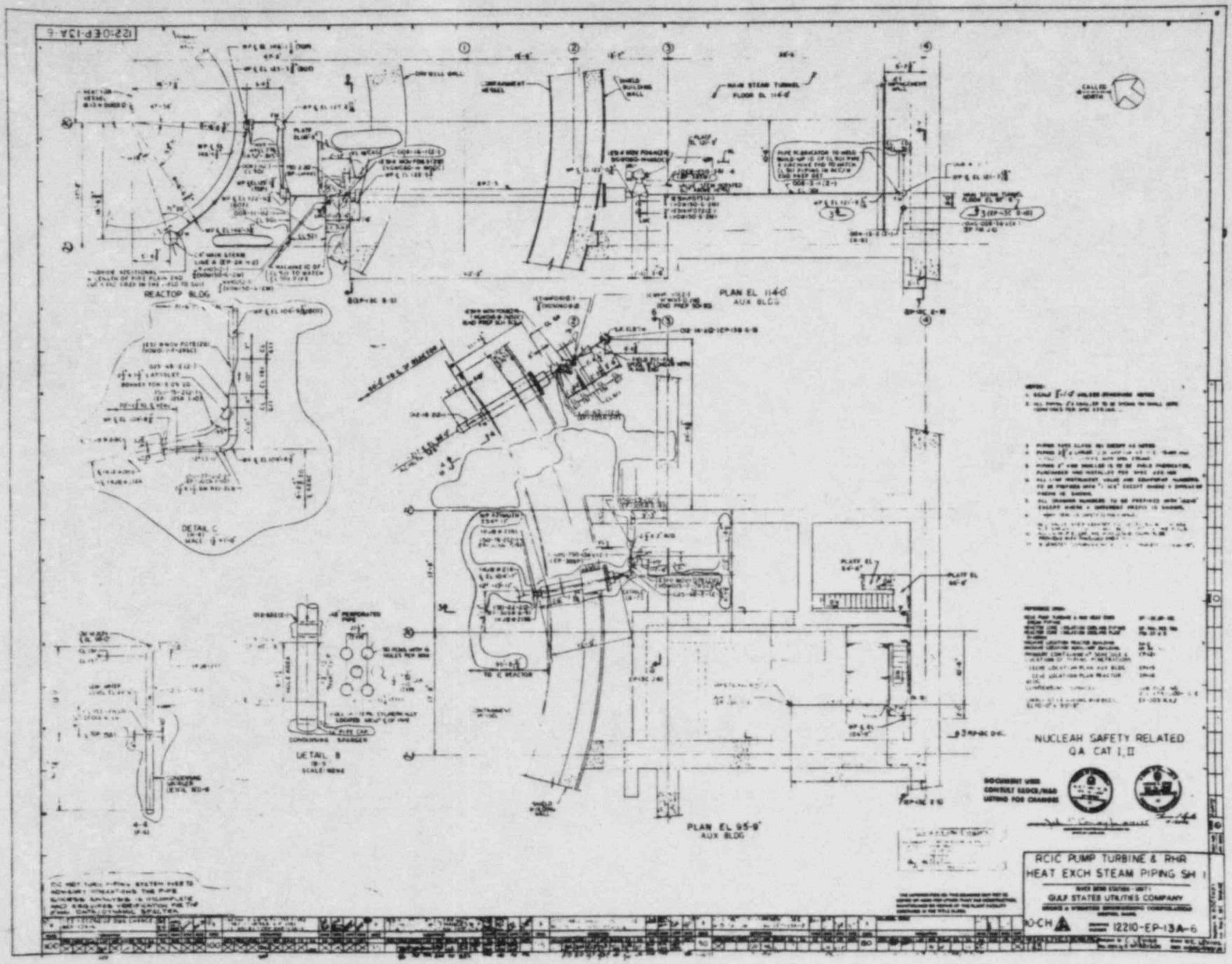
REACTOR BLDG
PLAN EL 114'-0"
AUX BLDG
PLAN EL 95'-0"
AUX BLDG
DETAIL C
DETAIL B
NUCLEAR SAFETY RELATED
QA CAT I, II
RCIC PUMP TURBINE & RHR
HEAT EXCH STEAM PIPING SH 1
GULF STATES UTILITIES COMPANY
12210-EP-13A-6

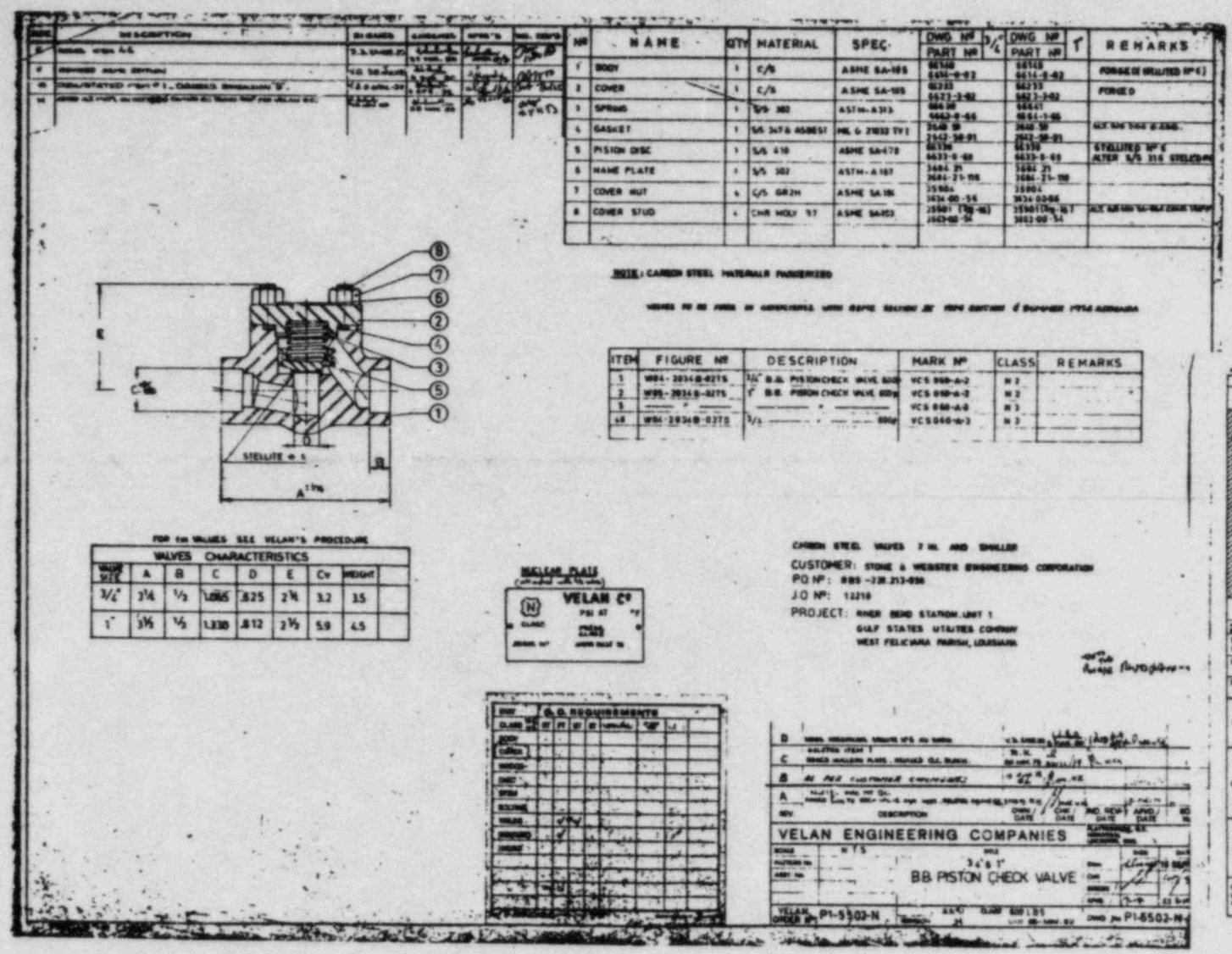

Nº	NAME	QTY	MATERIAL	SPEC.	DWG Nº / PART Nº 3/4"	DWG Nº / PART Nº 1"	REMARKS
1	BODY	1	C/S	ASME SA-105	66138 6636-B-02	66138 6636-B-02	FORGED (STELLITED Nº 6)
2	COVER	1	C/S	ASME SA-105	66233 6637-J-02	66233 6637-J-02	FORGED
3	SPRING	1	S/S 302	ASTM-A313	66438 6663-B-05	66441 6664-1-05	
4	GASKET	1	S/S 347& ASBEST	MIL G 21032 TY I	3648 50 3642-50-01	3648 50 3642-50-01	ALT S/S 304 & ASB.
5	PISTON DISC	1	S/S 410	ASME SA-479	66138 6633-B-03	66138 6633-B-03	STELLITED Nº 6 ALTER S/S 316 STELLITED
6	NAME PLATE	1	S/S 302	ASTM-A167	35684 21 3684-21-118	35684 21 3684-21-118	
7	COVER NUT	4	C/S GR2H	ASME SA 194	35804 3634-00-56	35804 3634-00-56	
8	COVER STUD	4	CHR MOLY 97	ASME SA-193	35801 (Typ-4) 3662-00-54	35801 (Typ-6) T 3662-00-54	ALT S/S 304 SA-194 ZINC TRIM

NOTE: CARBON STEEL MATERIALS PASSIVIZED

WELDS TO BE MADE IN ACCORDANCE WITH ASME SECTION IX 1974 EDITION & SUMMER 1974 ADDENDA

ITEM	FIGURE Nº	DESCRIPTION	MARK Nº	CLASS	REMARKS
1	W84-20348-0275	3/4" B.B. PISTON CHECK VALVE 600#	VCS 060-A-2	N 2	
2	W85-20348-0275	1" B.B. PISTON CHECK VALVE 600#	VCS 060-A-2	N 2	
3	" "	" " " "	VCS 060-A-3	N 3	
4	W84-20348-0275	1/2 " " " 800#	VCS 060-A-3	N 3	

FOR DIMENSIONAL VALUES SEE VELAN'S PROCEDURE

VALVES CHARACTERISTICS

VALVE SIZE	A	B	C	D	E	Cv	WEIGHT	
3/4"	3 1/4	1/2	1.065	.825	2 3/4	3.2	3.5	
1"	3 1/2	1/2	1.330	.812	2 1/2	5.9	4.5	

WELDS PLATE

VELAN Cº

CARBON STEEL VALVES 2 IN. AND SMALLER

CUSTOMER: STONE & WEBSTER ENGINEERING CORPORATION
PO Nº: BBS -238.253-036
J.O Nº: 12210
PROJECT: RIVER BEND STATION UNIT 1
GULF STATES UTILITIES COMPANY
WEST FELICIANA PARISH, LOUISIANA

QUALITY REQUIREMENTS								
CLASS	NDE RT	PT	MT	UT	VISUAL	"QR"	LT
BODY (CAST)							
WELDED							
INSERT							
STEM							
BONNET							
VALVE							
STANDARD							
ENDS							

REV	DESCRIPTION	DWN / CHK DATE	ENG. APPR. DATE	APVD. DATE
D				
C				
B				
A				

VELAN ENGINEERING COMPANIES

SCALE N.T.S
TITLE 3/4" & 1" BB PISTON CHECK VALVE
VELAN ORDER Nº P1-5502-N
DWG No P1-6502-N-1

STONE & WEBSTER ENGINEERING CORPORATION
RIVER BEND STATION - UNIT 1
GULF STATES UTILITIES COMPANY
A.E. 12210

MANUFACTURER'S DRAWING DATA FORM

RESP. ENG. F. VISHNEVETSKY (E1)
RESP. DES. ENG. (E1)

INSTRUCTIONS TO SUPPLIER (E2)
APPROVED
APPROVED AS REVISED
RELEASED FOR FABRICATION
RELEASED FOR MATERIAL PURCHASE
SUPPLIER TO RESUBMIT
NOTES:

INSTRUCTIONS TO DESIGN (E1)
INFORMATION ONLY
PRELIMINARY LAYOUT
PRODUCTION STUDIES
REVIEW AND COMMENT
FINAL DETAILS
NEW
REVISED

DATE TO DESIGN (E)
REQUIRED RETURN DATE (E1)
DESIGN ENGINEER'S DATE STAMP (D)
DESIGN GROUP ROUTING (D)
DESIGN ENGINEER'S DATE STAMP (D)
INITIALS OF SELECTED REVIEWERS
RESPONSIBLE ENGINEER'S DATE STAMP (E2)
SUPERSEDES S&W FILE NO (E)
S&W EQUIP. ID CODE (E)
P1-5502-N-1 REV H
VELAN
S&W FILE NO (E)
DISCIPLINES: ARCHITECTURE, CIVIL, CONCRETE, STEEL, BUILDING SERVICE, INSTRUMENT, MECHANICAL, PIPE SUPPORT, STRESS, MACHINE DESIGN/VESSEL, ELECTRICAL, LIGHTING, MODEL SHOP, EXTENSION OFFICE, CONTROL
F. Vishnevetsky
JOB ORDER NO 12210 00

Action Plan 7 - Plant Specific

I. Issues Addressed

3.2 The STRIDE design provided only 9 inches of submergence above the RHR heat exchanger relief valve discharge lines at low suppression pool levels.

II. Program for Resolution

The Humboldt Bay pressure suppression test data demonstrated the relationship of discharge submergence on condensation effectiveness. An evaluation based on this data will be submitted showing that the maximum discharge from the relief valves can be quenched under all possible submergence conditions.

III. Status*

Item 1 is complete and included in this submittal.

IV. Final Program Results*

Figure 7-1 shows condensation effectiveness data obtained during the Humboldt Bay pressure suppression tests (Reference 1). These tests investigated condensation effectiveness at vent submergences from 12 to 3 feet (i.e., 3-foot clearance between the discharge of the 14-inch diameter vertical vent and the pool surface) at vent steam mass fluxes of 50 to 250 lbm/sq ft sec. This mass flux considerably exceeds the mass flux of 92 lbm/sq ft sec associated with the River Bend Station RHR heat exchanger relief valve discharges. Also, the RBS RHR heat exchanger relief valve discharge lines are equipped with tees that are expected to provide more effective condensation due to more entrainment than a straight pipe which was used in the Humboldt Bay pressure suppression tests.

Condensation effectiveness is characterized by comparing the measured and calculated pressure in the suppression chamber air space. The calculated suppression chamber air space pressure is based on the assumption of complete condensation of steam in the pool; i.e., if the steam actually escapes to the air space without being condensed, the measured suppression chamber air space pressure would be much higher than the calculated value. The figure shows that nearly complete condensation of the steam still occurs when the vent exit is 2 feet above the water surface. Steam bypass is evident in the case of 3-foot clearance.

The River Bend Station design provides approximately 4 ft of suppression pool water above the RHR relief valve discharge lines after the pool level has been drawn down by ECCS operation and the pool water floods the drywell to the top of the weir wall. The normal minimum submergence is 7 ft 4 in.

Since the minimum submergence of the RHR discharge is approximately 4 ft, complete condensation is assured for River Bend Station.

Reference

1. C.H. Robbins, Tests of a Full Scale 1/48 Segment of the Humboldt Bay Pressure Suppression Containment, GEAP 3596, November 1960.

*This revision replaces the GSU submittal dated April 1, 1983.

HUMBOLDT BAY PRESSURE SUPPRESSION
TEST MAXIMUM SUPPRESSION CHAMBER
PRESSURE COMPARISON (Plotted from Ref. 1)

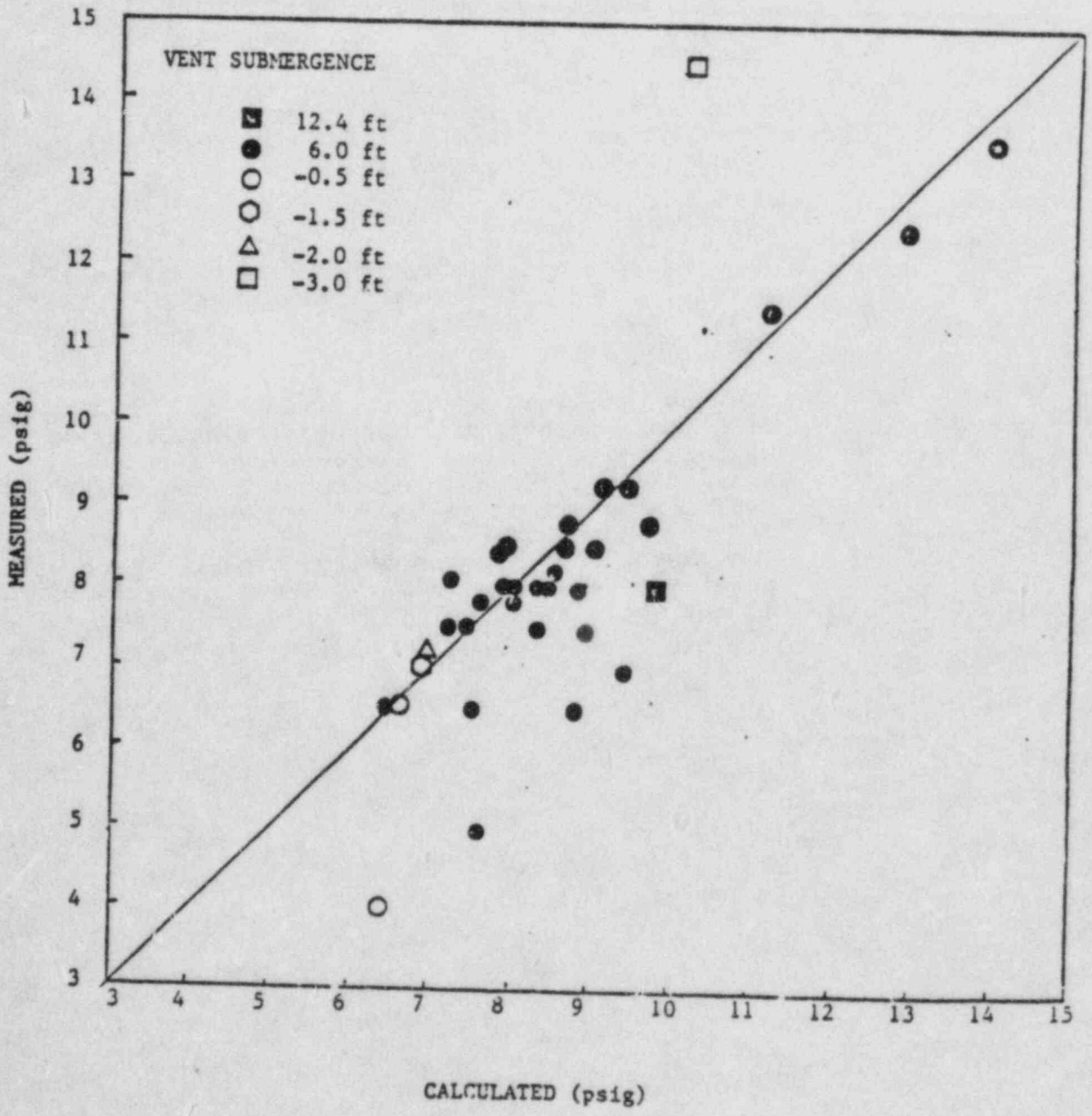

Figure 7-1

Action Plan 8 - Plant Specific

I. Issues Addressed

3.4 The RHR heat exchanger relief valve discharge lines are provided with vacuum breakers to prevent negative pressure in the lines when discharging steam is condensed in the pool. If the valves experience repeated actuation, the vacuum breaker sizing may not be adequate to prevent drawing slugs of water back through the discharge piping. These slugs of water may apply impact loads to the relief valve or be discharged back into the pool at the next relief valve actuation and apply impact loads to submerged structures.

3.5 The RHR relief valves must be capable of correctly functioning following an upper pool dump, which may increase the suppression pool level as much as 5 ft, creating higher back pressures on the relief valves.

II. Program for Resolution*

1. An analysis will be performed to determine if a water slug from the suppression pool is drawn into the RHR heat exchanger relief valve discharge line.

2. If the analysis shows that water is drawn up from the suppression pool, water slug loads on relief valve piping and submerged structures will be determined and appropriate design modifications implemented if necessary.

3. The River Bend Station design does not incorporate an upper pool dump. Hence, Issue 3.5 is not applicable.

III. Status*

Items 1 through 3 are complete and included with this submittal.

IV. Final Program Results*

A reflood analysis has been performed to determine the water leg rise in the RHR heat exchanger relief valve discharge line and a subsequent relief valve actuation analysis was performed. The analysis shows that the resulting maximum reflood water elevation is 106.2 ft. The relief valve is at elevation 118.75 ft and there is adequate margin to preclude reflood water from reaching the relief valves. The water clearing loads have been calculated for the relief valve discharge line itself and the adjacent submerged structures. RBS has no structure in the direct jet paths. The induced drag loads affect only a few adjacent structures. Piping and support evaluations for these structures were made and the structures were found to have sufficient design margin to accommodate these loads.

The reflood model developed in the Mark I and Mark II program (Reference 1) was used to calculate the water rise in the RHR heat exchanger relief valve discharge line. Following valve closure, the steam/water interface heat transfer coefficient used in the reflood analyses was scaled from vertical vent flow test data. SWEC computer code "STEHAM" (FSAR Appendix 3A) was used to calculate dynamic load on piping due to subsequent relief valve actuation. Subsequent actuation was postulated to occur at the maximum reflood level to determine the worst scenario load.

Reference 1: Wheeler, A. J.; Dougherty, D. A., "Analytical Model for Computing Water Rise in Safety Relief Valve Discharge Line Following Valve Closure". GE Document No. NEDE-23898-P, October 1978

Based on the above results, this issue is considered closed for RBS with this submittal.

*This revision replaces the GSU submittal dated April 1, 1983.

Action Plan 9 - Generic

I. Issues Addressed

3.6 If the RHR heat exchanger relief valves discharge steam to the upper levels of the suppression pool following a design basis accident, they will significantly aggravate suppression pool temperature stratification.

II. Program for Resolution*

1. The maximum quantity of energy which can be added to the suppression pool will be quantified. This will be based upon operator action to terminate relief valve discharge following discovery by the operator that the relief valve has actuated. This will include an evaluation of all scenarios which could lead to discharge from these relief valves.

2. The discharge plume from the relief valves will be investigated. This plume will establish the maximum area of the pool which can be affected.

III. Status

Items 1 and 2 are complete and included in this submittal.

IV. Final Program Results*

Item 1

The maximum quantity of energy which could be added to the suppression pool assuming that the pressure control valve fails full open, that all steam flowing through the control valve exits through the relief valve prior to reaching the heat exchanger, and that no heat is removed from flow into the heat exchanger, is approximately 1.06×10^7 Btu. This quantity of energy added to the suppression pool is limited to a discharge from the relief valve lasting for 2 minutes prior to termination of the event by operator action.

The maximum discharge time of 2 minutes for the relief valve before the operator terminates the event is based upon multiple sequences of control operation required prior to placing the steam condensing mode in service. Initiation of the RHR steam condensing mode is highly operator intensive and requires essentially continuous monitoring of heat exchanger pressure, temperature, and

water levels. The implementation of stable steam condensing operation normally requires a minimum of 30 minutes following initiation.

The operator must continuously monitor key variables, such as heat exchanger pressure, temperature, and water level, following actuation of the steam condensing mode. If the operator encounters situations in which important heat exchanger parameters, such as pressure, cannot be effectively controlled, i.e., the pressure control valve fails open, the operator will promptly close the steam supply block valve. A high temperature alarm downstream of the pressure control valve is set to alarm on reaching a temperature, corresponding to saturation at a pressure slightly higher than 200 psig, the upper end of the prescribed control range. This alarm will alert the operator that the control valve has failed. The operator will immediately isolate the steam supply to the heat exchanger within 1 minute of receipt of the alarm. The steam supply block valve will be fully closed within approximately 2 minutes of receipt of alarm.

The maximum quantity of energy postulated to be added to the suppression pool is quite conservative. The value of energy calculated is based upon full flow instead of partial flow through the relief valve for 2 minutes. In addition, the assumption that no energy is transferred out of the steam flowing to the heat exchanger is extremely conservative.

Item 2

A suppression pool mixing and stratification model has been developed to provide a conservative estimate of the suppression pool thermal response to continuous discharge of steam through the residual heat removal system heat exchanger relief valve. The worst case event evaluated with this model postulates a failure of the pressure control during steam condensing mode startup such that none of the steam flowing to the heat exchanger is condensed. A continuous discharge of 266,000 lbm/hr steam has been evaluated. The maximum choked flow for RBS which can be passed through the failed open pressure control valve is 2.6×10^5 lbm/hr.

The flow from the fully open relief valve exceeds the flow from the pressure control valve. Consequently, following actuation of the relief valve, the RHR heat exchanger and piping system will be depressurized below the pressure at which the relief valve closes. After

relief valve closes, the system will repressurize to the setpoint of the relief valve which will cause the valve to reopen. Consideration of discharge from the relief valve as continuous is therefore very conservative. The on/off charging of the pool will produce more mixing than would be accomplished by a steady uniform jet.

The length of the steam plume below the discharge line exit is slightly more than 3 feet based upon the known mass flux of the jet and the methodology contained in Reference 1. The steam jet momentum calculated for the given conditions is 1.35×10^5 lbm ft/sec^2. For a hot water jet with the same momentum, the following properties can be calculated from Reference 2 assuming a turbulent jet discharging into an infinite pool. The properties below are calculated at a location of 1.75 feet above the bottom of the pool at the center of the discharge pipe exit.

Jet half width	=	approximately 1.02 ft
Centerline velocity	=	28.6 ft/sec
Total jet flow	=	14,156 lbm/sec

The postulated flow configuration is shown in Figure 9-1. Based upon the parameters calculated for an infinite pool, the appropriate parameters for the jet discharge in the finite suppression pool can be estimated.

A drawing showing the nodalization used for evaluating the discharge from the jet is shown in Figure 9-2. A jet plume node (jet node) is located within a local sector of the pool defined as the mixing node. The entrainment into the jet is assumed to be the same as for a free field jet between the discharge pipe exit and 1.75 feet from the pool bottom. Flow which is entrained into the jet will come from and be returned to the mixing node. The only flow leaving the mixing node will be the inlet jet flow minus the amount the mixing node grows due to an increase in pool depth as a result of jet flow addition. Flow from the mixing node will enter a series of surface nodes which will stretch around the pool. Because of the symmetry of the pool, only half of the pool is modeled.

The mixing node consists of an 18-deg sector of the pool (which corresponds to a 36 deg sector in the full pool). The volume of the mixing node is approximately 12,554 cu ft in the pool, or about 10 percent of the pool volume. Based upon the entrained flow for the circular jet in an infinite pool which was calculated above, the entire volume of the mixing node will be

entrained and mixed through the jet plume every 56 seconds. The mixing node is assumed to be isolated from the rest of the pool, and no flow is entrained by the jet from the remainder of the pool. This represents a significant conservatism in the analysis.

The model considers convective heat transfer from the mixing node to the wetwell air space and conductive heat transfer from the mixing node is assumed to pass into adjacent surface nodes so that the lower regions of the pool are effectively excluded from the analysis with the exception of conductive heat transfer.

The predictions for jet node exit temperature and mixing node temperature as functions of time are shown in Figure 9-3. The mixing node temperature represents the local pool temperature surrounding the jet discharge. During the initial part of the transient, the mixing node temperature rise is not quite linear, but the rise is approximately 5.6°F per minute. The mixing node temperature follows the jet node exit temperature within 5°F for the selected mixing node as 10 percent of the total pool volume.

Figure 9-4 shows the predicted pool surface temperature stratification profiles. The stratification profiles are only important in terms of their effect on the average pool surface temperature, since the containment air space temperature will only be affected by the average pool surface temperature. The average pool surface temperature rise at the end of 12 minutes will be about 13°F. For a fixed volume and fixed air mass above the pool surface, this temperature rise could at most increase the wetwell air space pressure by about 2 percent, which is clearly inconsequential.

The sensitivity of the predicted results to changes in key assumptions was evaluated as part of the study. Parameters investigated include volume of the mixing node, jet entrainment flow, surface node thickness, and heat transfer from mixing and surface nodes. Table 9-1 summarizes the results of this sensitivity study.

As an example of how Table 9-1 should be interpreted, the model predicts a mixing volume temperature rise of about 70°F in 12 minutes. If the mixing volume were doubled, about a 50 percent decrease in the temperature rise could be expected, or about a 35°F rise over the same interval. Similarly, if we double the thickness of the surface nodes, the resulting temperature stratification profile would be reduced on average by about 20 percent near the mixing node and falling off more quickly moving away from the mixing node.

It is also interesting to observe that the jet entrainment flow has little effect on the mixing volume temperature. This results from the small mixing node volume and the high volumetric flow rate through the jet node. This sensitivity would change for a larger mixing node volume.

The most significant result from the model sensitivity studies is the confirmation that the size of the mixing node volume is the key parameter in the temperature predictions by the model. For the results shown in Figures 9-3 and 9-4, a mixing node volume was chosen such that the jet will mix the liquid inventory of the mixing node volume through the jet about once every minute. To demonstrate the effect of increasing this mixing volume size, Figure 9-5 shows the mixing node temperature history for various mixing node volume sizes. As this figure demonstrates, the mixing node temperature comes down rapidly as more of the pool becomes involved. It seems likely that as the RHR heat exchanger relief valve cycles open and close, the turbulence produced by the starting and stopping of the steam jet will create sufficient mixing to involve a large sector of the pool. However, solving this complicated mixing problem would require a detailed nodal analysis of the transient jet in the pool.

The simplified model used in the present analysis is intended to demonstrate with suitably conservative model assumptions that, if the pressure control valve in the RHR heat exchangers system should fail, the operator would have several minutes to detect the overpressure in the RHR heat exchanger and take action before there would be sufficient pool heatup to produce conditions in the pool which could lead to unstable condensation. For a more detailed discussion of the analysis, see Reference 3.

Each RBS RHR heat exchanger relief valve discharge line is equipped with a tee at the discharge end. The tee divides the discharge into two smaller jets and increases the mixing node volume. Since increasing the mixing node volume decreases the temperature as shown in Table 9-1, the results presented herein are conservative and bounding for the present RBS design.

Based on the above results, this issue is considered closed for RBS with this submittal.

References

1. Stanford, L.E. and C.C. Webster, Energy Suppression and Fission Product Transport in

Pressure Suppression Pools, ORNL-TM-3448, April 1972.

2. Schlichting, H., Boundary Layer Theory, 6th Edition, pages 699-702, McGraw Hill Book Co., 1968.

3. Healzer, J. M., A Model for Mixing and Stratification of the Suppression Pool During RHR Heat Exchange Relief Valve Discharge, SLI-8222-2, S. Levy, Inc., for General Electric Co., November 1982.

*These revised program results replace the GSU-submitted results dated April 1, 1983.

Table 9-1

Model Input Sensitivity

Input Parameter	% Changed	$\%(T_{mix} - T_o)$	$\%(T_n - T_o)$
Mixing Node Volume	+10	-10	0.01
Jet Entrainment Flow	±10	0	0
Surface Node Thickness	doubled	0	-20 near mixing node increasing to a higher percentage far away
Heat Transfer From Mixing and Surface Nodes	set to Zero	~ 0	0

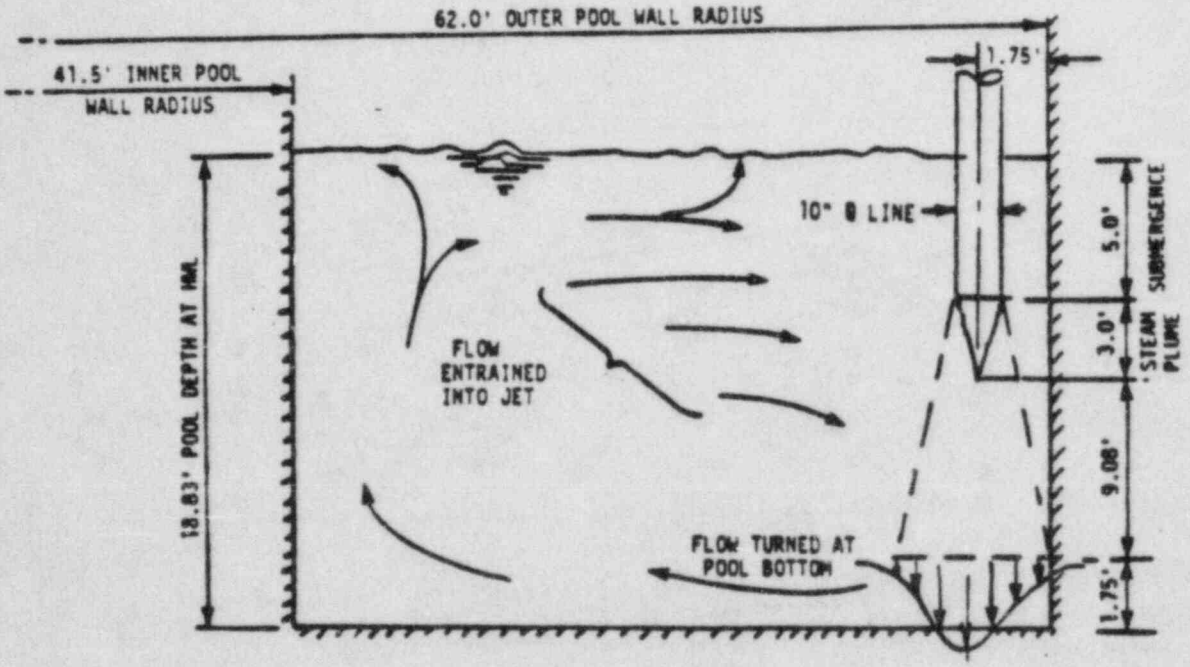

FIGURE 9-1
JET FROM RHR RELIEF VALVE DISCHARGE

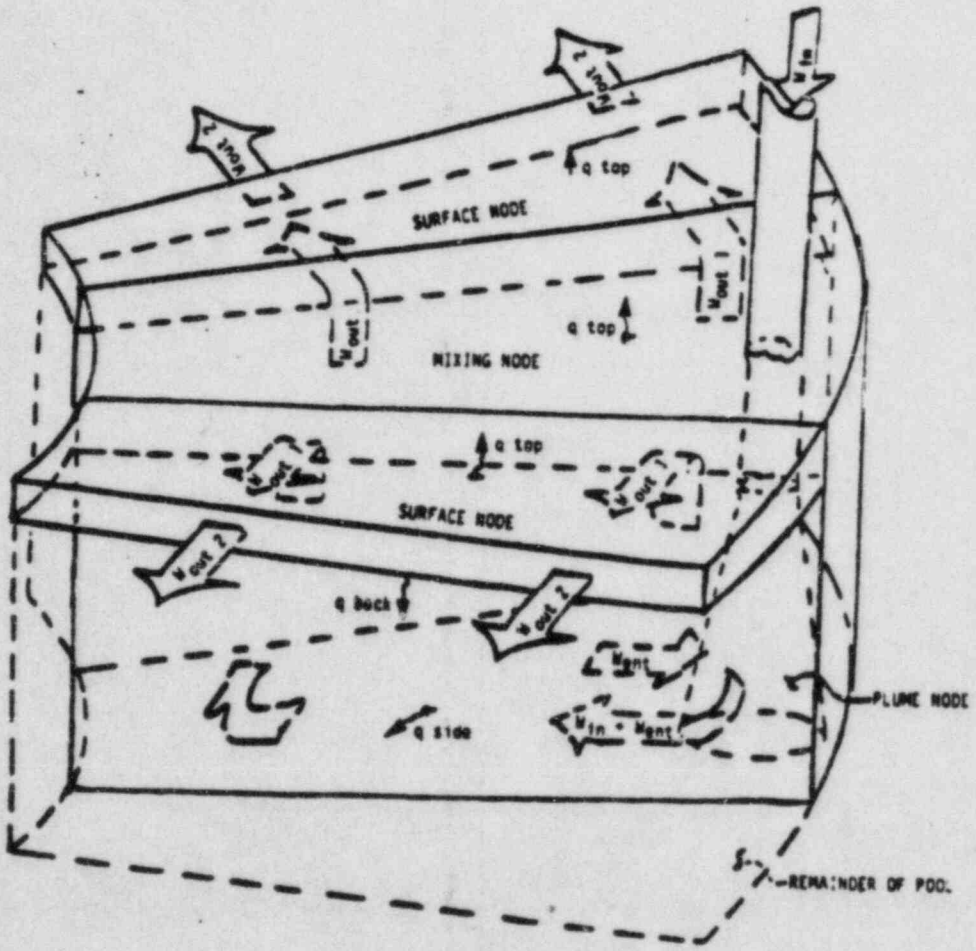

FIGURE 9-2
ISOMETRIC SKETCH OF JET DISCHARGE MODEL

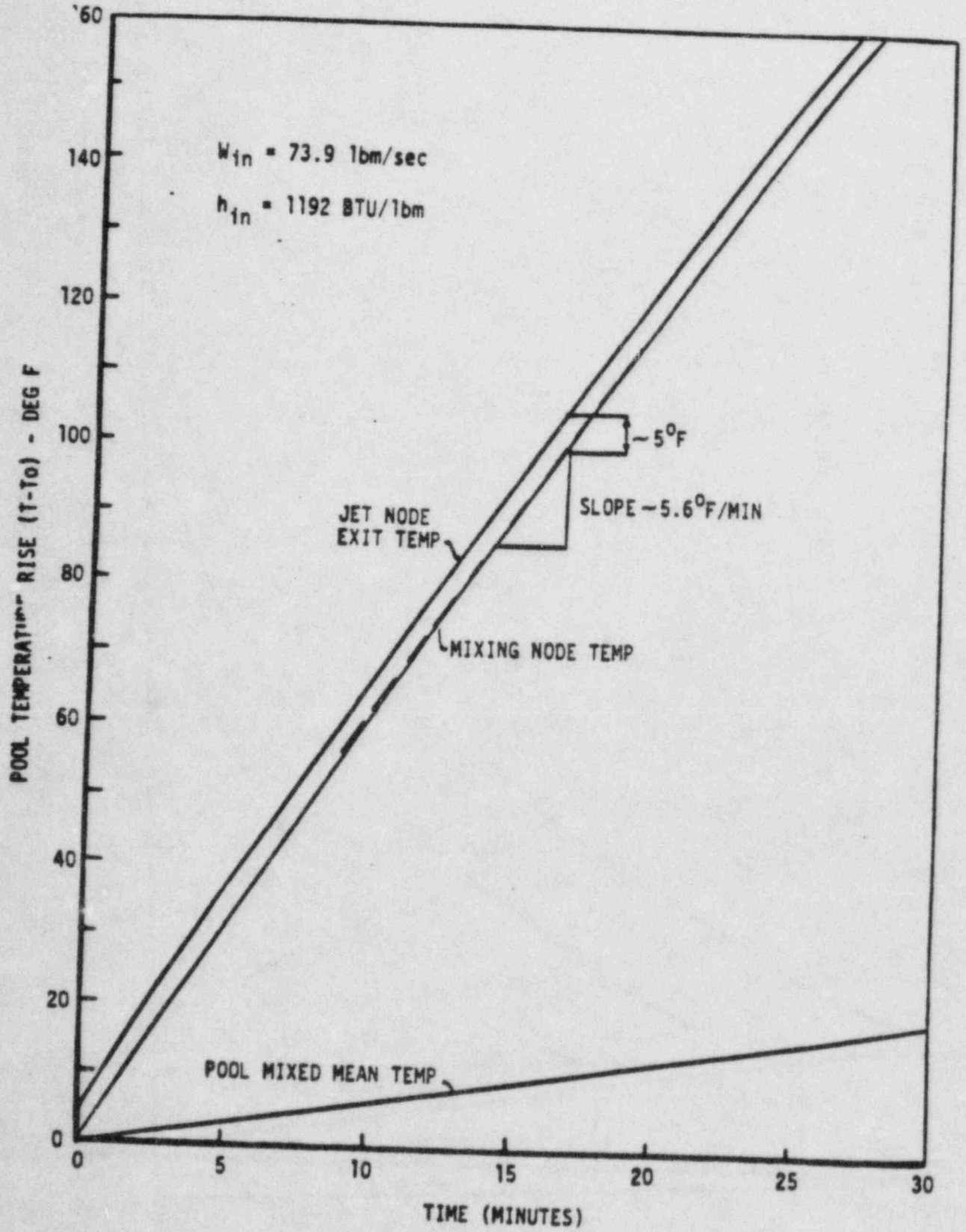

FIGURE 9-3
POOL HEAT-UP DUE TO RHR HEAT EXCHANGER DISCHARGE

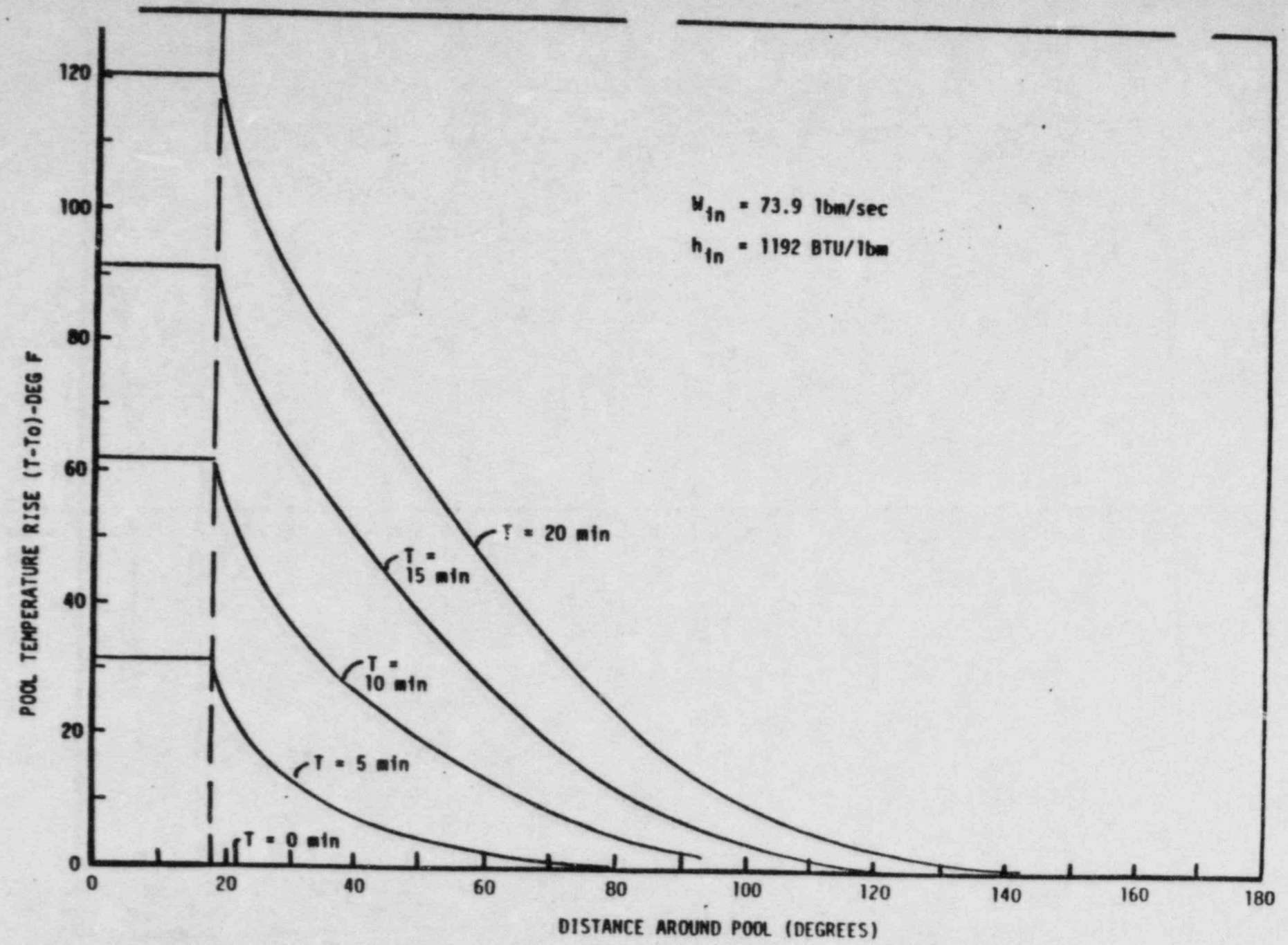

FIGURE 9-4
POOL STRATIFICATION PROFILES

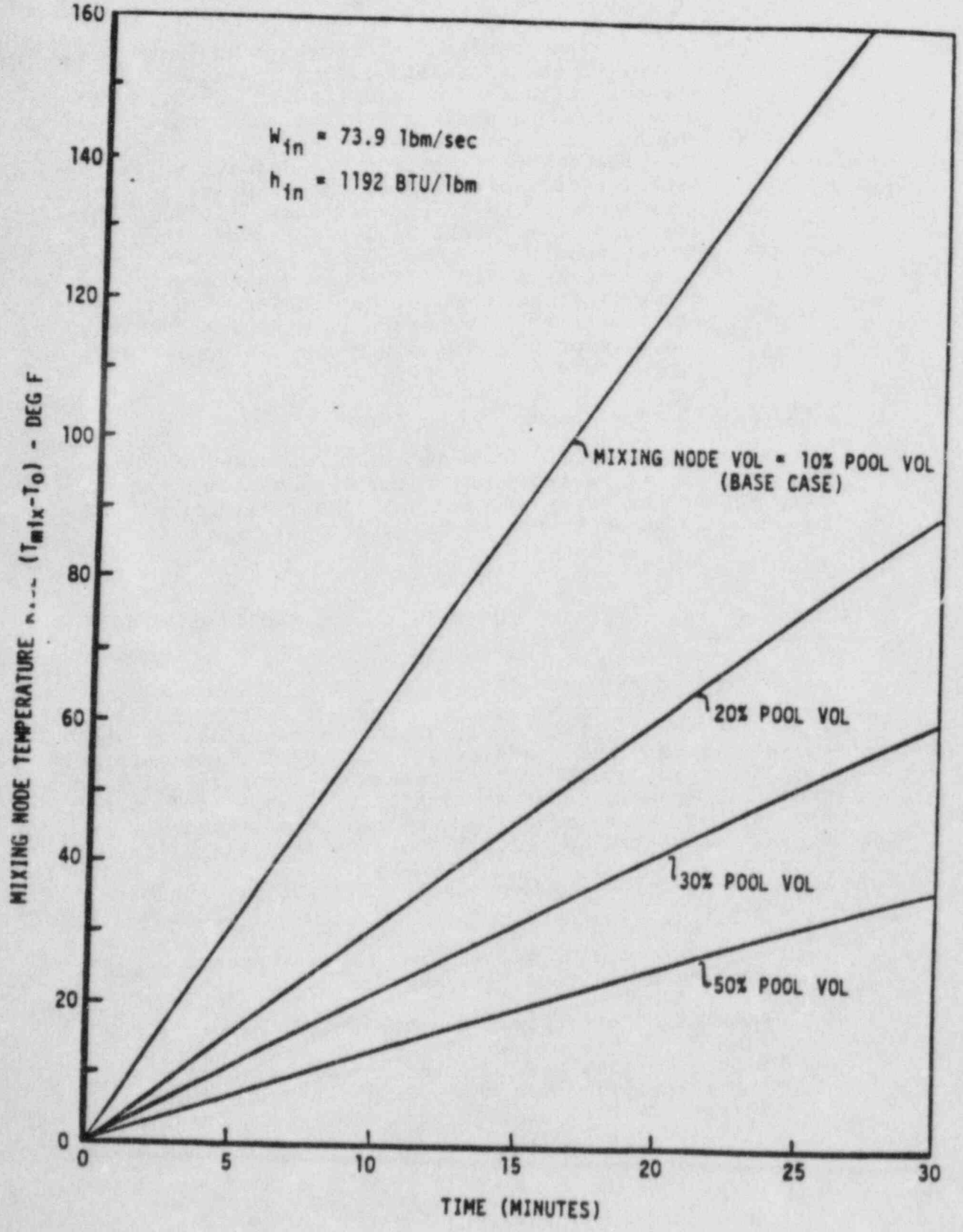

FIGURE 9-5
EFFECT OF MIXING NODE VOLUME ON LOCAL POOL TEMPERATURES

Action Plan 10 - Plant Specific

I. Issues Addressed

4.1 The present containment response analyses for drywell break accidents assume that the ECCS systems transfer a significant quantity of water from the suppression pool to the lower regions of the drywell through the break. This results in a pool in the drywell which is essentially isolated from the suppression pool at a temperature of approximately 135°F. The containment response analysis assumes that the drywell pool is thoroughly mixed with the suppression pool. If the inventory in the drywell is assumed to be isolated and the remainder of the heat is discharged to the suppression pool, an increase in bulk pool temperature of 10°F may occur.

II. Program for Resolution

A calculation will be made that assumes that the drywell pool is isolated after the blowdown fills up to the top of the weir wall and that the remainder of the blowdown is added to the suppression pool.

III. Status

Item 1 is complete and results are included in this submittal.

IV. Final Program Results*

GSU's River Bend FSAR analyses for large breaks in the drywell were conducted using the SWEC proprietary computer code LOCTVS. A general description of the code is given in Attachment 10.1. The following assumptions were made in the analyses for all pipe breaks postulated to occur inside the drywell:

1. The reactor is initially at 102 percent rated power.

2. A double-ended guillotine pipe rupture occurs instantaneously at time zero.

3. Loss of offsite power occurs at time zero.

4. Single active failure of the Division II diesel generator minimizes the availability of engineered safety feature (ESF) equipment for containment heat removal.

5. The maximum initial pool temperature is 100°F.

6. Conservatively low-heat transfer coefficients for heat transfer to heat sinks in drywell and containment are applied.

7. Metal water reaction energy is incorporated.

8. Decay heat, coastdown energy, and pump heat are absorbed by the coolant prior to release from the break.

9. Break flow is assumed to be a frictionless Moody critical flow after the initial inventory period.

The volume of the drywell pool is 20,353 cu ft to the top of the weir wall. With all the above assumptions, this volume is filled with water at an average temperature of 231°F, approximately 432 seconds after the LOCA. The formation of the drywell pool is due to the condensation of steam in the drywell from removal of heat by the passive heat sinks and ECCS water and the accumulation of the unflashed portion of the blowdown. Once the drywell pool is formed, any additional water is assumed to overflow the weir wall and enter into the suppression pool.

Drywell depressurization and reverse flow from the suppression pool is predicted to start approximately at 764 seconds. After this time, the drywell is at a negative pressure for the remainder of the transient as shown in FSAR Figure 6.2-4. The peak suppression pool temperature is 167.5°F at 17,203 seconds.

Considering the sources of the water which accumulates on the drywell floor (i.e., unflashed reactor coolant and heat sink condensate), there is no basis for assuming a pool of water isolated at the initial drywell temperature of 135°F. However, the increase in peak suppression pool temperature resulting from minimizing the temperature of the water isolated on the drywell floor was evaluated with manual calculations described in the following paragraphs.

The manual assessment was based on the LOCTVS results discussed previously, and modified to reflect no water storage on the drywell floor until drywell depressurization and subsequent weir wall overflow at 764 seconds. Prior to this time, all unflashed blowdown and heat sink condensate were added to the containment pool. As shown in Attachment 10.2, the addition of 20,353 cu ft of 231°F water to the containment pool resulted in a containment pool

temperature of 155.7°F at 764 seconds. This represents the minimum temperature of the water which could be isolated on the drywell floor for the remainder of the analysis.

Assuming that the drywell negative pressure is relieved at the time of peak suppression pool temperature predicted by LOCTVS (17,203 sec) yields an upperbound estimate of the increase in peak pool temperature resulting from drywell floor water mixing with the containment suppression pool. Excluding 20,353 cu ft of water at 155.7°F, we calculate an increase in peak suppression pool temperature from 167.5°F to 181°F as shown in Attachment 2.

The above analyses indicate that the suppression pool temperature may increase by as much as 13.5°F, considering the drywell pool to be isolated at the minimum temperature of 155.7°F. However, as shown above, the peak suppression pool temperature does not exceed the design value of 185°F.

Based on the above results, this issue is considered closed for RBS with this submittal.

*These revised program results replace the GSU-submitted results dated April 1, 1983.

TABLE 1

MASS AND ENERGY IN DRYWELL (DW) POOL AND SUPPRESSION POOL

	t = 769 sec(1)	t = 17,203 sec(2)
Mass of water on DW floor, LBM	1.239664×10^4	3.027529×10^4
Mass of water in suppression pool, LBM	7.734599×10^4	5.554833×10^4
Mass of water in vents and annulus, LBM	8.43568×10^3	1.209471×10^4
Energy of water on DW floor, Btu	2.3349×10^6	5.1235×10^6
Energy of water in suppression pool, Btu	8.8432×10^6	7.5242×10^6
Energy of water in vents and annulus, Btu	9.7014169×10^7	1.63825814×10^6

NOTE:

(1) Depressurization and weir overflow begins.
(2) Time of Peak Pool temperature.

ATTACHMENT 10.1

Description of LOCTVS Computer Code

LOCTVS is a SWEC proprietary computer code that has BWR Mark III containment system and phenomena simulation capability. A schematic diagram of LOCTVS code modeling is shown in Figure 10.1.

The code models the reactor coolant system, drywell, containment, suppression pool, and vents. In addition, the code includes models for the containment unit coolers, RHR heat exchangers, dynamic vent clearing, and heat transfer between the drywell and containment atmosphere to the respective concrete and steel structures.

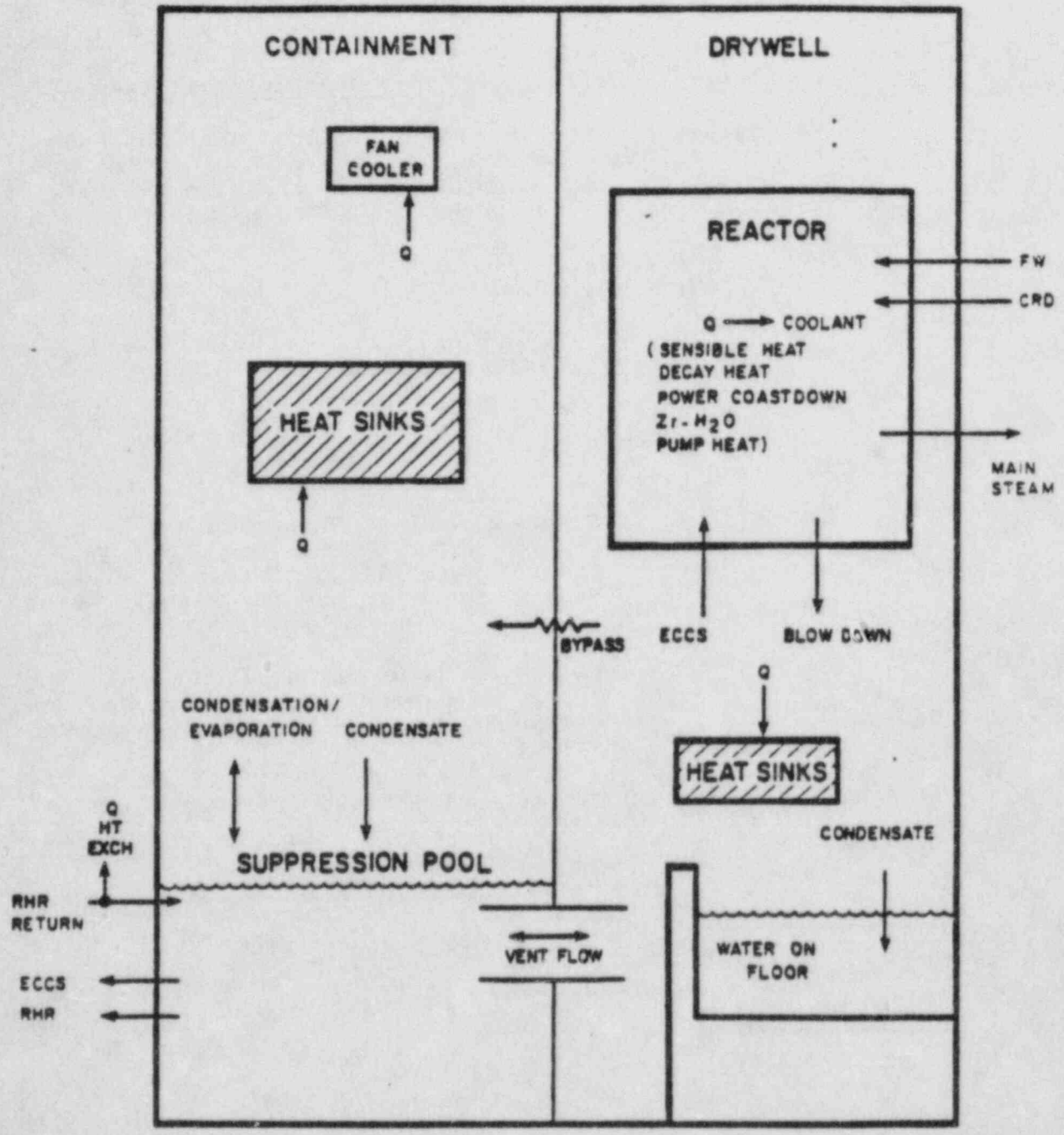

FIGURE 10-1 SCHEMATIC DIAGRAM OF LOCTVS CODE MODELLING

ATTACHMENT 10.2

Supplemental Calculations for Resolution of Issue 4.1

If we assume all the unflashed blowdown mass and heat-sink condensate is added to the suppression pool instead of accumulating on the drywell floor, the temperature of the suppression pool at 764 seconds would be as follows:

$$T_{pool} = \frac{(U_1+U_2+U_3)}{(M_1+M_2+M_3)} + 32$$

$$= \frac{(2.3349+8.8432+0.9701)\ 10^6}{(1.239664+7.734599+0.843568)\ 10^6} + 32$$

$$= 155.7^\circ F$$

Where:

T_{pool}	-	Suppression Pool Temperature (°F)
M_1	-	Mass of Water on DW Floor (lbm)
M_2	-	Mass of Water in Suppression Pool (lbm)
M_3	-	Mass of Water in the Annulus and Vents (lbm)
U_1	-	Energy of Water on DW Floor (Btu)
U_2	-	Energy of Water in Suppression Pool (Btu)
U_3	-	Energy of Water in the Annulus and Vents (Btu)

NOTE: Values of variables are taken from Table 1

1. Drywell Pool at 155.7°F

If the operator relieves drywell negative pressure at the time of peak suppression pool temperature, the water on the drywell floor, except that which is assumed isolated within the weir wall, would flow into the containment suppression pool. Also, if we make the assumption that the drywell floor water within the weir wall is isolated at 155.7°F, the resulting peak suppression pool temperature would be:

$$T_{pool} = \frac{(U_1+U_2+U_3) - V/v(155.7-32)}{(M_1+M_2+M_3) - V/v} + 32$$

$$= \frac{(7.5242+5.1235+1.638)\ 10^8 - \frac{20,353}{0.016374}(155.7-32)}{(5.554833+3.027529+1.209471)\ 10^6 - \frac{20,353}{0.016374}} + 32$$

$$= 181.1°F$$

Where:

V - Volume of water on drywell floor to the top of the weir wall = 20,353 cu ft

v - Specific volume of water on drywell floor to the top of the weir wall = 0.016374 cu ft/lbm

2. Drywell Pool at 135°F

If the drywell pool is assumed to be isolated at 135°F, the resulting peak suppression pool temperature would be equal to 184.1°F using the above equation.

3. No Drywell Pool

If we assume no drywell pool is formed, the resulting peak suppression pool temperature would be equal to 178°F.

Action Plan 11 - Plant Specific

I. Issues Addressed

4.2 The existence of the drywell pool is predicated upon continuous operation of the ECCS. The current emergency procedure guidelines require the operators to throttle ECCS operation to maintain vessel level below level 8. Consequently, the drywell pool may never be formed.

9.1 The current FSAR analysis is based upon continuous injection of relatively cool ECCS water into the drywell through a broken pipe following a design basis accident. The EPGs direct the operator to throttle ECCS operation to maintain reactor vessel level at about level 8. Thus, instead of releasing relatively cool ECCS water, the break will be releasing saturated steam, which might produce higher containment pressurizations than currently anticipated. Therefore, the drywell air which would have been drawn back into the drywell will remain in the containment, and higher pressures will result in both the containment and the drywell.

II. Program for Resolution

1. A calculation will be performed, demonstrating that continuous addition of saturated steam to the drywell, and the failure to form the drywell pool will not produce pressures or temperatures above the design conditions.

III. Status

Item 1 is complete and results are included in this submittal.

IV. Final Program Results*

The operators' action to maintain water level in the reactor vessel below level 8 may impact the following items:

1. Suppression Pool Temperature and Volume

Since the drywell remains pressurized due to the continuous addition of steam from the break, there may not be any weir overflow from the suppression pool, and the drywell pool may not be formed.

Therefore, the suppression pool temperature and volume may be different than that which is published in the RBS FSAR.

2. Containment and Drywell Pressures

Due to sustained drywell pressurization, the drywell air that is purged into the containment during the early part of the accident transient may not return to the drywell. This may result in containment and drywell pressures that are different in the long term than those published in the FSAR.

3. Drywell Bypass Leakage

Because of the continued drywell pressurization, the maximum allowable suppression pool bypass leakage capability may be lower than that which is published in the FSAR.

The above items are addressed separately as discussed below. Four break sizes ranging from small to large were analyzed with the SWEC CONSBA Computer Code.

CONSBA is a SWEC proprietary computer code that has Mark III system and phenomena simulation capability. A schematic of the CONSBA code modeling is shown in Figure 1. In general, CONSBA models the reactor coolant system, drywell, containment, suppression pool, emergency core cooling systems (ECCS), and safety relief valve (SRV) system. The code also includes models for passive heat sinks, containment unit coolers, residual heat removal heat exchangers, and suppression pool steam bypass leakage. Written primarily for small break analysis, CONSBA models static vent clearing, reactor water level for on-and-off control of the ECCS, and various modes of SRV operation, including operator-controlled reactor cooldown at a specified rate.

The CONSBA code has an input option of all-steam blowdown. The analyses were performed with the all-steam blowdown option, and the results are shown in Figures 2 through 9.

1. Suppression Pool Temperature and Volume

The predicted peak temperature results are as below:

Break Size (sq ft)	Suppression Pool Temp (°F)
0.01	178.3
0.1	176.5
1.0	173.5
2.6	168.4

The suppression pool temperature analysis described in FSAR Appendix 6A identifies the limiting case as a stuck-open relief valve (SORV) event. The peak suppression pool temperature for this case is 185°F. Therefore, failure to form the drywell pool after a LOCA does not result in a more limiting or higher peak pool temperature than previously analyzed.

2. Containment and Drywell Pressures

The peak pressures in the drywell and containment for the four break sizes analyzed are given below. It should be noted for all these cases, the drywell air remains in the containment due to sustained drywell pressurization.

Break Size (sq ft)	Peak Drywell Pressure (psia)	Peak Containment Pressure (psia)
0.01	22.6	19.79
0.1	22.6	19.73
1.0	21.7	19.67
2.6	25.9	19.36

As can be seen, the maximum peak containment pressure is reached for a small break accident. Even if it is assumed unrealistically that the containment temperature reaches the design temperature of 185°F, the peak containment pressure will be only 22 psia (7.3 psig). This gives 105-percent margin between the maximum expected and the containment design pressure. For the drywell, the peak pressure of 33.76 psia is reached at 1.17 seconds after a main steam line DER as shown in FSAR Figure 6.2-4.

3. Drywell Bypass Leakage

This is addressed under Action Plan 19.

Based on the above results, these issues are considered closed for RBS with this submittal.

*These revised program results replace the GSU-submitted results dated April 1, 1983.

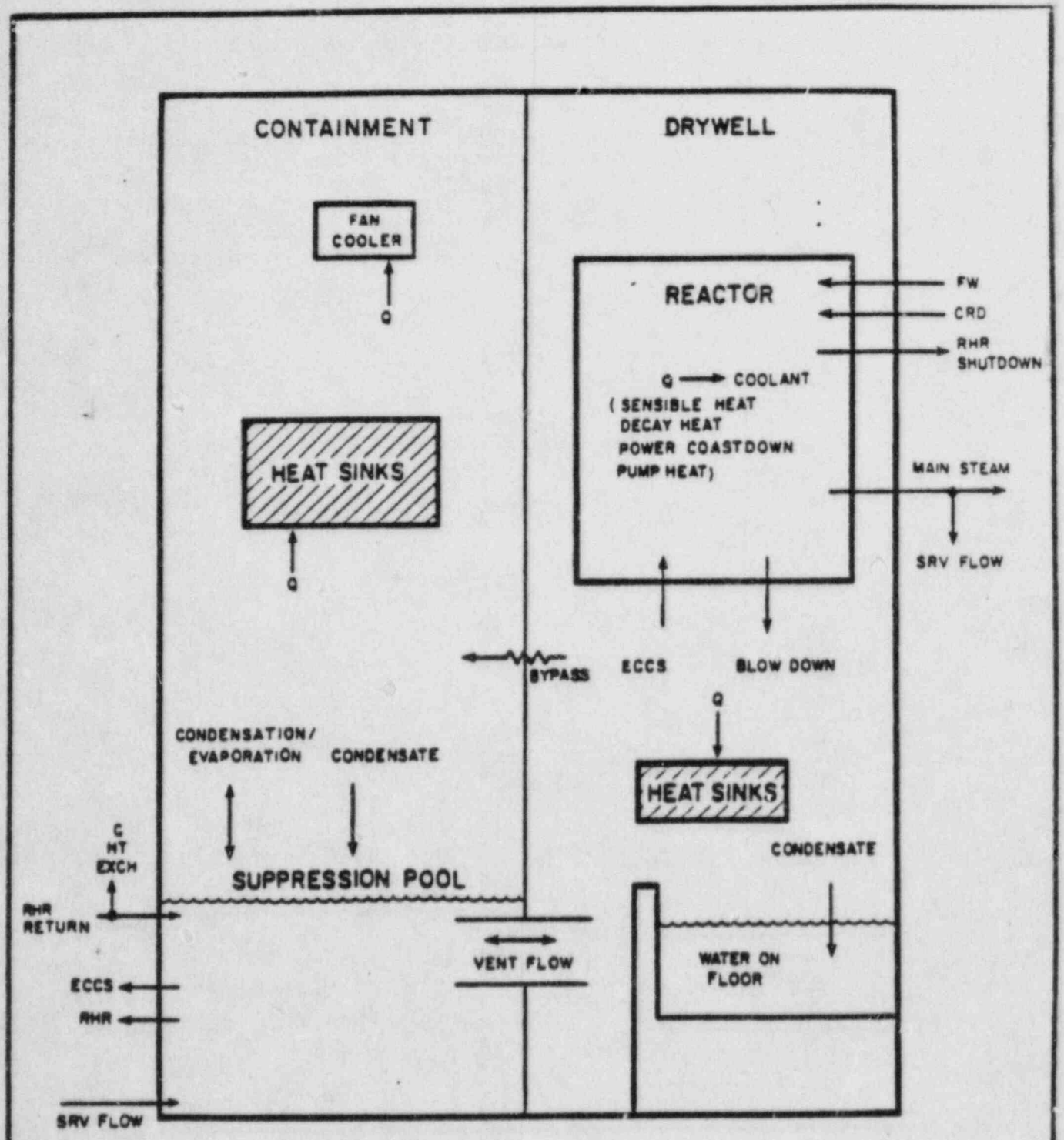

Figure 11.1

SCHEMATIC DIAGRAM OF CONSBA CODE MODELLING

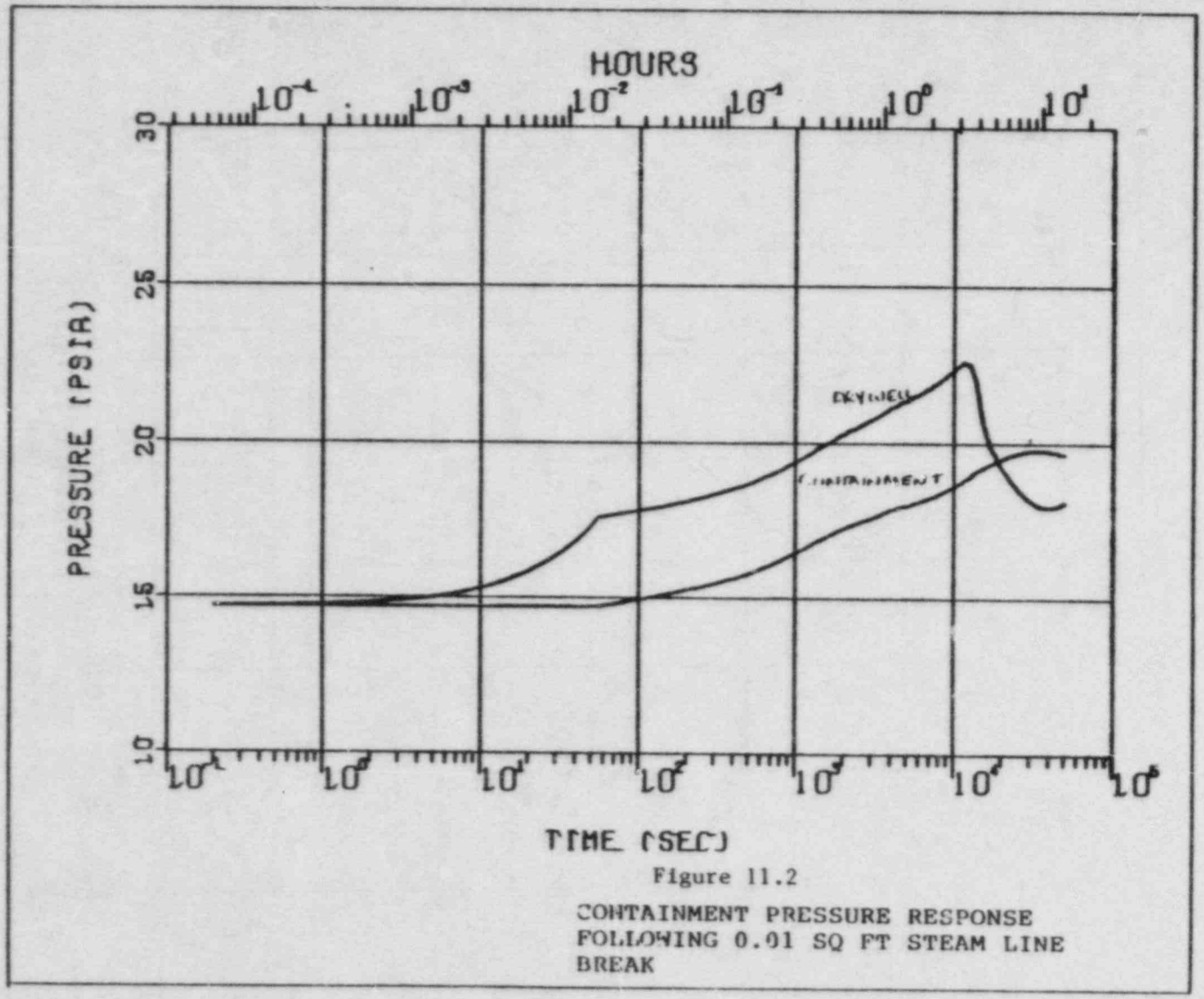

Figure 11.2

CONTAINMENT PRESSURE RESPONSE FOLLOWING 0.01 SQ FT STEAM LINE BREAK

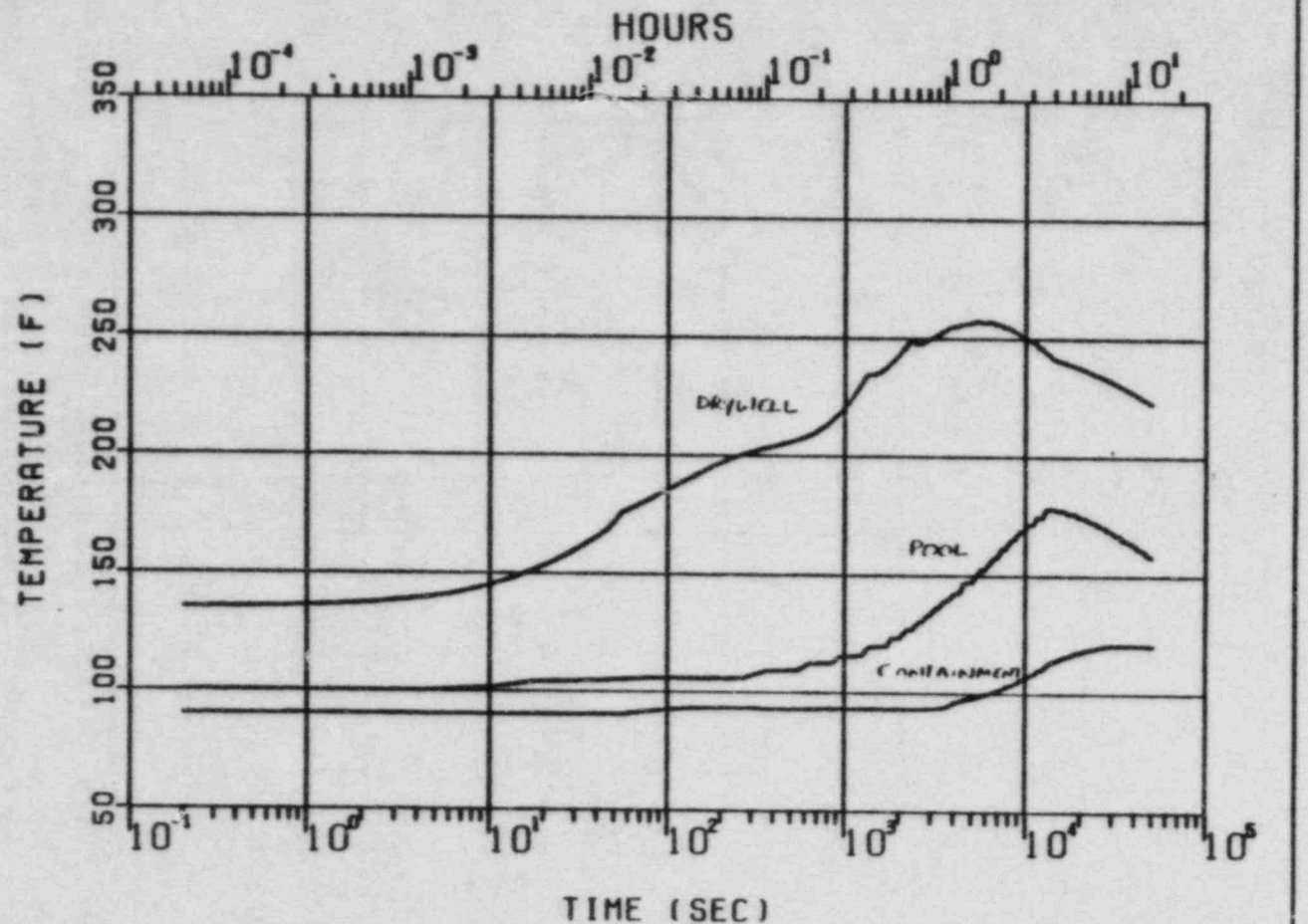

Figure 11.3

CONTAINMENT TEMPERATURE RESPONSE FOLLOWING 0.01 SQ FT STEAM LINE BREAK

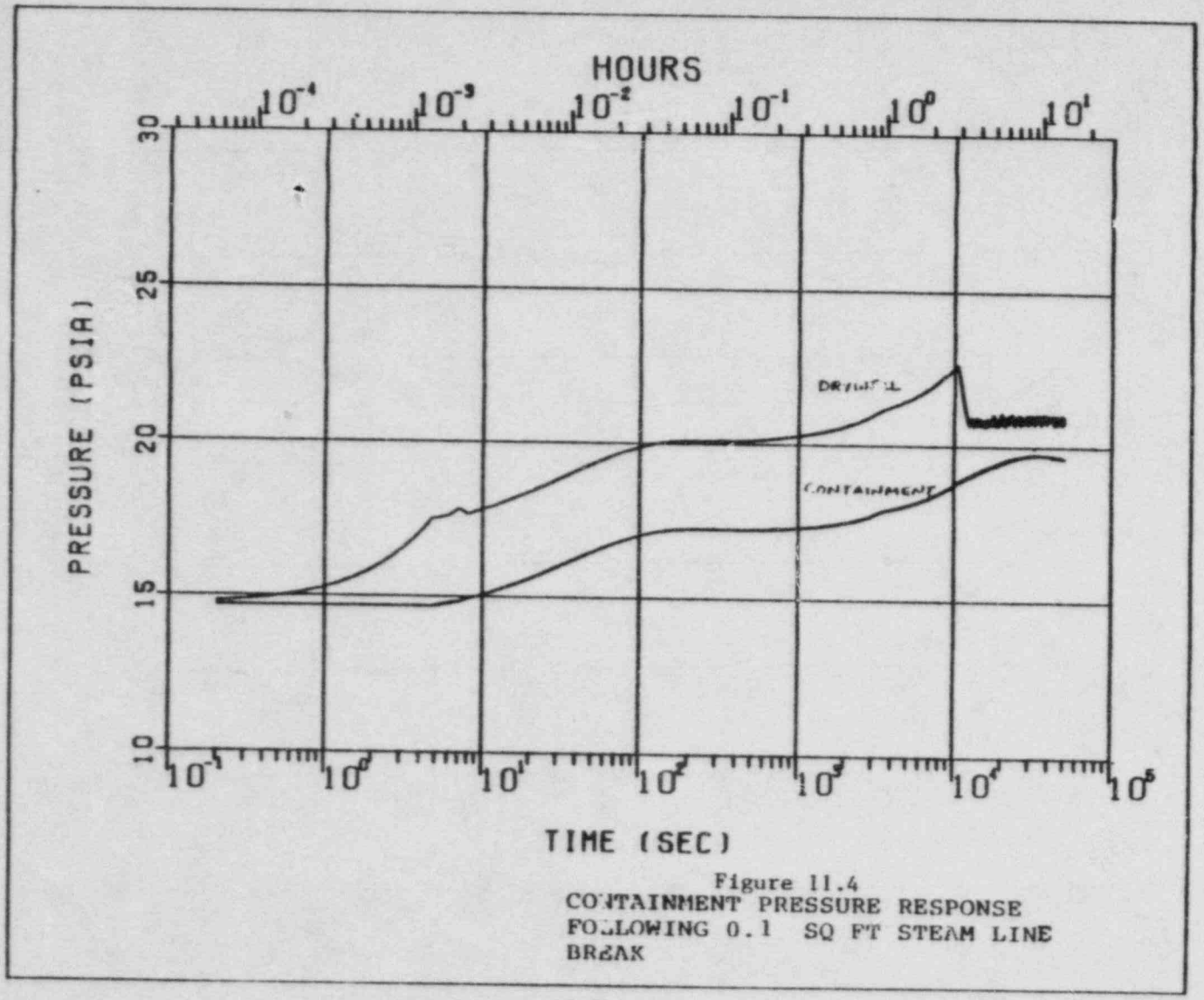

Figure 11.4
CONTAINMENT PRESSURE RESPONSE
FOLLOWING 0.1 SQ FT STEAM LINE
BREAK

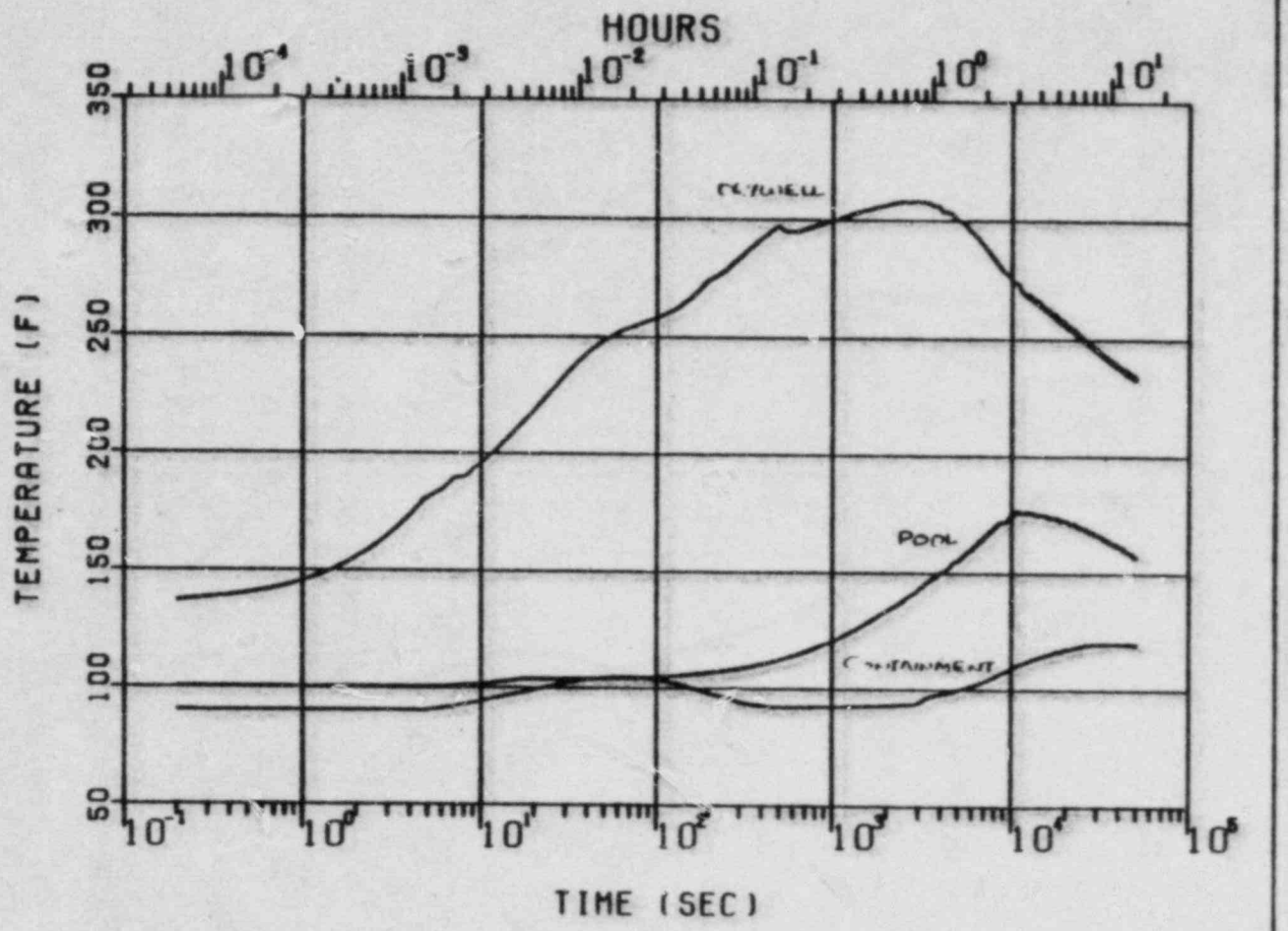

Figure 11.5
CONTAINMENT TEMPERATURE RESPONSE
FOLLOWING 0.1 SQ FT STEAM LINE BREAK

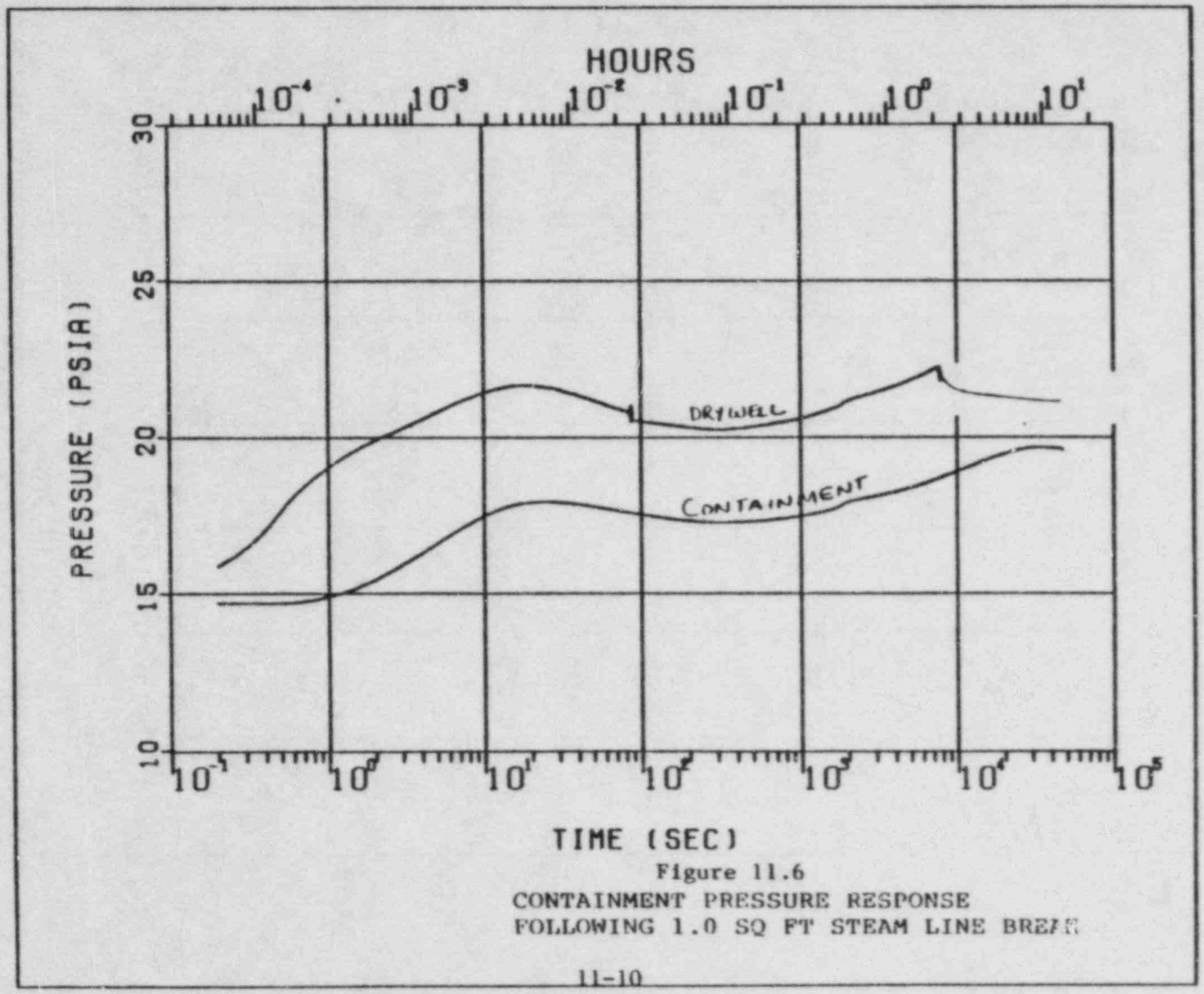

Figure 11.6
CONTAINMENT PRESSURE RESPONSE
FOLLOWING 1.0 SQ FT STEAM LINE BREAK

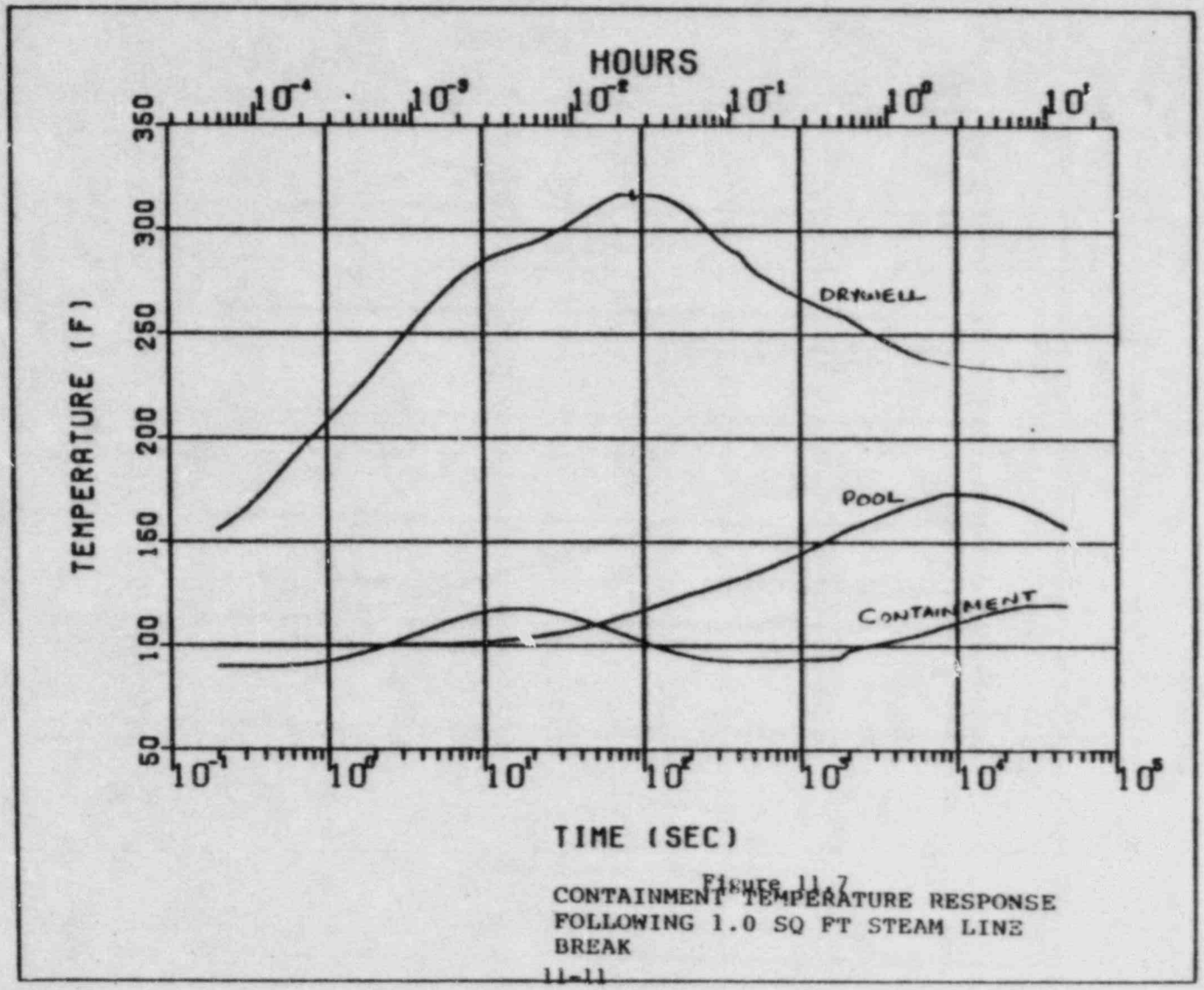

Figure 11.7
CONTAINMENT TEMPERATURE RESPONSE FOLLOWING 1.0 SQ FT STEAM LINE BREAK

KUN 53611RK7 3979

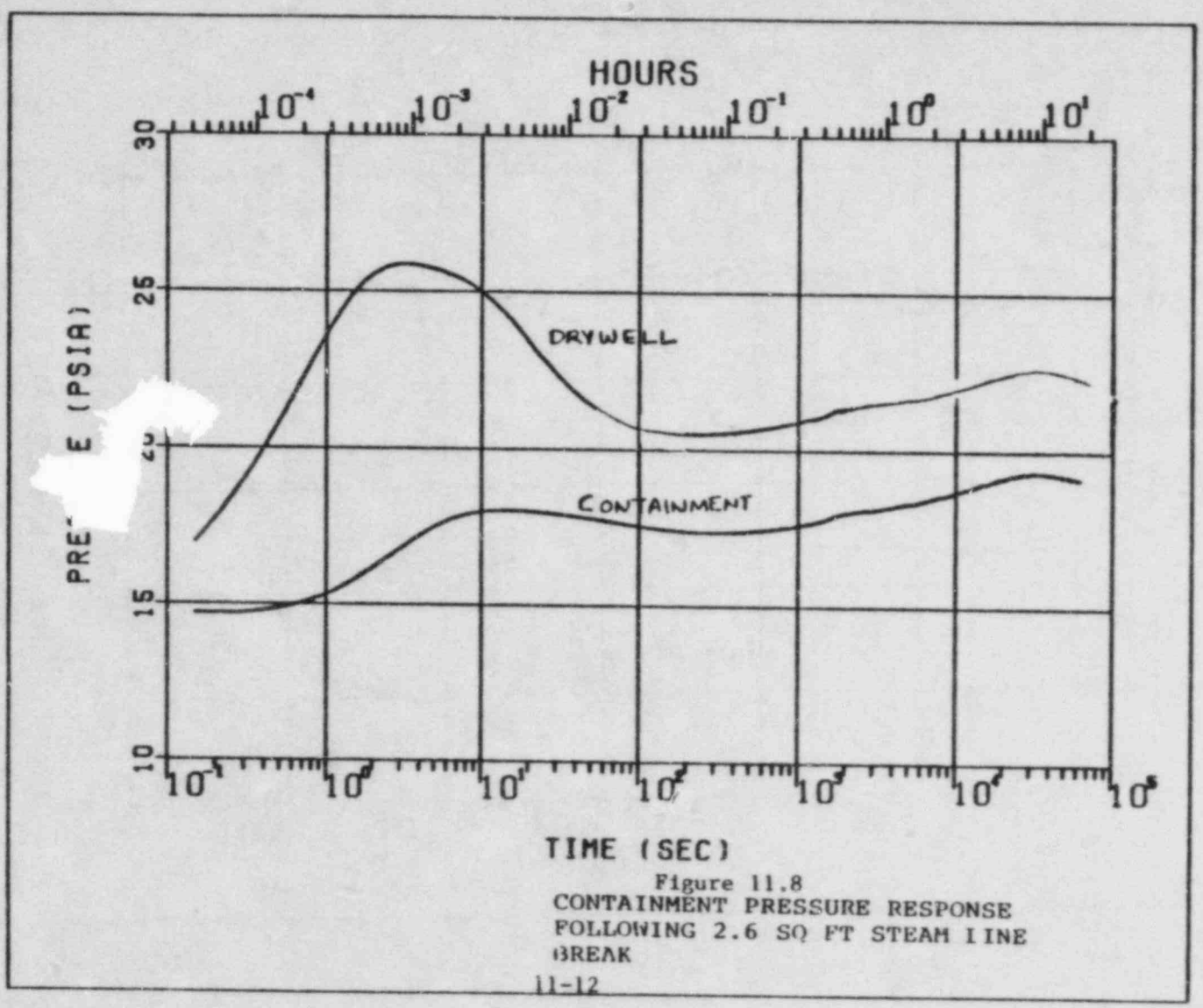

Figure 11.8
CONTAINMENT PRESSURE RESPONSE
FOLLOWING 2.6 SQ FT STEAM LINE
BREAK

RUN 5361I RA7 3979

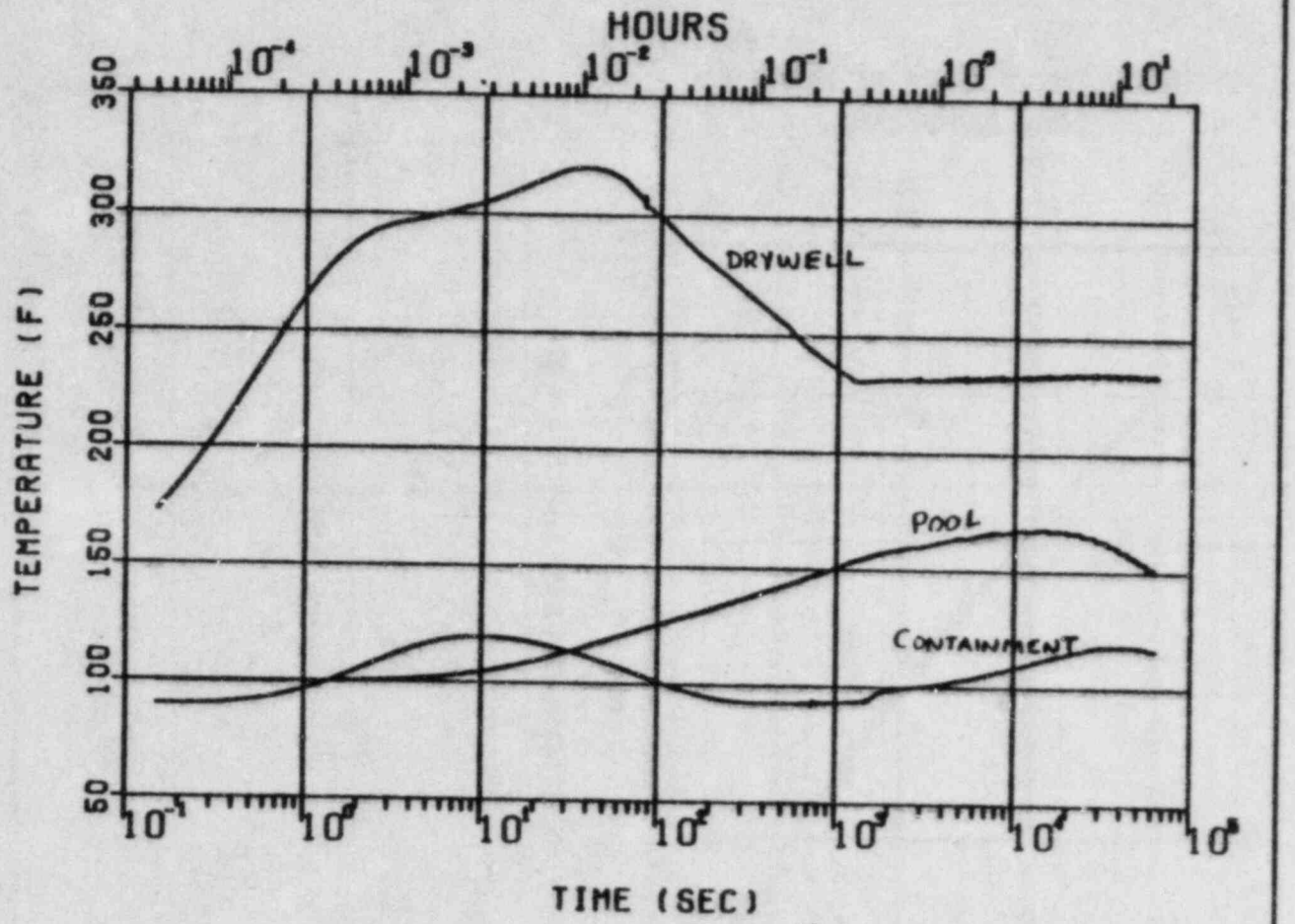

Figure 11.9
CONTAINMENT TEMPERATURE
RESPONSE FOLLOWING 2.6 SQ FT
STEAM LINE BREAK

Action Plan 12 - Plant Specific

I. Issues Addressed

4.3 All Mark III analyses presently assume a perfectly mixed, uniform suppression pool. These analyses assume that the temperature of the suction to the RHR heat exchangers is the same as the bulk pool temperature. In actuality, the temperature in the lower part of the pool where the suction is located will be as much as 7 1/2°F, cooler than the bulk pool temperature. Thus, the heat transfer through the RHR heat exchanger will be less than expected.

II. Response

The River Bend Station analysis assumes that the RHR suction temperature is 5°F less than the bulk suppression pool temperature. In addition, a sensitivity analysis on the RHR heat exchanger heat transfer coefficient shows that containment peak pressure is not very sensitive to the RHR Hx heat transfer coefficient (see FSAR Figure 6.2-36 included as Attachment 12.1).

III. Status

Based on the above response, this issue is considered closed for RBS with this submittal.

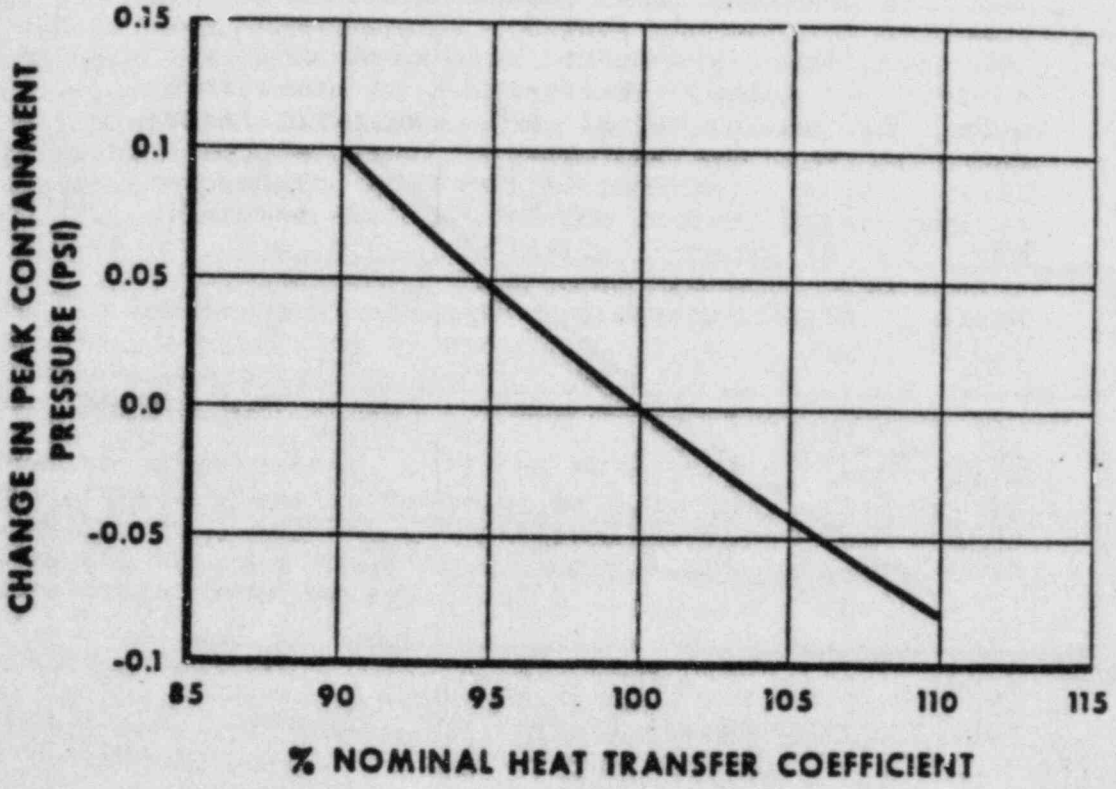

FIGURE 6.2-36

SENSITIVITY OF PEAK CONTAINMENT PRESSURE TO RHR HEAT EXCHANGER HEAT TRANSFER COEFFICIENT

RIVER BEND STATION

FINAL SAFETY ANALYSIS REPORT

Action Plan 13 - Plant Specific

1. Issues Addressed

4.4 The long-term analysis of containment pressure/temperature response assumes that the wetwell airspace is in thermal equilibrium with the suppression pool water at all times. The calculated bulk pool temperature is used to determine the airspace temperature. If pool thermal stratification were considered, the surface temperature, which is in direct contact with the airspace, would be higher. Therefore the airspace temperature (and pressure) would be higher.

7.1 The containment is assumed to be in thermal equilibrium with a perfectly mixed, uniform temperature suppression pool. As noted under Topic 4, the surface temperature of the pool will be higher than the bulk pool temperature. This may produce higher-than-expected containment temperatures and pressures.

II. Response

The River Bend Station analysis assumes that the surface temperature of the suppression pool is 5°F greater than the bulk temperature. The containment and LOCA analysis, documented in FSAR Section 6.2.1, incorporates this assumption.

III. Status

Based on the above response, these issues are considered closed for RBS with this submittal.

Action Plan 14 - Generic

I. Issues Addressed

4.5 A number of factors may aggravate suppression pool thermal stratification. The chugging produced through the first row of horizontal vents will not produce any mixing from the suppression pool layers below the top vent row. An upper pool dump may contribute to additional suppression pool temperature stratification. The large volume of water from the upper pool further submerges RHR heat exchanger effluent discharge, which will decrease mixing of the hotter, upper regions of the pool. Finally, operation of the containment spray eliminates the heat exchanger effluent discharge jet, which contributes to mixing.

II. Program for Resolution*

Testing information will be submitted to demonstrate the effectiveness of chugging as a mixing mechanism in the suppression pool. Additionally, River Bend design does not use the upper pool dump concept and does not have containment sprays.

III. Status

Item 1 is complete and results are included in this submittal.

IV. Final Program Results*

Data from the 1/3-Area Scale Condensation and Stratification Tests (Test Series 5807) performed in GE's Pressure Suppression Test Facility (PSTF) shows that chugging is effective in mixing the suppression pool. These tests are described completely in Reference 1.

Briefly, these tests were performed to quantify both chugging loads and also the degree of thermal stratification that could occur during the blowdown phase of a LOCA. Part of the instrumentation of these tests consisted of drag discs to measure flow velocities in the bottom two vents of the three-vent system. The location of these instruments is shown in Figure 14-1.

Following a break in the drywell and the resultant vent clearing process, steam will be injected into the

suppression pool through the vents. Some 20 to 30 seconds later, as the vent mass flowrate and drywell pressure decrease, water will rise in the vent system, eventually flooding the bottom and middle vents with water. At some 30 to 60 seconds post-LOCA, as the mass flowrate decreases further, chugging will begin in the top vent.

Figure 14-2 shows the response of the drag discs from PSTF Test 5807 Run 16, a 1-inch (approximately 16 percent DBA) blowdown having an initial pool temperature of 150°F. As may be seen, the drag discs are initially excited during the vent clearing and steam flow portions of the transient, but then become quiescent during the period of quasi-steady steam flow through the top vent. Chugging begins about 55 seconds into the transient, after which periodic swings in the liquid flow occur in both the middle and bottom vents. This same behavior is seen in all chugging data.

By performing a time integration of the vent liquid flowrates, it may be concluded that on the average, more flow is entering the vent system through the bottom two vents during the inflow portion of the transient than is exiting during the outflow portion. Obviously, the excess water must exit through the top vent. Hence, the phenomenon of Mark III chugging, although confined to the top vent in terms of condensation, does affect the response of the entire vent system. In fact, the vent system performs as a pump, pulling water in from the lower portions of the suppression pool and expelling it through the top vent and into the upper half of the pool.

This behavior is caused by the relative inertia of the water in the weir and vents, and the directional nature of the vent turning and exit loss coefficients.

An analysis was performed to quantify the effectiveness of chugging in mixing the suppression pool. The analysis included runs with break sizes ranging from 1-inch to 3-inch and initial suppression pool temperatures ranging from 75°F to 155°F.

A mass balance was calculated on the bottom two vents by integrating the curves of vent flowrate versus time, concluding that the remaining flow enters the top vent on the weir annulus side and then flows into the suppression pool. Knowing the amount of mass entering the suppression pool from the top vent for a given interval of time, the time required for the total volume of the pool to enter the bottom vents and exit via the top vent could be calculated. Suppression pool

turnover times due to chugging were found to be less than 10 minutes for all cases considered. Table 14-1 shows the results of these calculations.

Pool turnover times were also calculated due solely to the RHR System. These turnover times were found to be 135 minutes for the case of one pump running and 45 minutes when all three pumps were activated. The startup tests performed at the Kuo-Sheng BWR/6 Mark III plant in Taiwan demonstrated that operation of the RHR system effectively mixed the suppression pool and limited thermal stratification. A comparison of pool turnover times due to the RHR system and the phenomena of chugging clearly support the latter as an effective means of suppression pool mixing.

A plot of pool turnover time versus mass flux shown in Figure 14-3 illustrates that pool turnover time is not dependent on the mass flux or initial pool temperature. Therefore, this data would be expected to be valid for any set of conditions which might occur during an actual plant transient.

Figure 14-4 shows measured pool thermal stratification from PSTF Test 5807 Run 29, a 1-inch (approximately 16 percent DBA) blowdown having an initial pool temperature of 75°F. Since in a 1-inch break case all steam is input to the pool via the top vent, energy is added to the pool only at an elevation of 11 feet. As the pool heatup transient progresses, it is seen that temperature increases occur over the entire elevation of the suppression pool. Temperature increases below the 11-ft elevation are due solely to the effect of mixing by flow through the bottom two vents. If chugging were not effective in mixing the suppression pool, a sharp increase in temperature would be seen above the top vents with no increase in temperature at low levels. Clearly, this is not the case.

In summary, it has been shown that the effects of Mark III chugging are not limited to the top vent, and that the fluid mechanics of weir and vent clearing and recovery is such that mass is effectively moved from the lower regions of the suppression pool to the upper regions. This pumping action is at least as, and probably more, efficient than the RHR system for mixing the pool and limiting thermal stratification.

V. Conclusions

Chugging through the top row of horizontal vents provides an exceptional mechanism for thoroughly mixing the Mark III suppression pool. The pool is turned over

completely as frequently as once every 10 minutes, which is substantially more rapidly than the RHR system processes the water. Chugging will be present under all accident conditions and will be sufficient to completely mix the pool. Therefore, adequate assurance exists that sufficient mixing will occur and effectively prevent excessive stratification.

References

1. A.M. Varzaly et al, Mark III Confirmatory Test Program - 1/3-Scale Condensation and Stratification Phenomena - Test Series 5807, NEDE-21596-P, March 1977. (General Electric Company Proprietary Report)

*This revision replaces the GSU submittal dated April 1, 1983.

Table 14-1

CHUGGING - POOL MIXING

TEST SERIES 5807

Run	Time of Analysis (sec)	Venturi Diameter (in.)	Initial Pool Temperature (°F)	Vent Steam Mass Flux (lbm/ft²sec)	Mean Middle Vent Liquid Flow (lbm/sec)	Mean Bottom Vent Liquid Flow (lbm/sec)	Turnover Time (min)
15	30.5	1.0	148	3.05	-65.3	-35.8	9.1
16	22	1.0	150	3.35	-113.6	-62.7	5.32
11	20	1.0	76	3.16	-158.8	-29.8	4.98
29	30.5	1.0	75	2.54	-90.3	-19.9	8.52
17	21	3.0	152	2.55	-142.5	-3.4	6.43
18	20	3.0	155	1.81	-123.3	-43.7	5.62
30	21	3.0	75	2.36	-87.2	-19.1	8.82
12	21.5	3.0	79	1.89	-152.5	-14.6	5.6

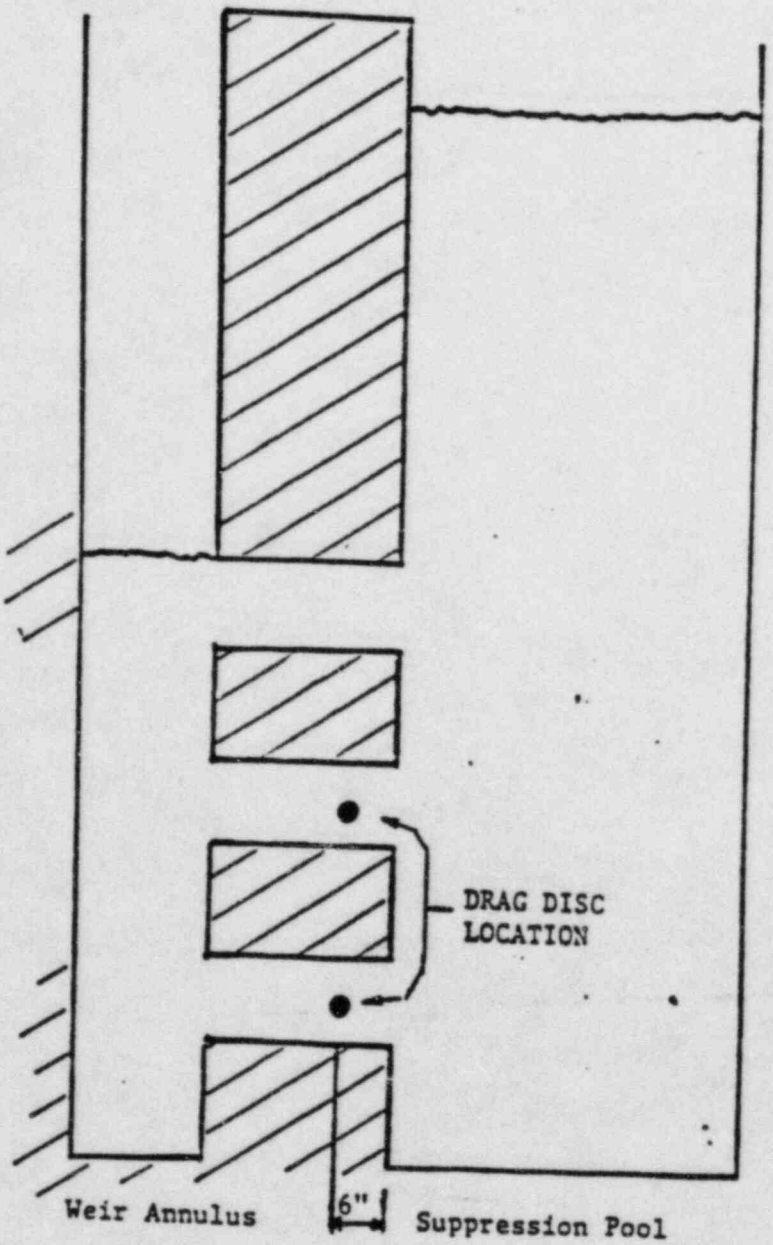

Figure 14-1 Drag Disc Location

Pages 14-7 through 14-9

These pages represent General Electric Company Proprietary Figures 14-2 through 14-4. These figures have been previously provided to the NRC via MP&L's August 19, 1982 submittal (Reference No. AECM-82/353).

Action Plan 15 - Plant Specific

I. Issues Addressed

The initial suppression pool temperature is assumed to be 95°F, while the maximum expected service water temperature is 90°F for all GGNS accident analyses as noted in FSAR Table 6.2-50. If the service water temperature is consistently higher than expected, as occurred at Kuosheng, the RHR system may be required to operate nearly continuously in order to maintain suppression pool temperature at or below the maximum permissible value.

II. Program for Resolution

1. A discussion of peak service water temperature which is expected under nonaccident conditions will be provided. Also the expected peak suppression pool temperature under normal operating conditions will be discussed.

2. The conservatisms in the analysis defining peak service water temperature will be quantified to the extent possible.

III. Status

Items 1 and 2 are complete and are included with this submittal.

IV. Final Results

The River Bend Station analysis uses an initial suppression pool temperature of 100°F and a service water temperature of 95°F. The worst-case maximum standby service water temperature is 90°F for RBS, as described in FSAR Section 9.

During the normal plant operation (excluding test conditions), the only possible mechanism to raise the pool temperature is leakage through the main steam safety relief valves. A simplified suppression pool heatup analysis assuming 20 lb/hr steam leakage from each of the 16 main steam safety relief valves was performed. The result, as shown in Figure 15.1, shows that it takes 4.4 days to raise the pool temperature from 100 to 105°F and 2.25 hr for the RHR system (with 95°F service water temperature) to cool the pool back down to 100°F.

The RHR system is capable of reducing the pool temperature in a relatively short time. Thus no

problems should develop which would mandate long-term operation of RHR system to control suppression pool temperature.

Based on the above response, this issue is considered closed for RBS with this submittal.

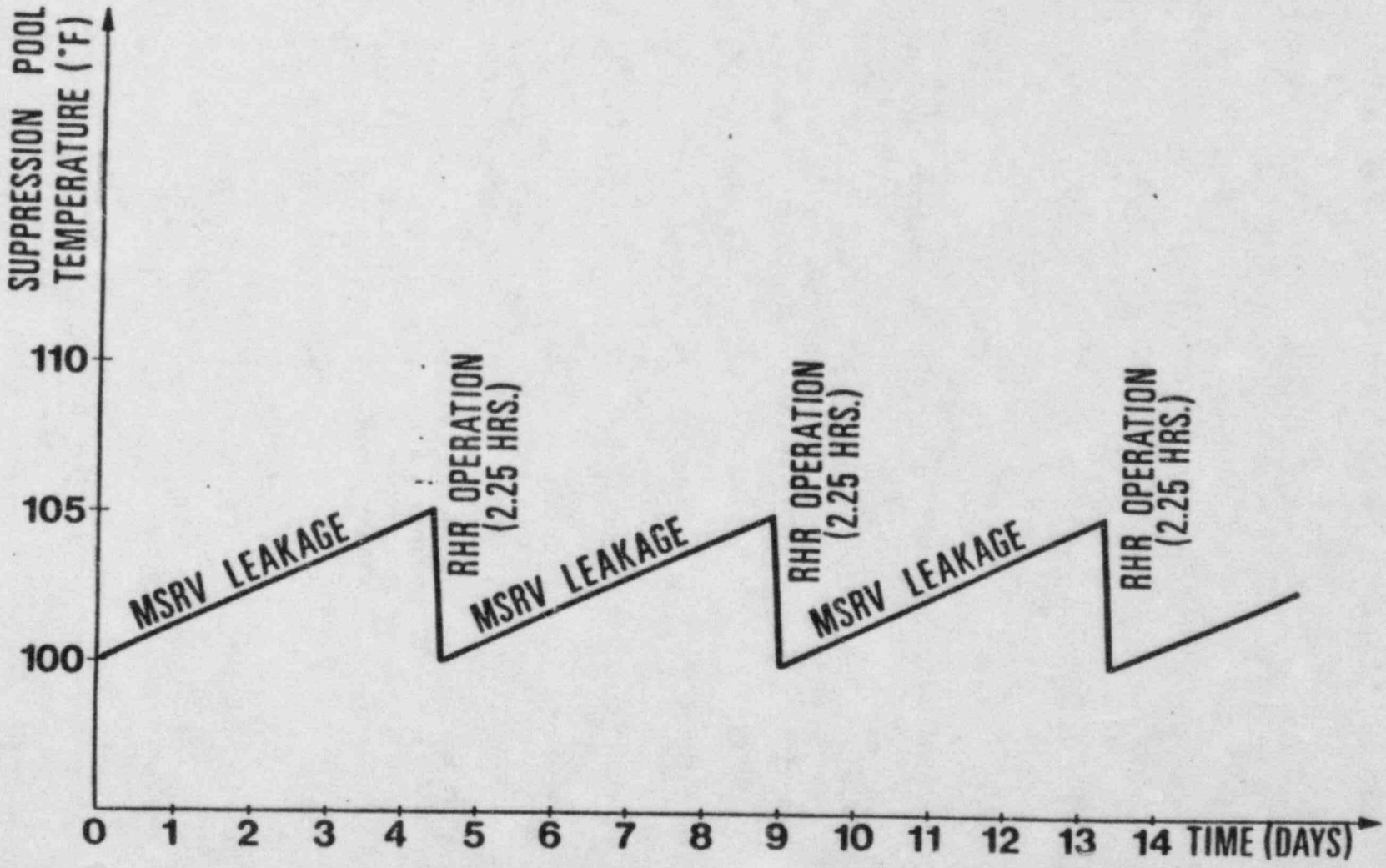

FIGURE 15.1 SUPPRESSION POOL TEMPERATURE DURING NORMAL OPERATION

Action Plan 16 - Generic

I. Issues Addressed

4.7 All analyses completed for the Mark III are generic in nature and do not consider plant-specific interactions of the RHR suppression pool suction and discharge.

4.10 Justify that the current arrangement of the discharge and suction points of the pool cooling system maximizes pool mixing (pages 150 through 155 of the May 27, 1982, transcript).

II. Program for Resolution

Information regarding RHR system effectiveness tests that have previously been conducted or that are in the planning stages will be evaluated. The evaluation is expected to show that a wide variety of RHR suction and discharge arrangements have been tested and are being tested under a variety of initial conditions. The arrangements used in the owners' plants will be compared to the various arrangements used in the previously noted tests.

III. Status

Item 1 is complete and included with this submittal.

IV. Final Results

A study has been performed using results from various RHR system effectiveness tests and analyses which have been completed. The results of this study are included as Attachment 16.1 of this submittal. Based on the results of this study, GSU has concluded that the present arrangement of RHR suction and discharge points is acceptable.

QUAD-1-82-245
Revision A

ATTACHMENT 16.1

A SURVEY OF TESTS AND ANALYSES ON THE EFFECTIVENESS OF THE RHR SYSTEM IN THE POOL-COOLING MODE

Prepared for:

Mark III Containment Issues Owners Group

By

Quadrex Corporation
1700 Dell Avenue
Campbell, California

November 1982

TABLE OF CONTENTS

1.0 INTRODUCTION

At the request of the Mark III Containment Issues Owners Group, Quadrex Corporation undertook a study of the existing test data and analyses pertaining to the effectiveness of the residual heat removal (RHR) system as a means of thermal mixing within the pressure suppression pool. The purpose of the study was to determine if sufficient data and supporting analyses existed to demonstrate the effectiveness of the RHR system in four plants with Mark III containments (Grand Gulf, Clinton, Perry, and River Bend) without the need for in-plant testing. Specifically, the questions to be addressed are the positions of the RHR suction and discharge and the possibility of short-circuiting and reduced mixing from a lack of suppression pool bulk motion.

The first task was to study the RHR suction and discharge geometry and the orientation of the discharge flow in the four plants. This was done by using drawings and documents supplied by the plants' architect-engineers.

The next task was to review existing test and analysis reports and summarize the pertinent findings that might be applicable to plants with Mark III containments. In some cases, complete reports were available; in other cases, only facts found in public-domain reports could be utilized.

The final task was to draw conclusions regarding the effectiveness of the RHR systems of the four Mark III containments on the basis of the findings resulting from the survey of the existing test and analysis reports.

A summary of the findings is presented in section 2.0, and section 3.0 gives a description of the RHR system suction and return geometries and orientations for each of the four plants. This description is followed by a brief summary in section 4.0 of each test or analysis report reviewed. Section 5.0 presents the conclusions drawn from the available data and information.

2.0 SUMMARY OF FINDINGS

- Short-circuiting of the RHR flow, i.e., the direct flow of some of the RHR system discharge to the RHR system suction line, is not likely to occur.

- After about 15 minutes of RHR system operation, the suction temperature is close to the bulk temperature.

- Operation of one RHR system loop breaks up initial pool stratification at the rate of 1.5 to 1.8°F/min; therefore, a period of 10 to 15 minutes of RHR system operation is sufficient to produce practically uniform temperature distribution in an initially stratified pool.

- Three to four minutes of operation of one RHR system loop can produce an average suppression pool bulk velocity of approximately 0.4 ft/s in an initially quiescent pool.

- The data and analyses reviewed dealt exclusively with the operation of one RHR system loop. No data could be found on the operation of two loops or on the effect of the two loops' discharging in opposite circumferential directions. However, based on considerations of continuity and conservation of momentum, global flow patterns were developed. They show the effectiveness of the existing RHR system suction and discharge arrangements in domestic plants with Mark III containments.

- The concern regarding the effect of opposing RHR system discharges and the claim that each jet will impede the effectiveness of the other in providing suppression pool mixing are without technical bases. Opposing jets produce a different flow pattern but probably afford as much thermal mixing as jets that point in the same direction.

3.0 SURVEY OF RHR SYSTEM SUCTION AND RETURN ARRANGEMENTS

Some of the information presented in this section was obtained from preliminary drawings, and some of the dimensions were estimated and may not be accurate. As far as thermal mixing of the pool is concerned, the main features of the RHR system of interest are:

- Azimuthal location of the discharge nozzles or elbows,
- Direction of the return flow,
- Distance between the discharge nozzle and the pool bottom, and
- Location of the suction strainers and their distance from the discharge nozzles and from the pool bottom.

The above information is summarized in figures 1 through 7 and described below.

3.1 Clinton Power Station, Unit 1

The RHR system return elbows are located at azimuthal angles 275° and 94°; the suction strainers, at 37° and 323° (see figure 1). The discharge flow makes a 55° angle with the radial axis, and both pumps discharge counterclockwise. The discharge points are 14 feet 11 inches from the bottom of the pool and 3 feet 6 inches from the containment shell (see figure 2). The suction strainers are located 8 feet above the pool bottom and 3 feet 11 inches from the containment shell.

3.2 Grand Gulf Power Station

The RHR system return lines have 45° elbows at the discharge ends. The elbows are located at azimuthal angles of 90° and 270° (figure 3) and are pointed in opposite circumferential directions, i.e., one discharges clockwise and the other counterclockwise. The suction strainers are located at 32° and 328°.

The discharge points are at a distance of 14 feet 4 1/2 inches from the bottom of the pool, and the suction strainers are 10 feet 6 inches from the bottom (see figure 4) and 3 feet 10 inches from the containment wall.

3.3 Perry Power Station

The only information available for Perry Power Station is that contained in reference 1. Figure 5 shows the general arrangement of the suction and disharge for one of the RHR system pumps. The azimuthal angle between the suction and discharge points is estimated to be 18°. The discharge point is 16 feet 3/4 inch from the bottom of the pool and 5 feet 3/4 inch from the containment wall. The suction strainer is estimated to be 5 feet above the pool bottom. The locations of the second discharge and suction points are not known.

3.4 River Bend Station, Unit 1

The RHR system return points for pumps A and B are located at azimuthal angles 30° and 310°, respectively (see figure 6). They terminate at 90° elbows pointed in opposite circumferential directions. The discharge flow is tangential. Suction strainers are located at 165° (pump A) and 195° (pump B). Locations of the discharge and suction relative to the pool boundaries are shown in figure 7. The return point is 14 feet from the pool bottom and 2 feet 9 inches from the containment wall. The suction strainers are 3 feet 4 3/4 inches above the pool bottom and 2 feet 3 7/8 inches from the containment wall. These dimensions were obtained from preliminary drawings.

The results of the survey of RHR system suction and return arrangements are summarized in table 3.1. There is a certain amount of variation in the arrangement of RHR system discharge and suction among these four plants. For instance, the azimuthal angle between the two discharge points varies from 80° to 181°; the minimum angle between discharge and suction varies from 18° to 115°; and the distance of the suction strainer from the pool bottom ranges from 3 feet 4 3/4 inches to 10 feet 6 inches.

TABLE 3.1--Summary of RHR system discharge and suction locations

Geometry \ Plant	Clinton	Grand Gulf	Perry	River Bend
Angle between discharges	181°	180°	X	80°
Minimum angle between suction and discharge	48°	58°	~18°	115°
Direction of discharge flow	same	opposite	X	opposite
Distance of discharge from bottom	14'11"	14'4 1/2"	16' 3/4"	14'
Distance of suction from bottom	8'	10'6"	~5'	3'4 3/4"
Distance of discharge from containment	3'6"	X	5'3/4"	2'9"
Distance of suction from containment	3'11"	3'10"	X	2'3 7/8"
Angle of discharge relative to radial	55°	~55°	X	90°

X: Dimension unknown

4.0 SURVEY OF EXISTING TEST DATA AND ANALYSES

In the pool-cooling mode, the role of the RHR system is:

- To mix the water in the pressure suppression pool to avoid any hot spots in the vicinities of the quenchers and to eliminate thermal stratification and

- To remove thermal energy from the pressure suppression pool in a manner that will reduce the temperature uniformly throughout the pool.

The rate of heat removal is proportional to the difference between the temperature at the suction side of the RHR pump and the service water temperature (neglecting energy-transfer mechanisms other than the heat exchanger). It is therefore desirable to withdraw water at the point where the highest temperature exists. However, if the pool is well mixed, it does not make any difference where the suction takes place as long as cold water returning from the RHR heat exchanger is not drawn back in, i.e., as long as there is no short-circuiting.

Another important consideration is the net positive suction head (NPSH), which must be maintained under all postulated conditions to avoid cavitation. Starting with a stratified pool, discharge of the cold water near the surface where the temperatures are higher is desirable. However, there are other considerations, such as pool draw-down and bulk motion of the pool induced by momentum transfer from the discharge jet to the suppression pool.

When two RHR system loops are used in the pool-cooling mode, other questions arise regarding the relative location of the two discharge nozzles, the direction of the jets (same circumferential direction or opposite

directions), the angle between the jets and the radial axis, the locations of the suction strainers, and the elevation of discharge and suction points. These questions have been investigated analytically and experimentally (small scale and in-plant tests). In most cases, satisfactory solutions have been found.

A summary of each of the investigations and their major findings follows.

4.1 Perry One-Tenth-Scale Test

A one-tenth-scale model of the Perry Nuclear Power Plant suppression pool was used in this test program. The model included 19 X-quenchers and various structural members, main vents, etc., to simulate the real flow resistance conditions that exist in the actual plant. A simplified sketch of the model is shown in figure 5.

4.1.1 Scaling Factors

The scaling factors were as follows:

Length: 10^{-1},

Area: 10^{-2},

Volume: 10^{-3},

Time: $10^{-1/2}$,

Velocity: $10^{-1/2}$, and

Flow rate: $10^{-5/2}$.

4.1.2 Purpose of the Test

The purpose of the test was to investigate the following concerns:

- Short-circuiting between RHR system discharges and suctions.
- Optimum injection angle for the RHR system discharge jets.
- Bulk pool motion from operation of one RHR system loop.
- Hot spots around discharging quenchers.
- Temperature of the bottom liner of the suppression pool.

The RHR system discharge was simulated by using 50°F water at the rate of 22 gpm (corresponding to 7,000 gpm full scale). Water at 180°F, pumped at a rate of 6 gpm, was used to simulate the discharge of steam through the quenchers. This corresponds to approximately 256 lb/s of condensate in the full scale.

To simulate stratified pool conditions, a linear temperature gradient was established, with a temperature variation of 79°F at the bottom to 91°F at the top.

4.1.3 Summary of Perry One-Tenth-Scale Test Results

a. Test Series O. Orientation of Discharge Jet

- The optimum jet angle was found to be 55° from the radial axis. In a uniform temperature pool at 47°F, this arrangement resulted in an average bulk velocity of 0.15 ft/s (prototype) in 19 seconds (prototype).

- In a stratified pool (with water temperatures ranging from 91°F at the surface to 79°F at the bottom), a prototype bulk velocity of 0.17 ft/s was established in 25 seconds (prototype) with a 55° jet angle.

- A jet angle of 75° produced considerable backflow and turbulent flow conditions, particularly near the bottom and close to the drywell wall around quenchers 2 and 3 (figure 5). A potentially stagnant region was observed at the bottom near quencher 1.

- No stagnant areas were found for the case in which the jet angle was 55°. Flow patterns and constant velocity lines for this case are shown in figures 8 and 9, which show a considerable amount of turbulent mixing and backflow.

b. Test Series 1. Short-Circuiting

To investigate the possibility of short-circuiting between the discharge and suction of the RHR system, dye was injected in the discharge flow and tracked by movie and still photography. Quenchers 2 and 10 were operated, one at a time. These studies showed that short-circuiting did not occur with or without operating quenchers.

c. Test Series 2. Velocity and Temperature Measurements

A three-dimensional transient temperature distribution, starting with an initially stratified temperature field, is shown in figures 10 and 11. It can be seen that the initial stratification of approximately 12°F is reduced to 1 or 2°F in about 15 minutes.

The temperature at the suction point remained above the discharge temperature of 50°F, indicating that there was no short-circuiting.

The suppression pool water accelerated from zero velocity to an average velocity of 0.4 ft/s in 3 to 4 minutes (prototype values) of RHR system operation.

d. Test Series 3. Velocity and Temperature Measurements with a Quencher Operating

In this series of tests, a jet angle of 55° was used (as in series 2); and quenchers 2, 4, and 10 were actuated, one at a time, to study their effects on the velocity and temperature distributions.

Figure 12 shows the variation of velocity with elevation upstream of the operating quencher (number 2, see figure 5 for the locations of the quenchers). There is a velocity gradient in the vertical direction, particularly between levels 1 and 2 (levels are shown on figure 10) and between levels 2 and 3. In the lower half of the suppression pool, velocities seem to be uniform except near the bottom where backflow occurs. This velocity gradient is more pronounced directly downstream of the jet and diminishes with distance from the jet and with time. Figure 13 shows the variation of velocity with elevation and with time for the case where quencher number 4 is operating. Measurements were taken downstream of the operating quencher. Similarly, figure 14 is a plot of velocity versus time upstream of the jet with quencher number 10 operating.

In figure 15, the temperature of the water at the suction of the RHR system pump is plotted versus time for three tests in test series 3. Temperatures measured at the specified locations at level 4 are also plotted for comparison. It can be seen that the suction temperature is always higher than the discharge temperature of 50°F, thereby indicating that there was no short-circuiting. Also, after about 15 minutes (prototype time) of RHR system operation, the suction temperature stays above the temperature at level 4. Judging from figures 10 and 11, the suction temperature seems to be at or slightly above the bulk temperature of the suppression pool after about 15 minutes of operation of the RHR system.

4.2 Monticello In-Plant Test

The RHR system in the Monticello Nuclear Generating Station has two discharges at azimuthal angles of approximately 74° and 299° and four suction headers at azimuthal angles of 45°, 135°, 225°, and 315° (see figures 16 and 17).

Extended safety-relief-valve (SRV) blowdown tests were conducted at Monticello in December 1977 and February 1978. In the first test, the pressure suppression pool was brought to a uniform temperature of 50°F with the help of the RHR system. After a 50-minute wait for the motion of the pool to cease (this waiting period was later determined to be insufficient) the SRV discharging into Bay D (figure 16) was opened and left open for 7 minutes and 55 seconds. The reactor pressure was approximately 1,000 psia, and the steam flow rate varied between 200 to 220 lb/s. The maximum difference between the measured local temperature and the calculated bulk temperature was 43°F (reference 2) for the duration of discharge. In the same period, the maximum temperature difference in the bay of discharge (Bay D, figure 16) was 12°F. This indicated good mixing in that bay, even in the absence of any RHR system flow. Thirty minutes after closure of the SRV, there was a 52°F-temperature variation in the pool from thermal stratification.

The second test was conducted similarly, except that one RHR system loop was used in the recirculation mode (no cooling). The maximum difference between the local and bulk temperatures was reduced to 38°F (reference 2); the maximum stratification was 21°F at 20 minutes after valve closure; and uniform temperature was established throughout the suppression pool after 30 minutes of RHR system operation (in the recirculation mode).

A series of tests were conducted in November 1978 after two modifications were made:

- Forty holes were drilled in the end-cap of one of the quencher arms. The purpose was to enhance the bulk motion of the suppression pool by introducing steam, in the circumferential direction, through the end-cap holes.

- A 90° elbow, terminating at a 10-to-8-inch reducing nozzle, was installed at the end of the RHR system discharge line, oriented tangentially. The purpose of this modification was to impact momentum to the pool and induce bulk motion in the suppression pool. The reduction of the flow area increased the rate of momentum transfer by about 50 percent.

Tests were run with and without the operation of the RHR system. The duration of the SRV blowdown was 12 minutes for the former and 11 minutes for the latter case. The results showed that the end-cap holes did not produce a significant improvement in the suppression pool mixing but that the modification of the discharge nozzle did. In fact, with the RHR system operation, the maximum local-to-bulk temperature was reduced to 15°F; and 6 minutes after SRV closure all temperature readings in the suppression pool were within 5°F.

The Monticello test results indicate:

- Quenchers provide adequate thermal mixing in the bay where they discharge.

- Properly directed, the RHR system discharge jet is an effective means of producing bulk motion and thermal mixing of the pressure suppression pool.

4.3 Caorso In-Plant Test

The geometry of the Caorso RHR system discharge device is quite different from that of the plants with Mark III containments (see figures 18 and 19 for the details). Each of the two 16-inch-diameter discharge lines has a 9.2-foot perforated section with thirty 2-inch holes in two horizontal rows, 180° apart. (The four 20-inch suction lines are located at azimuthal angles of 140°, 164°, 222°, and 235°.)

The locations of the temperature sensors and the activated quencher A are shown in figure 20. The extended SRV blowdown test was conducted with the reactor pressure at 975 psig and an SRV flow rate of 237 lb/s. The initial suppression pool temperature was brought to a uniform 60°F by running the RHR system in the pool-cooling mode. The initial temperature distribution in the suppression pool (just before SRV actuation) is shown in figure 21. The RHR system operation was stopped after a uniform, 60°F suppression pool temperature was established and 4 1/2 hours before SRV actuation. This waiting period was for ensuring that all suppression pool motion had stopped before SRV actuation.

SRV A (figure 20) was actuated and left open for 13 minutes and 7 seconds. Figure 22 shows the temperature distribution and the end of the blowdown. The maximum temperature at this time was 116°F, registered by sensor T13. The sensor T307 on the opposite side of the suppression pool was at 94°F, 15 degrees above its initial temperature, thus indicating the extent of suppression pool mixing caused by the quencher.

After SRV closure, it was 3 minutes and 40 seconds before the RHR system pumps A and C began operating in the pool-mixing mode (no cooling). Stratification began immediately after SRV closure, as can be seen in figures 23 and 25. Figure 24 shows the temperature distribution after 4 minutes of RHR system operation. The maximum temperature difference at that time was only 5°F.

The Caorso test results (reference 3) indicate:

- The X-quencher is an effective device for distributing the thermal energy of the condensing steam over a large volume of the suppression pool.

- The RHR system discharge device used in Caorso is effective in mitigating pool stratification and providing pool mixing. Starting with a stratified pool, it takes only a few minutes of RHR system operation to reach approximately equal temperatures throughout the suppression pool.

4.4 Kuo-Sheng In-Plant Test (Reference 4)

The Kuo-Sheng extended SRV blowdown test consisted of a 9-minute blowdown of one SRV into an initially quiescent suppression pool at a uniform temperature of 90°F. Five minutes into the blowdown, one RHR system loop was put in the pool-mixing mode. At the start of RHR

system operations, a 17°F thermal stratification existed; it was reduced to a 2°F stratification after 10 minutes of RHR system operation.

Both the results and the conclusions of this test are similar to those of the Caorso test, in spite of the major differences in the RHR system discharge geometries of the two plants. In both plants, the thermal stratification was reduced at the rate of 1.5 to 1.8°F/min by the operation of one RHR system loop in the pool-mixing mode.

4.5 Thermal Stratification Study of a Mark III Containment Suppression Pool (Reference 5)

The purpose of this study was to determine the effectiveness of one RHR system loop in the thermal mixing of the suppression pool following a design basis accident (DBA).

The suppression-pool and containment data used in the analysis are given in table 4.1, and the RHR system suction and return arrangement is shown in figure 26. Table 4.2 is a summary of the sequence of events analyzed. The analysis starts at 15.5 minutes following the postulated DBA and covers the ensuing 30 minutes. The conditions at 15.5 minutes after DBA are given in table 4.3 and constitute the initial conditions for the analysis. The emergency core-cooling system (ECCS) flow was assumed to be 14,700 gpm for the first 14.5 minutes and 7,800 gpm thereafter. The RHR system flow rate was assumed to be 6,500 gpm (table 4.2). The conditions in the suppression pool at the start of RHR system operation are given in table 4.4. The ECCS and RHR system return temperatures were assumed to be 200°F and 111°F, respectively.

The RELAP4/MOD3 computer program was used to simulate the events and obtain temperature distributions for the pressure suppression pool. A 32-node, half-pool model was used for the first 14.5 minutes; and a 39-node, full-pool model was used for the remainder of the time when the RHR system was in operation.

The results of the RELAP4/MOD3 analysis showed that 15 minutes of operation of one RHR system loop (starting at 30 minutes after DBA) was sufficient to:

- Maintain the peak suppression pool temperature below 166°F (+2°F/-0°F).

- Maintain the average suppression pool surface temperature below 166°F (+2°F/-0°F).

- Decrease the difference between the peak and bulk temperatures of the suppression pool from a maximum of 17°F to 13°F (+2°F/-0°F) and decrease the difference between the average surface and the bulk temperatures of the suppression pool from 15°F to 11°F (+2°F/-0°F).

Another important conclusion, which is supported by the Caorso in-plant test data, was that 5 minutes of operation of a single RHR system loop was sufficient to provide nearly complete breakup of the initial thermal stratification.

Two other observations in reference 5 are either obvious or wrong:

- "Operation of a single RHR system is insufficient to maintain or decrease the rise of the bulk temperature of the suppression pool up to 45 minutes after LOCA."

This should be obvious, since the ECCS is introducing 200°F water at a rate of 7,800 gpm while the RHR system is discharging into the pool at a rate of 6,500 gpm and a temperature of 111°F; the suction temperature for both systems is approximately 155°F.

- "The observed short-circuiting in the RELAP4/MOD3 simulation is conservatively estimated to be between 20% and 40% of the potential short circuiting. Because of the conservative choices for temperature input data to the estimate, it is believed that the actual observed short-circuiting may be less."

This conclusion was reached by calculating a rate of increase of bulk temperature (0.09°F/min), based on computer-calculated suction temperatures and given discharge temperatures for the RHR system and the ECCS, and comparing it with the rate calculated by the computer program (0.21°F/min). The latter was higher, and the conclusion was that short-circuiting occurred. In the absence of any errors (in the computer program or the hand calculations), the two answers should have been the same. Therefore, the discrepancy invalidates either the entire analysis (if the computer program indeed does not conserve energy) or the hand calculations. The hand calculations (appendix H of reference 5) were checked and found to be reasonably accurate (except the wrong ECCS flow rate was used in calculating the maximum rate of temperature rise). However, the conclusion about short-circuiting is without foundation and not supported by test data.

TABLE 4.1.--Mark III 238 suppression pool and containment data

Containment ID	120'
Weir Wall OD/ID (ft)	68'-8"/65'-0"
Weir Wall Thickness	1'-10"
Weir Annulus Width	2'-2"
Weir Annulus Area (ft^2)	482
Obstructed Weir Annulus Area (ft^2)	14
Total Vent Area (horizontal vent) (ft^2)	495
No. Vent Azimuth Locations	40
Vent Azimuth ℄ Spacing on Drywell I.D.	5'-9"
Total No. Vents (3 levels)	120
Vent I.D. (E,F,G)	27-1/2"
Vent Length (D)	5'-0"
Vent Centerlines	Ht. from Basemat
Top Row (J)	12'-11"
Middle Row (M)	8'-5"
Bottom Row (H)	3'-11"
Containment Gross Volume	1,965,000 ft^3
Suppression Pool Volume outside drywell	119,000 ft^3
Water Depth After Drawdown - (Q)	16'-0"
High Water Level (N)	20'-5"

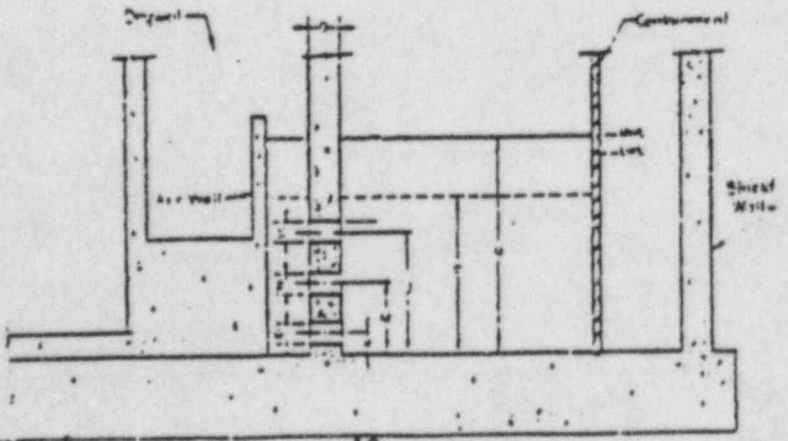

TABLE 4.2.--Sequence of events for ECCS and RHR system activity following LOCA

System Activity	Time (minutes)	Flow Rate (gallons per minute)
1. ECCS Suction & Discharge	0 - 15.5	Pool height and pool thermal stratification at 15.5 minutes are provided by GE
2. ECCS Suction & Discharge	15.5 - 30	14,700 gpm
3. ECCS Suction & Discharge	30 - shutoff	7,300 gpm
RHR Suction & Discharge	30 - shutoff	6,500 gpm

TABLE 4.3.--Initial conditions
15½ minutes following
LOCA (ECCS)

Water Level (ft)	16.0
Temperature (^{o}F)	
Level IV (Top)	139.5
Level III	136.8
Level II	135.5
Level I (Bottom)	128.0
Flow Rates in Pool	Negligible
ECCS Return Temperature	200.0

TABLE 4.4.--Initial conditions
30 minutes following
LOCA (RHR)

Water Level (Ft.)	16.0
Temperature (^{o}F)	
Level III (Top)	165.8
Level II	165.0
Level I (Bottom)	142.7
Flow Rates in Pool	None
ECCS Return Temperature (^{o}F)	200.0
RHR Return Temperature (^{o}F)	111.0

5.0 CONCLUSIONS

The test data and analyses compiled in this report lead to the following conclusions regarding the effectiveness of one RHR system loop in providing mixing within a boiling-water-reactor (BWR) pressure suppression pool:

- Scaled tests at the Perry Power Station demonstrated that even when the suction point is less than 20° degrees from the discharge, no short-circuiting of the flow occurs.

- The same tests demonstrated that, after approximately 15 minutes of RHR system operation, the suction temperature is close to the bulk temperature.

- Both the Perry and Monticello tests indicated the importance of directing the RHR system discharge flow in such a way that suppression pool bulk motion is induced. This bulk motion enhances the uniform distribution of the thermal energy throughout the pool.

- Caorso test results demonstrated that other RHR system discharge devices, such as the sparger design used at Caorso, are equally effective in affording suppression pool mixing. In fact, pool stratification was reduced at about the same rate (1.5 to 1.8°F/min) at Caorso (with a sparger) and at Kuo-Sheng (with a 90° elbow).

- The X-quencher is an effective means of distributing the thermal energy of the condensing steam.

The question of the consequences of having two RHR system discharge elbows facing each other (when both RHR system loops are in the pool-cooling mode) was not directly addressed in any of the reports. That being the main question, it will be discussed in the following paragraphs.

The main concern regarding the effect of opposing RHR system jets is that this arrangement may impede the bulk motion of the suppression pool and adversely affect suppression pool mixing. Regarding the bulk motion of the suppression pool, several points need clarification:

- Circumferential bulk motion by itself is only effective in distributing the thermal energy circumferentially. This type of mixing is necessary when the thermal energy is deposited locally, such as in the case when an SRV is stuck in the open position. However, many other mechanisms contribute to and are essential for thermal mixing:

  - Secondary flow patterns induced by RHR system suction, ECCS suction and return (when operating), quencher discharge, and the turbulence caused by submerged structures and pool geometry.

  - Free convection, which is particularly effective in spreading the hot water over the top layer of the pool. The Caorso test, as well as an earlier test at Quad Cities, indicates that, even in the absence of RHR system activity, the temperature on the other side of the pool rises in a very short time after SRV discharge begins.

- The concern that opposing RHR discharge jets will impede pool mixing is a misconception. Whereas it is true that a rigid body subjected to two equal and opposing forces will not move, the same is not always true for a body of liquid. To clarify this point, one may picture a global view of the flow patterns for the two cases, i.e., with two jets in the same direction versus opposing jets. For simplicity, secondary flow patterns will not be shown; and transient effects will be ignored, i.e., steady-state flow rate will be indicated. Taking River Bend as an example, the global flow rates for the cases of jets discharging in the same direction and in opposing directions are shown in figures 27 and 28.

If the discharge jets are pointing in the same direction, the overall flow will be in one direction with the flow introduced at azimuthal angles of 310° and 30° (the locations of return lines) and withdrawn at azimuthal angles of 190° and 165° (suction points). The flow rate for each loop is called $\dot{m}_1$, and the entrained flow is denoted by $\dot{m}_2$.

In the actual case of opposing jets, there are two planes of symmetry at azimuthal angles of 180° and 350°. The planes behave more or less as rigid boundaries. When the two opposing streams meet at these points, they are deflected, as shown in figure 28. Again, each jet induces a flow rate of $\dot{m}_2$; and each loop has a flow rate of $\dot{m}_1$. The flow pattern shown in figure 28 is ideal for suppression pool mixing, since there is not only a circumferential flow but also a flow in the vertical direction to break up any stratification.

At the planes of symmetry, i.e., at azimuthal angles of 350° and 180°, mixing of the two streams takes place. In other words, these two planes act as very effective parallel-flow heat exchangers, providing energy transfer between the two halves of the suppression pool.

This is admittedly a highly simplified presentation of the actual flow, but it serves the purpose of refuting the notion that in some manner two opposing jets will cancel each other's effect and reduce the degree of thermal mixing afforded by the bulk motion of the suppression pool.

Similar flow patterns exist in the Grand Gulf plant and lead to the same conclusion.

To summarize, all of the domestic plants with Mark III containments have RHR system discharge and suction arrangements that preclude short-circuiting and provide effective thermal mixing of the pressure suppression pool. The remarks about the disadvantages of opposing discharge jets, particularly the suggestion that two opposing jets will tend to impede the effectiveness of each other, are without technical basis. Uniform and unidirectional bulk motion is not the only and not necessarily the best way of effecting thermal mixing. Opposing jets provide a different flow pattern, which is equally effective in distributing the thermal energy.

Existing tests and analyses provide sufficient support for the above conclusions; additional testing is not necessary.

References

1. "Model Study of Perry Nuclear Power Plant Suppression Pool." Final Report. November 10, 1977.

2. Su, T. M. "Suppression Pool Temperature Limits for BWR Containment." NUREG-0783.

3. Holan, J., and Mintz, S. "Mark II Containment Program, Caorso Extended Discharge Test Report." NEDE-24798-P. July 1980.

4. Author's notes, taken at the site during the Kuo-Sheng in-plant SRV test.

5. "Mark III Suppression Pool Thermal Stratification Study." Revision 0. EDS Report No. A-77-122. December 5, 1977.

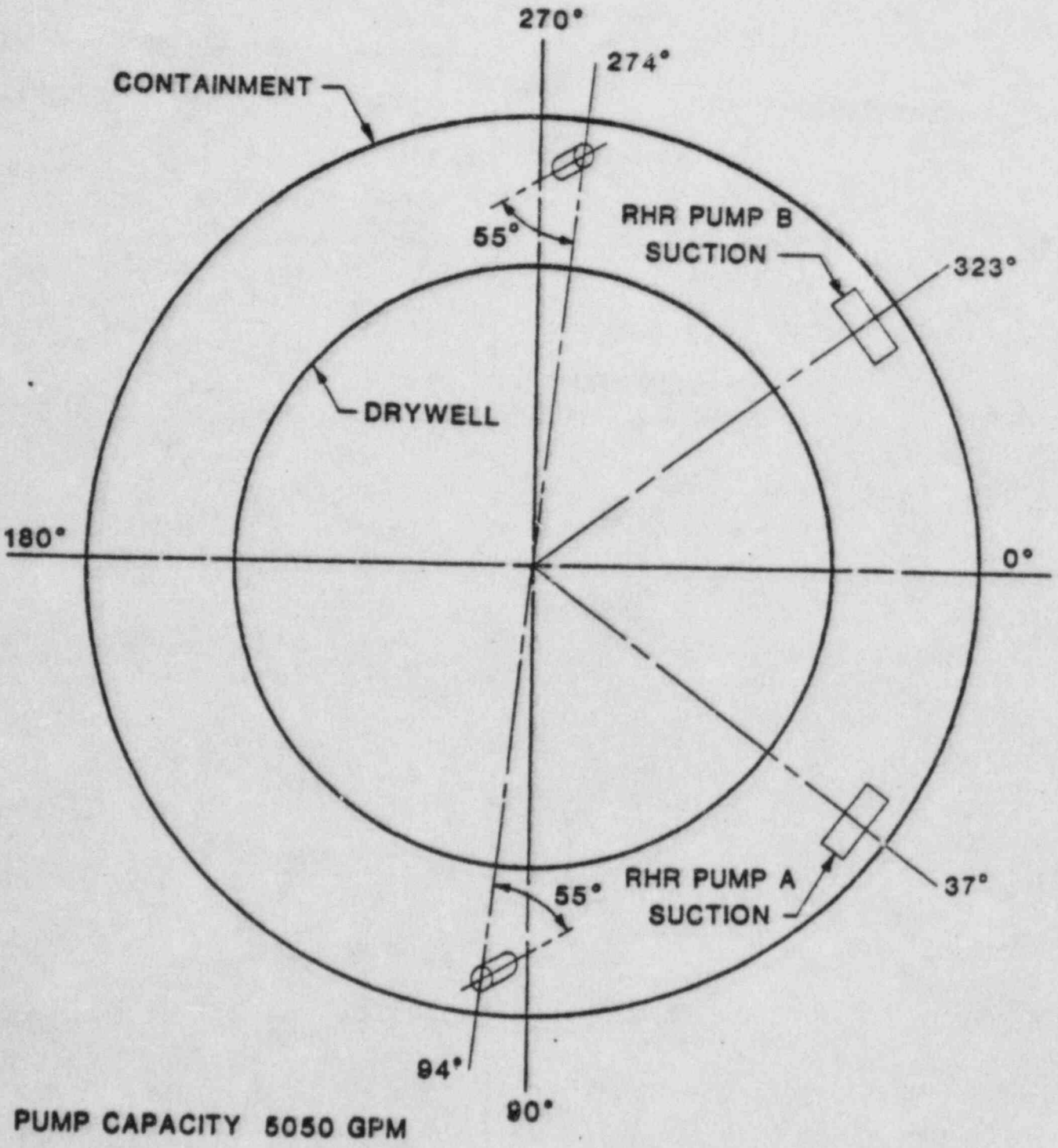

FIG. 1 LOCATIONS OF RHR SUCTION AND DISCHARGE

CLINTON POWER STATION

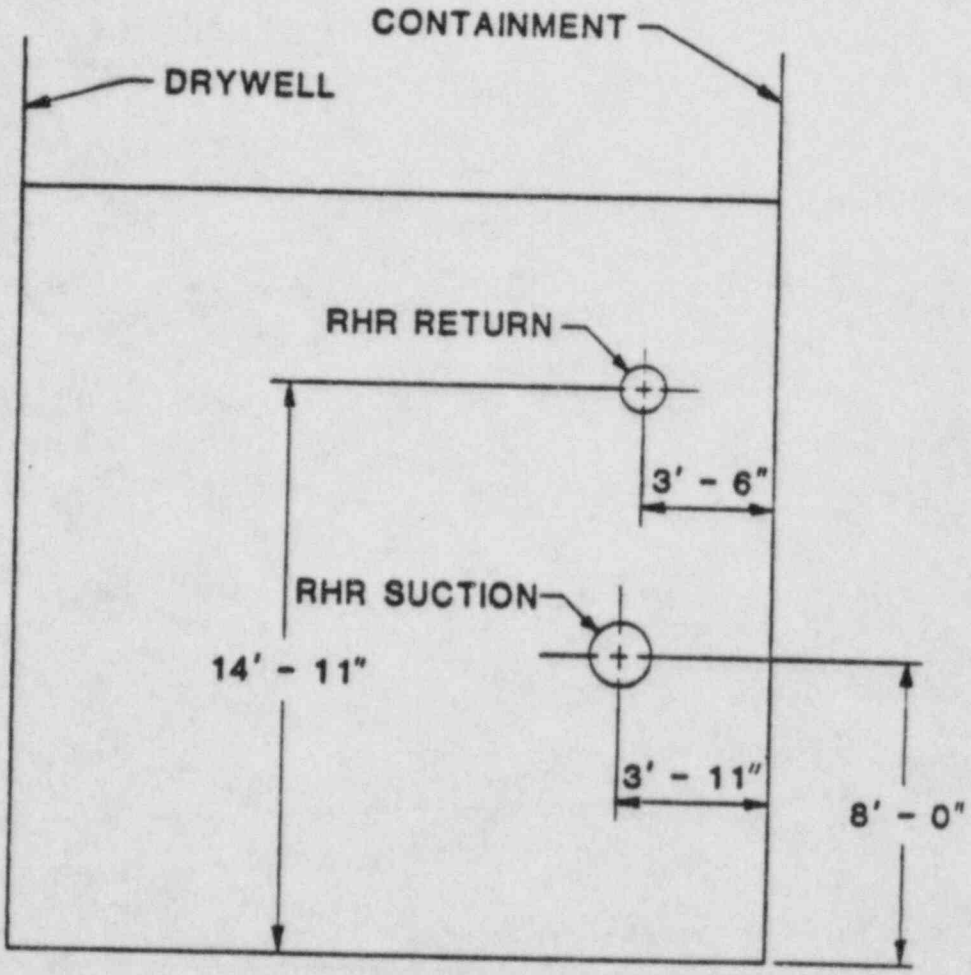

FIG. 2 ELEVATIONS OF RHR SUCTION AND DISCHARGE

CLINTON POWER STATION

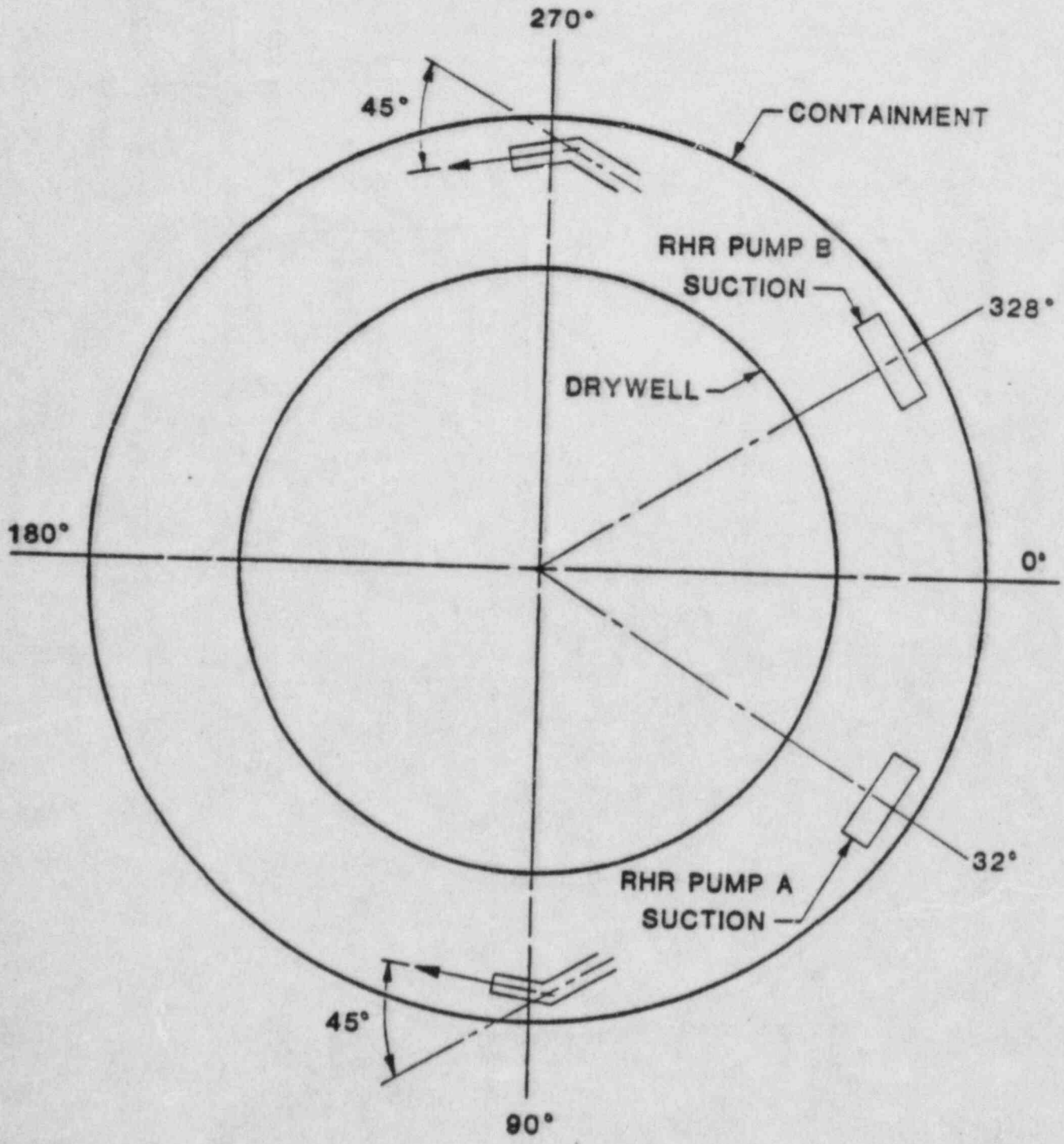

FIG. 3 LOCATIONS OF RHR SUCTION AND DISCHARGE

GRAND GULF POWER STATION

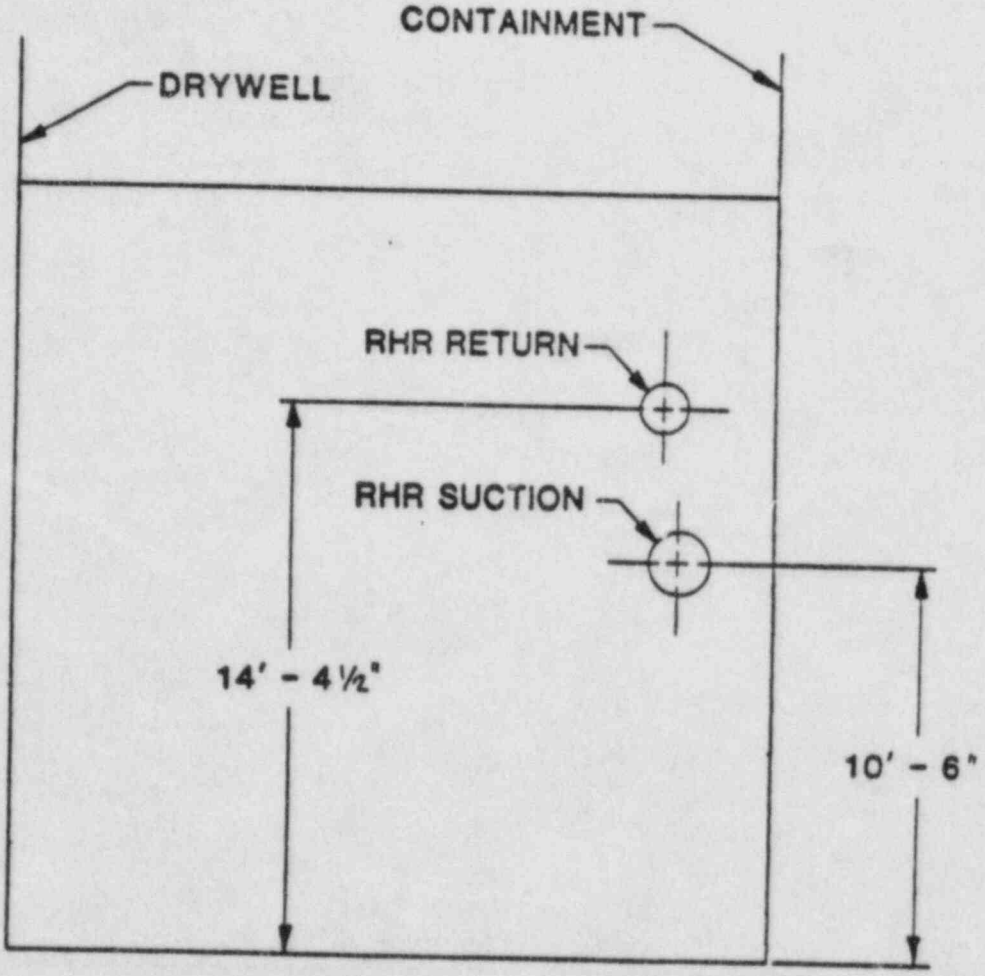

FIG. 4 ELEVATIONS OF RHR SUCTION AND DISCHARGE

GRAND GULF POWER STATION

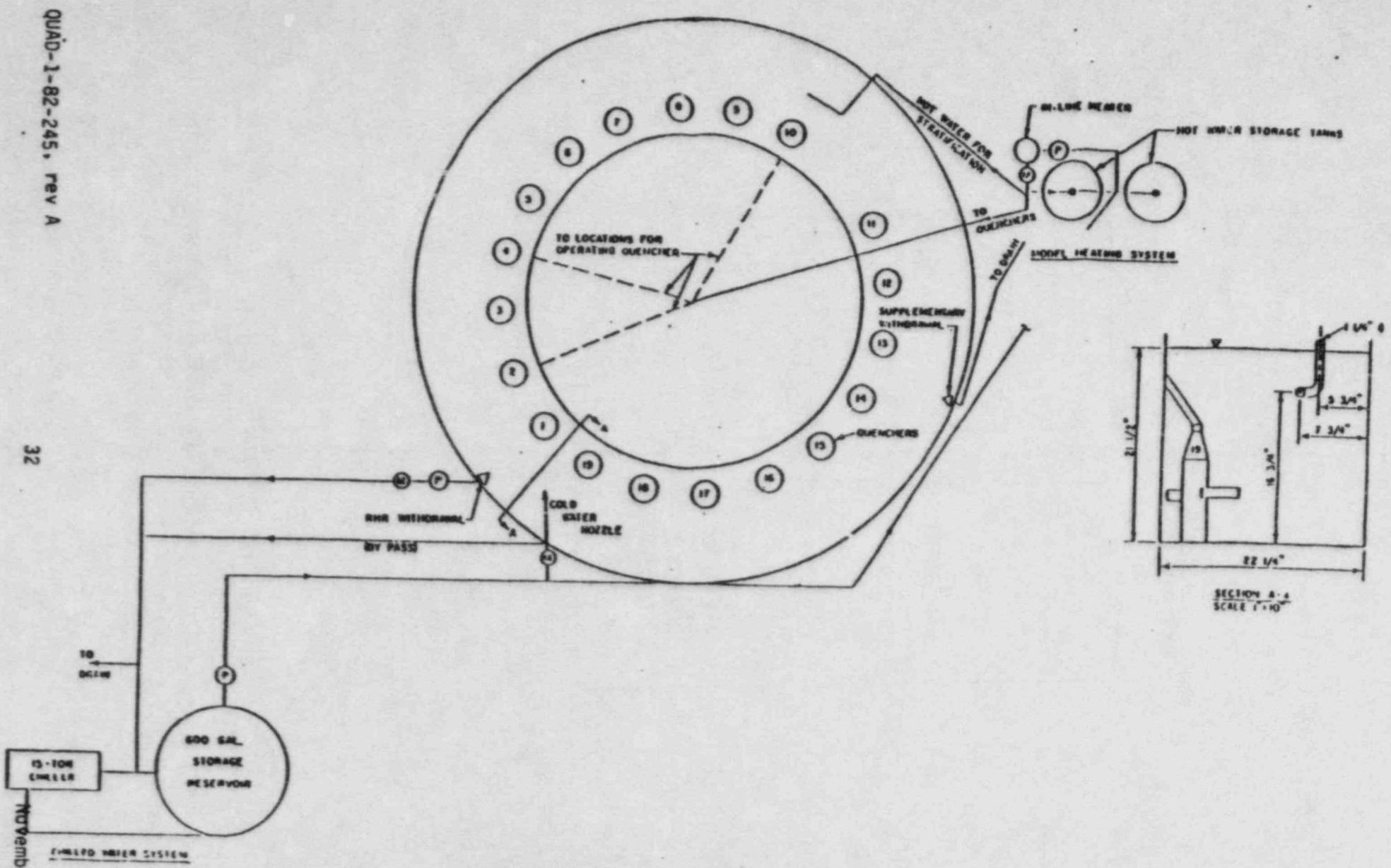

FIG.5-LOCATION OF RHR SUCTION AND DISCHARGE

PERRY POWER STATION (MODEL)

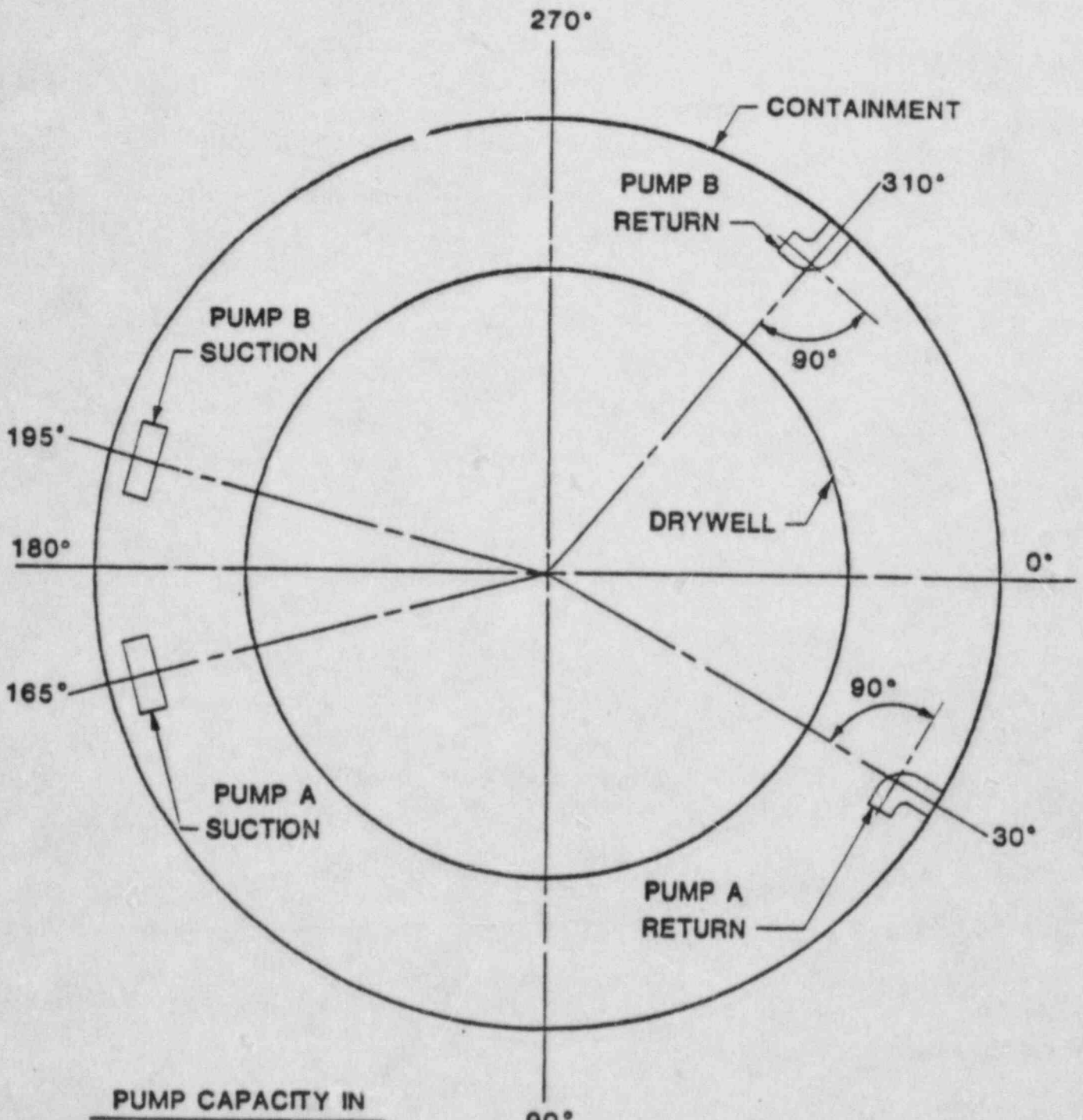

PUMP CAPACITY IN POOL COOLING MODE	
PUMP A	5050 GPM
PUMP B	5050 GPM

FIG. 6 LOCATIONS OF RHR SUCTION AND DISCHARGE

RIVERBEND (PRELIMINARY)

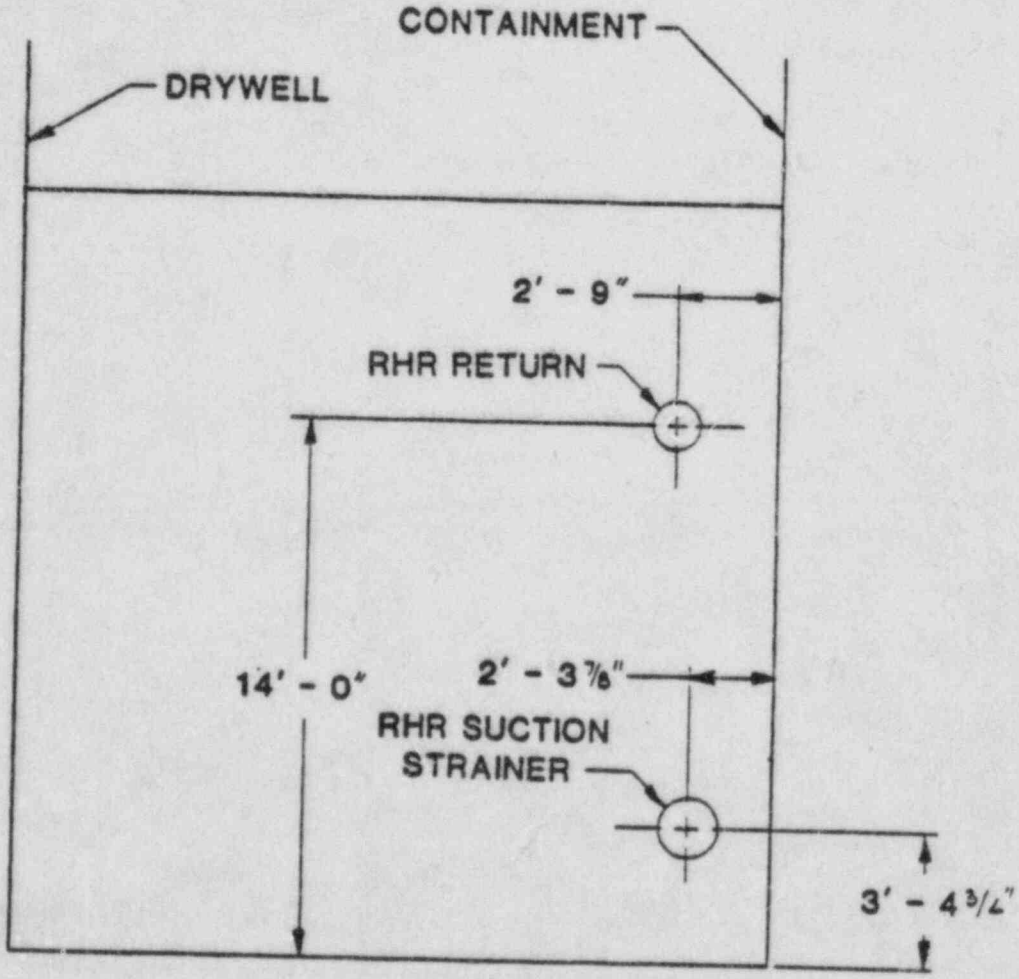

FIG. 7 ELEVATIONS OF RHR SUCTION AND DISCHARGE

RIVERBEND (PRELIMINARY)

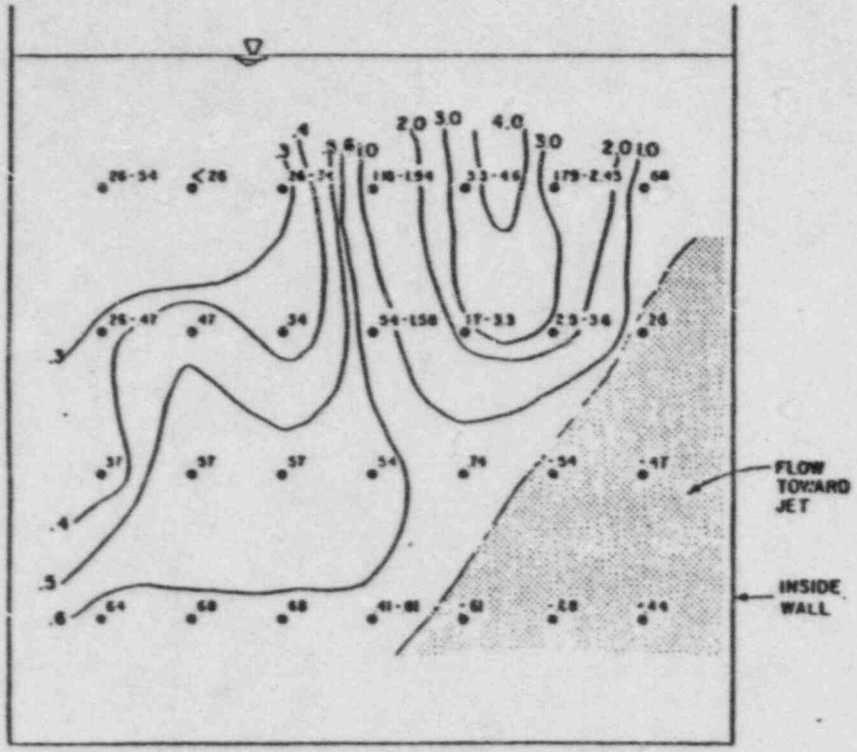

VELOCITIES MEASURED BETWEEN THE JET AND QUENCHER No. 1

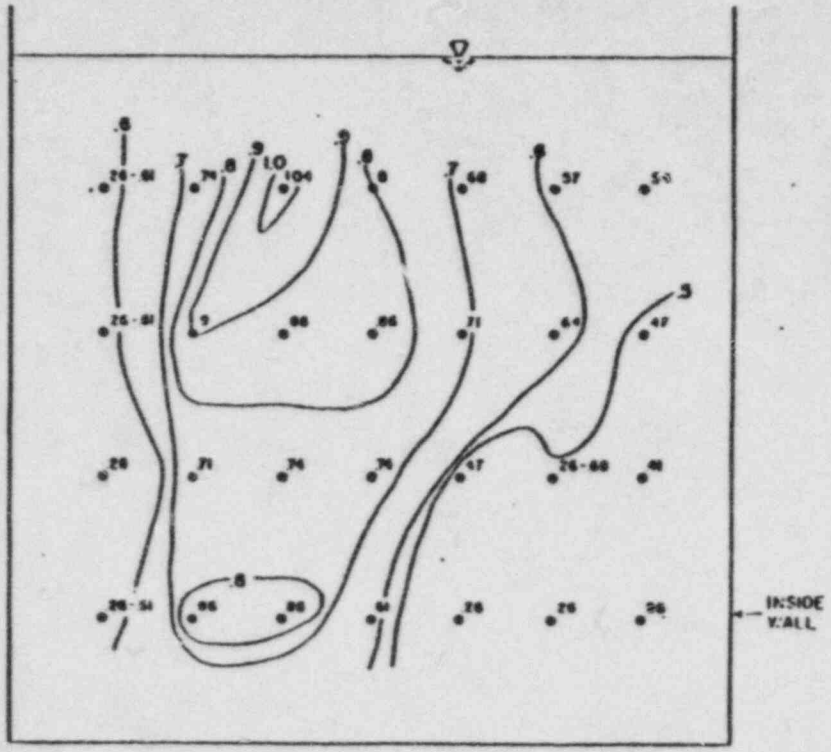

VELOCITIES MEASURED BETWEEN QUENCHERS No 1 AND No. 2

JET ANGLE 55°

FIG.8-VELOCITY FIELD FOR JET ANGLE OF 55 DEGREES

GILBERT ASSOCIATES INC.

POINT VELOCITIES AND ISO-VELS - TEST 0 D

JUNE 1977

5

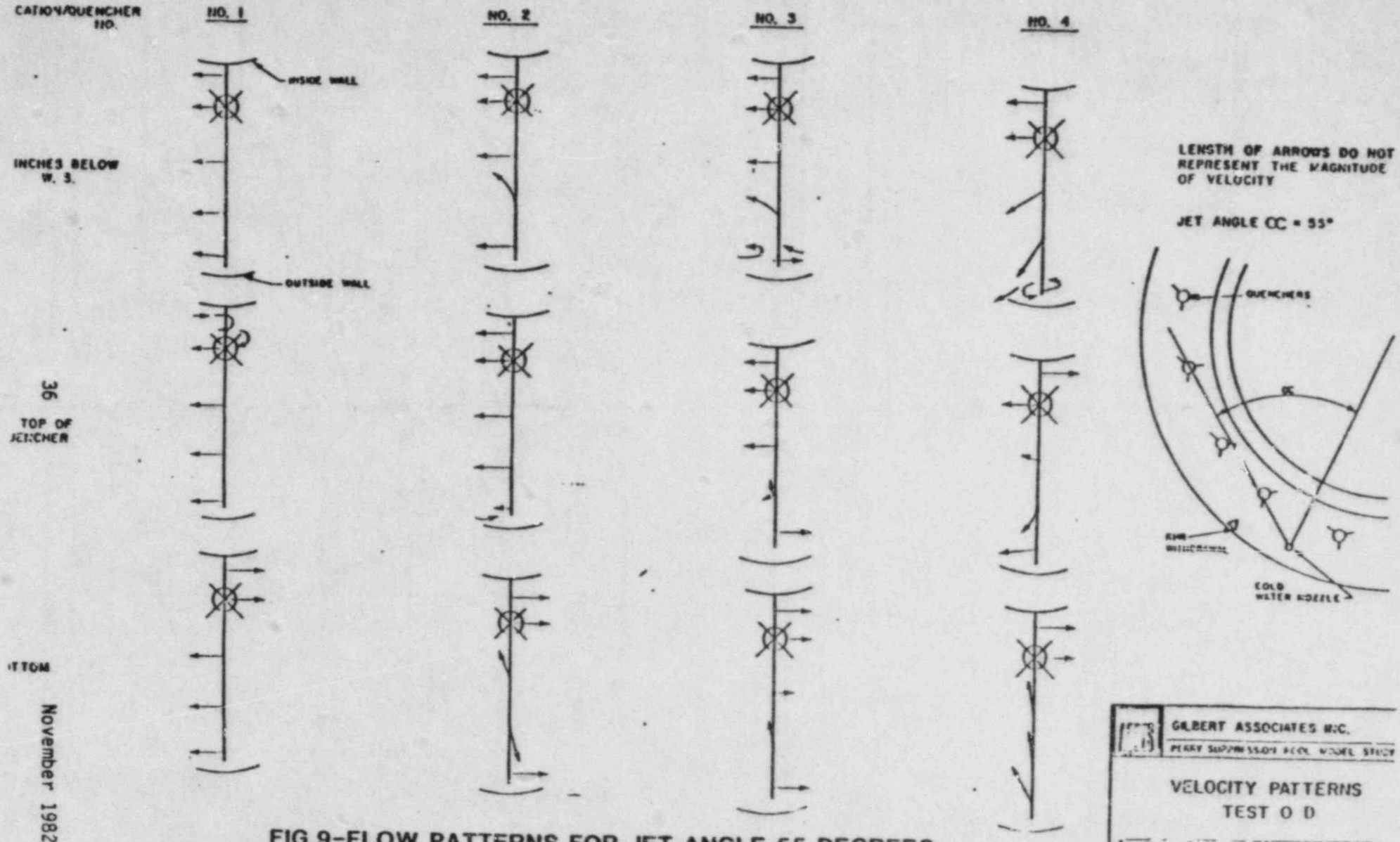

FIG.9-FLOW PATTERNS FOR JET ANGLE 55 DEGREES

November 1982

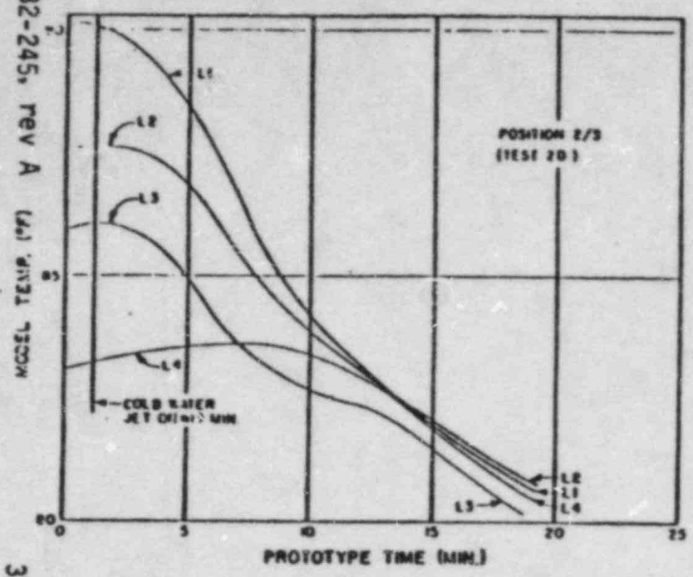

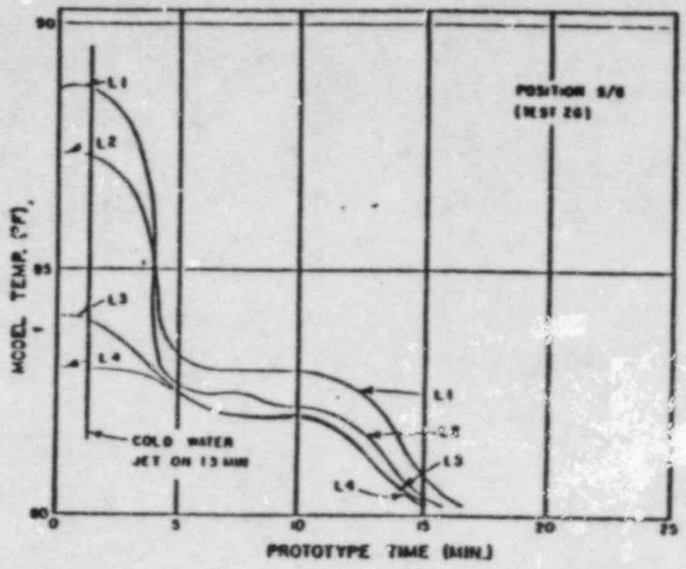

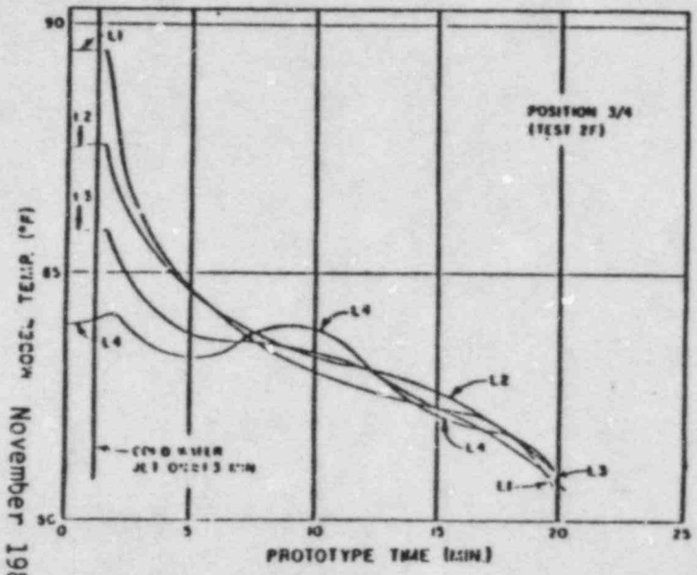

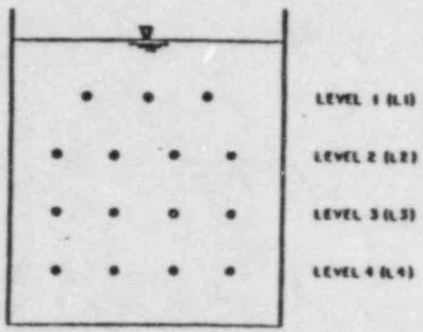

TEMPERATURE SENSOR GRID

GILBERT ASSOCIATES INC.

TIME VERSUS TEMPERATURE
PLOTS – SERIES 2
LOCATIONS BETWEEN QUENCHER
203, 304, 506

JUNE 1977

FIG.10-POOL THERMAL MIXING

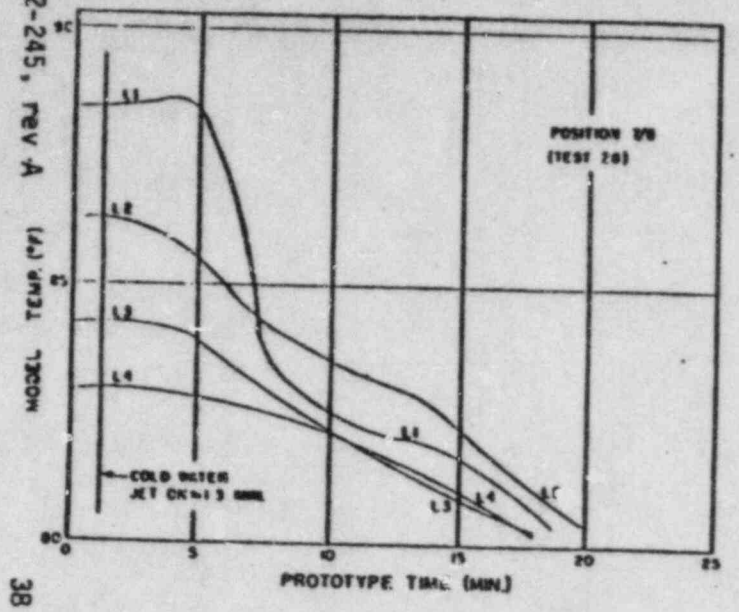

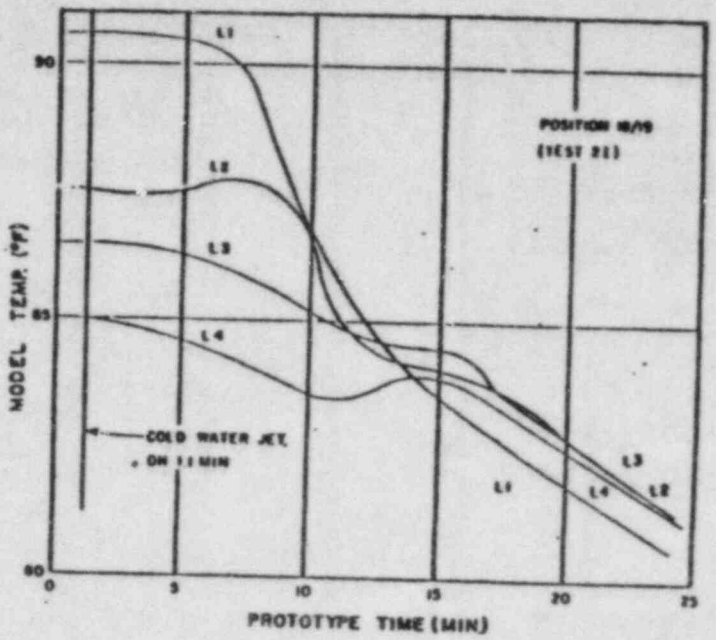

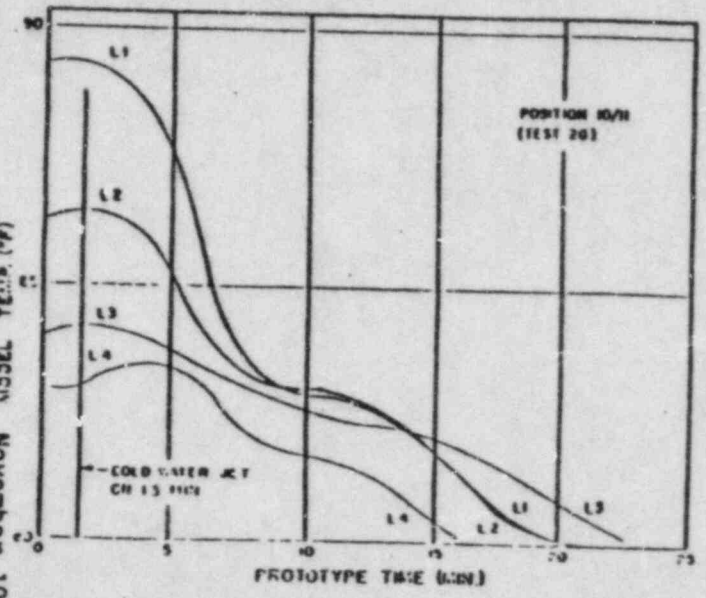

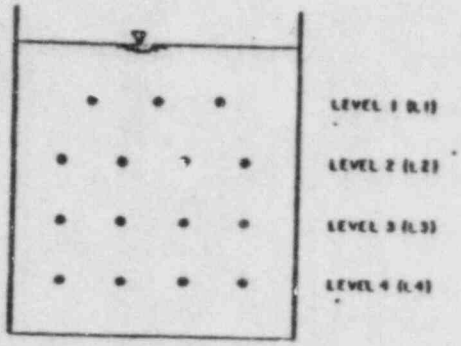

GILBERT ASSOCIATES INC.
PERRY SUPPRESSION POOL MODEL STUDY
TIME VERSUS TEMPERATURE
PLOTS — SERIES 2
LOCATIONS DETAILED ON FIGS 7-8, 10 & 11
JUNE 1982
7

FIG.11-POOL THERMAL MIXING (CONT'D)

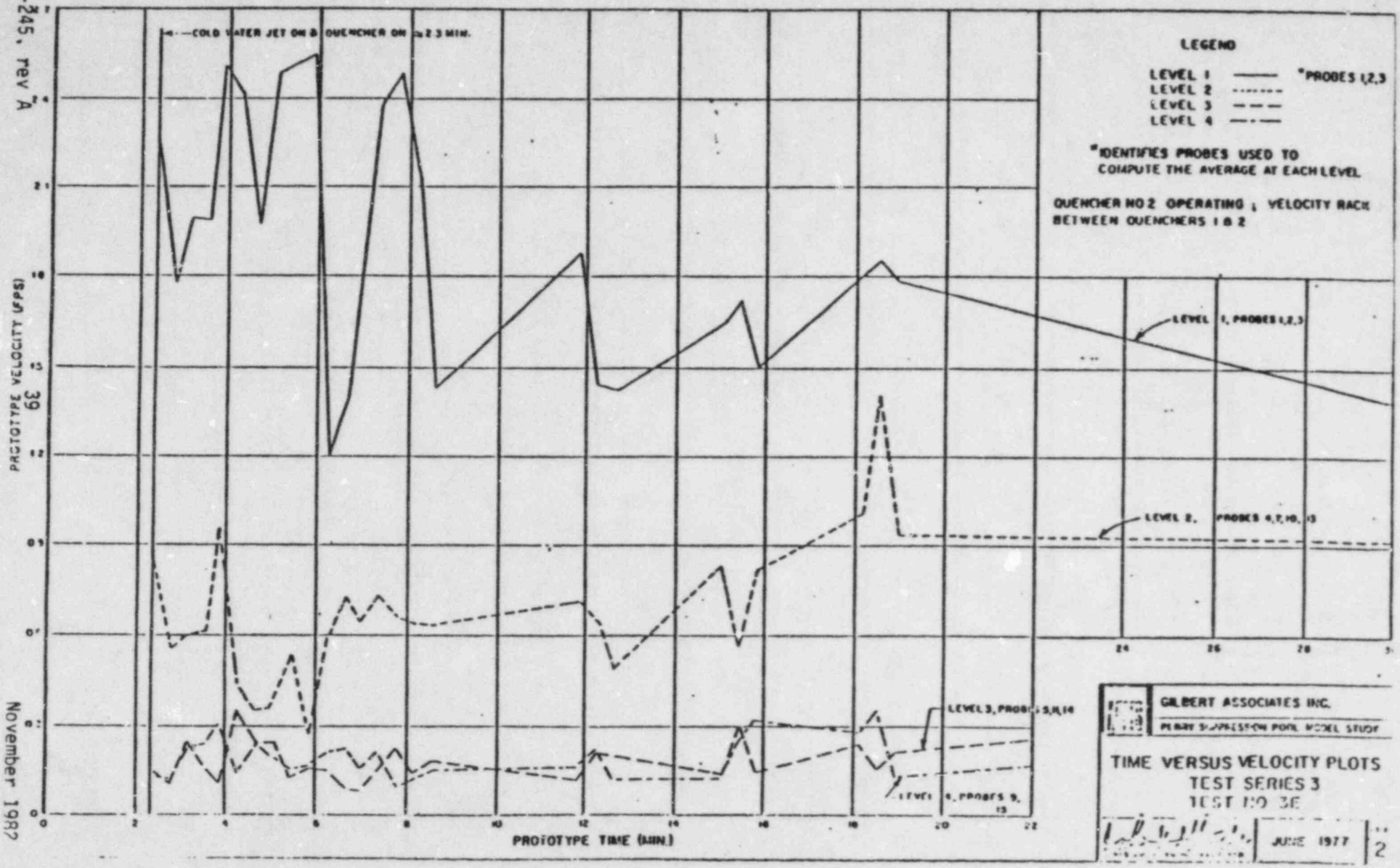

FIG. 12-VARIATION OF VELOCITY WITH DEPTH AND WITH TIME

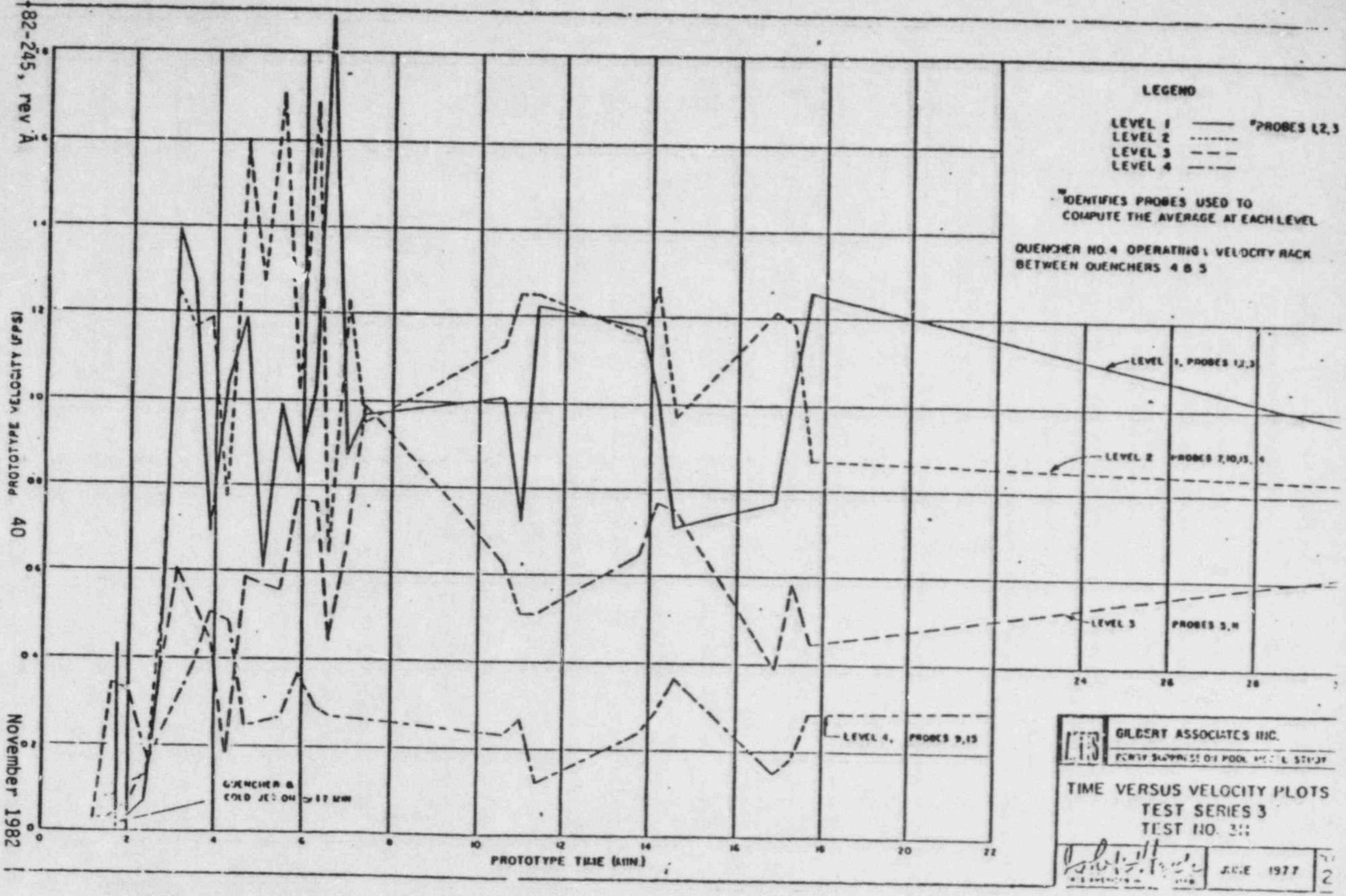

FIG.13–VELOCITY VARIATIONS OF OPERATING QUENCHER NO.4

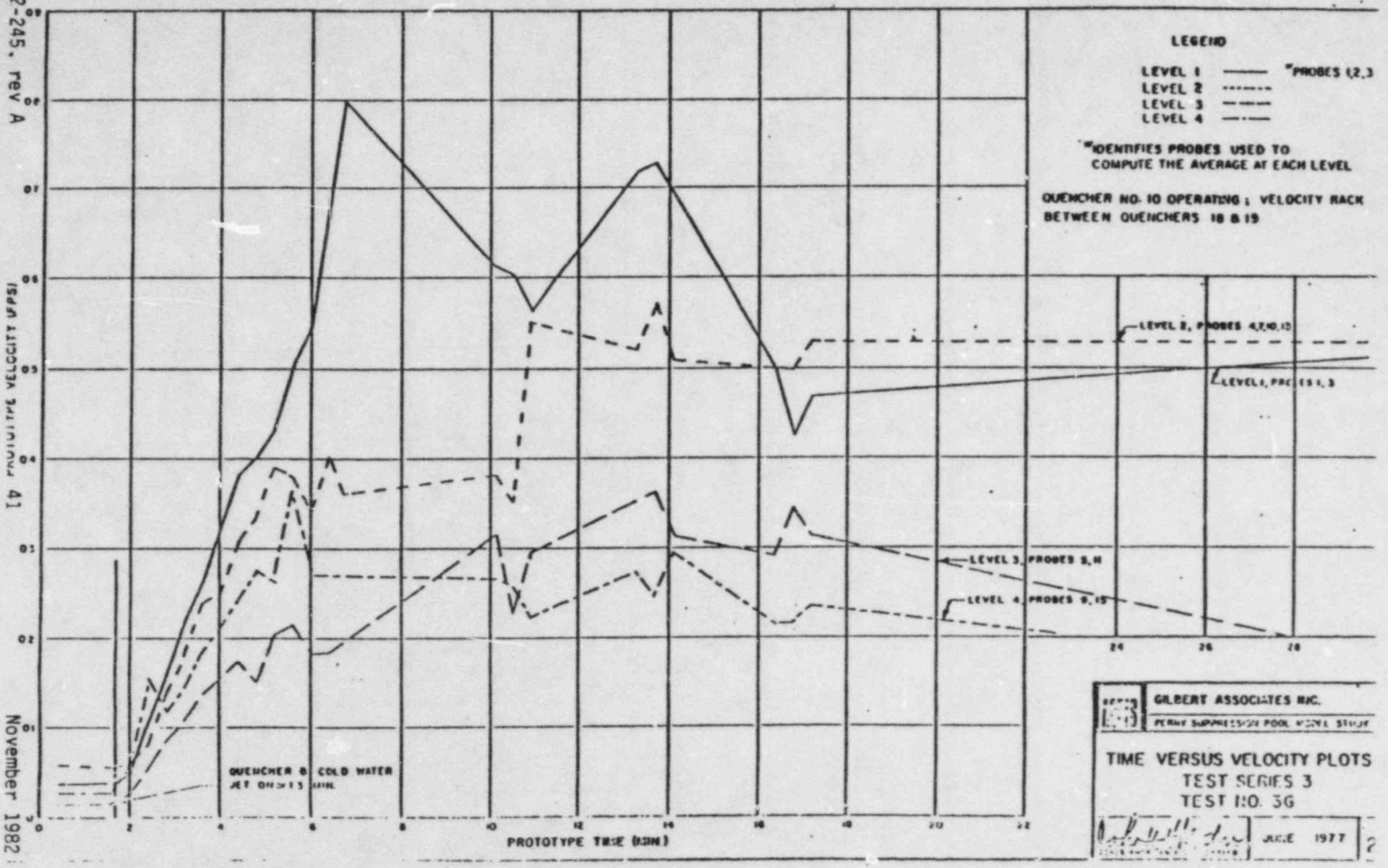

FIG.14-VELOCITY DISTRIBUTION UPSTREAM OF THE JET

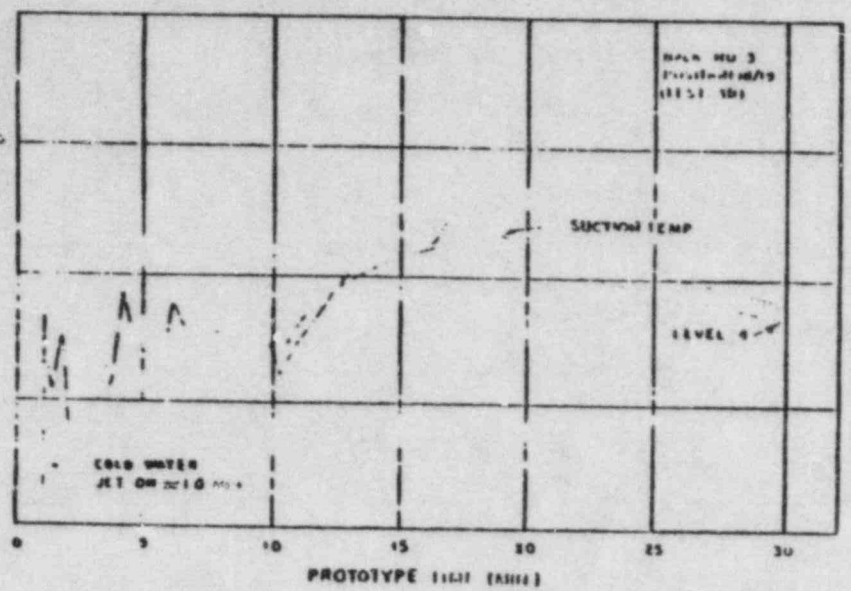

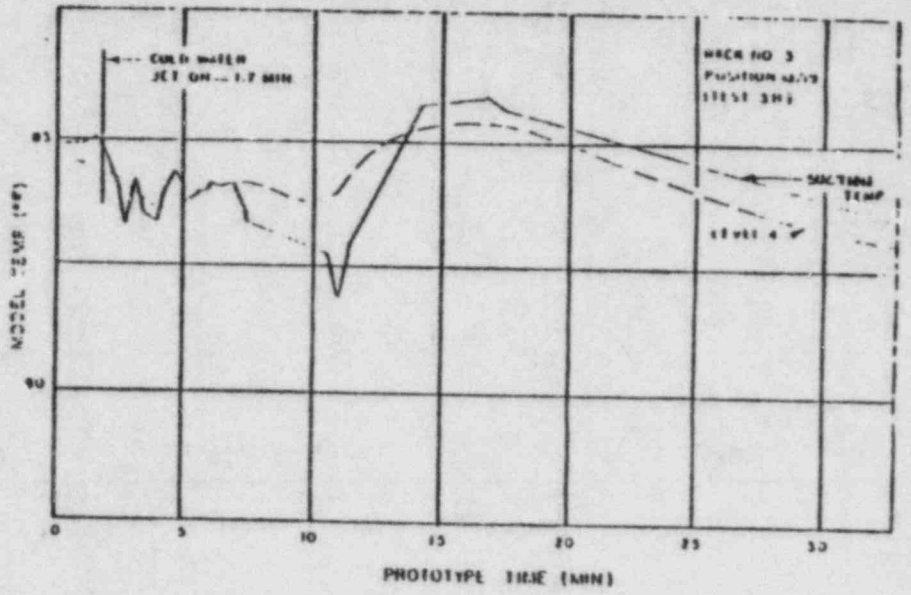

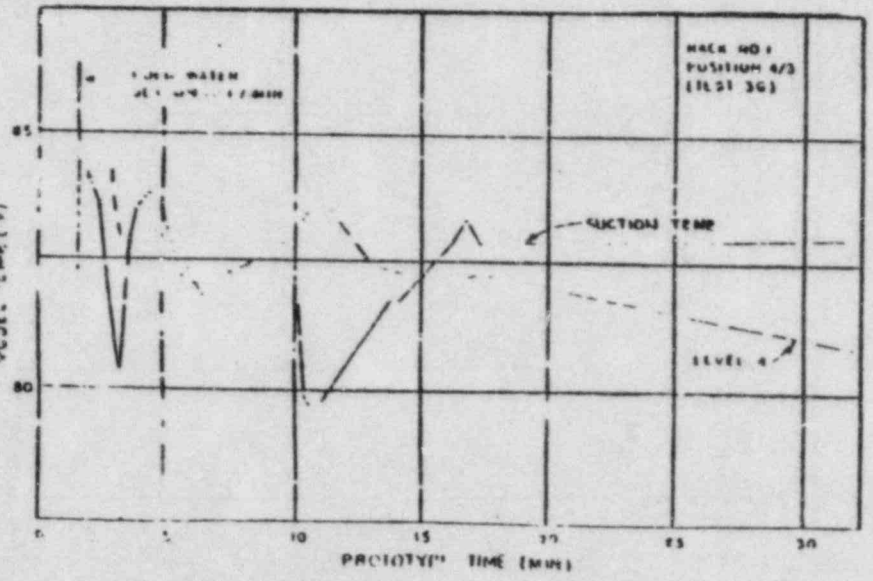

GILBERT ASSOCIATES INC

TEST SERIES 3

FIG.15-VARIATION OF SUCTION TEMPERATURE WITH TIME

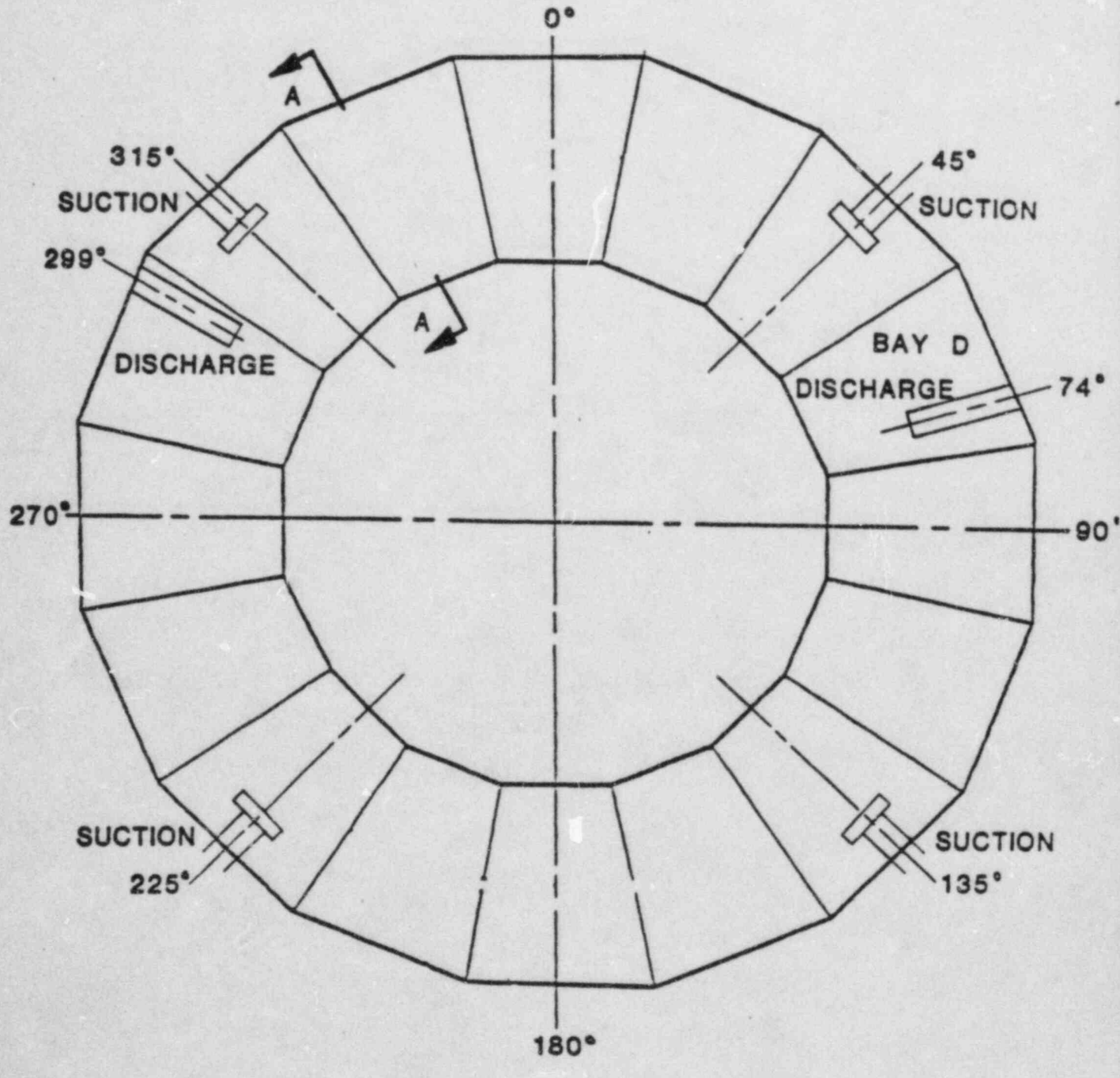

FIG. 16 RHR SUCTION AND DISCHARGE LOCATIONS

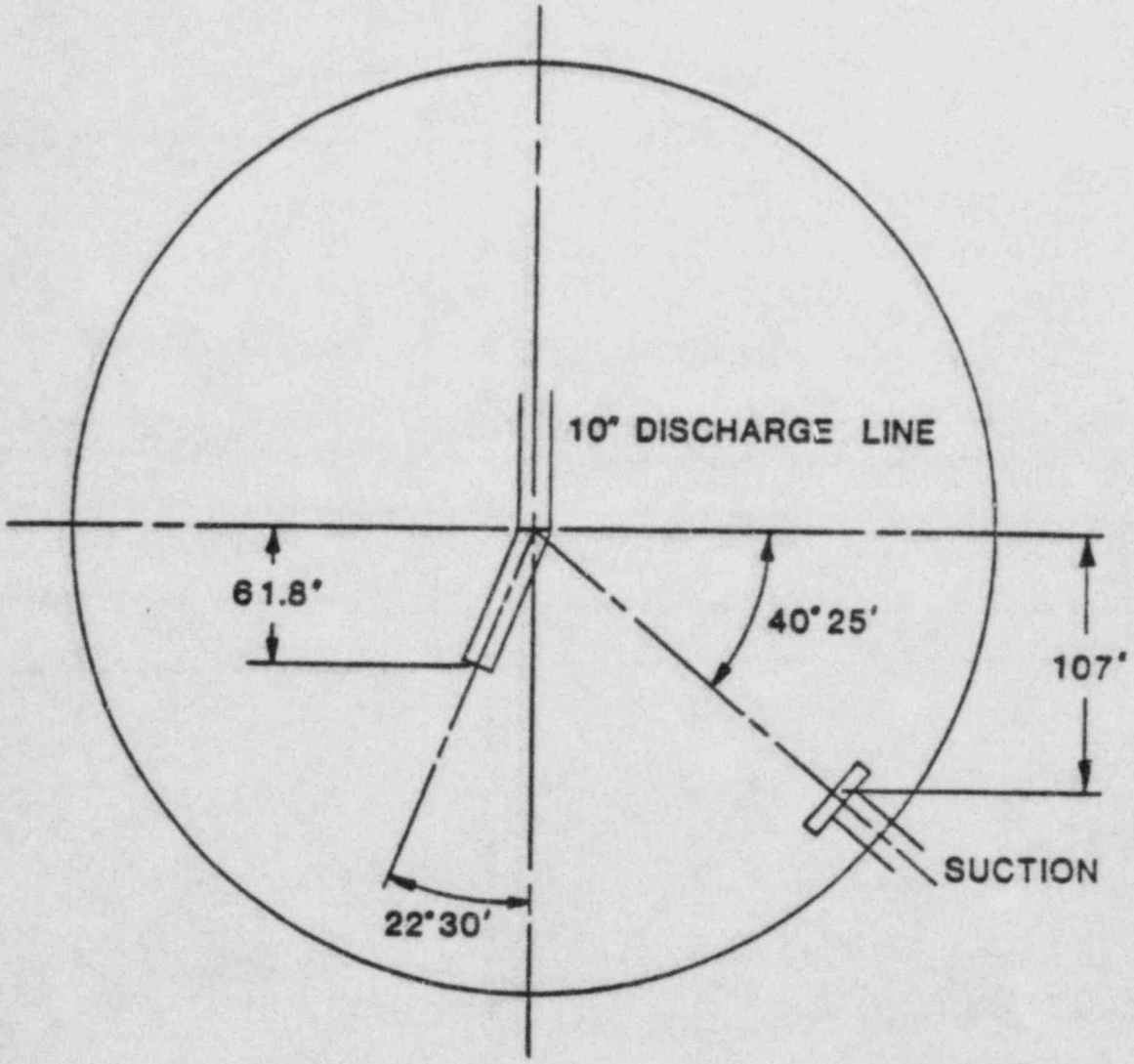

VIEW A-A

FIG. 17 RHR SUCTION AND DISCHARGE ARRANGEMENT

Pages 45 through 52

These pages represent General Electric Company Proprietary Figures 18 through 25 of NEDE-24798-P.

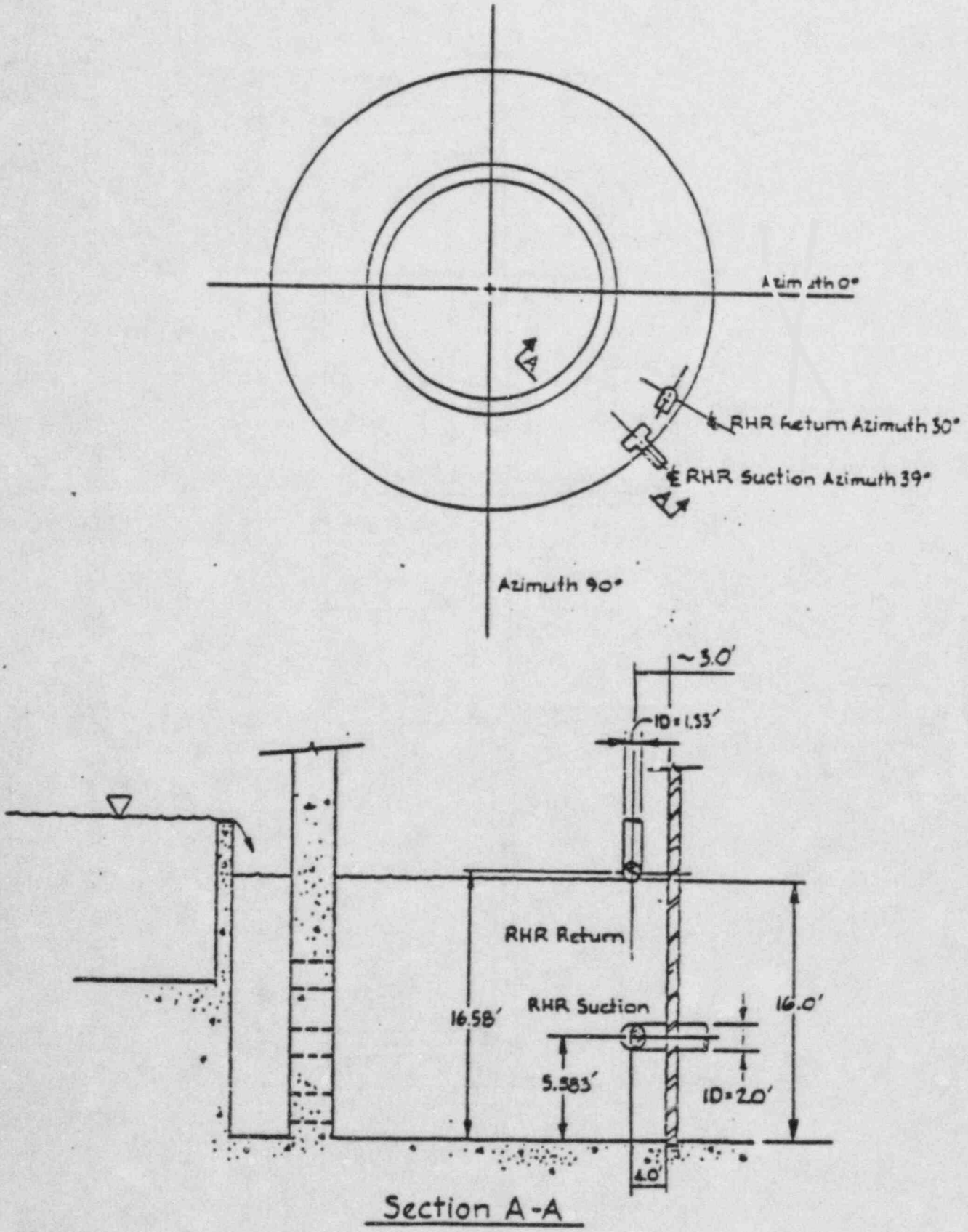

FIGURE 26

RHR RETURN AND SUCTION DETAIL

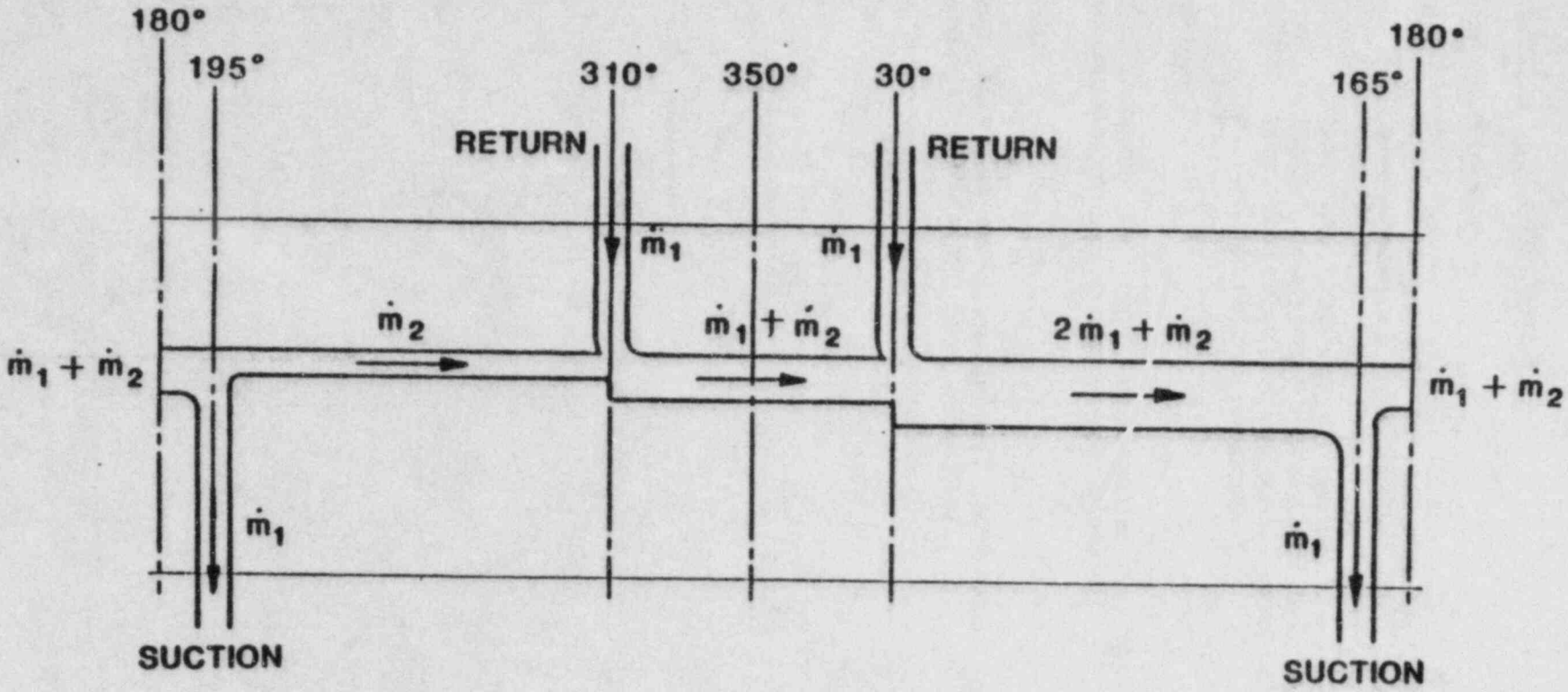

FIG. 27 GLOBAL FLOW FOR DISCHARGE JETS POINTING IN THE SAME DIRECTION

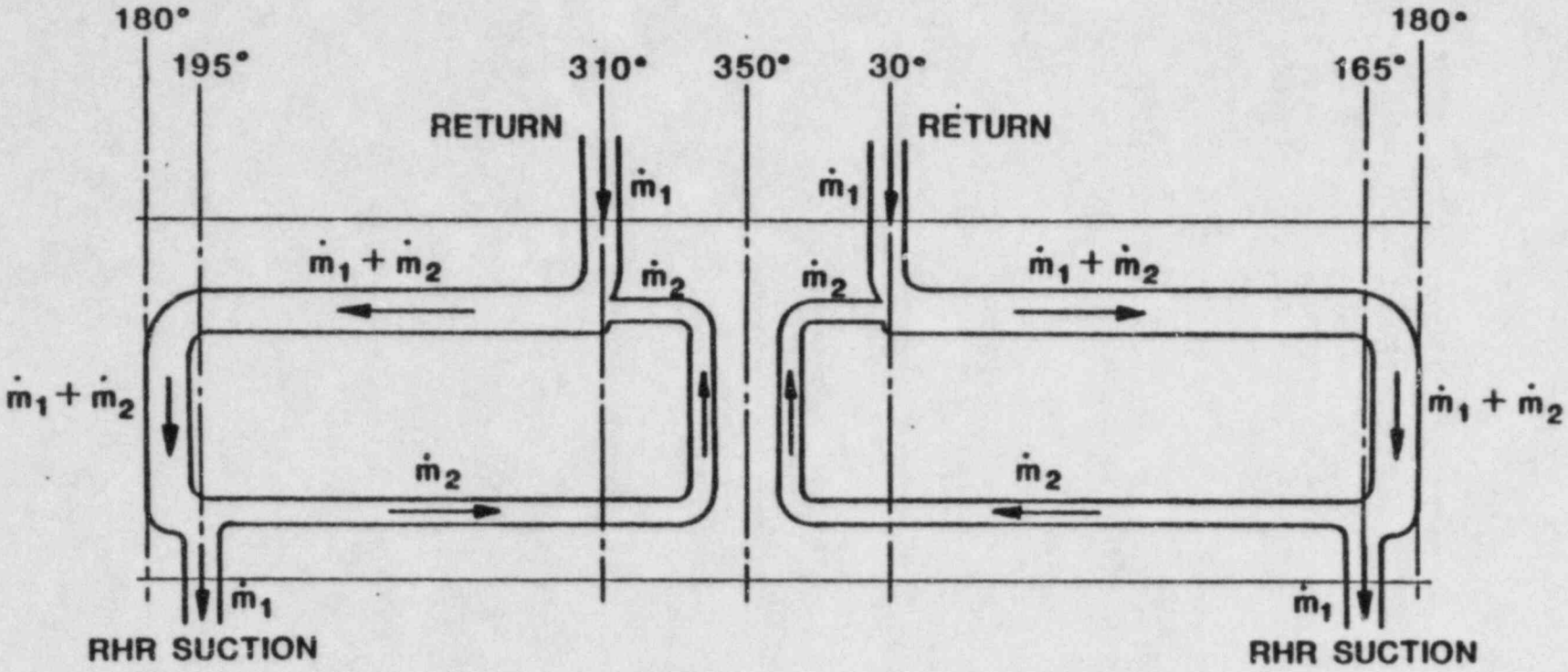

FIG. 28 GLOBAL FLOW FOR THE CASE OF OPPOSING DISCHARGE JETS

Action Plan 17 - Plant Specific

I. Issues Addressed

4.8 Operation of the RHR system in the containment spray mode will decrease the heat transfer coefficient through the RHR heat exchangers due to decreased system flow. The FSAR analysis assumes a constant heat transfer rate from the suppression pool, even with operation of the containment spray.

II. Response

This concern is not applicable to the River Bend Station design (no containment spray).

III. Status

Based on the above response, this issue is considered closed for RBS with this submittal.

Action Plan 18 - Plant Specific

I. Issues Addressed

4.9 The effect on the long-term containment response and the operability of the spray system due to cycling the containment spray on and off to maximize pool cooling needs to be addressed. Also provide and justify the criteria used by the operator for switching from the containment spray mode to pool cooling mode, and back again.

5.3 Leakage from the drywell to containment will increase the temperature and pressure in the containment. The operators will have to use the containment spray in order to maintain containment temperature and pressure control. Given the decreased effectiveness of the RHR system in accomplishing this objective in the containment spray mode, the bypass leakage may increase the cyclical duty of the containment sprays.

II. Response

These concerns are not applicable to GSU's River Bend Station design (no containment sprays).

III. Status

Based on the above response, these issues are considered closed for RBS with this submittal.

Action Plan 19 - Plant Specific

I. Issues Addressed

5.1 The worst case of drywell-to-containment bypass leakage has been established as a small-break accident. An intermediate-break accident will actually produce the most significant drywell-to-containment leakage prior to initiation of containment sprays.

5.6 The test pressure of 3 psig specified for the periodic operational drywell leakage rate tests does not reflect additional pressurization in the drywell which will result from upper pool dump. This pressure also does not reflect additional drywell pressurization resulting from throttling of the ECCS to maintain vessel level which is required by the current EPGs.

9.2 The continuous steaming produced by throttling the ECCS flow will cause increased direct leakage from the drywell to the containment. This could result in increase containment pressures.

II. Response

1. The River Bend Station Project considered the entire spectrum of breaks for the bypass study. The resulting allowable bypass capacity ($A/\sqrt{K}$) versus break area is shown in FSAR Figure 6.2-27 (see Attachment 19.1). From this figure it can be seen that the worst-case break for RBS is 0.1 sq ft. The drywell and containment pressures for the worst-case break with a bypass area equal to 1.15 sq ft is shown in FSAR Figure 6.2-27a (see Attachment 19.1).

2. Concern 5.6 is not applicable to GSU's River Bend Station because there is no upper pool dump and because the limiting bypass analyses assumes continuous steaming.

3. The bypass analyses for RBS for break sizes 0.008 sq ft to 1.5 sq ft were performed with SWEC proprietary computer code CONSBA. The analyses for break sizes 1.5 sq ft to 2.5 sq ft were done with SWEC proprietary computer code LOCTVS. The CONSBA code has an all steam blowdown input option. The CONSBA

analyses were performed with an all steam blowdown option. The blowdown history for the worst-case break of 0.1 sq ft with a bypass area equal to 1.15 sq ft is given in Table 19.1. A brief description of the LOCTVS and CONSBA codes is given in Action Plans 10 and 11.

III. Status

Based on the above response, these issues are considered closed for RBS with this submittal.

TABLE 19.1

BLOWDOWN DATA

STEAM LINE BREAK AREA 0.1 SQ FT, BYPASS AREA 1.15 SQ FT

Time	Blowdown Mass (lbm/sec)	Blowdown Enthalpy (Btu/lbm)	Reactor Coolant System Pressure (psia)
0.1	219.9	1190.63	1060.59
0.5	220.25	1190.57	1061.50
1.0	220.02	1190.61	1060.23
10	231.53	1188.44	1113.36
20	213.33	1191.8	1029.08
50	210.2	1192.29	1015.56
100	198.84	1194.10	962.702
200	170.78	1198.23	834.725
500	107.71	1204.38	538.480
1000	72.69	1204.13	358.626
1928	51.07	1201.13	250.742
2000	39.81	1197.98	194.55
2932	25.32	1190.77	122.714
3000	24.12	1189.94	116.90
3600	16.83	1183.82	83.335

NOTES: (1)Peak drywell pressure occurs at 1928 seconds and is equal to 30.565 psia.
(2)Peak containment pressure occurs at 2932 seconds and is equal to 29.101 psia.
(3)Credit is taken for drywell and containment heat sinks and also containment unit coolers.

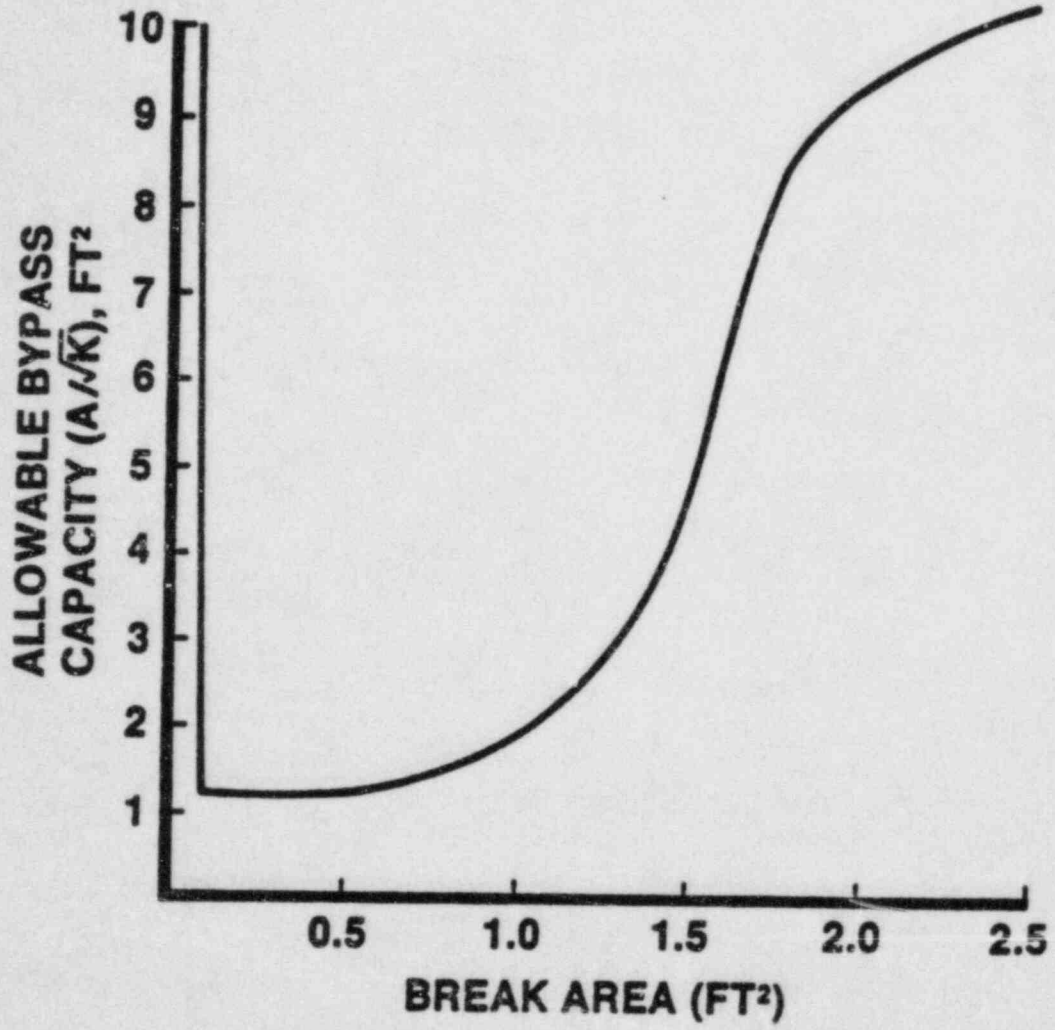

FIGURE 6.2-27

ALLOWABLE SUPPRESSION POOL STEAM BYPASS LEAKAGE CAPACITY

RIVER BEND STATION
FINAL SAFETY ANALYSIS REPORT

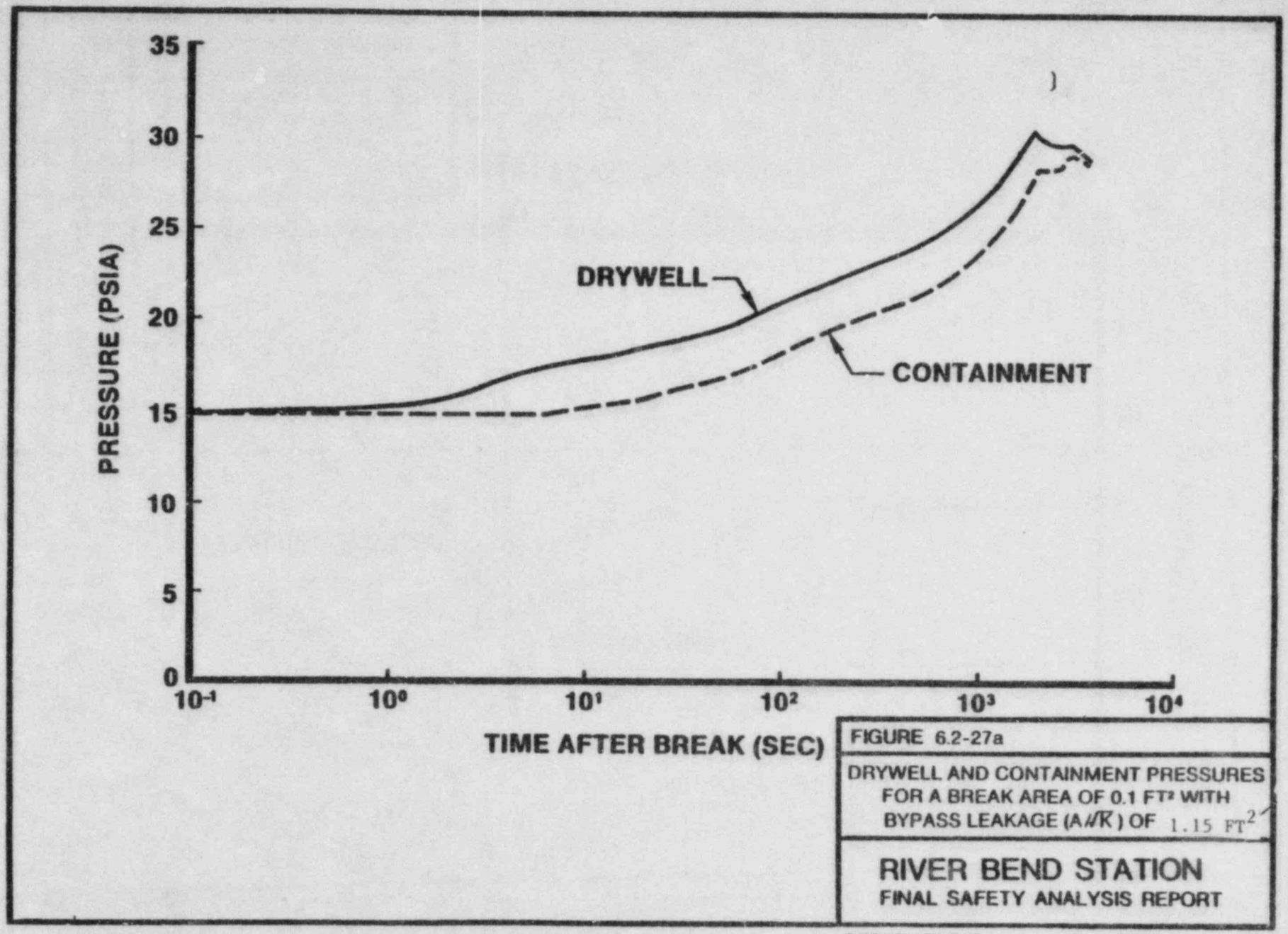

FIGURE 6.2-27a

DRYWELL AND CONTAINMENT PRESSURES FOR A BREAK AREA OF 0.1 FT² WITH BYPASS LEAKAGE ($A/\sqrt{K}$) OF 1.15 FT²

RIVER BEND STATION
FINAL SAFETY ANALYSIS REPORT

Action Plan 20 - Plant Specific

I. Issues Addressed

5.4 Direct leakage from the drywell to the containment may dissipate hydrogen outside the region where the hydrogen recombiners take suction. The anticipated leakage exceeds the capacity of the drywell purge compressors. This could lead to pocketing of hydrogen exceeding the concentration limit of 4 percent by volume.

II. Response*

River Bend Station design does not use drywell purge compressors. Instead, the mixing system is manually initiated when the concentration of H_2 in the drywell reaches 3.5 v/o. The two mixing system penetrations that allow air to flow into the drywell from the containment are located diametrically opposite each other on the circumference of the drywell wall above the suppression pool. The drywell atmosphere is exhausted into the larger containment volume through two other penetrations located at the top of the drywell by means of two recirculation fans. Opening the mixing system inlet flow path has the immediate function of equalizing the containment and drywell pressures. The mixing system recirculation fans draw from the drywell during operation and hence, the possibility of direct leakage from the drywell by any other path is eliminated. The design of the mixing system is based upon the operation of one of two redundant systems. Failure of one system will not affect the potential of hydrogen pocketing.

Any leakage from drywell to containment before the mixing system initiation is likely to happen through the electrical penetrations. The electrical penetrations are not located near any major obstructions and hence any hydrogen leakage does not result in hydrogen pocketing. The highest electrical penetration is at elevation 156 feet-6 inches. The containment unit coolers are located at elevation 162 feet-3 inches and will provide mixing of the containment atmosphere. The recombiners are located on the refueling platform at elevation 186 feet-3 inches.

III. Status

Based on the above response, this issue is considered closed for RBS with this submittal.

*This response replaces the GSU-submitted response dated April 1, 1983.

Action Plan 21 - Plant Specific

I. Issues Addressed

5.5 Equipment may be exposed to local conditions which exceed the environmental qualification envelope as a result of direct drywell-to-containment bypass leakage.

II. Program for Resolution*

1. A list of essential equipment located near electrical penetrations in the drywell wall will be provided. The list will include a qualitative assessment of the equipment's sensitivity to temperature and the distance of the equipment from the drywell wall.

III. Status

Item 1 is complete and included in this submittal.

IV. Final Program Results*

Following a LOCA or a small break accident, the drywell temperature envelope is higher than the containment. The assumed drywell bypass leakage path is via the drywell electrical penetrations. The safety-related equipment which may be sufficiently near the drywell wall to be affected by higher local temperatures is provided in Table 21.1-1. The maximum distance from the penetrations considered was 10 feet. Actual distances are provided for each item. An assessment of the equipment's sensitivity to temperature is also provided in the "Qualification" column.

It has been determined that those equipment items not qualified for the drywell temperature profile are qualified to perform their safety function for the containment temperature profile with margin in accordance with NUREG-0588. Their exact location in relation to the drywell penetrations has been reviewed to determine that they are a minimum of 3 feet from the drywell penetrations and on or below the elevation of the drywell penetrations. This minimum spacing will be more than sufficient to diffuse any warmer air filtering through the 5-inch conduits filled with cable in the 5-foot thick drywell wall. In addition, the drywell wall and drywell penetration boxes will act as a heat sink which will decrease the leakage temperature.

There is no essential equipment which may be adversely affected by bypass leakage from the drywell. Consequently, GSU considers this issue to be closed.

*This revised Action Plan 21 replaces Action Plan 21 submitted by GSU on the previous submittal date of December 3, 1982.

Table 21.1-1

Safety-Related Equipment
Near the Drywell Electrical Penetrations

Mark Number	Equipment Description	Minimum Distance	Qualification
1E12*MOV37A	Motor-Operated Valve	5 feet	Qualified to DW conditions
1E12*MOV42A	Motor-Operated Valve	6 feet	Qualified to DW conditions
1E12*MOV42B	Motor-Operated Valve	3 feet	Qualified to DW conditions
1CCP*MOV142	Motor-Operated Valve	3 feet	Qualified to DW conditions
1CCP*MOV143	Motor-Operated Valve	3 feet	Qualified to DW conditions
1SWP*MOV4A	Motor-Operated Valve	6 feet	Qualified to DW conditions
1SWP*MOV4B	Motor-Operated Valve	4 feet	Qualified to DW conditions
1CPM*MOV2B	Motor-Operated Valve	2 feet	Qualified to DW conditions
1CPM*MOV4B	Motor-Operated Valve	1 foot	Qualified to DW conditions
1HVR*AOV126	Air-Operated Valve	6 feet	Qualified to DW conditions
1H22*PNLP005	RV Level and Pressure Local Panel	4 feet	Located below the level of the electrical penetrations. The instruments in these panels are nuclear safety related but not essential, i.e., they perform no active safety function
1H22*PNLP006	Recirc Pump A Local Panel	4 feet	
1H22*PNLP010	Jet Pump Instrumentation A Local Panel	3 feet	

Action Plan 22 - Plant Specific

I. Issues Addressed

5.8 The possibility of high temperatures in the drywell without reaching the 2 psig high-pressure scram level because of bypass leakage through the drywell wall should be addressed.

II. Program for Resolution*

1. A new analysis will be performed using the capability bypass leakage. This analysis will show that a temperature of 330°F is not reached in the drywell until after 10 minutes. In this interval, the operator will have received sufficient information to manually scram the reactor.

III. Status

Item 1 is complete and is included with this submittal.

IV. Final Results*

The steam bypass analysis performed for River Bend Station considered break sizes ranging from 0.008 sq ft to 2.5 sq ft. The resulting bypass area versus break size is shown in Figure 1.0 of Action Plan 19. From this figure it can be seen the worst size break for RBS is 0.1 sq ft. The following table provides a summary of small break accident analyses for break sizes ranging from 0.1 to 0.008 sq ft with a bypass area equal to 1.15 sq ft.

Break Size Sq Ft	2 psig Scram Signal Time (sec)	Peak Drywell Temperature(°F)/ at Time(sec)
0.1(1)	3.7	251.3 /1940 sec
0.08(1)	4.7	250.33/1900 sec
0.03(1)	17.2	190.78/2590 sec
0.008(1)	570	169.8 /1025 sec
0.08(2)	4.5	249.3 /2540 sec
0.008(2)	668	215.3 /4560 sec
0.008(3)	628	221.5 /3150 sec

For large breaks the 2 psig scram signal is reached nearly instantaneously and the temperature in drywell remains below the design temperature of 330°F. For small breaks, the energy addition is at a slower rate, and due to the large heat sink availability, the tem-

perature of drywell will not exceed the design drywell temperature as shown in the above table.

Based on the above response, this issue is considered closed for RBS with this submittal.

NOTES: (1) Analysis assumes pure steam bypass and 100 percent revaporization of steam condensate from heat sinks.

(2) Analysis assumes homogeneous flow through bypass area and 100 percent revaporization of steam condensate from heat sinks.

(3) Analysis assumes homogeneous flow through bypass area and 8 percent revaporization from heat sinks.

*This revision replaces the GSU submittal dated April 1, 1983.

Action Plan 23 - Plant Specific

I. Issues Addressed

6.3 The recombiners may produce "hot spots" near the recombiner exhausts that might exceed the environmental qualification envelope or the containment design temperature.

6.5 Discuss the possibility of local temperatures due to recombiner operation being higher than the temperature qualification profiles for equipment in the region around and above the recombiners. State what instructions, if any, are available to the operator to actuate containment sprays to keep this temperature below design values.

II. Program for Resolution

Arrangement drawings of the hydrogen recombiner areas of the containment will be submitted to demonstrate that no essential equipment could be affected by the recombiner thermal plume, which is only 50°F above the ambient temperature at the recombiner exhaust.

III. Status

Item 1 is complete and is included with this submittal.

IV. Final Program Result*

A review of equipment arrangements has been performed. No safety-related Class 1E equipment has been found located in the vicinity of the recombiner. In any event, the recombiners are not expected to be activated until approximately 13 days after the accident, at which time the ambient temperature in the containment has returned to the normal range of 90°F. This will result in a localized temperature rise to 140°F, which is within the accident qualification peak temperature. In addition, there are no containment temperature sensors located in the vicinity of the hydrogen recombiners which would indicate any local temperature effects.

In addition, detailed analysis considering the unit coolers and heat sinks show that the containment bulk temperature rise due to operation of two hydrogen recombiners is less than 3°F as shown in Figures 23.1 through 23.3. Also RBS has three containment temperature monitors located at elevation 166 feet-9 inches and seven monitors located at

elevation 118 feet-6 inches to detect any temperature stratification in the containment.

Based on the above results, these issues are considered closed.

*This revision replaces the GSU submittal dated April 1, 1983.

KEY ASSUMPTIONS
- POOL EVAPORATION CONSIDERED
- HEAT TRANSFER COEFF FOR COOLERS FROM VENDOR DATA
- CREDIT FOR HEAT SINKS
- CONSERVATIVE INITIAL TEMP OF 130°F

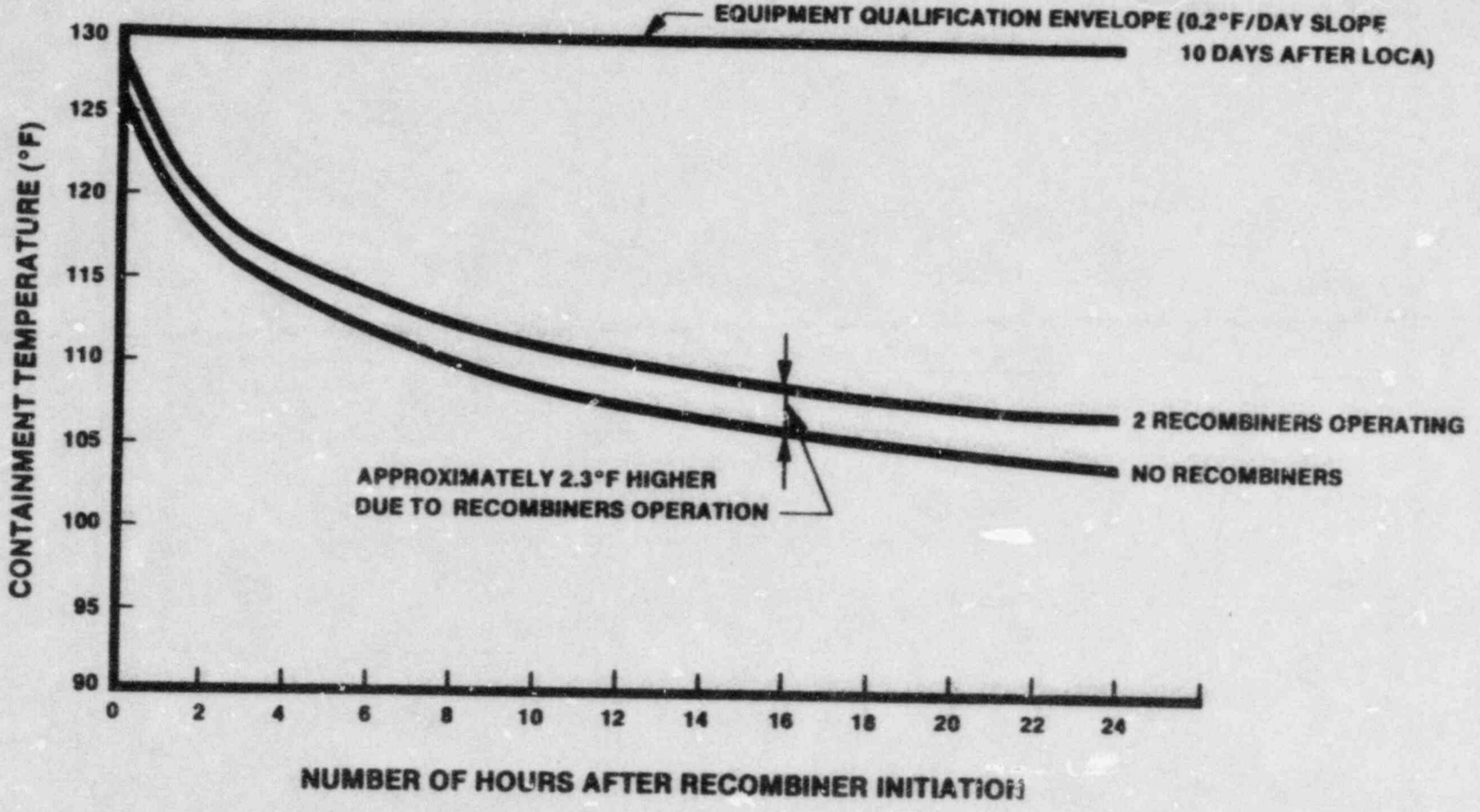

FIGURE 23.1 CONTAINMENT BULK TEMPERATURE DUE TO H_2 RECOMBINER OPERATION

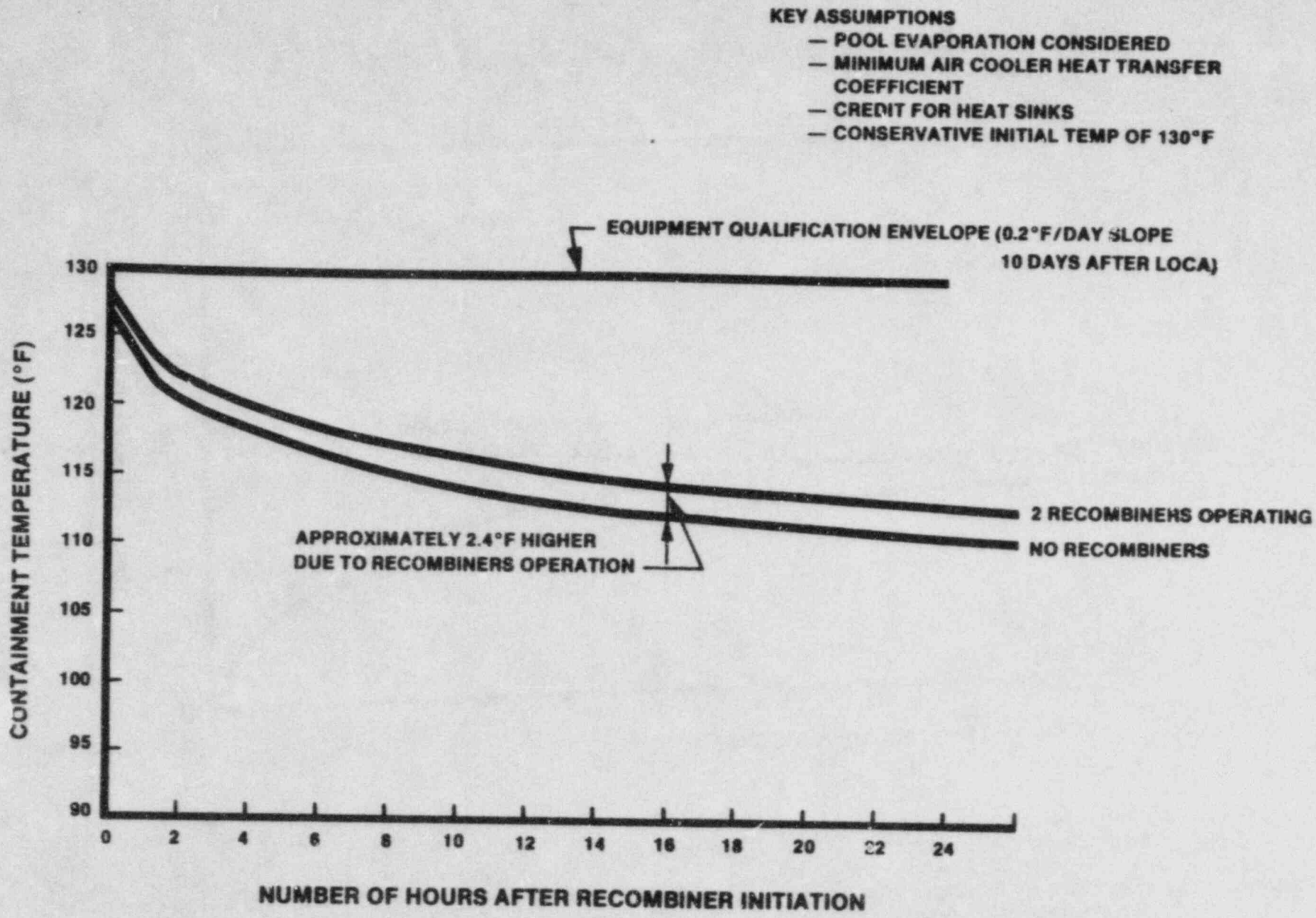

FIGURE 23.2 CONTAINMENT BULK TEMPERATURE DUE TO H_2 RECOMBINER OPERATION

KEY ASSUMPTIONS
- NO POOL EVAPORATION
- MINIMUM AIR COOLER HEAT TRANSFER COEFFICIENT
- CREDIT FOR HEAT SINKS
- CONSERVATIVE INITIAL TEMP OF 130°F

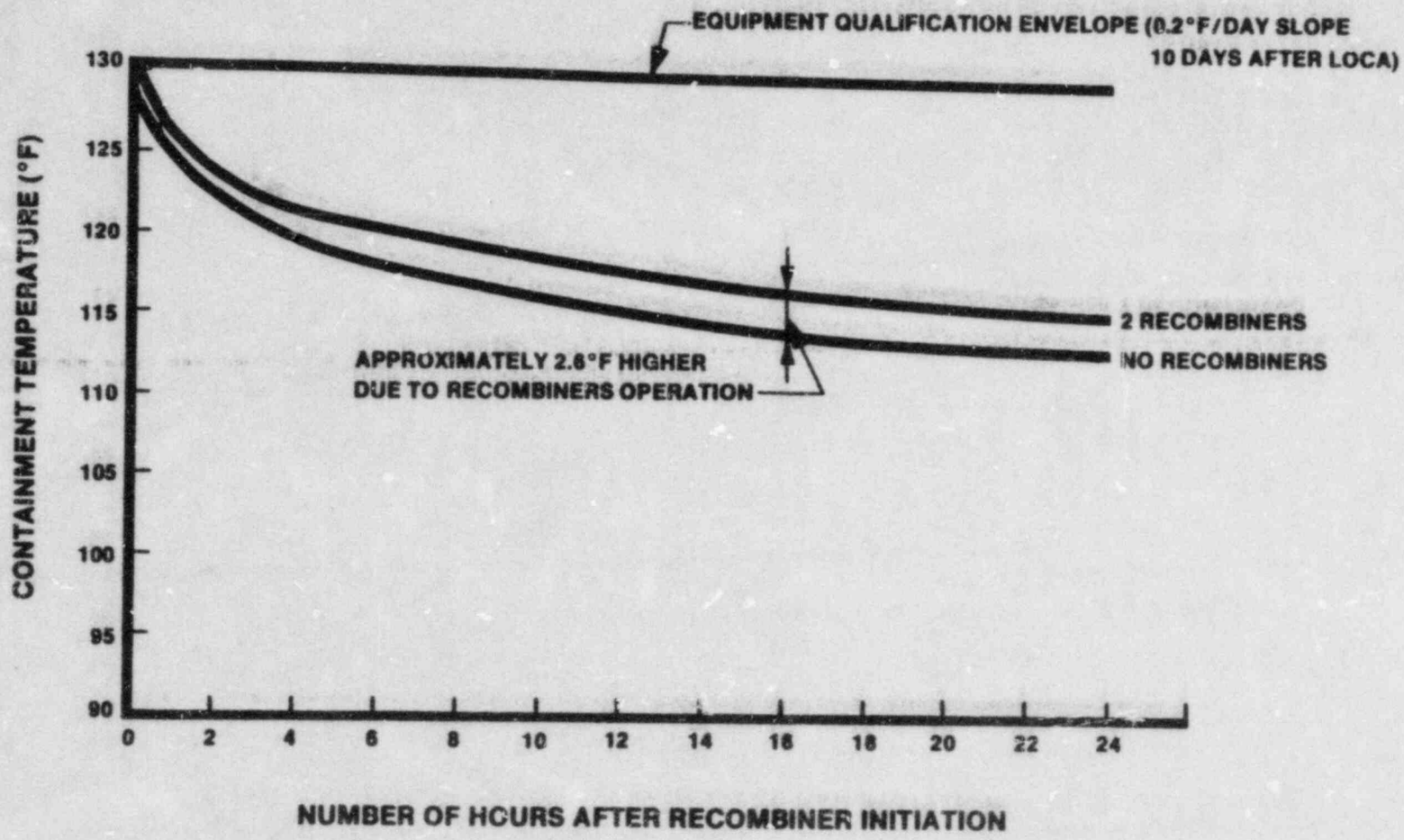

FIGURE 23.3 CONTAINMENT BULK TEMPERATURE DUE TO RECOMBINER OPERATION

Action Plan 24 - Plant Specific

I. Issues Addressed

7.2 The computer code used by General Electric to calculate environmental qualification parameters considers heat transfer from the suppression pool surface to the containment atmosphere. This is not in accordance with the existing licensing basis for Mark III environmental qualification. Additionally, the bulk suppression pool temperature was used in the analysis instead of the suppression pool surface temperature.

II. Response

The RBS analysis was done using SWEC codes. The environmental design criteria (EDC) was developed in accordance with NUREG 0588. Additionally, the analysis assumes that the surface temperature of the pool is 5°F greater than the bulk pool temperature.

III. Status

Based on the above response, this issue is considered closed for RBS with this submittal.

Action Plan 25 - Plant Specific

I. Issues Addressed

8.1 This issue is based on consideration that some technical specifications allow operation at parameter values that differ from the values used in assumptions for FSAR transient analyses. Normally, analyses are done assuming a nominal containment pressure equal to ambient (0 psig) and a temperature near maximum operating temperature (90°F) and do not limit the drywell pressure equal to the containment pressure. The technical specifications permit operation under conditions such as a positive containment pressure (1.5 psig) and temperatures less than maximum (60 or 70°F), and drywell pressure can be negative with respect to the containment (-0.5 psid). All of these differences would result in transient responses different than the FSAR descriptions.

II. Response*

The post-LOCA containment peak pressure is sensitive to variables that affect long-term analysis, such as initial suppression pool temperature, decay heat rate, containment unit cooler heat transfer coefficient, and passive heat sink area. The main steam line break (MSLB) sensitivity analysis results for the above-mentioned variables for RBS are presented in FSAR Figures 6.2-33 through 6.2-37, included as Attachment 25.1. The sensitivities of drywell and containment peak pressure and temperature to initial conditions varied over their expected ranges are given in Table 1. These results indicate that the calculated peak pressures and temperatures are relatively insensitive to variations in the initial conditions.

III. Status

Based on the above response, this issue is considered closed for RBS with this submittal.

*This revised response replaces the response submitted by GSU in the previous submittal dated April 1, 1983.

TABLE 1. SENSITIVITY OF CALCULATED DRYWELL PRESSURE AND TEMPERATURE TO INITIAL CONDITIONS FOR 24 INCH MAIN STEAM LINE BREAK

Initial Conditions						Peak Pressure (psig)		Peak Temperature (°F)	
Pressure (psig)		Temperature (°F)		Mass of Air (lbm)					
DW	Cont	DW	Cont	DW	Cont	Drywell	Cont	Drywell	Cont
0.0	0.0	135	90(1)	14,405	83,937	19.06	5.19	316.0	137.8
1.0	0.0	135	90(1)	15,477	83,937	19.34	5.37	307.44	137.7
2.0	0.0	135	90(1)	16,550	83,937	19.68	5.56	299.20	137.8
0.0	0.0	135	70(2)	14,405	88,386	19.06	4.9	316.0	127.2
2.0	0.0	135	70(2)	16,550	88,386	19.68	5.27	299.15	127.2
2.0	0.0	135	70(3)	16,550	88,386	19.68	7.86	299.15	155.9

NOTES: (1) The service water temperature to the containment unit coolers is at a maximum temperature of 95°F.
(2) The service water temperature to the containment unit coolers is assumed to be at a temperature of 70°F.
(3) No credit taken for containment coolers.

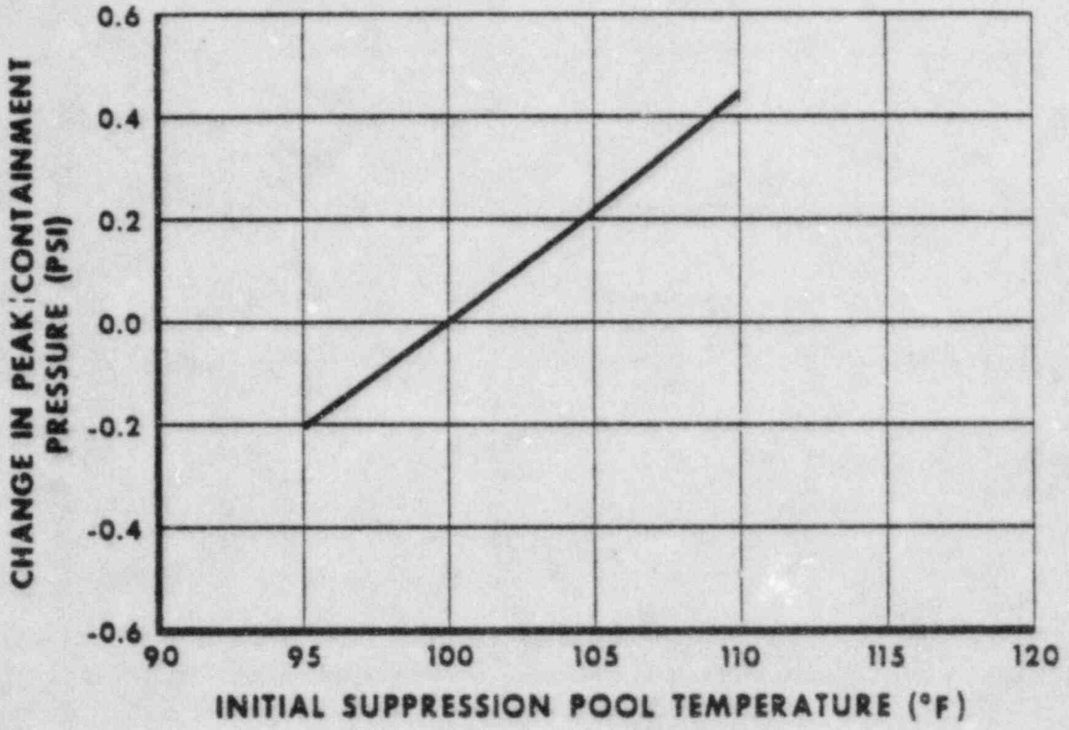

FIGURE 6.2-33

SENSITIVITY OF PEAK CONTAINMENT PRESSURE TO INITIAL SUPPRESSION POOL TEMPERATURE

RIVER BEND STATION
FINAL SAFETY ANALYSIS REPORT

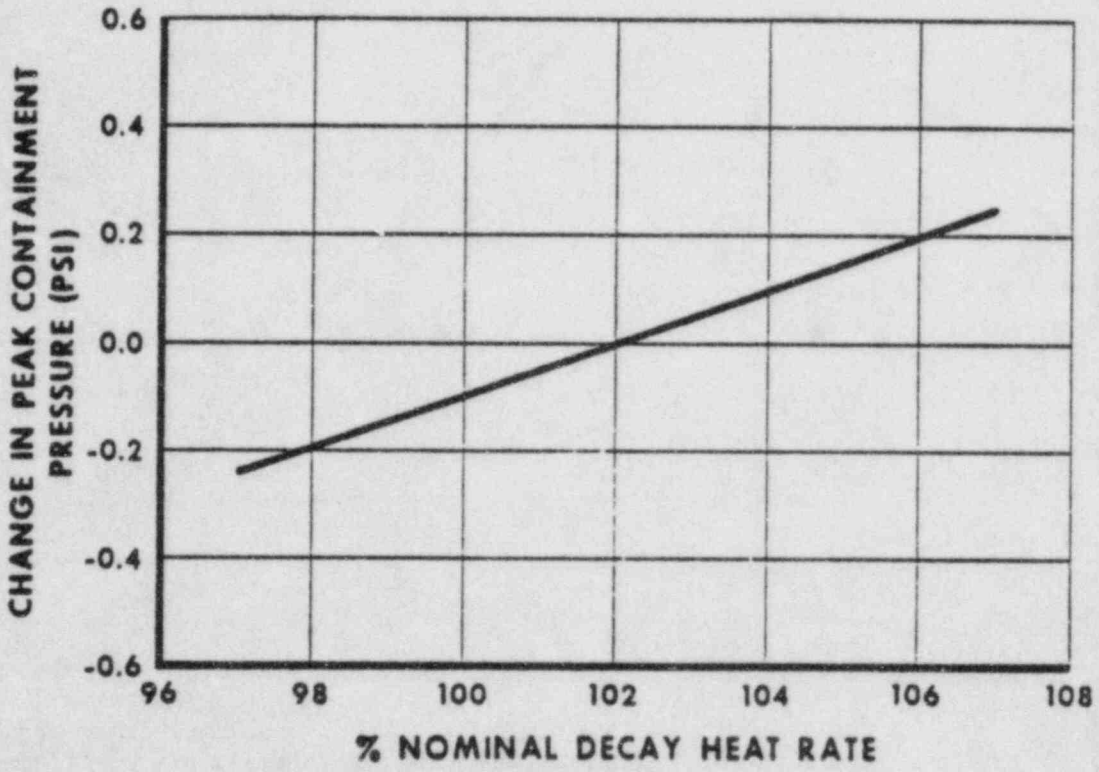

FIGURE 6.2-34

SENSITIVITY OF PEAK CONTAINMENT PRESSURE TO DECAY HEAT RATE

RIVER BEND STATION
FINAL SAFETY ANALYSIS REPORT

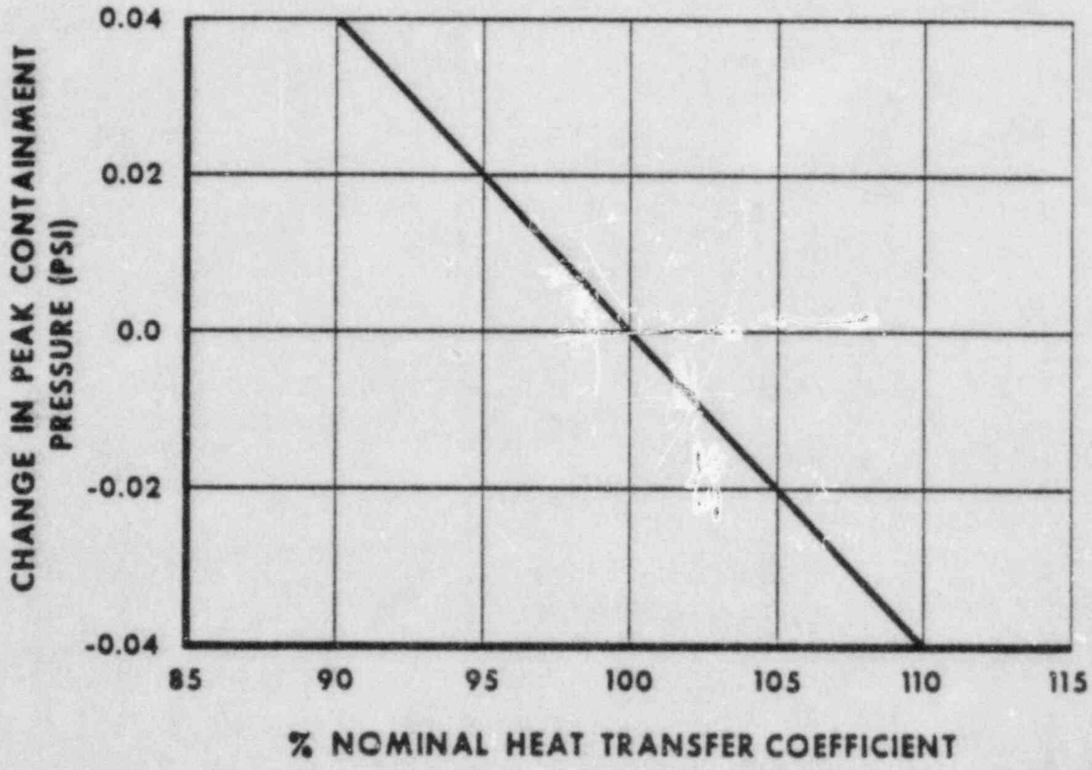

FIGURE 6.2-35

SENSITIVITY OF PEAK CONTAINMENT PRESSURE TO CONTAINMENT UNIT COOLER HEAT TRANSFER COEFFICIENT

RIVER BEND STATION
FINAL SAFETY ANALYSIS REPORT

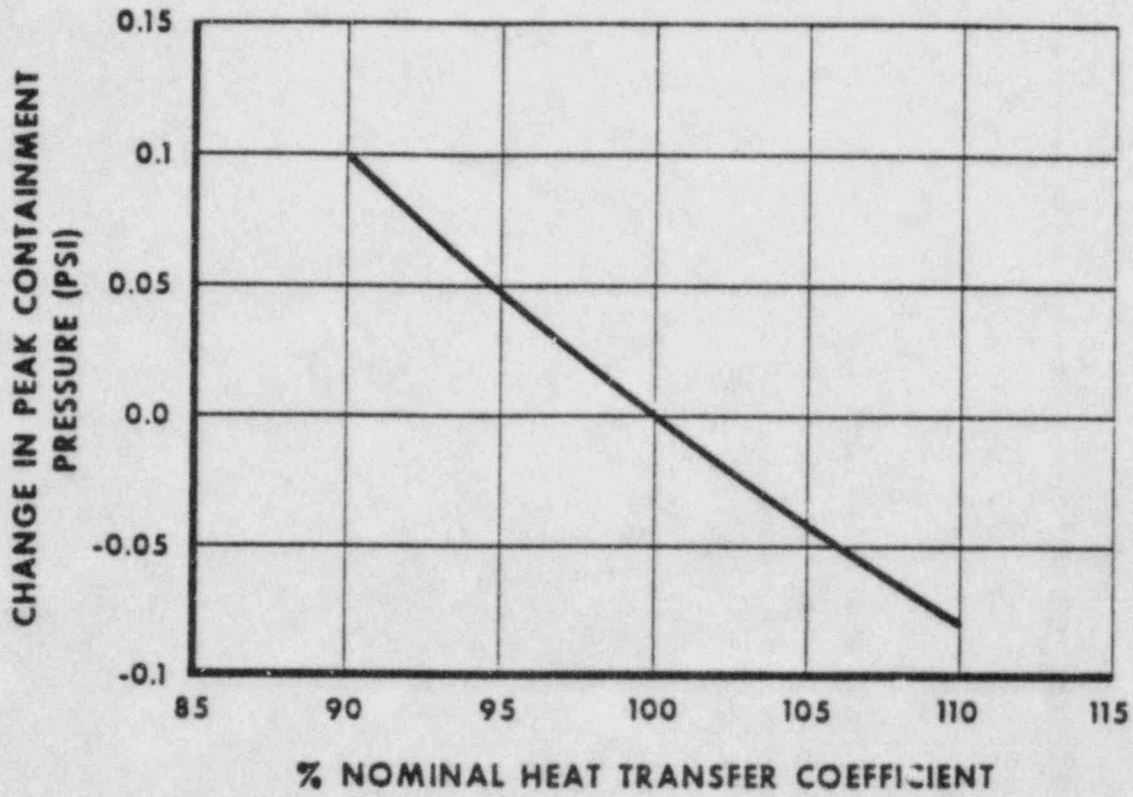

FIGURE 6.2-36

SENSITIVITY OF PEAK CONTAINMENT PRESSURE TO RHR HEAT EXCHANGER HEAT TRANSFER COEFFICIENT

RIVER BEND STATION
FINAL SAFETY ANALYSIS REPORT

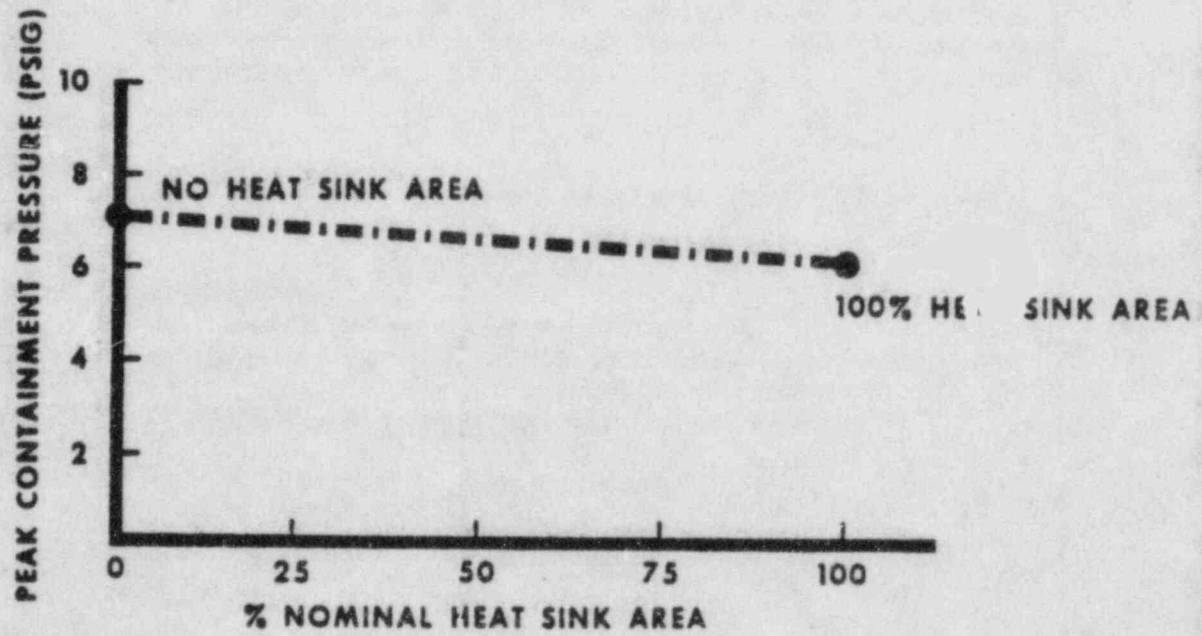

FIGURE 6.2-37

SENSITIVITY OF PEAK CONTAINMENT PRESSURE TO PASSIVE HEAT SINK AREA

RIVER BEND STATION
FINAL SAFETY ANALYSIS REPORT

Action Plan 26 - Plant Specific

I. Issues Addressed

8.2 The draft GGNS technical specifications permit operation of the plant with containment pressure ranging between 0 and -2 psig. Initiation of containment spray at a pressure of -2 psig may reduce the containment pressure by an additional 2 psig, which could lead to buckling and failures in the containment liner plate.

8.3 If the containment is maintained at -2 psig, the top row of vents could admit blowdown to the suppression pool during an SBA without a LOCA signal being developed.

II. Response*

1. The proposed RBS technical specifications limit the containment pressure range to -0.3 to 0.3 psig. Also, RBS does not have containment sprays. RBS does, however, have containment unit coolers, and analyses have been done that consider the failure of chilled water control valves to close and isolate chilled water to one containment unit cooler. Supplied with a continuous flow of 57°F chilled water, one containment unit cooler continues reducing containment pressure and temperature. At -12 in. WG (-0.43 psig) pressure, the chilled water isolation valves are closed automatically by redundant signals from differential pressure transmitters that sense the differential pressure between the containment and the shield building annulus.

2. Concern 8.3 is not applicable to RBS. The containment pressure range during normal conditions is -0.3 to 0.3 psig. Therefore, the top row of vents cannot admit blowdown without a LOCA signal being generated.

III. Status

Based on the above response, these issues are considered closed for RBS with this submittal.

*This response replaces the GSU-submitted response on April 1, 1983.

Action Plan 27 - Plant Specific

I. Issues Addressed

8.4 Describe all of the possible methods, both before and after an accident, of creating a condition of low air mass inside the containment. Discuss the effects on the containment design external pressure of actuating the containment sprays.

II. Program for Resolution*

1. A complete list of scenarios which might result in reduced containment air mass will be developed.

2. The list of scenarios developed in Item 1 will be reviewed and a worst case, bounding scenario will be selected.

3. An evaluation will be completed to establish the containment response under the bounding scenario.

III. Status*

Items 1 through 3 are complete and are included in this submittal.

IV. Final Program Results*

The following scenarios have been identified as mentioned in Item 1 of the Program for Resolution as leading to reduced air mass in the containment:

Scenario 1 - Containment purge exhaust operating with no purge supply.

Scenario 2 - RWCU line break with purge exhaust operating and no purge supply.

Scenario 3 - Instrument line break with purge exhaust operating and no purge supply.

Scenario 4 - Loss of containment HVAC with purge exhaust operating and no purge supply.

All scenarios were analyzed, and it was concluded that Scenario 2 is the bounding case.

The sequence of events for this scenario is described as follows:

- RWCU line break in the containment with the purge supply line inadvertently closed.

- Purge exhaust continues.

- At -12 inches WG, containment unit coolers automatically isolate.

- Operator isolates the purge exhaust system.

The analysis was performed using SWEC computer code THREED to simulate RWCU line break with purge supply isolated and purge exhaust operating.

The final containment pressure was calculated by assuming that the containment atmosphere cools down to 90°F with a relative humidity of 20 percent (corresponding to initial conditions).

The results show that the purge exhaust system must be isolated within 100 seconds after the RWCU line break to keep the final containment pressure within the design pressure of -0.6 psig.

Design modification will be initiated for providing an interlock on purge exhaust and supply valves and for preventing such inadvertent closure of purge supply line with exhaust continuing.

Conclusions

RBS containment will not experience a reduction of air mass after including the design modification stated above. This issue is considered closed for RBS with this submittal.

*This revision replaces the GSU submittal dated April 1, 1983.

Action Plan 28 - Plant Specific

I. Issues Addressed

9.3 It appears that some confusion exists as to whether SBAs and stuck-open SRV accidents are treated as transients or design basis accidents. Clarify how they are treated, and indicate whether the initial conditions were set at nominal or licensing values.

II. Response

The RBS analysis discussed in FSAR Section 6.2 considers SBAs and stuck-open SRV accidents as design basis accidents, assuming:

- Maximum initial suppression pool temperature
- Maximum initial conditions
- Loss of offsite power
- Single active failure (i.e., minimum availability of engineered safety features).

III. Status

Based on the above response, this issue is considered closed for RBS with this submittal.

Action Plan 29 - Plant Specific

I. Issues Addressed

10.1 The suppression pool may overflow from the weir wall when the upper pool is dumped into the suppression pool. Alternatively, negative pressure between the drywell and the containment that occurs as a result of normal operation or sudden containment pressurization could produce a similar overflow. Any cold water spilling into the drywell and striking hot equipment may produce thermal failures.

II. Program for Resolution

Although RBS does not incorporate an upper pool dump, an evaluation currently in progress will be completed that will define the extent of drywell flooding due to weir wall overflow. The effect of cold water striking safety-related equipment will be evaluated to ensure that no thermal failures occur.

III. Schedule

Item 1 is complete and is included with this submittal.

IV. Final Results*

The containment pressurization following a worst 4-in. RWCU line break in the RWCU heat exchanger room is considered. Blowdown from upstream of the break is calculated using Moody choked flow model and the blowdown from downstream is obtained using RELAP4MOD(5) computer code. Table 29.1 provides the total blowdown. This blowdown is used in SWEC proprietary computer code THREED to determine containment pressurization. The initial containment conditions used in the analysis are:

Pressure = 0 psig
Temperature = 90°F
Relative Humidity = 0.5

The peak calculated containment pressure with the above initial conditions is 0.54 psid. The required containment to drywell differential pressure for the suppression pool to overflow the weir wall is 0.58 psid. Therefore, no pool overflow can occur with the above initial conditions. However, if the drywell to containment pressure difference is at the lower technical specification limit of -0.3 psid (the technical specification allowable range is $-0.3 \leq \Delta P_{DW-CONT} \leq 1.2$ psid),

an RWCU line break in containment would result in weir wall overflow. However, negative values of drywell to containment differential pressure are unlikely to occur as the drywell temperature is higher (135°F) than containment and all the heat load from the reactor vessel, steam lines, etc, tend to maintain positive pressure in the drywell atmosphere. Therefore, the condition resulting in drywell to containment differential pressure of -0.3 psid ($P_{DW} - P_{CONT} = 0.0 - 0.3$) is an extremely rare event and not considered in the analysis.

Further, the drywell to wetwell differential pressure can be controlled by opening the inlet valves of the mixing system.

In addition, as shown in Attachment 29.1, the drywell flooding is a rare event occurring only once or twice during a 40-year plant life, and the resulting peak stresses due to thermal shock are important only for fatigue and fatigue usage.

Based on the above response, this issue is considered closed for RBS with this submittal.

*This final program result replaces the results submitted by GSU on April 1, 1983.

TABLE 29.1 BLOWDOWN DATA 4-IN. RWCU
DER IN RWCU HX ROOM

Time sec	Blow Down Mass Flow Rate lb/sec	Blow Down Energy Flow Rate btu/sec	Time sec	Blow Down Mass Flow Rate lb/sec	Blow Down Energy Flow Rate btu/sec	Time sec	Blow Down Mass Flow Rate lb/sec	Blow Down Energy Flow Rate btu/sec
0.0	0.0	0.0	3.50	278.65	132730.8	45.00	48.86	6201.6
0.001	319.07	168807.45	4.00	266.02	127881.9	46.00	48.73	6085.3
0.002	334.56	177013.68	4.50	257.80	124639.9	47.00	48.57	5972.3
0.002	349.56	184953.87	5.00	251.75	122233.9	48.00	48.43	5864.4
0.003	363.97	192575.96	5.50	247.60	120537.2	49.00	48.24	5756.4
0.004	377.72	199841.61	6.00	245.03	119417.3	50.00	48.05	5653.7
0.005	390.72	206708.07	6.50	243.10	118553.7	51.00	47.83	5552.0
0.006	403.00	213185.62	7.00	233.34	113506.2	52.00	47.58	5451.4
0.006	415.12	219597.21	7.50	167.46	78731.5	53.00	47.31	5353.1
0.007	427.22	225999.14	8.00	101.76	44036.8	54.00	46.99	5254.8
0.008	439.30	232390.86	8.50	36.18	9398.6	55.00	46.63	5155.5
0.009	451.36	238771.42	9.00	35.34	9009.8	56.00	46.07	5039.0
0.010	463.40	245139.77	9.50	34.54	8648.4	57.00	45.59	4936.4
0.010	469.41	248319.43	10.00	33.76	8309.4	58.00	45.00	4826.5
0.020	616.94	326348.44	10.50	32.98	7981.9	59.00	44.41	4720.5
0.030	756.90	400351.43	11.00	32.27	7687.2	60.00	44.66	4708.0
0.040	885.52	468319.01	11.50	31.59	7408.9	62.00	45.23	4693.4
0.050	994.00	525594.90	12.00	30.90	7137.7	64.00	45.56	4682.5
0.060	973.08	514500.80	13.00	29.40	6600.1	66.00	45.67	4618.1
0.070	951.33	502963.52	14.00	27.73	6062.0	68.00	45.49	4553.8
0.080	928.77	491002.31	15.00	26.20	5586.5	70.00	45.55	4521.9
0.090	9[illegible].38	478600.01	16.00	26.34	5463.5	72.00	46.46	4582.9
0.100	881.16	465763.65	17.00	29.30	5947.9	74.00	47.05	4619.4
0.150	818.73	432505.45	18.00	29.02	5780.4	76.00	46.76	4578.3
0.200	761.74	401951.37	19.00	25.28	4944.6	78.00	46.04	4503.2
0.250	687.97	362245.89	20.00	19.86	3820.7	80.00	44.84	4388.6
0.300	600.82	314789.15	21.00	12.59	2387.2	82.00	43.21	4237.4
0.350	533.46	276696.99	22.00	13.48	2500.0	84.00	41.05	4039.6
0.400	515.20	263591.57	23.00	28.63	5244.5	86.00	38.55	3809.6
0.450	527.72	266763.27	24.00	36.78	6648 9	88.00	35.97	3572.7
0.500	548.89	275080.30	25.00	37.56	6691.7	90.00	33.63	3358.0
0.550	566.25	282032.40	26.00	33.74	5919.9	92.00	31.47	3160.5
0.600	576.37	285761.66	27.00	27.63	4771.2	94.00	29.71	3001.2
0.650	579.60	286418.16	28.00	21.56	3666.6	96.00	28.16	2863.0
0.700	577.02	284476.57	29.00	15.55	2605.6	98.00	26.75	2735.8
0.750	569.82	280465.72	30.00	46.91	7750.5	100.00	25.42	2616.1
0.800	559.17	274926.08	31.00	51.23	8333.4	102.00	24.16	2502.1
0.850	545.98	268302.31	32.00	50.73	8116.4	104.00	23.17	2415.5
0.900	531.20	261068.37	33.00	50.42	7925.5	106.00	23.13	2425.8
0.950	516.59	254008.00	34.00	50.05	7726.9	108.00	23.48	2479.5
1.000	502.50	247263.12	35.00	49.66	7526.6	110.00	23.95	2546.8
1.050	488.02	240432.87	36.00	49.20	7320.1	112.00	24.44	2618.8
1.100	373.11	180494.45	37.00	48.66	7108.1	114.00	24.84	2682.3
1.200	343.46	166861.52	38.00	48.03	6890.5	116.00	25.07	2729.5
1.300	314.14	153535.43	39.00	48.31	6806.4	118.00	25.11	2756.7
1.400	289.76	142516.55	40.00	48.64	6731.5	120.00	24.84	2749.5
1.500	273.31	134908.19	41.00	48.86	6642.9	120.10	25.00	4891.1
2.000	294.23	139661.43	42.00	49.01	6548.1	443.00	25.00	4891.1
2.500	315.33	146510.08	43.00	49.16	6452.5	443.10	0.0	0.0
3.000	298.82	140177.03	44.00	48.98	6320.8	4000.00	0.0	0.0

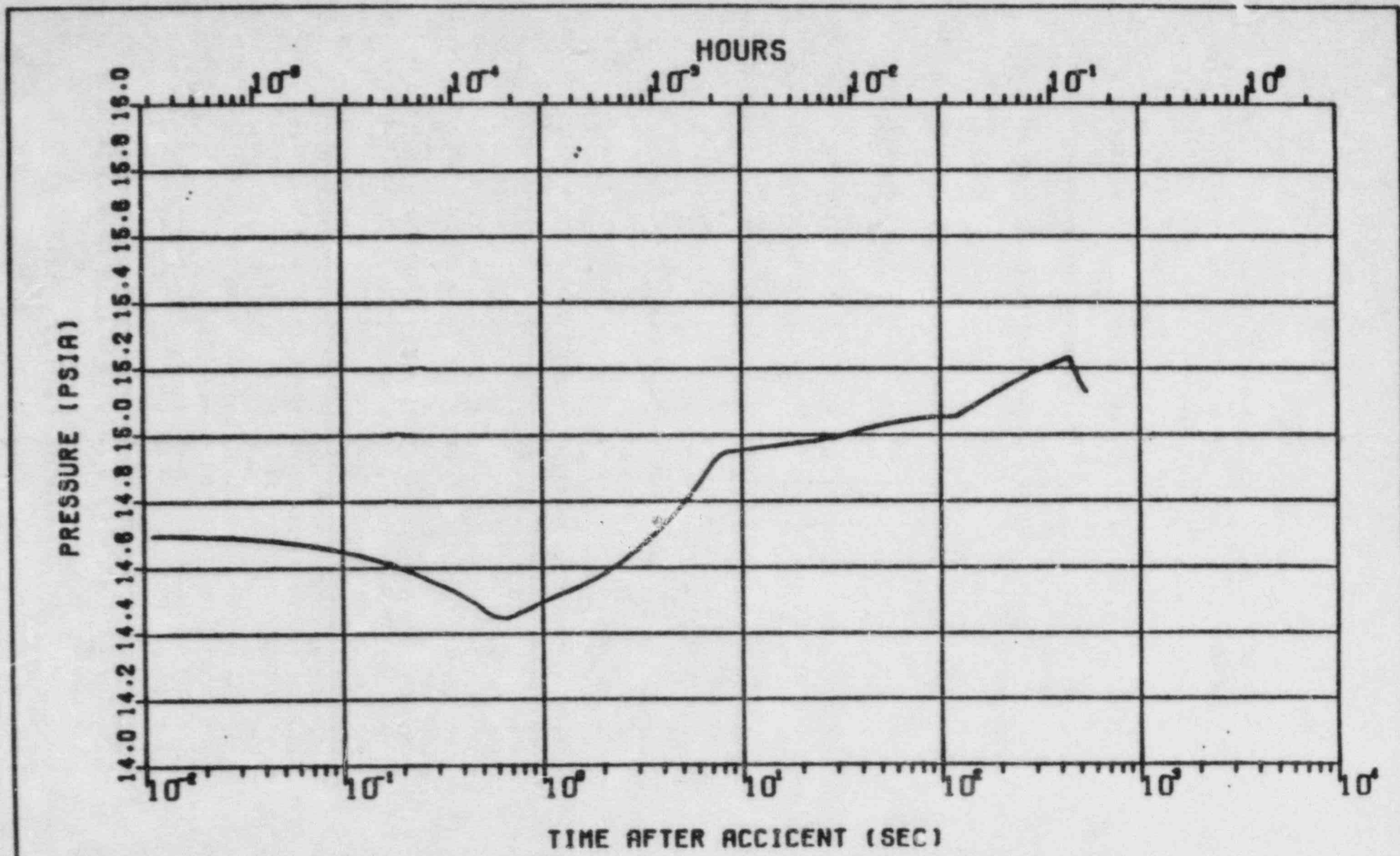

Figure 29.1
CONTAINMENT BUILDING PRESSURE TRANSIENT
4" RHCU DER LINE BREAK ANALYSIS
FOR SUPPRESSION POOL OVERFLOW
RIVER BEND NUCLEAR POWER PLANT

ATTACHMENT 29.1

GENERAL ELECTRIC CO.
NUCLEAR ENERGY DIVISION
SAN JOSE, CA 95125
DESIGN MEMO #123-8324
DRF #124-98

CONTAINMENT ISSUE

ISOLATION TRANSIENT

Prepared by: H. M. Srivastava 7/18/83
H. M. Srivastava, Principal Engineer
Plant Piping Design

Reviewed by: H. L. Hwang 7/21/83
H. L. Hwang, Principal Engineer
Plant Dynamic Methods & Applications

Approved by: J. C. Atwell 7/21/83
J. C. Atwell, Manager
Plant Piping Design

JULY 1983

CONTENTS

1.0 INTRODUCTION.

Various Scenarios lead to conditions where suppression pool water may overflow/backflow over the weir, splashing onto, or partial immersion of, recirculation pumps and piping become possible. Thermal shock, and resulting fatigue, will add to the system imposed (Service Levels A and B) fatigue life for the recirculation piping system and may consume all remaining useful life. Occurrence of any other concurrent, or subsequent, loading could result in a recirculation break LOCA.

2.0 PURPOSE.

The purpose of this report is to show that if this incredible event, were to occur it would not damage the piping system to an extent whereby loading could cause a recirculation break LOCA.

3.0 CLASSIFICATION OF EVENT.

Drywell flooding is a rare event and it is postulated to occur only once or twice during a 40 year plant life. This event can be classified as Service Level C or Service Level D event (Reference 7.1) and no fatigue analysis is required.

4.0 DRYWELL FLOODING TRANSIENT STRESS EVALUATION.

Although this event is classified as Service Levels C or D event, simplified fatigue analyses were made (Reference 7.2) for the pump casing and a typical BWR-6 recirculation piping system subjected to this postulated transient. The assumptions for this evaluation were as follows.

4.1 RECIRCULATION PUMP

The present capability of the recirculation pumps as documented by the Byron Jackson stress report, states the pump casing can withstand a maximum temperature gradient of 350°F without any fatigue evaluation. However, a fatigue evaluation was made with a pump casing temperature gradient of 450°F.

4.2 RECIRCULATION PIPING

A fatigue evaluation was made for this event and the stresses were added to the piping stresses due to system loading and thermal transients. The thermal gradient was evaluated for this event using the LION401 computer program. The surface temperature of the pipe was assumed to be 70° immediately after water reaches the pipe surface. The boundary temperature and heat transfer coefficient were conservatively assumed as follows:

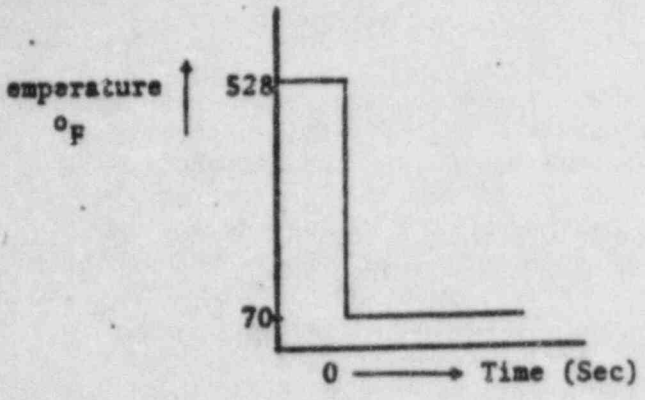

TEMPERATURE PROFILE

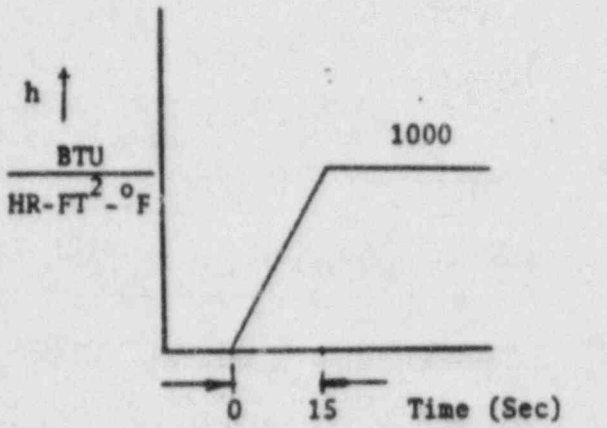

HEAT TRANSFER COEFFICIENT

The heat transfer to water increases rapidly in 15 seconds to 1000 BTU/hr°F Ft^2 and partially destroy the insulation. This causes high thermal gradient in the pipe.

5.0 RESULTS.

The results of the evaluation (Section 4.0) were:

5.1 RECIRCULATION PUMP

5.1.1 The calculated allowable cycles for this transient were 150 cycles which gives a fatigue usage factor of 0.007 (1/150).

5.1.2 Distortion

There is a chance the 450°F temperature difference would cause local yielding such that a dimensional check of the critical parts would be required. The recirculation pump motor cannot tolerate flooding without subsequent cleaning, oil change and drying its' winding. These operations and check have to be done after this event.

5.1.3 Fracture Toughness

The pump casing is cast austenitic stainless steel, so brittle fracture is not a concern.

The pump cover case bolts are ferritic steel. The mean temperature of the cover is: 1/2 (450) + 100 = 350°F. This temperature is above NDTT (Nil Ductility Transition Temperature) of ferritic steel.

5.2 RECIRCULATION PIPING

5.2.1 The calculated maximum temperature gradients for this transient described in Section 4.2 were:

ΔT_1 = 354°F

ΔT_2 = 88°F

T_{AB} = 46°F (Due to thick pump casing and thin pipe)

The stresses due to the above thermal gradients were added to the stresses due to the system loads and thermal gradients. The allowable cycles with these stresses were 900, which gives a fatigue usage factor of 0.001 (1/900).

5.2.2 Distortion

The temperature gradient may distort the pipe at the pipe to pump casing weld location which will not affect the function of the recirculation piping.

5.2.3 Fracture Toughness

For the austenitic stainless steel recirculation piping, fracture is not a concern for this event.

6.0 CONCLUSIONS AND RECOMMENDATIONS.

The above transient is similar to events of "Improper Start of a Cold Loop", except the temperature shock ΔT is 398°F instead of 450°F. So the transient is not totally new for the recirculation piping system design. This event is not a safety concern based on the fatigue evaluation and the following reasons.

1) The stresses produced by the event are in a category (secondary & peak) that do not require evaluation except for Service Levels A & B conditions. These peak stresses produced by the thermal shock are important only for fatigue and fatigue usage which, for a few rare events, is not required by the Code or by NRC rules.

2) If it were necessary to consider the fatigue usage due to this thermal shock, calculations show; based on worst case conditions, that significant fatigue usage would not result unless there were more than one hundred such cycles.

3) Under a worst case condition the potential damage to the piping could be slight distortion at the weld joints. The worst case condition is defined as the insulation being removed and a 450° temperature difference between the outside and inside of the recirculation pipe. In the event that suppression pool water immersed part of the recirculation piping, we would recommend the insulation of the piping be removed and the weld joints connecting the recirculation piping to the recirculation pump be visually examined for deformation at the next shutdown.

Additionally, a dimensional and alignment check of the pump is recommended. The pump motor must be reconditioned by decontamination and drying the insulation, an electrical check, and an oil change. This assumes the motor was flooded.

7.0 REFERENCES.

7.1 ASME Boiler and Pressure Vessel Code, Section III Division I - 1980 Edition upto and including Winter 1982 Addenda.

7.2 Design Record File #124-98, Recirculation Flooding.

APPENDIX A

LION401 PROGRAM

LION401 is a digital computer program which is used to solve the steady state or transient temperature distribution in any three-dimensional configuration. The heat source may be externally conducted or internally generated.

In addition to the solving of heat conduction in structural elements, LION401 may also be used in such cases as forced convection, free convection, or radiation where the output will yield temperatures and heat fluxes for points representing the surface of the structure.

The program solves the transient heat conduction equations for a three-dimensional field using a first forward difference method.

Input to the program consists of structural geometry, physical properties, boundary conditions, internal heat generation rates and coolant flow properties and rates.

Action Plan 30 - Plant Specific

I. Issues Addressed

10.2 Describe the interface requirement (A42) that specifies that no flooding of the drywell shall occur. Describe your intended methods to follow this interface.

II. Response

There is no A42 document applicable to RBS which specifies that no flooding of the drywell occurs. The concerns relates to ensuring that the weir wall has sufficient height to account for an upper pool dump without overflowing the weir wall. Since RBS does not have an upper dump, this issue is not applicable to RBS.

III. Status

Based on the above response, this issue is considered closed for RBS with this submittal.

Action Plan 31 - Plant Specific

I. Issues Addressed

11.0 Mark III load definitions are based upon the levels in the suppression pool and the drywell weir annulus being the same. The GGNS technical specifications permit elevation differences between these pools. This may affect load definition for vent clearing.

II. Program for Resolution

1. An evaluation of the maximum elevation differences that can exist between the weir annulus and the suppression pool will be made for each owner. If these elevation variations are outside the parameters established for GGNS, a bounding set of parameters will be defined.

2. A discussion will be given of how pressure differences between the wetwell and the drywell will be controlled.

3. The changes in hydrodynamic loads that may result from these maximum possible level differences will be evaluated.

III. Status*

Items 1 through 3 are complete, and the results included in this submittal.

IV. Final Program Results*

The differential pressure between drywell and containment for RBS is constrained within the nominal range $-0.3 \leq \Delta P_{DW-CONT} \leq 1.2$ psi.

If the drywell pressure is greater than the containment airspace pressure, the water level in the weir annulus will be depressed and thus the liquid inertia above the top vent will be reduced. This will cause top vent clearing to occur earlier, which implies the drywell pressure at top vent clearing, and also peak drywell pressure will be less than the FSAR values. The lower driving pressures decrease the pool swell velocities, accelerations, and loads.

If, on the other hand, the initial containment airspace pressure is greater than the initial drywell pressure,

top vent clearing would be delayed, which would increase the peak drywell pressure. An analysis was performed to determine the upper limit of this effect for the RBS Nuclear Power Station when the $\Delta P_{DW-CONT}$ is -0.3 psid. This corresponds to the water in the weir annulus being elevated by almost 8 inches. The effect of this pressure difference is to delay top vent clearing by approximately 0.04 sec and increase the drywell pressure at the time of top vent clearing by 0.82 psi. The peak drywell pressure is increased by 0.74 psi.

The changes in the drywell pressure change the driving conditions for submerged structure bubble loads and pool swell. The changes are small, however. Taking the ratio of the drywell pressure increase due to the deeper weir annulus submergence (0.74 psi) to the drywell peak pressure (19.06 psi), it may be seen that the change is about 3.9 percent, clearly a negligible change.

The pressure difference between the wetwell and the drywell will be equalized by opening the inlet valves of the hydrogen mixing system.

Based on the above response this issue is considered closed for RBS with this submittal.

*This revision replaces the GSU submittal dated April 1, 1983.

Action Plan 32 - Plant Specific

I. Issues Addressed

14.0 A failure in the check valve in the LPCI line to the reactor vessel could result in direct leakage from the pressure vessel to the containment atmosphere. This leakage might occur as the LPCI motor operated isolation valve is closing and the motor operated isolation valve in the containment spray line is opening. This could produce unanticipated increases in the containment pressure.

II. Response

This concern is not applicable to RBS (no containment sprays).

III. Status

Based on the above response, this issue is considered closed for RBS with this submittal.

Action Plan 33 - Plant Specific

I. Issues Addressed

16.0 Some of the suppression pool temperature sensors are located (by GE recommendation) 3 in. to 12 in. below the pool surface to provide early warning of high pool temperature. However, if the suppression pool is drawn down below the level of the temperature sensors, the operator could be misled by erroneous readings, and the required safety action could be delayed.

II. Response

The RBS Emergency Procedures will be written to either require the operator to verify level in the suppression pool before reading suppression pool temperature or to specify which suppression pool temperature instruments can be used following an accident.

III. Status

Based on the above response, this issue is considered closed for RBS with this submittal.

Action Plan 34 - Plant Specific

I. Issues Addressed

19.1 The chugging loads were originally defined on the basis of 7.5 feet of submergence over the drywell to suppression pool vents. Following an upper pool dump, the submergence will actually be 12 feet, which may affect chugging loads.

II. Response

This concern is not applicable to RBS (no upper pool dump).

III. Status

Based on the above response, this issue is considered closed for RBS with this submittal.

Action Plan 35 - Generic

I. Issues Addressed

19.2 The effect of local encroachments on chugging loads needs to be addressed.

II. Program for Resolution

1. An evaluation of the adequacy of available models to investigate the impact of longer acoustic paths on chugging load definition will be performed. A model will be selected, and the effects of encroachments will be quantified.

2. The inertial impedance effect on chugging loads will be quantified to the maximum extent possible.

III. Status*

Items 1 and 2 are complete and results are included in this submittal.

IV. Final Program Results*

Item 1

A three-dimensional acoustic model of the suppression pool was used to determine the effects of the GGNS TIP platform pool swell deflector on pool boundary loads due to chugging. Actual test data from the PSTF test yielding the maximum chug pressure in a clean pool (Test Run No. 5707-11, Chug 78) was input into the acoustic model with and without the encroachment in place. The maximum pressure at each location on the containment wall was averaged to obtain the area-averaged peak pressure on the wall for both the encroached and unencroached cases. A ratio of the pressures between cases was found. This ratio was applied to the ARS of the maximum measured PSTF chug and then compared with the ARS of the local load definition. The local load definition was used for comparison because the TIP encroachment only covers a small portion of the total pool (less than 5 percent).

The above procedure was also performed on the drywell wall and the basemat. Comparison plots are shown in Figures 1 through 3. Figure 35.1 shows that a small amount of exceedance exists on the containment wall. This exceedance is less than 15 percent at its maximum and is judged to be negligible because, as can be seen,

the integrated area of exceedance (indicative of energy) is very small in the range of concern. Furthermore, the total load definition energy easily bounds that of the encroached signal energy. Figure 35.2 shows that the drywell wall load definition bounds the encroached load everywhere. Finally Figure 35.3 shows that there is up to 60 percent exceedance of the basemat local load definition in the frequency range from 12 Hz to 22 Hz.

This load exceedance is not of any consequence, since it is a local load and the basemat liner is the structure involved. The hydrostatic head of the pool is greater than 8 psid (18.5 feet of submergence). This 8 psid ensures that the liner will never see a negative pressure in the frequency range of exceedance, and, since the liner is backed by concrete everywhere, no natural modes in this range are excitable.

It is therefore concluded that the existing load definition adequately covers the localized effects of the TIP encroachment.

Item 2

The hydrodynamic mass, M_h, associated with spherical bubble collapse is found from

$$1/2M_h\dot{R}^2 = \int_R^\infty 1/2(p4\ r^2dr)\ \ \dot{R}^2\left(\frac{R}{r}\right)^4 \qquad (1)$$

R - bubble radius
R - bubble surface collapse rate

where the right-hand side represents the summing of the kinetic energy of each differential element of mass between the bubble surface and infinity. The result is

$$M = 3\left(\rho\frac{4}{3}R^3\right) \qquad (2)$$

Equation (2) implies that the majority of the mass affecting bubble collapse is contained within a volume of water surrounding the bubble that is three times that of the bubble volume. This volume of water is contained in a shell of thickness.

$$t = R\left(\sqrt[3]{4} - 1\right) \qquad (3)$$

or

$$t = 0.6R \qquad (4)$$

Visual observations of chugging bubble collapse during full-scale Mark III chugging tests have shown that the bubble diameter is on the order of the vent diameter, and the collapse location is near the top vent (Reference 1). This places the bubble and its hydrodynamic mass greater than one bubble diameter away from the encroachment. It is therefore concluded that the effect of the encroachment on the inertial impedance is negligible.

Since the collapse of steam bubbles during chugging is inertia controlled, there will be no encroachment effect on bubble collapse rate. It follows, then, that the excitation to the suppression pool is independent of the presence of an encroachment. Chug source pressures measured in unencroached tests are therefore valid and may be used as input to the model developed in Action Plan Element 35.1 to quantify the encroachment effect.

Reference

1. A.M. Varzaly et al, Mark III Confirmatory Test Program - Full Scale Condensation & Stratification Phenomena - Test Series 570, NEDE-21853P, August 1978. (General Electric Proprietary)

*This revision replaces the GSU submittal dated April 1, 1983.

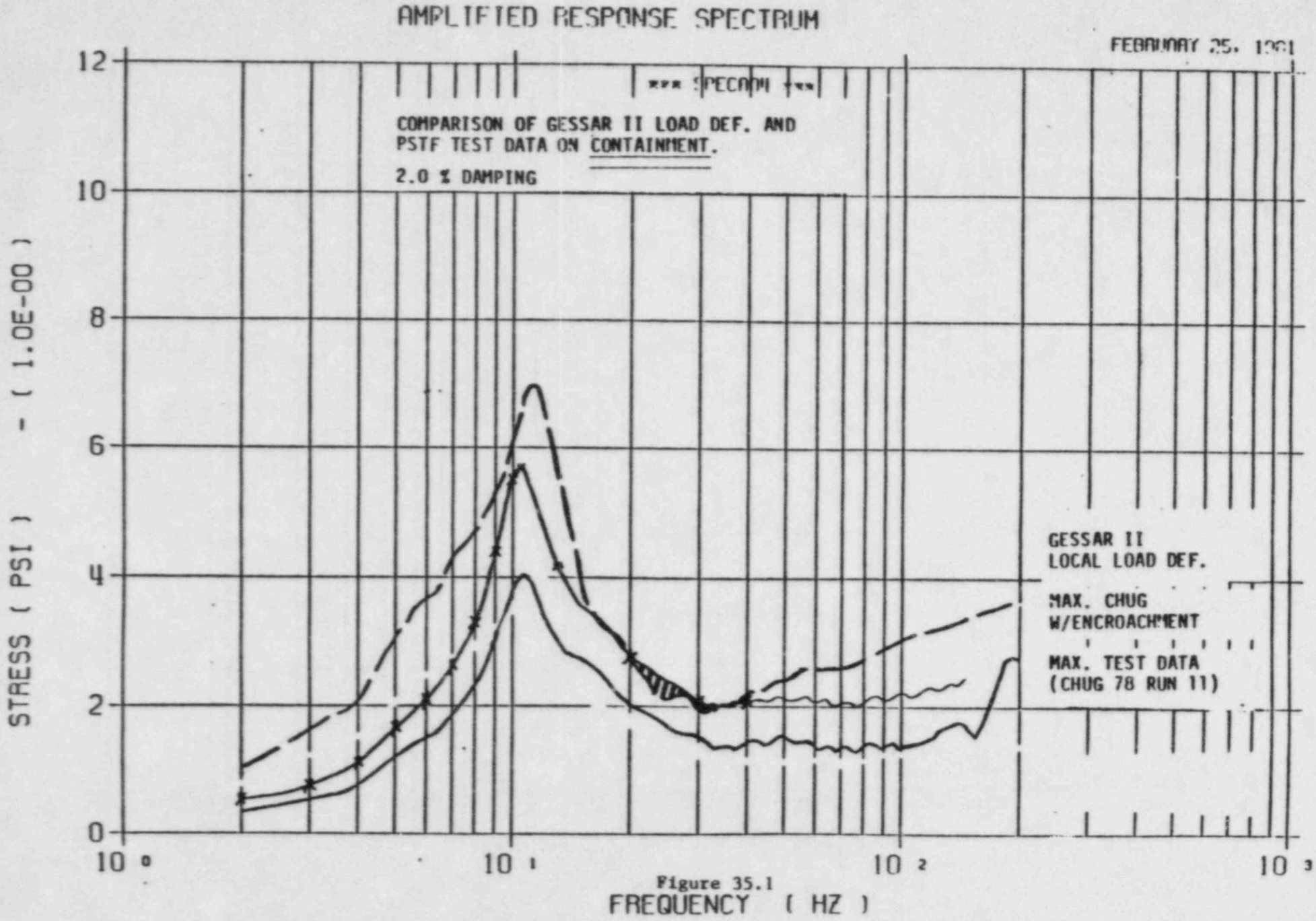

Figure 35.1

PL 1

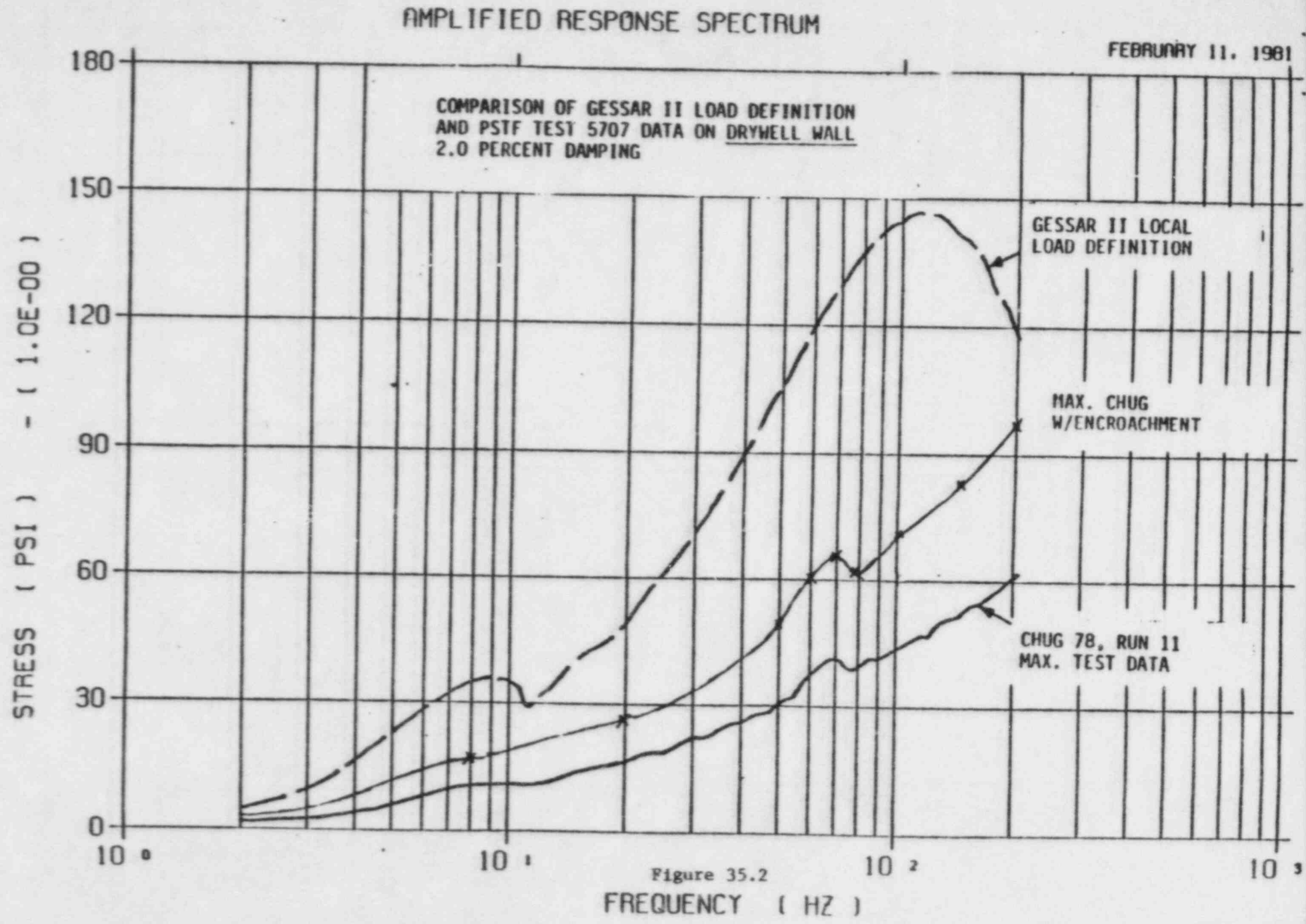
AMPLIFIED RESPONSE SPECTRUM
FEBRUARY 11, 1981
COMPARISON OF GESSAR II LOAD DEFINITION
AND PSTF TEST 5707 DATA ON DRYWELL WALL
2.0 PERCENT DAMPING
GESSAR II LOCAL
LOAD DEFINITION
MAX. CHUG
W/ENCROACHMENT
CHUG 78, RUN 11
MAX. TEST DATA
STRESS (PSI) - (1.0E-00)
FREQUENCY (HZ)
180
150
120
90
60
30
0
10 0
10 1
10 2
10 3

Figure 35.2

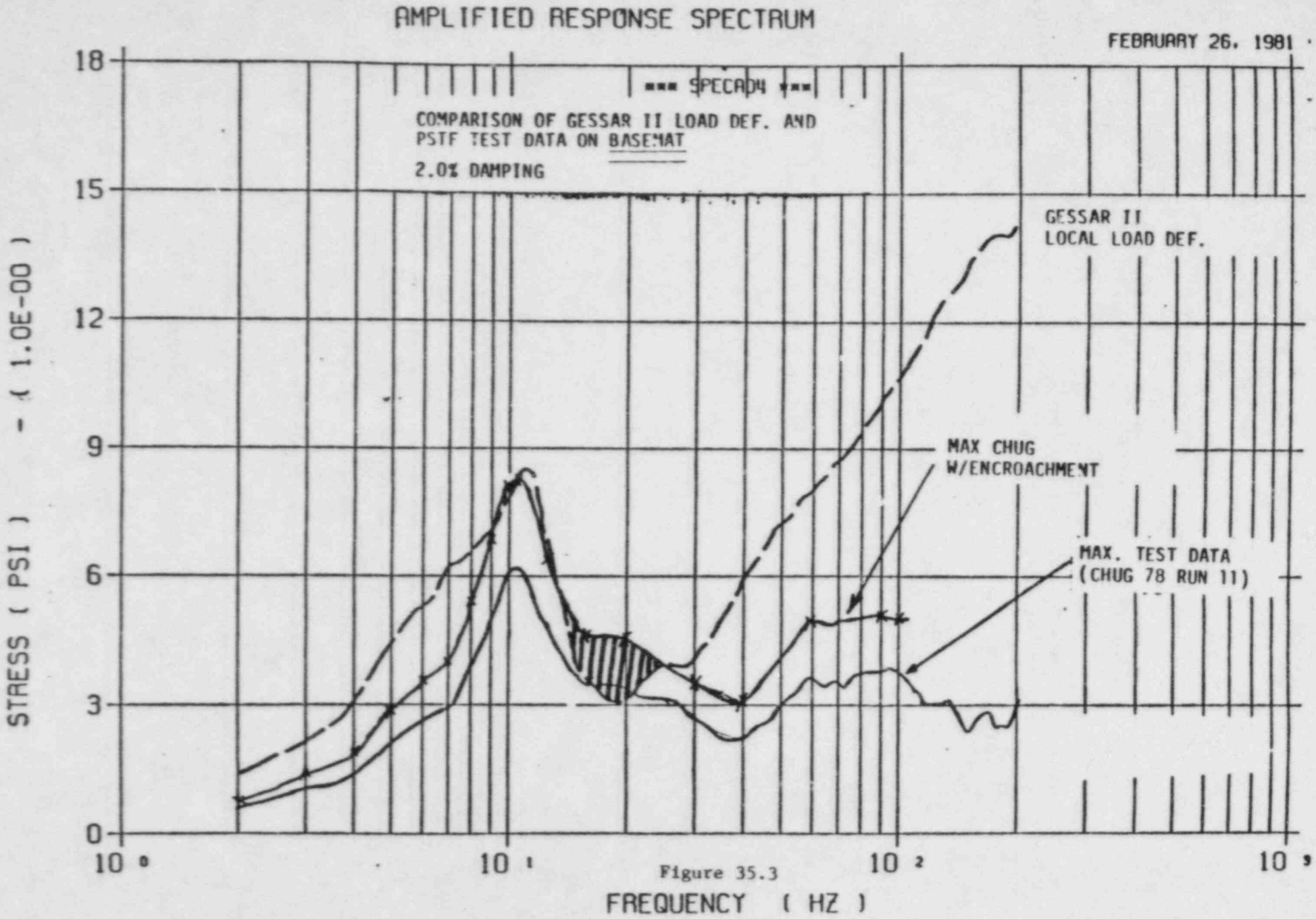
AMPLIFIED RESPONSE SPECTRUM
FEBRUARY 26. 1981
*** SPECAD4 ***
COMPARISON OF GESSAR II LOAD DEF. AND
PSTF TEST DATA ON BASEMAT
2.0% DAMPING
GESSAR II
LOCAL LOAD DEF.
MAX CHUG
W/ENCROACHMENT
MAX. TEST DATA
(CHUG 78 RUN 11)
STRESS (PSI) - (1.0E-00)
FREQUENCY (HZ)
0
3
6
9
12
15
18
10 0
10 1
10 2
10 3

Figure 35.3

Action Plan 36 - Generic

I. Issues Addressed

20.0 LOADS ON STRUCTURES, PIPING, AND EQUIPMENT IN THE DRYWELL DURING REFLOOD

During the latter stages of a LOCA, ECCS overflow from the primary system can cause drywell depressurization and vent backflow. The GESSAR defines vent backflow, vertical impingement, and drag loads to be applied to drywell structures, piping, and equipment, but no horizontal loading is specified.

II. Response

No action is required, based on discussion between MP&L and the NRC Staff. The basis for this decision is applicable to RBS.

III. Schedule

Based on the above response, this item is considered closed for RBS with this submittal.

Action Plan 37 - Generic

I. Issues Addressed

22.0 The EPGs currently in existence have been prepared with the intent of coping with degraded core accidents. They may contain requirements conflicting with design basis accident conditions. Someone needs to carefully review the EPGs to assure that they do not conflict with the expected course of the design basis accident.

II. Response*

The Owners Group believes that the development program through which the emergency procedure guidelines have passed has adequately addressed this concern. As a result of this issue, the Mark III Owners Group has brought this concern to the attention of the BWR Owners Group. A generic resolution of this issue will be pursued with the BWR Owners' Group. In addition, GSU and SWEC are reviewing the EPGs to ensure that they do not nonconservatively conflict with the expected course of the design basis accident. Any conflicts that are identified will be either addressed on a plant-specific basis or addressed to the BWR Owners' Group for resolution.

III. Status

Based on the above response, this issue is considered closed for RBS with this submittal.

*This revised response replaces the GSU-submitted response dated April 1, 1983.

Action Plan 38 - Plant Specific

I. Issues Addressed

6.2 GE has recommended that an interlock be provided to require containment spray prior to starting the recombiners because of the large quantities of heat input to the containment. Incorrect implementation of this interlock could result in the inability to operate the recombiners without containment spray.

II. Response*

This concern is not applicable to RBS (no containment sprays, no interlocks).

RBS has redundant containment unit coolers. These coolers are automatically initiated within 10 minutes after a LOCA signal and do not have any interlocks with the combustible gas control systems.

III. Status

Based on the above response, this item is considered closed for RBS with this submittal.

*This revised response replaces the GSU-submitted response dated April 1, 1983.

Action Plan 39 - Plant Specific

I. Issues Addressed

6.4 For the containment air monitoring system furnished by GE, the analyzers are not capable of measuring hydrogen concentration at volumetric steam concentrations above 60 percent. Effective measurement is precluded by condensation of steam in the equipment.

II. Response

The RBS hydrogen analyzers are not supplied by GE. The analyzers will have the capability to measure under the following conditions:

- Pressure: -10 to 25 psig
- Temperature: 330°F max
- Relative humidity: 100 percent

In addition, containment atmosphere monitoring lines are heat-traced to preclude condensation.

III. Status

Based on the above response, this issue is considered closed for RBS with this submittal.

Action Plan 40 - Plant Specific

I. Issues Addressed

7.3 The analysis assumes that the containment airspace is in thermal equilibrium with the suppression pool. In the short term, this is nonconservative for Mark III due to adiabatic compression effects and finite time required for heat and mass to be transferred between the pool and containment volumes.

II. Response

This concern is not applicable to RBS, since the analysis applies the first law of thermodynamics in determining containment pressure and temperature, i.e., adiabatic compression effects are accounted for.

III. Status

Based on the above response, this issue is considered closed for RBS with this submittal.

Action Plan 41 - Plant Specific

I. Issues Addressed

12.0 SUPPRESSION POOL MAKEUP LOCA SEAL-IN

The upper pool dumps into the suppression pool automatically following a LOCA signal with a 30-minute delay timer. If the signal that starts the timer disappears on the solid-state logic plants, the timer resets to zero, preventing upper pool dump.

II. Response

This concern is not applicable to RBS (no upper pool dump).

III. Status

Based on the above response, this issue is considered closed for RBS with this submittal.

Action Plan 42 - Plant Specific

I. Issues Addressed

13.0 NINETY SECOND SPRAY DELAY

The "B" loop of the containment sprays includes a 90-second timer to prevent simultaneous initiation of the redundant containment sprays. Because of instrument drift in the sensing instrumentation and the timers, GE estimates that there is a 1 in 8 chance that the sprays will actuate simultaneously. Simultaneous actuation could produce negative pressure transients in the containment and aggravate temperature stratification in the suppression pool.

II. Response

This concern is not applicable to RBS (no containment sprays).

III. Status

Based on the above response, this issue is considered closed for RBS with this submittal.

Action Plan 43 - Plant Specific

I. Issues Addressed

15.0 SECONDARY CONTAINMENT VACUUM BREAKER PLENUM RESPONSE

The STRIDE plants had vacuum breakers between the containment and the secondary containment. With sufficiently high flows through the vacuum breakers to containment, vacuum could be created in the secondary containment.

II. Response

This concern is not applicable to RBS (no containment vacuum breakers).

III. Status

Based on the above response, this issue is considered closed for RBS with this submittal.

Action Plan 44 - Plant Specific

I. Issues Addressed

18.0 EFFECTS OF INSULATION DEBRIS

18.1

Failures of reflective insulation in the drywell may lead to blockage of the gratings above the weir annulus. This may increase the pressure required in the drywell to clear the first row of drywell vents and perturb the existing load definitions.

18.2

Insulation debris may be transported through the vents in the drywell wall into the suppression pool. This debris could then cause blockage of the suction strainers.

II. Program for Resolution

1. The amount of insulation that will be displaced by jet impingement from pipe breaks in the drywell will be quantified, and the effects of increased vent loss will be evaluated to ensure that any post-LOCA drywell pressure caused by this effect does not exceed the drywell design pressure.

2. An evaluation of the potential effects of possible ECCS suction strainer blockage will be provided.

III. Status

Items 1 and 2 are complete and are included with this submittal.

IV. Final Results

Item 1

RBS design provides a clearance of 3.75 ft between the top of the weir wall and the grating above the weir annulus. This clearance provides a vent area of 707 square feet. Even if the unrealistic assumption is made that the entire grating is blocked by insulation, the available flow area is 707 sq ft as indicated in Figure 44.1. Comparing this greater flow area with the

made that the entire grating is blocked by insulation, the available flow area is 707 sq ft as indicated in Figure 44.1. Comparing this greater flow area with the weir annulus flow area of 515.5 sq ft indicates no significant blockage of flow area.

Item 2

The type of insulation that will be used for River Bend Station has not been determined. However, one of the following two insulation types will be selected: a) metallic insulation or b) Owens Corning Fiberglas' (OCF) Nu'k'on. Either of these insulations would not create any problems as explained below:

a) Metallic Insulation

The metallic insulation that may be used for the primary coolant system piping has a heavy outer stainless steel casing and rigid, thin inner stainless steel spacers.

The assumption is made that a number of panels of the metallic insulation rupture catastrophically and the spacers become debris. However, the outer casing completely encloses the spacers, and the spacers are spot welded to the casing. The physical construction of the assembly is such that the assembly is quite strong.

To achieve substantial blockage of the ECCS suction strainers, it must be assumed that a number of panels totally fail and that the spacers are evenly distributed around the drywell. In addition, it must be assumed that the spacers would all enter the weir annulus and be transported through the horizontal vents into the suppression pool. The spacers then must be carried across the suppression pool and must wrap around the ECCS strainer, clogging it. It is excessively conservative and not reasonable to assume that all of these factors would occur during an accident.

It should also be noted that each strainer can become 50 percent clogged and still perform its design function. Furthermore, the approach velocity of the water through the strainer is 0.71 ft/sec. These design factors further reduce the potential for debris to adversely affect ECCS system performance.

b) Owens Corning Fiberglas' (OCF) Nu'k'on Insulation

The OCF Nu'k'on insulation was tested under design basis accident (DBA) and the nozzle/sump clogging tests. The methodology of testing and results were published in the topical report OCF-1 submitted to the NRC in August 1977. The summary of the conclusions of the above-mentioned tests are as follows:

- Owens-Corning Fiberglas' nuclear containment insulation system (Nu'k'on) will not deteriorate or lose its mechanical integrity during a loss-of-coolant accident.

- The only parts of the system which might be dislodged would be those that are blasted off as a direct result of a component rupture. This would include sections of insulation adjacent to the break and those dislodged by a pipe whip action or direct impingement of the water blast resulting from the rupture. In short, only those sections which experience extremely violent forces will be dislodged.

- Owens-Corning Fiberglas' Nu'k'on on system's blanket insulation will not clog containment area sumps or drains.

- No portions of the Owens-Corning Fiberglas' nuclear containment insulation system (Nu'k'on) will be washed off or dislodged from the surfaces, to which it is attached, as a result of the emergency spray systems. (It should be noted that RBS does not have any containment spray systems.)

- Owens-Corning Fiberglas' Nu'k'on system's blanket insulation will not interfere with nuclear containment emergency recirculation pumps.

- Owens Corning Fiberglas' Nu'k'on insulation blankets will not clog nuclear containment area emergency spray nozzles. (It should be noted that RBS does not have any containment spray systems.)

- Owens Corning Fiberglas' Nu'k'on system will not interfere with the safe

operation of emergency spray system in nuclear containment areas of light water nuclear power plants.

In addition to the above conclusions, it should be noted that the large number of physical obstructions such as piping, structural supports, walkways, cable trays, and restraints make it very difficult for anything other than water to fall all the way to the suppression pool. Even if any insulation debris does fall into the pool, it would tend to settle on the bottom of the pool. Since the ECCS suction strainers are located approximately 3 ft above the bottom of the pool, it would be extremely difficult and unlikely for a piece of insulation to be picked up by the strainers. Further, each strainer can become 50 percent clogged and still perform its design function.

III. Status

Based on the above response, this issue is considered closed for RBS with this submittal.

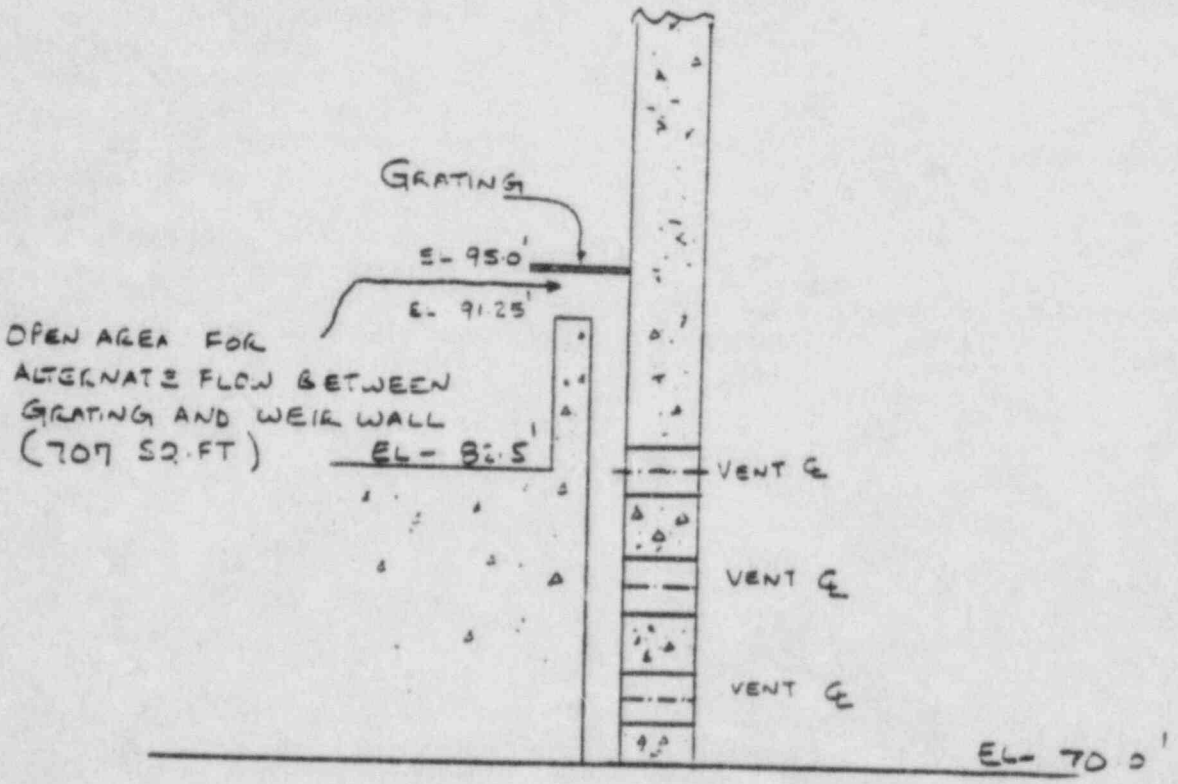

Figure 44.1

Schematic showing elevation of weirwall and drywell grating above weir annulus.

Action Plan 45 - Plant Specific

I. Issues Addressed

6.1 GE had recommended that the drywell purge compressors and the hydrogen recombiners be activated if the reactor vessel water level should drop to within 1 ft of the top of active fuel. This requirement was not incorporated in the emergency procedure guidelines.

II. Response*

Appropriate guidance for activation of these systems will be provided in the RBS Emergency Operating Procedures.

III. Status

Based on the above response, this issue is considered closed for RBS with this submittal.

*This revision replaces the GSU submittal dated April 1, 1983.

Action Plan 46 - Plant Specific

I. Issues Addressed

17.0 EMERGENCY PROCEDURE GUIDELINES

The EPGs contain a curve that specifies limitations on suppression pool level and reactor pressure vessel pressure. The curve presently does not adequately account for upper pool dump. At present, the operator would be required to initiate automatic depressurization when the only action required is the opening of one additional SRV.

II. Response

This concern is not applicable to RBS (no upper pool dump).

III. Status

Based on the above response, this issue is considered closed for RBS with this submittal.

Action Plan 47 - Plant Specific

I. Issues Addressed

1.7 GE suggests that at least 1,500 sq ft of open area should be maintained in the HCU floor. In order to avoid excessive pressure differentials, at least 1,500 sq ft of opening should be maintained at each containment elevation.

II. Response*

The RBS design provides an open area of 2,481 sq ft (i.e., a 39-percent open area) at the HCU floor. The analysis conservatively uses 1600 sq ft as the open area at the HCU floor. The open area at all other elevations, except at refueling floor (el 186 feet-3 inches) exceed 1500 sq ft. The open area at the refueling floor is approximately 689 sq ft. The pressure differential across this floor is calculated using the Darcy equation given below.

$$\Delta P_2 = \frac{\rho_2}{\rho_1} \frac{K_2}{K_1} \left(\frac{A_1}{A_2}\right)^2 \left[\frac{V_3}{V_2 + V_3}\right]^2 \Delta P_1$$

The definition of the variables in the above equation is given in Figure 47.1. As can be seen from Table 47.1, the resultant differential pressure across the refueling floor is very small. Also, the effect on drywell pressure due to the additional backpressure as a result of the restricted area at the refueling floor is very small.

III. Status

Based on the above response, this issue is considered closed for RBS with this submittal.

*This revised response replaces the GSU-submitted response dated April 1, 1983.

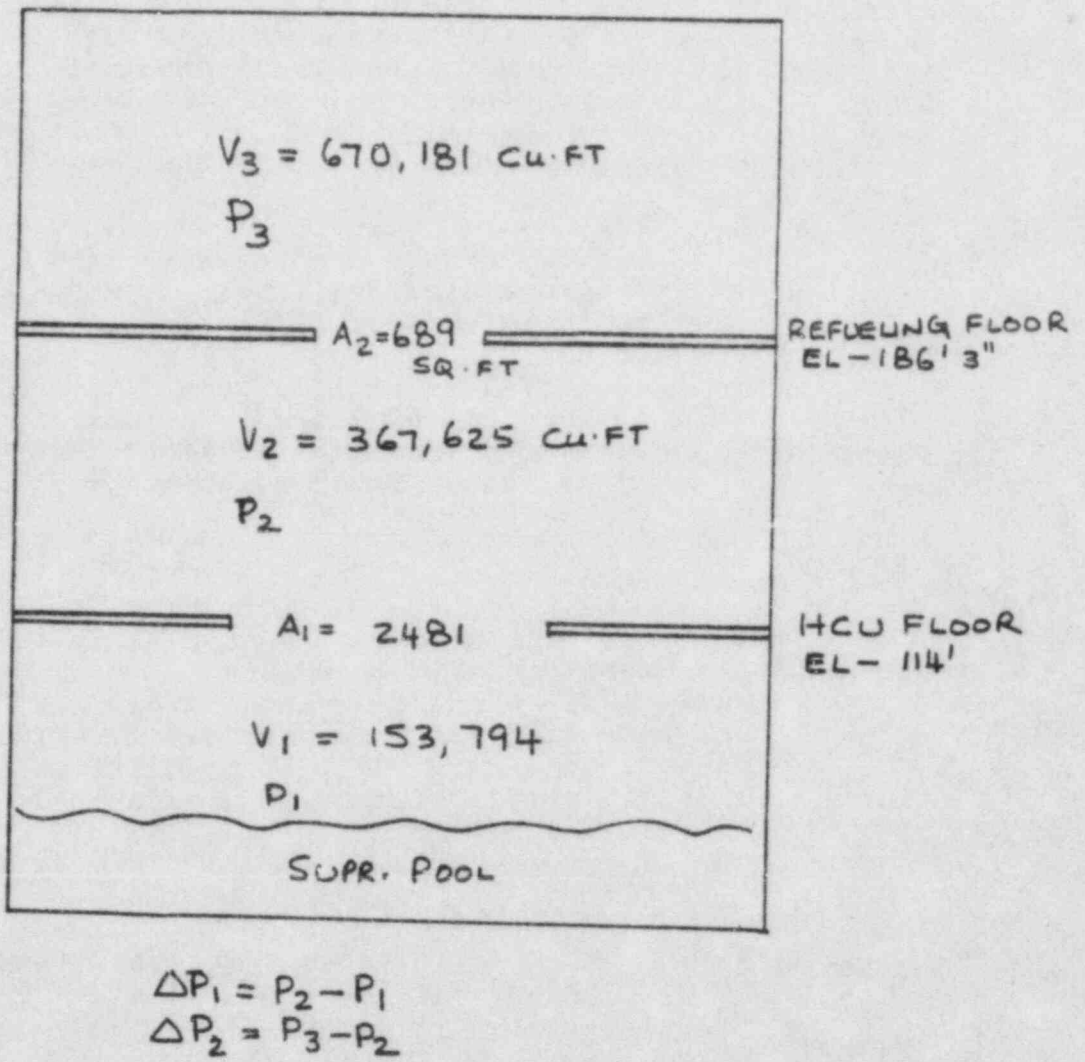

Figure 47.1

Open Flow Areas in RBS Containment

TABLE 47.1

PRESSURE DIFFERENTIAL ACROSS HCU AND REFUELING FLOORS

Time (Sec)	Calculated Pressures DW (psia)	WW (psia)	Cont. (psia)	ΔP1 (psid)	Adjustments P1	ΔP2	Adjusted DW Pressure	% Diff.
0	14.7	14.7	14.7	0	0.07	0	14.7	0
1.0	33.12	14.914	14.87	0.044	0.07	0.099	33.219	0.30
1.64	32.0	16.402	16.19	0.212	0.08	0.478	32.478	1.49
1.65	31.88	16.540	16.21	0.33	21.56	0.001	31.881	0.003
2.0	30.02	19.205	16.31	2.895	20.78	0.013	30.033	0.043
2.5	30.43	20.168	16.67	3.498	19.24	0.021	30.451	0.069
2.77	30.78	20.256	16.88	3.376	18.42	0.022	30.802	0.071
3.0	31.00	20.220	17.06	3.16	17.76	0.022	31.022	0.071
3.5	30.87	19.938	17.36	2.578	16.65	0.020	30.890	0.065
4.5	31.28	19.207	18.07	1.137	14.60	0.010	31.290	0.032
5.5	30.05	18.788	18.48	0.308	13.44	0.003	30.053	0.010

NOTE:

ΔP1 = Pressure differential across HCU floor.
ΔP2 = Pressure differential across refueling floor.

Action Plan 48 - Plant Specific

I. Issues Addressed

5.7 After upper pool dump, the level of the pool will be 6 ft higher, and drywell-to-containment differential pressure will be greater than 3 psid. The drywell hydrogen purge compressor head is nominally 6 psid. The concern is that after an upper pool dump, the purge compressor head may not be sufficient to depress the weir annulus enough to clear the upper vents. In such a case, hydrogen mixing would not be achieved.

II. Response

This concern is not applicable to the River Bend Station design (no upper pool dump).

III. Status

Based on the above response, this item is considered closed for RBS with this submittal.

Action Plan 49 - Plant Specific

I. Issues Addressed

21.0 CONTAINMENT MAKEUP AIR FOR BACKUP PURGE

Regulatory Guide 1.7 requires a backup purge hydrogen removal capability. This backup purge for Mark III is via the drywell purge line, which discharges to the shield annulus, which in turn is exhausted through the standby gas treatment system (SGTS). The containment air is blown into the drywell via the drywell purge compressor to provide a positive purge. The compressors draw from the containment; however, without hydrogen-lean air makeup to the containment, no reduction in containment hydrogen concentration occurs. It is necessary to ensure that the shield annulus volume contains a hydrogen lean mixture of air to be admitted to the containment via containment vacuum breakers.

II. Response

RBS has no containment vacuum breakers. The RBS hydrogen purge system design has provisions to discharge filtered outside air into the containment/drywell and exhausts through the SGTS.

III. Status

Based on the above response, this issue is considered closed for RBS with this submittal.

Action Plan 50 - Generic

I. Issues Addressed

5.2 Under technical specification limits, bypass leakage corresponsing to $A/\sqrt{K}$ = 0.1 sq ft constitutes acceptable operating conditions. Smaller-than-IBA-sized breaks can maintain break flow into the drywell for long time periods, however, because the RPV would be depressurized over a 6-hr period. Given, for example, an SBA with $A/\sqrt{K}$ = 0.1, projected time period for containment pressure to reach 15 psig is 2 hours. In the latter 4 hours of the depressurization, the containment would presumably experience ever-increasing overpressurization.

II. Response

GSU's River Bend Station design allows a maximum bypass area ($A/\sqrt{K}$) of 1.1 sq ft for small breaks (0.1 sq ft). The bypass capacity is larger for intermediate and large breaks (see FSAR Figure 6.2-27 included as Attachment 19.1 to Action Plan 19). River Bend Station's redundant containment unit coolers and heat sinks provide more than adequate heat removal capability to prohibit containment overpressurization during the later part of reactor vessel depressurization. Finally, the operator can initiate rapid reactor vessel depressurization if containment pressure and temperature continue to rise.

III. Status

Based on the above response, this issue is considered closed for RBS with this submittal.